Dynamic Real-Time Optimization of a Solar Thermal Plant with Storage Management

Alix Untrau

THÈSE

UNIVERSITE DE PAU ET DES PAYS DE L'ADOUR

École doctorale des Sciences Exactes et leurs Applications (ED2011)

Soutenue le 18 septembre 2023

par **Alix Untrau**

pour obtenir le grade de docteur
de l'Université de Pau et des Pays de l'Adour
Spécialité : Energétique

Dynamic Real-Time Optimization of a Solar Thermal Plant with Storage Management

Optimisation dynamique en temps-réel d'une centrale solaire thermique avec gestion du stockage

MEMBRES DU JURY

PRESIDENT

• Lorenz T. BIEGLER	Professeur des Universités / Université Carnegie Mellon

RAPPORTEURS

• Argimiro R. SECCHI	Professeur des Universités / Université Fédérale de Rio de Janeiro
• Marc CLAUSSE	Professeur des Universités / Institut National des Sciences Appliquées de Lyon

EXAMINATEURS

• Galo A. CARILLO LE ROUX	Professeur des Universités / Université de São Paulo
• Sabine SOCHARD	Maître de Conférences / Université de Pau et des Pays de l'Adour

DIRECTEUR

• Sylvain SERRA	Maître de Conférences HDR / Université de Pau et des Pays de l'Adour

MEMBRES INVITES

• Jean-Michel RENEAUME	Professeur des Universités / Université de Pau et des Pays de l'Adour
• Frédéric MARIAS	Professeur des Universités / Université de Pau et des Pays de l'Adour

UNIVERSITÉ DE PAU ET DES PAYS DE L'ADOUR

Dynamic Real-Time Optimization of a Solar Thermal Plant with Storage Management

Abstract

With the aim of mitigating climate change, solar thermal plants represent a good alternative to fossil fuels for the production of low temperature heat. Because of the intermittency of solar irradiation and the uncertainty of its forecast, the operation of a solar thermal plant is particularly challenging. Especially, the use of storage, required to decouple the heat production from the heat supply, makes the operation even more complex. In this thesis, a methodology was presented to optimize the operation of a solar thermal plant with storage, minimizing the operating costs. The methodology is composed of two dynamic optimization levels. A planning phase is in charge of storage management, benefiting from a longer term strategic vision and using weather forecasts. Then, a Dynamic Real-Time Optimization (DRTO) adapts the optimal trajectories to the current disturbances and updated forecasts, with a shorter time horizon. The methodology is tested online, on a detailed simulation model representing the real solar thermal plant. In order to achieve a better compromise between the accuracy of the model and the computational time, a spatial discretization scheme for the 1D storage tank model, based on orthogonal collocation on finite elements, was proposed in replacement of the traditional finite volumes. The DRTO methodology developed was tested in various case studies, representing different seasons and real-time disturbances. Storage management at the DRTO level was studied in particular. It was found that the planning phase can help to avoid overheating by providing a reference trajectory for the stored energy that can be tracked at the DRTO level. The tracking term in the objective function of DRTO should be adjusted to achieve the best compromise between the tracking of the planned stored energy and the minimization of the operating costs. In situations without a risk of overheating, determined at the planning phase, maximizing the stored energy at the end of each DRTO increases the solar fraction of the heat supply and thus reduces the operating costs. Additionally, it was found that the simulated solar thermal plant showed improved thermal and economic performances when using DRTO to operate it rather than offline dynamic optimization. This work shows interesting directions on how to use a planning phase to improve storage management in a DRTO methodology for a solar thermal plant.

Optimisation dynamique en temps-réel d'une centrale solaire thermique avec gestion du stockage

Résumé

Afin de limiter le réchauffement climatique, une transition énergétique est nécessaire. Les centrales solaires thermiques sont une bonne alternative aux combustibles fossiles pour la production de chaleur à basse température, à destination de procédés industriels ou pour le chauffage et l'eau chaude sanitaire. Malheureusement, la ressource solaire est intermittente et difficile à prédire, ce qui complexifie le fonctionnement des centrales solaires thermiques. Une cuve de stockage thermique ajoutée au système permet de découpler la production et la fourniture de chaleur pour pallier leur déphasage. Cela accroît les degrés de liberté du fonctionnement de la centrale solaire et le rend encore plus complexe. Cette thèse présente une méthodologie d'optimisation du fonctionnement des centrales solaires thermiques dans le but de minimiser les coûts d'opération et de proposer une bonne gestion du stockage tout en satisfaisant la demande en chaleur. Cette méthodologie se décompose en deux niveaux d'optimisation dynamique. Le premier niveau est une phase de planification qui prévoit l'utilisation optimale du stockage sur un horizon de temps de quelques jours en utilisant des prévisions météorologiques. Le second niveau est une optimisation dynamique en temps-réel (Dynamic Real-Time Optimization, DRTO), qui adapte les trajectoires optimales des débits de la centrale sur un horizon de temps plus court et en utilisant des prévisions mises à jour, plus fiables. La méthodologie est testée en temps-réel sur un modèle de simulation détaillé représentant la centrale réelle. Afin d'améliorer la modélisation de la centrale, une étude a été réalisée sur la discrétisation spatiale de la cuve de stockage en 1D. La collocation orthogonale sur éléments finis a été proposée pour remplacer le traditionnel schéma de discrétisation utilisant les volumes finis, car elle permet d'obtenir des résultats plus précis avec un temps de calcul réduit. La méthodologie de DRTO développée a été testée sur plusieurs cas d'étude représentant différentes saisons et des scénarios en temps-réel variés. Une attention particulière a été donnée à la gestion du stockage. Les résultats obtenus montrent que l'utilisation pour la DRTO d'une planification pour fournir une trajectoire de référence pour l'énergie stockée au cours du temps permet d'éviter des risques de surchauffe dans la centrale solaire. Le suivi de la planification de la gestion du stockage se fait par l'ajout d'un terme dans la fonction objectif permettant de minimiser l'écart à la fin de l'horizon de temps entre la planification et la DRTO. Ce terme de suivi est affecté d'un poids qui doit être ajusté pour obtenir le meilleur compromis entre le suivi de la planification et la minimisation des coûts d'opération. Lorsque la planification ne montre aucun risque de surchauffe, il est préférable de maximiser l'énergie stockée à la fin de l'horizon de temps de chaque DRTO pour augmenter la fraction solaire de l'énergie fournie et ainsi réduire les coûts d'opération. Enfin, la centrale solaire simulée atteint de meilleures performances thermiques et économiques lorsqu'elle fonctionne en suivant les trajectoires optimales obtenues avec la DRTO que lorsque l'optimisation dynamique hors ligne est utilisée. Ce travail de thèse présente des perspectives intéressantes quant à l'utilisation d'une phase de planification pour améliorer la gestion du stockage dans une méthodologie de DRTO appliquée à une centrale solaire thermique.

Remerciements

Je souhaite tout d'abord remercier les membres de mon jury de thèse qui ont apporté d'enrichissantes discussions grâce à leur expertise dans les différents domaines scientifiques impliqués dans mon travail. Merci aux professeurs Marc Clausse et Argimiro Secchi pour leur relecture attentive de mon manuscrit et leurs rapports constructifs. Je suis également très sensible à l'honneur que m'a fait le professeur Lorenz Biegler en acceptant de présider mon jury. Je me souviendrai toujours de sa bienveillance lors de nos échanges à l'issue de ma soutenance.

Je tiens également à remercier tous mes encadrants de thèse pour leur accompagnement lors de ces trois années. Je leur suis particulièrement reconnaissante pour la confiance et l'autonomie qu'ils m'ont accordées, tout en se rendant disponibles dès lors que je rencontrais des difficultés. Un encadrement à cinq peut sembler compliqué à gérer mais j'ai vraiment senti les atouts d'avoir une telle équipe pour m'entourer (hormis lorsqu'il s'agissait de trouver une date pour une réunion !). Merci à Frédéric et Jean-Michel pour votre aide sur la convergence difficile d'un modèle de simulation ou d'optimisation, j'ai beaucoup appris à vos côtés. Je remercie chaleureusement Sabine pour son aide sur la collocation orthogonale et pour toutes les discussions non scientifiques que l'on a pu avoir. Galo, je me souviendrai toujours de mon passage dans ta ville de São Paulo, où tu m'as si bien accueillie. Enfin, Sylvain, merci d'avoir dirigé ma thèse avec autant de bienveillance et d'humanité. Je savais qu'en allant frapper à ta porte, je trouverais toujours une oreille attentive pour des questions scientifiques mais pas que. Je suis vraiment ravie de continuer à travailler avec vous tous, merci pour votre confiance !

Ma gratitude va également à l'ensemble du personnel du LaTEP et de l'ENSGTI pour leur accueil chaleureux et la bonne humeur qui règne dans notre petit labo. En particulier, je remercie Patricia et Jean-Michel pour leur aide sur les aspects administratifs et logistiques.

Ces trois années de thèse ont aussi vu de belles amitiés se créer. En tout premier lieu je souhaite remercier mes partenaires du bureau terrasse, Malik et Matheus. Que ce soit pour des défis sportifs, des discussions personnelles ou des blagues toujours plus imaginatives, vous étiez là. Je vous souhaite bon courage pour ces derniers mois. Buriti, merci d'avoir toujours été là pour moi, y compris quand j'étais à São Paulo et toi à Pau, ton écoute et ta sensibilité sont de précieuses qualités qui me manqueront quand tu rentreras au Brésil. Jean, merci pour le coaching sportif, le partage des traditions alsaciennes et toutes les discussions à midi. Merci à Régis et Amina, mon papa et ma maman de thèse, pour votre accueil et votre bonne humeur communicative. Marie, je te remercie pour tous les conseils que tu nous donnes sur la thèse et sur la vie, tu trouves toujours les bons mots et tu nous fais aussi bien rire. Je remercie le clan des brésiliens, Arthur, Jeff, Giberto, pour les soirées repas et jeux de société. Ces trois années ont été particulièrement sportives alors je remercie mes autres partenaires d'aventure Cassie, Perla, Sonia, Julie, Diane. Enfin merci à tous les autres doctorants/post-docs/ATER avec qui j'ai partagé de bon moments culinaires, sportifs ou festifs. Je vous souhaite à tous une bonne continuation dans votre thèse ou l'après-thèse et j'espère qu'on gardera le contact.

Je tiens aussi à remercier mes amis hors du labo, qui m'ont permis de déconnecter et retrouver un peu le monde hors de la thèse. Tout d'abord, merci au CUB pour l'accueil et l'apprentissage de l'ultimate, je compte bien continuer à jouer au frisbee avec vous le plus longtemps possible. Merci aux amis d'enfance avec qui les retrouvailles sont toujours aussi drôles et agréables, malgré la distance et les années. Enfin merci aux amis de l'INSA, en particulier les C10 et les GEn, que j'ai pu régulièrement revoir pendant ces années. Vos messages et votre soutien pour le jour de ma soutenance m'ont profondément touchée. Merci d'être là et de toujours m'intégrer aux plans même si la probabilité que je vous rejoigne depuis mon petit coin de France est souvent faible. Célia, merci d'être venue jusqu'à Pau pour me voir (et voir MichMich je sais), notre amitié m'est extrêmement précieuse et durera toujours je l'espère. Je te souhaite le meilleur pour la suite de ta thèse.

Merci à toute ma famille pour leur accueil dans le Nord-Est aux vacances, pour quelques jours de déconnexion et de bons moments partagés. Je remercie mon très grand frère Théo pour m'avoir montré la voie jusqu'à la fin de nos études. C'était une chance de partager les années de thèse entre frère et soeur. Papa et Maman, je ne pense pas qu'on puisse trouver un meilleur soutien que vous deux. Que ce soit pour déménager au $4^{ème}$ étage, traverser la France en voiture ou écouter mes bavardages incessants et mes angoisses, vous êtes là. Papa, je te décerne le diplôme de docteur en tetris de coffre, entretien de jardin et oeufs au plat. Je ne sais pas ce qu'on ferait sans toi. Maman, tu étais parfois ma $6^{ème}$ encadrante mais tu es bien plus que ça. Je continuerai toujours à optimiser le soleil !

Pour finir, Tibo, tu as rendu ces trois années beaucoup plus amusantes. Je compte bien manger des risottos et des quiches poireaux-munster entre deux randonnées avec toi pour les nombreuses années à venir.

Résumé détaillé

L'atténuation du changement climatique est un des enjeux majeurs de notre temps. Pour cela, il est nécessaire de procéder à une transition énergétique réduisant les émissions de gaz à effet de serre liés à la production d'énergie. Les centrales solaires thermiques permettent de produire de la chaleur sans émissions directes de CO_2 et constituent donc une bonne alternative aux combustibles fossiles. Leur usage est particulièrement adapté à la production de chaleur à basse température pour certains procédés industriels et pour alimenter des réseaux de chaleur urbains, pour le chauffage des locaux et la distribution d'eau chaude sanitaire. Malheureusement, le rayonnement solaire est intermittent, avec des variations journalières et saisonnières. De plus, les variations journalières dues à la couverture nuageuse sont difficiles à prévoir précisément longtemps à l'avance et impactent fortement la prodution de chaleur. La demande en chaleur peut quant à elle être continue et importante à des moments où le rayonnement solaire est faible. Afin de pallier le déphasage de la production et de la fourniture de chaleur, un stockage thermique est ajouté à la centrale solaire. Cela permet d'étendre la période de fourniture de chaleur solaire au consommateur mais cela nécessite une bonne connaissance des conditions météorologiques futures pour anticiper les besoins en stockage et déstockage. Au vu des conditions environnementales variables et des degrés de liberté du système, l'exploitation d'une centrale solaire thermique est particulièrement délicate. L'objectif de cette thèse est de développer une méthodologie d'optimisation du fonctionnement d'une centrale solaire thermique dans le but d'en minimiser les coûts d'opération, en portant une attention particulière à la gestion du stockage.

Le chapitre I présente l'état de l'art sur l'optimisation des centrales solaires thermiques. Le dimensionnement des éléments de la centrale, tels que le champ solaire ou la cuve de stockage, est classiquement optimisé pour minimiser les coûts d'investissement tout en satisfaisant la demande en chaleur. En revanche, l'exploitation des centrales est souvent effectuée en utilisant des stratégies de contrôle standard, basées sur des règles heuristiques. Des contrôleurs, de plus en plus avancés, se chargent ensuite de suivre les trajectoires de contrôle standard. Il est cependant possible d'utiliser un objectif économique pour déterminer des trajectoires optimales, soit directement dans le contrôleur, soit en ajoutant un niveau supérieur d'optimisation. L'optimisation dynamique permet de déterminer des trajectoires optimales de fonctionnement, qui minimisent les coûts d'opération de la centrale sur un horizon de temps. Si cet horizon est suffisamment long, il permettra de bien gérer le stockage pour étendre la fourniture de chaleur solaire. Cela a rarement été testé dans la littérature pour une centrale solaire thermique mais plus fréquemment pour des centrales solaires à concentration pour la production d'électricité. Dans les différentes études publiées, l'optimisation dynamique a permis d'améliorer les performances énergétiques et économiques des centrales solaires par rapport à une stratégie de contrôle standard. Cependant cela nécessite de connaître les conditions météorologiques et la demande en chaleur en avance. Il est possible d'utiliser des prévisions pour cela mais elles peuvent contenir des erreurs qui conduiraient à un fonctionnement sous-optimal, voire impossible. Dès lors, l'optimisation dynamique en temps-réel (Dynamic Real-Time Optimization, DRTO) apparaît plus adaptée. En effet,

la DRTO permet de ré-optimiser régulièrement le fonctionnement d'un système en utilisant des mesures des perturbations et de l'état du système. Ainsi, le fonctionnement optimal s'adapte aux conditions environnementales variables. Le chapitre I présente les différentes manières d'implémenter la DRTO sur un système, en utilisant des exemples issus de différents domaines scientifiques, notamment le génie des procédés. En effet, cette méthodologie est très peu appliquée aux centrales solaires thermiques et n'a jamais été utilisée pour optimiser le fonctionnement de toute la centrale avec stockage. La possibilité d'utiliser deux niveaux d'optimisation, la planification et la DRTO, pour gérer deux problèmes d'optimisation avec des échelles de temps différentes et les connecter est aussi présentée. Cela est particulièrement adapté pour la gestion du stockage dans une centrale solaire thermique, bien que n'ayant jamais été étudié dans la littérature. En effet, anticiper les besoins de stockage et déstockage nécessite un horizon de temps plus long, et implique donc l'utilisation de prévisions peu précises et des temps de calcul longs. D'un autre côté, le problème de DRTO doit être résolu rapidement pour pouvoir l'implémenter en temps réel, et nécessite donc un horizon de temps court. Les prévisions utilisées seront alors plus précises mais la gestion du stockage pourrait être dégradée. C'est pourquoi la décomposition de l'optimisation du fonctionnement d'une centrale solaire thermique en plusieurs niveaux hiérarchiques est proposée dans ce chapitre.

Le chapitre II présente la méthodologie introduite dans le premier chapitre avec plus de détails et les résultats obtenus sur quelques cas d'étude simples. Les modèles utilisés pour représenter la centrale solaire thermique sont détaillés. Les caractériqtiques des deux problèmes d'optimisation à résoudre (planification et DRTO) sont énumérées: contraintes, fonction objectif économique, méthode de résolution. Idéalement, il faudrait tester la méthodologie sur le système réel afin de bénéficier de mesures pour connaître l'état du système et les perturbations. Comme cela n'était pas possible dans le cadre de cette thèse, un modèle détaillé d'équations est utilisé pour représenter la centrale réelle. Ce modèle de simulation fournit toutes les données de retour nécessaires à la méthodologie. Une étude simple a été réalisée dans un premier temps. La planification est faite sur deux jours, puis la DRTO est testée sur la première journée uniquement. Une nouvelle DRTO est relancée chaque heure, avec un horizon de temps jusqu'à la fin de la journée, qui se réduit donc d'une DRTO à l'autre. La demande en chaleur est considérée constante et parfaitement connue. En revanche, une perturbation artificielle est introduite sur le rayonnement solaire en temps-réel. Dans un premier temps, la connection entre la planification et la DRTO pour la gestion du stockage est étudiée. Le suivi de l'énergie stockée planifiée se fait dans la fonction objectif de la DRTO en minimisant l'écart entre l'énergie stockée planifiée et réelle à la fin de l'horizon de temps de la DRTO, ce qui correspond à la fin de la journée. Ce terme est affecté d'un poids dans la fonction objectif économique qui doit être ajusté afin d'obtenir le meilleur compromis entre le suivi de la planification et la minimisation des coûts d'exploitation de la journée. Une fois ce poids choisi, une étude de cas plus étendue a été menée. Les données météorologiques correspondant à 3 saisons différentes ont été utilisées et différentes pertubations en temps-réel ont été introduites dans le rayonnement solaire. Les performances de la centrale virtuelle utilisant les trajectoires optimales pour les débits déterminées par la DRTO sont comparées à celles de la centrale utilisant l'optimisation dynamique hors ligne (Dynamique optimisation, DO). Dans la majorité des cas d'étude, les coûts d'opération de la centrale ont été ré-

duits, grâce à la diminution de la consommation électrique mais aussi à une meilleure utilisation de l'énergie thermique qui conduit à une augmentation de la fraction solaire jusqu'à 35% par rapport à l'utilisation de la DO. Le suivi de l'énergie stockée planifiée est correct, avec une différence maximale de -14% entre l'énergie finale stockée dans les simulations avec la DRTO et celles avec la DO. Ce chapitre a montré que la DRTO connectée à une phase de planification permet d'adapter le fonctionnement optimal de la centrale solaire thermique aux perturbations et prévisions mises à jour tout en utilisant une bonne gestion du stockage determinée lors de la planification grâce à une meilleure vision stratégique.

Le chapitre III porte sur la modélisation en 1D de la cuve de stockage, qui est une partie essentielle de la centrale solaire thermique. Un stockage stratifié est particulièrement difficile à modéliser parce qu'il présente un très fort gradient de température dans la zone de la thermocline, qui sépare les zones chaude et froide. Le modèle utilisé doit donc être suffisamment précis pour représenter cette zone tout en conduisant à des temps de calcul raisonnables pour la simulation d'un système énergétique complet et son optimisation, particulièrement en temps-réel. Le modèle 1D le plus commun utilise les volumes finis pour discrétiser l'axe vertical de la cuve de stockage. Avec un faible nombre de strates, le profil de température obtenu est adouci autour de la thermocline par un effet appelé diffusion numérique (le gradient de température est réduit). Ainsi, le profil de température et l'énergie stockée ne sont pas bien estimés avec peu de strates. Cependant, avec un nombre de strates important, les temps de calcul deviennent trop long, en particulier pour l'optimisation. Dans ce chapitre, un autre schéma de discrétisation est proposé : la collocation orthogonale sur éléments finis. Ce schéma combine les avantages de la collocation orthogonale, qui ne nécessite pas beaucoup de points de discrétisation pour converger vers la solution, et ceux des volumes finis, dont la résolution est rapide grâce aux matrices creuses générées. Ce schéma permet d'obtenir une représentation précise du profil de température dans la cuve, et donc de l'énergie stockée, avec un temps de résolution inférieur à celui des volumes finis utilisés précédemment. Ce nouveau schéma a été validé avec des données réelles. Ensuite, une discussion sur la modélisation de la convection naturelle dans la cuve de stockage pour l'optimisation est présentée. Elle montre les difficultés de représenter ce phénomène grâce à un modèle continu, adapté à un problème d'optimisation.

Enfin, le chapitre IV présente les améliorations effectuées sur la méthodologie de DRTO présentée dans le chapitre II ainsi que des cas d'étude plus réalistes. Tout d'abord, le modèle de cuve de stockage utilisé dans le modèle détaillé représentant la centrale réelle a été modifié et est basé sur la collocation orthogonale sur éléments finis, comme présenté dans le chapitre précédent. En revanche, le modèle utilisé pour l'optimisation, bien que peu précis, a été conservé car il n'a pas été possible d'améliorer la précision sans trop augmenter les temps de calcul. Dans ce chapitre, la méthodologie est testée sur des simulations de 96 heures. La planification est effectuée au début, une fois pour toute la période. Ensuite, la DRTO est relancée toutes les six heures avec un horizon de temps glissant de 12 heures. Les cas d'étude sont plus réalistes que dans le Chapitre II, ils utilisent une demande en chaleur journalière variable et des données météorologiques réelles, à la fois pour les prévisions et les mesures en temps-réel. Plusieurs scénarios ont été considérés, en été et au printemps. L'objectif de cette partie est de déterminer quelle est la meilleure gestion du stockage à l'étape de DRTO. Pour cela, plusieurs fonctions objectif ont été testées avec différents termes

pour la gestion du stockage ajoutés à la partie économique. Les résultats montrent que si il n'y a aucun risque de surchauffe dans la centrale, ce qui est déterminé à l'étape de planification, alors maximiser l'énergie stockée à la fin de chaque DRTO permet de réduire les coûts d'opération en augmentant la fraction solaire. En revanche, si il y a un risque de surchauffe, suivre la planification, comme étudié dans le chapitre II, peut permettre d'éviter les surchauffes. En effet, la planification bénéficie d'une meilleure vision stratégique et peut donc anticiper les surchauffes. Ainsi, elle peut par exemple éviter de trop charger la cuve de stockage en prévision des périodes à fort ensoleillement et faible demande. Finalement, des conseils sur la gestion du stockage à l'étape de DRTO dans des scénarios variés ont pu être formulés.

Cette thèse montre que l'utilisation de la DRTO en association avec une phase de planification peut améliorer les performances économiques d'une centrale solaire thermique, par rapport à des stratégies de contrôle standard et à une optimisation dynamique hors ligne. La collocation orthogonale sur éléments finis permet de modéliser la cuve de stockage plus finement tout en réduisant les temps de calcul, ce qui permet d'améliorer les essais sur la méthodologie de DRTO développée. Enfin, des conseils sur la gestion du stockage à l'étape de DRTO, en fonction du risque de surchauffe et en utilisant la planification, sont formulés. Ce travail apporte d'intéressants résultats sur l'optimisation des systèmes énergétiques avec stockage d'énergie et qui évoluent dans des conditions environnementales variables et incertaines.

Contents

List of Figures

List of Tables

Introduction

Global warming is a threatening phenomenon for our planet, characterized by a general increase in the average surface temperature of the globe, caused by human activities. The emissions of greenhouse gases such as CO_2 and CH_4 by human activities are directly responsible for the climate change. They are due to the combustion of fossil fuels such as coal, oil and gas for energy production but also to agriculture and deforestation. The Intergovernmental Panel on Climate Change has noted an increase of 1.1°C in the global surface temperature for the period 2011-2020 compared to the pre-industrial period between 1850 and 1900 (Intergovernmental Panel on Climate Change; 2023). The increase in the surface temperature has numerous impacts on the ecosystems and natural equilibriums, such as melting of glaciers, rising of sea level, extreme meteorological phenomenons, ocean acidification, extinction of species, etc. Human kind will be affected in many ways if the temperature continues to increase: health hazards, crises related to food and water resources, migrations. Mitigating climate change should therefore be a priority in the next years for our societies. Most developed countries have been incorporating measures towards the reduction of CO_2 emissions in their policies in the last decades, but it has not been enough to reduce global warming. Hence, more restrictive agreements are necessary. In 2015, 193 countries (plus the European Union) signed the Paris agreement aiming at keeping global warming well below 2°C above the pre-industrial levels, and continuing the efforts to achieve a global warming below 1.5°C. In order to honor this commitment, the emissions of CO_2 should be reduced drastically, in all sectors of our societies. Figure 1a shows the distribution of the final energy consumption between its different forms. More than half of the final energy consumption in the world is in the form of heat, providing industrial process heat, space heating and domestic hot water (Collier; 2018). Around the globe, nearly half of the heat consumed is for industrial needs, including the production of steam, and the other half is dedicated to space and water heating as well as cooking. Figure 1b shows the distribution of various sources of energy used to produce the heat consumed in the world. Almost three quarters of the heat is produced by direct combustion of fossil fuels such as coal, oil and natural gas, largely contributing to the CO_2 emissions on the planet. Thus, shifting the heat production sources towards renewable sources is imperative.

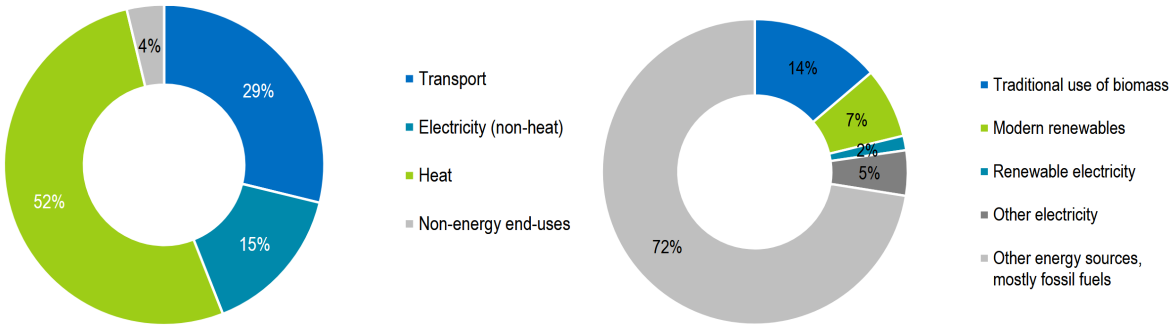

(a) Final energy consumption form (b) Energy consumption for heat

Figure 1: Heat in the energy consumption (data from 2015) (Collier; 2018)

In order to boost this change, the Revised Renewable Energy Directive fixed a target of 1.3% increase in the share of renewable energy for heating and cooling, for each state member of the European Union each year (Renewable Energy Directive; 2018).

Similar objectives are fixed locally around the world to reduce the share of fossil fuels in the heating sector. One way to produce heat with a renewable source is solar thermal energy, which is the focus of this thesis. Solar thermal energy is the heat transmitted to a heat transfer fluid by solar irradiation. Several collector technologies can be used to transform solar irradiation into heat at various levels of temperature, depending on the application (summarized in (Gil et al.; 2022) for example). In southern countries where the direct solar irradiation is high, concentrating solar collectors can be used to reach temperatures suitable for steam and electricity generation (Faninger; 2010). In this thesis, only low temperature heat production is considered. For domestic hot water or space heating, the required temperature is below 100°C. Individual solar thermal systems can be installed to provide solar heat for a house or a single building, using a few solar collectors. Solar district heating is a large scale application of solar thermal energy where the solar irradiation is collected in a solar field composed of many solar collectors and the heat produced feeds a District Heating Network (DHN) (Pauschinger; 2016). In a DHN, the heat is generated in a centralized heat production plant, such as a large solar thermal plant, and distributed through a network of insulated pipes in urban quarters, small communities or large cities. Both residential and commercial buildings can be connected to a DHN for space and water heating. Some industrial processes also require low temperature heat, such as pasteurization, drying, dehydration, and sterilization for the food and beverage industry and also paper and textile industries (Koçak et al.; 2020). Pre-heating of some higher temperature processes is also possible with solar thermal energy. Flat plate collectors and evacuated tube collectors are the most commonly used technologies for heat production at low temperature, collecting both direct and diffuse irradiation. The latter plays an important role for solar energy conversion in central and northern countries (Faninger; 2010). In this thesis, flat plate collectors will be considered. In 2009, experts evaluated that solar thermal energy only provides around 0.5% of the heating demand in the building sector, whereas the potential in the European Union is estimated around 47% of the overall low-temperature heat demand in 2050 (Weiss and Biermayr; 2009). It is thus necessary to accelerate the development of solar thermal energy. Figure 2 presents the global solar thermal capacity in operation each year from 2000 to 2020, along with the annual energy for glazed and unglazed water collectors. It shows that solar thermal energy has increased in terms of installed capacity and energy in the last two decades, even though the growth seems to slow down in the recent years. This is due to a slower increase in the installation of individual solar heaters. However, the number of large scale solar thermal plants for district heating and industrial process heat, which are the focus of this work, is in constant growth. The use of all installed solar thermal systems in 2020 saved 43.8 million tons of oil, corresponding to 141.3 million tons of CO_2 emissions avoided (Weiss and Spörk-Dür; 2021). This shows that solar thermal energy can greatly contribute to mitigate climate change. In this context, it is not only important to install more solar thermal systems but also to make the most of them.

A major downside of solar thermal energy, which has hindered its development, is the intermittency of solar irradiation. There are both seasonal and daily variations in the solar irradiation so the production of solar heat cannot be continuous. Yet, the heat consumption might be continuous in some industrial processes or might happen at times when no solar irradiation is available. In particular, space heating is necessary in winter, when solar irradiation is lower, and in the evenings when the sun goes down.

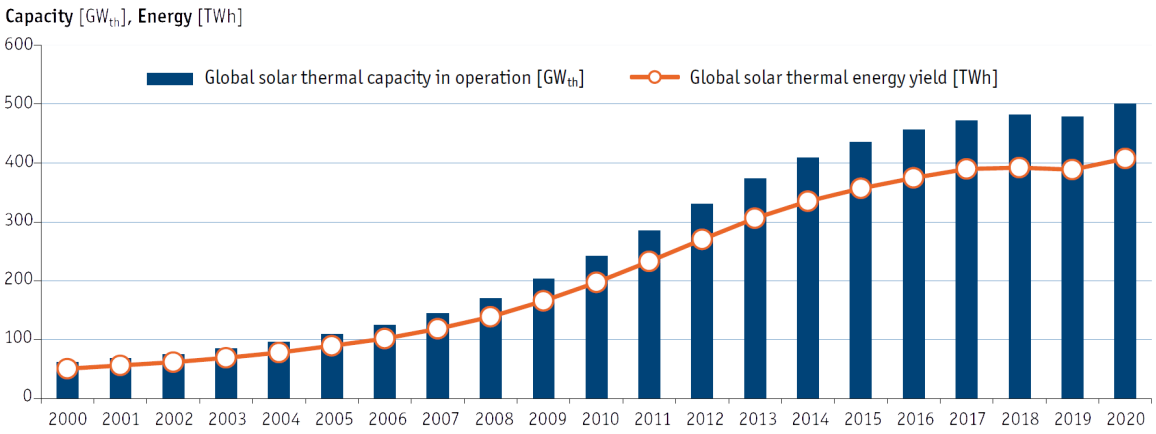

Figure 2: Global solar thermal capacity in operation and annual energy between 2000 and 2020 (Weiss and Spörk-Dür; 2021)

To overcome this issue, Thermal Energy Storage (TES) is usually used. Both long term (seasonal) and short term (daily) storage technologies exist. They allow to store the excess heat produced when the solar irradiation is high and the heat demand low, and then discharge the stored heat when needed. That way, solar heat can still be supplied, even when heat production and heat demand are not simultaneous. In this thesis, only short term storage is considered, in the form of a stratified water tank. Even with a TES, a back up burner is added to the solar thermal plant to make sure that the heat demand can be satisfied in any environmental conditions. Natural gas is generally chosen as the back up fuel because the burner can start rapidly. Adding a storage solution to the solar field improves the flexibility of the solar thermal plant but also complicates its operation. Indeed, there are several operational modes for the plant: direct heat supply, charge, discharge, shut down. In order to make an intelligent use of storage, the solar irradiation and heat demand in the next days should be known so that the necessary charge and discharge phases can be anticipated. Unfortunately, it is difficult to predict accurately the solar irradiation. Although the night and day cycle is well known in advance, the impact of the cloud cover on the solar irradiation throughout the day is much more difficult to estimate. Similarly, heat demand forecasts are uncertain, the real-time values can differ from the forecasted values. Therefore, the daily operation of a solar thermal plant, satisfying the heat demand and minimizing the operating costs, remains a challenge.

Given the various degrees of freedom in the system, mathematical optimization is particularly promising to achieve a better operation. With a fixed design for the system, that might have been optimized previously (Delubac et al.; 2023), the operation of the solar thermal plant can be optimized. The optimization could ensure a better use of thermal energy, leading to reduced operating costs and CO_2 emissions coming from the gas back up burner and the electric pumps in the solar thermal plant. Since both the heat source and demand are time varying, dynamic optimization is more suitable than static optimization. Indeed, it will compute optimal trajectories for the decision variables over a time horizon, taking into account the dynamic behavior of the system (Biegler and Grossmann; 2004). In a previous PhD thesis conducted at LaTEP, the dynamic optimization of the operation of a solar thermal plant over 5 days

in summer was carried out (Scolan; 2020). It achieved an improved use of storage, a reduced electricity consumption and reduced operating costs for the period tested, compared to standard operating strategies determined by logic control rules. However, the trajectories obtained from dynamic optimization were not tested in real-time on the real system or a virtual plant representing the real system. Thus, the weather and load forecasts used for optimization were never compared to the real values. In order to optimize such a system operating in uncertain conditions, Dynamic Real-Time Optimization (DRTO) is more suitable (Kadam et al.; 2002). In this optimization scheme, the trajectories obtained from dynamic optimization are regularly updated. The real system provides some feedback to the optimization algorithm in the form of measurements of some state variables and disturbances. A new optimization starts with the actual system state and disturbances as initial conditions, as well as updated forecasts. DRTO is thus able to adapt the optimal operation of the system to the actual environmental conditions. In a solar thermal plant, not all the elements vary on the same time scale. For example, the temperature in the solar field can vary in a few seconds if a cloud impacts the solar irradiation, while the stored energy in the storage tank varies slowly throughout the day. As suggested in (Gil et al.; 2022), a hierarchical optimization framework could deal with optimization objectives of different time scales. That way, the storage management could be planned on a slower time scale and a long time horizon providing a good strategic vision, while the daily operation of the plant could be optimized more frequently and over a shorter time horizon, using more accurate forecasts.

The main objective of the thesis is to develop a DRTO methodology for a solar thermal plant, following the work conducted in (Scolan; 2020). The methodology developed should be able to adapt the optimal operation to the current disturbances, thus correcting errors in forecasts. Moreover, it should also make the best use of storage, which might require a longer term strategic vision. The methodology should ideally be tested and validated on a real operating plant. However, because such plant and associated data were not available yet, it was chosen to apply the methodology to a virtual plant. This one is a knowledge-based model, with fast numerical solving, representing the real plant, and for which all relevant data can be collected. LaTEP has experience in dynamic optimization of energy systems and a collaboration with the research group of Professor Galo Antonio Carillo Le Roux, from the University of São Paulo, has been initiated to benefit from his experience with real-time optimization. Moreover, a collaboration with the French company NEWHEAT, specialized in solar heat, was established. The thesis is composed of four chapters, corresponding to four journal papers, describing the development of the methodology, the choices made, and the results obtained.

Chapter I presents the state of the art on the optimization of the operation of solar thermal plants. An analysis of the system characteristics is conducted to show the potential of DRTO to improve the operation of solar thermal plants. A literature review on real-time optimization is then carried out, with a focus on DRTO, using papers from various fields, mostly in chemical engineering. Adaptations on the typical DRTO framework are presented, including the incorporation of a planning phase. Then, perspectives on the application of DRTO to solar thermal plants are provided, with the use of a planning phase to improve storage management. The methodology described in this chapter presents the main characteristics of the methodology further developed

in this thesis.

Chapter II presents the DRTO methodology developed and its first testing. The model used to represent the solar thermal plant in the optimization algorithm and the virtual plant for online testing is presented. The DRTO methodology is described, following the suggestions from Chapter I. A simple case study, with an online testing for only one day is then carried out. Artificial test data are used for the weather and heat demand. A comparison between DRTO and offline dynamic optimization is conducted to show the potential of DRTO to improve the solar thermal plant operation.

Chapter III is a focus on the storage tank modeling. Indeed, the storage tank is an important part of the solar thermal plant and the accuracy of the model used for its representation has a direct impact on the optimized solar thermal plant performances. Unfortunately, an accurate model for the storage tank requires long computational times. This chapter presents an alternative to the traditional 1D solution strategy using finite volumes. Orthogonal Collocation on Finite Elements (OCFE) is explained and the performances of the new solution strategy are compared to the ones of the original solution strategy which was using finite volumes for spatial discretization. The OCFE model is validated using experimental data. Finally, perspectives on natural convection modeling in an optimization framework are discussed.

Chapter IV presents a more realistic testing of the DRTO methodology developed. The virtual plant model used for the online testing is improved with the storage tank model presented in Chapter III. Several scenarios are used in case studies. The data used for the weather forecasts and real-time measurements are real data. The heat demand is variable. The testing is carried out for 96 hours, and the DRTO uses a rolling time horizon. The incorporation of storage management into the DRTO methodology is tested and discussed. The results for the case studies are analyzed and guidelines for the optimal operation of a solar thermal plant are formulated in two distinct cases: when there is a risk of overheating in the plant and when there is no risk.

Introduction [français]

Le réchauffement climatique est caractérisé par l'augmentation de la température globale à la surface du globe due aux activités humaines, et met en péril notre planète. Les émissions de gaz à effet de serre, tels que le CO_2 et le CH_4, sont directement responsables du dérèglement climatique. Les principales sources d'émissions sont la combustion de combustibles fossiles, tels que le charbon, le pétrole et le gaz naturel, pour la production d'énergie. L'agriculture et la déforestation participent également à ces émissions. Le Groupe d'experts Intergouvernemental sur l'Evolution du Climat (GIEC) a constaté une augmentation de la température de surface globale de 1,1°C sur la période de 2011 à 2020 comparée à l'époque pré-industrielle entre 1850 et 1900 (Intergovernmental Panel on Climate Change; 2023). L'augmentation de la température de surface du globe a de nombreux effets néfastes sur les écosystèmes et les équilibres naturels tels que la fonte des glaciers, l'augmentation du niveau des mers, l'acidification des océans, des phénomènes météorologiques extrêmes plus fréquents, l'extinction d'espèces, etc. Le réchauffement climatique impactera aussi l'espère humaine si la température globale continue d'augmenter, avec des risques sur la santé, des crises liées aux ressources alimentaires et en eau ou encore des migrations climatiques. Limiter le réchauffement climatique est donc un enjeu prioritaire des prochaines années. La plupart des pays développés ont déjà mis en place des mesures pour réduire les émissions de CO_2 mais cela n'a pas suffit à endiguer le réchauffement climatique. Des mesures plus restrictives sont donc nécessaires. En 2015, 193 pays (et l'Union Européenne) ont signé les accords de Paris, qui visent à maintenir l'augmentation de la température bien en-dessous de 2°C par rapport au niveau pré-industriel et à poursuivre les efforts pour limiter l'augmentation à 1.5°C. Afin d'honorer cet engagement, les émissions de CO_2 doivent être réduites drastiquement dans tous les secteurs de nos sociétés. La Figure 3a montre la part des différentes formes d'énergie dans la consommation finale d'énergie dans le monde. Plus de la moitié de la consommation finale d'énergie est sous la forme de chaleur, qui peut être utilisée pour des procédés industriels, le chauffage des bâtiments et la production d'eau chaude sanitaire (Collier; 2018). Au niveau mondial, environ la moitié de la chaleur consommée répond aux besoins de l'industrie, dont la production de vapeur, tandis que l'autre moitié est utilisée pour le chauffage des locaux et de l'eau ainsi que pour la cuisine. La Figure 3b montre la répartition des sources d'énergie utilisées pour la production de chaleur dans le monde. Presque les trois quarts de la chaleur produite reposent sur l'utilisation de combustibles fossiles, ce qui contribue largement aux émissions de CO_2 sur la planète. Par conséquent, il est impératif de remplacer les combustibles fossiles par des sources renouvelables pour la production de chaleur.

Afin d'encourager cette transition énergétique, la directive révisée sur les énergies renouvelables a fixé un objectif de 1,3% d'augmentation de la part d'énergies renouvelables pour la production de chaleur et de froid, chaque année, pour chaque membre de l'Union Européenne (Renewable Energy Directive; 2018). Des objectifs similaires ont été fixés dans différentes régions du monde afin de réduire la part de combustibles fossiles dans la production de chaleur. L'énergie solaire thermique constitue un moyen de produire de la chaleur renouvelable, en chauffant un fluide caloporteur grâce au rayonnement solaire. Il s'agit du sujet d'étude de cette thèse. Différents capteurs solaires peuvent être utilisés pour collecter le rayonnement solaire et le transformer en

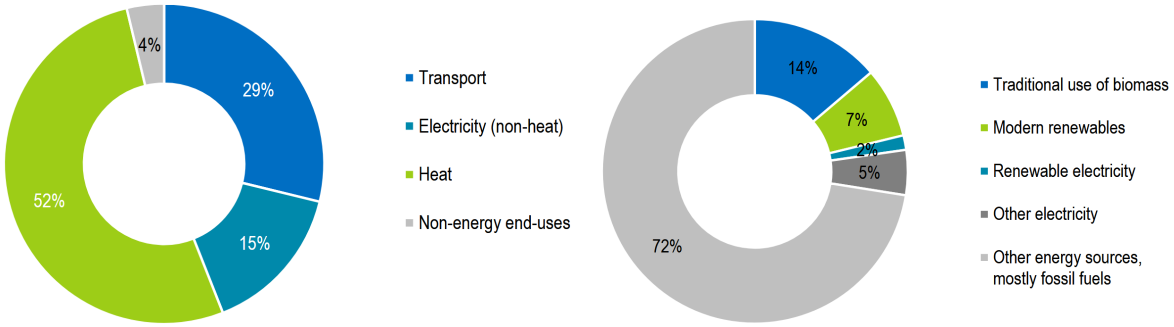

(a) Formes d'énergie dans la consommation finale

(b) Sources d'énergie pour la production de chaleur

Figure 3: La place de la chaleur dans la consommation d'énergie (données de 2015) (Collier; 2018)

chaleur en fonction de l'application visée et de la température souhaitée (les différents capteurs et leurs applications sont présentés dans (Gil et al.; 2022) par exemple). Dans les pays où le rayonnement direct est particulièrement fort, proche de l'équateur, des capteurs solaires à concentration peuvent être utilisés pour atteindre des températures suffisamment élevées pour la production de vapeur et la génération d'électricité (Faninger; 2010). Dans cette thèse, uniquement la chaleur à basse température est étudiée. La production d'eau chaude sanitaire et le chauffage des locaux nécessitent une température inférieure à 100°C. Des systèmes solaires thermiques individuels peuvent être installés pour fournir de la chaleur à une maison ou un bâtiment en utilisant seulement quelques capteurs. Le rayonnement solaire peut également être collecté dans un champ solaire, composé de nombreux capteurs, pour produire de la chaleur pour un réseau de chaleur urbain (RCU) (Pauschinger; 2016), ce qui constitue une utilisation à grande échelle de l'énergie solaire thermique. Dans un RCU, la chaleur est produite de manière centralisée dans une centrale de production, telle qu'une centrale solaire thermique, puis distribuée dans des quartiers, petites communautés ou villes grâce à un réseau de canalisations isolées thermiquement. Les consommateurs de chaleur du RCU sont des bâtiments résidentiels ou commerciaux, qui ont besoin de chauffage et d'eau chaude sanitaire. L'énergie solaire thermique peut aussi alimenter en chaleur des procédés industriels à basse température tels que la pasteurisation, le séchage, la déshydratation ou encore la stérilisation, pour l'industrie agroalimentaire, l'industrie textile ou du papier (Koçak et al.; 2020). L'énergie solaire thermique peut également servir à préchauffer un procédé industriel à haute température. Pour la production de chaleur solaire à basse température, les technologies de capteurs couramment utilisées sont les capteurs plans et les capteurs à tubes sous vide, qui collectent les rayonnements direct et diffus. Dans les pays éloignés de l'équateur, le rayonnement diffus est important et participe largement à la production de chaleur solaire (Faninger; 2010). Dans cette thèse, des capteurs plans seront considérés. En 2009, un groupe d'experts a évalué que l'énergie solaire thermique couvrait seulement environ 0,5% de la demande en chaleur du secteur du batiment, alors que le potentiel du solaire thermique dans l'Union Européenne est estimé à 47% de la demande en chaleur globale à basse température en 2050 (Weiss and Biermayr; 2009). Il est donc nécessaire d'accélérer le développement de l'énergie solaire thermique. La Figure 4 présente la capacité des installations so-

laires thermiques en opération chaque année entre 2000 et 2020 ainsi que l'énergie annuelle correspondante pour les capteurs vitrés et non vitrés fonctionnant avec de l'eau comme fluide caloporteur. Cette figure montre que la capacité ainsi que l'énergie produite ont fortement augmenté au cours des deux dernières décennies, bien que la croissance ait légèrement ralenti ces dernières années. Cela est dû à un ralentissement dans l'installation de nouveaux systèmes solaires thermiques individuels. En revanche, le nombre d'installations à grande échelle pour les RCU et industries, qui sont étudiées dans cette thèse, est en augmentation constante. L'utilisation de tous les systèmes solaires thermiques installés en 2020 a permis d'économiser 43,8 millions de tonnes de pétrole, ce qui corresponds à 141,3 millions de tonnes de CO_2 émis évitées (Weiss and Spörk-Dür; 2021). Cela montre que l'énergie solaire thermique peut jouer un rôle important dans la transition énergétique pour réduire le réchauffement climatique. Dans ce contexte, il est important d'installer de nouveaux systèmes solaires thermiques mais également d'en tirer le meilleur parti en améliorant leur utilisation.

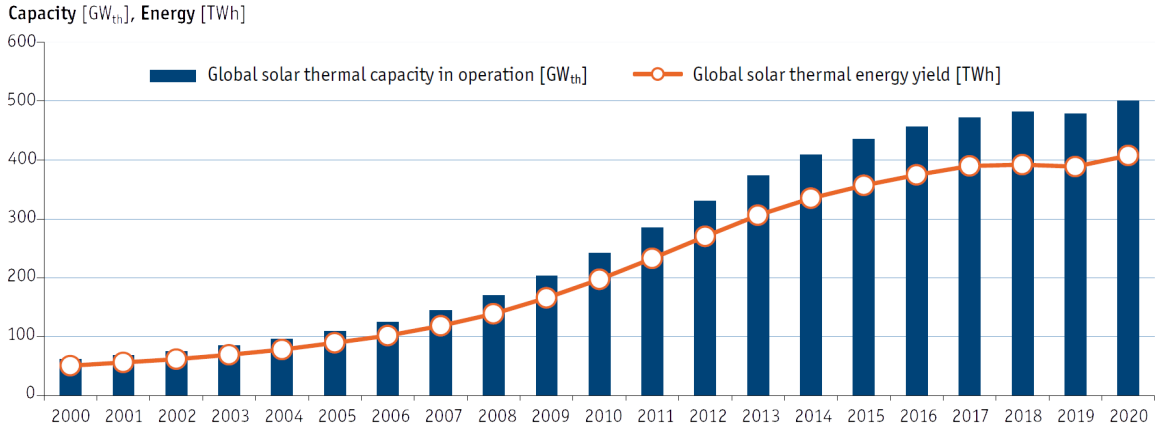

Figure 4: Capacité globale des installations solaires thermiques en opération et énergie annuelle correspondante entre 2000 et 2020 (Weiss and Spörk-Dür; 2021)

L'inconvénient majeur de l'énergie solaire thermique, qui a freiné son développement, est l'intermittence du rayonnement solaire. Il existe des variations journalières et saisonnières dans le rayonnement solaire, la production de chaleur solaire ne peut donc pas être continue. Pourtant, la demande en chaleur peut être continue dans certains procédés industriels ou bien être importante à des moments où le rayonnement solaire est faible. Par exemple, le besoin en chauffage est important en hiver alors que le rayonnement solaire est faible en cette saison. Ou encore, le besoin en chaleur du secteur résidentiel est plus important en soirée, lorsque le soleil se couche. Pour pallier ce problème, un stockage thermique est généralement employé. Il existe des technologies de stockage à long terme (saisonnier) ou à court terme (journalier). Le stockage permet de stocker l'excès de chaleur produite lorsque le rayonnement solaire est important et la demande en chaleur faible pour ensuite déstocker la chaleur quand c'est nécessaire. Ainsi, de la chaleur solaire peut être fournie même lorsque la production et la consommation de chaleur ne sont pas simultanées. Dans cette thèse, seul le stockage court terme est étudié, sous la forme d'une cuve de stockage d'eau stratifiée. Malgré l'utilisation d'un stockage thermique, une chaudière d'appoint est ajoutée à la centrale solaire thermique afin d'assurer la satisfaction de la demande en chaleur quelles que soient les conditions météorologiques. Le gaz naturel est généralement choisi comme

combustible de la chaudière d'appoint car il permet un démarrage rapide. Ajouter une solution de stockage thermique au champ solaire permet d'améliorer la flexibilité de la centrale solaire thermique mais cela rend son exploitation plus complexe. En effet, il existe plusieurs modes de fonctionnement dans la centrale : fourniture directe de chaleur, stockage, déstockage ou encore arrêt complet. La connaissance du rayonnement solaire et de la demande en chaleur des prochains jours est nécessaire pour utiliser intelligemment le stockage thermique. Ainsi, les phases de stockage et déstockage nécessaires pourraient être anticipées. Malheureusement, il est difficile de prévoir le rayonnement solaire précisément. Bien que les cycles de nuit et jour soient connus à l'avance, l'impact de la couverture nuageuse sur le rayonnement solaire au cours de la journée est bien plus difficile à estimer. De la même façon, la demande en chaleur n'est pas connue parfaitement en avance, et la demande réelle peut être différente de celle prévue. L'exploitation quotidienne d'une centrale solaire thermique satisfaisant la demande en chaleur tout en minimisant les coûts d'exploitation, reste donc un défi.

Au vu des nombreux degrés de liberté dans l'exploitation de la centrale solaire thermique, l'optimisation mathématique est particulièrement prometteuse pour améliorer le fonctionnement du système. Avec un dimensionnement du système fixé, qui a pu être optimisé précédemment (Delubac et al.; 2023), le fonctionnement de la centrale solaire thermique peut être optimisé. L'optimisation pourrait permettre une meilleure utilisation de l'énergie thermique, conduisant à une réduction des coûts d'exploitation et des émissions de CO_2 provenant de la chaudière d'appoint fonctionnant au gaz et des pompes électriques permettant le fonctionnement de la centrale. Puisque la source et la consommation d'énergie sont toutes deux variables dans le temps, l'optimisation dynamique semble plus adaptée que l'optimisation statique. En effet, cela permet de calculer des trajectoires optimales pour les variables de décision sur un horizon de temps, en prenant en compte le comportement dynamique du système (Biegler and Grossmann; 2004). Dans une thèse menée précédemment au LaTEP, l'optimisation dynamique de l'exploitation d'une centrale solaire thermique sur 5 jours en été a été étudiée (Scolan; 2020). Cela a permis une meilleure utilisation du stockage thermique et une réduction de la consommation électrique et des coûts d'exploitation sur la période testée, en comparaison à l'utilisation de stratégies de fonctionnement standard basées sur des règles de contrôle issues de l'expérience des opérateurs et ingénieurs. Cependant, les trajectoires obtenues avec l'optimisation dynamique n'ont pas été testées en temps-réel sur la centrale solaire réelle ou bien une représentation numérique de celle-ci. Ainsi, les prévisions météorologiques et de demande en chaleur utilisées pour l'optimisation n'ont pas été comparées avec les valeurs réelles. Pour optimiser un système évoluant dans un environnement incertain, l'optimisation dynamique en temps-réel (Dynamic Real-Time Optimization, DRTO) est plus adaptée (Kadam et al.; 2002). Dans ce schéma d'optimisation, les trajectoires obtenues grâce à l'optimisation dynamique sont régulièrement mises à jour. Le système réel fournit un retour à l'algorithme d'optimisation grâce à des mesures des variables d'état et des perturbations. Une nouvelle optimisation commence donc avec des conditions initiales déduites des mesures effectuées ainsi qu'avec des prévisions mises à jour et plus précises. Ainsi, la DRTO est capable d'adapter le fonctionnement optimal d'un système aux conditions environnementales en temps-réel. Dans une centrale solaire thermique, l'état des différents éléments qui la composent ne varie pas à la même échelle de temps. Par exemple, la température dans le champ solaire peut varier en quelques secondes à cause du pas-

sage d'un nuage qui impacte le rayonnement solaire reçu tandis que l'énergie stockée dans la cuve de stockage varie lentement au cours de la journée. Comme suggéré dans (Gil et al.; 2022), une structure hiérarchique d'optimisation peut permettre de gérer plusieurs objectifs à différentes échelles de temps. Ainsi, la gestion du stockage pourrait être planifiée avec une échelle de temps longue et un horizon de temps suffisamment long pour bénéficier d'une bonne vision stratégique. L'exploitation quotidienne de la centrale solaire thermique pourrait quant à elle être optimisée plus régulièrement sur un horizon de temps court en utilisant des prévisions plus précises.

L'objectif principal de cette thèse est de développer une méthodologie de DRTO pour une centrale solaire thermique, suite aux travaux menés par Simon Scolan dans sa thèse (Scolan; 2020). La méthodologie développée doit être capable d'adapter le fonctionnement optimal de la centrale aux perturbations réelles, corrigeant ainsi les erreurs dans les prévisions. De plus, elle doit utiliser au mieux le stockage thermique, ce qui pourrait nécessiter une vision stratégique à plus long terme. La méthodologie devrait idéalement être testée et validée sur un système réel en fonctionnement. Cependant, comme une telle centrale et les données associées n'étaient pas disponibles pour ce travail, il a été décidé d'appliquer la méthodologie à une centrale virtuelle. Il s'agit d'un modèle de connaissances avec une résolution numérique rapide qui représente la centrale réelle et sur lequel toutes les données souhaitées peuvent être collectées. Le LaTEP a de l'expérience sur l'optimisation dynamique des systèmes énergétiques. Une collaboration avec le professeur Galo Antonio Carillo Le Roux, de l'Université de São Paulo, a été mise en place pour bénéficier de son expertise sur l'optimisation en temps-réel. De plus, un partenariat avec l'entreprise française NEWHEAT, spécialiste des centrales solaires thermiques, a été établi. La thèse comporte quatre chapitres, qui sont quatre articles de journaux, décrivant la méthodologie développée, les choix effectués et les résultats obtenus.

Le chapitre I présente l'état de l'art sur l'optimisation du fonctionnement des centrales solaires thermiques. Une analyse des caractéristiques du système étudié est menée pour montrer le potentiel de la DRTO pour améliorer l'exploitation des centrales solaires thermiques. La littérature sur l'optimisation en temps-réel et la DRTO en particulier, est examinée. Les articles proviennent de domaines d'étude variés, notamment le génie des procédés. Des adaptions au schéma de DRTO classiques sont ensuite présentées, en particulier l'utilisation d'une étape de planification dans la méthodologie. Des perspectives sur l'application de la DRTO aux centrales solaires thermiques sont détaillées par la suite, avec l'incorporation d'une étape de planification à la méthodologie pour améliorer la gestion du stockage. Ce chapitre permet de positionner ces travaux de thèse dans la littérature actuelle. La méthodologie décrite dans la fin de ce chapitre va ensuite être dévelopée dans les chapitres suivants.

Le chapitre II présente la méthodologie de DRTO développée et les premiers resultats obtenus sur des cas d'étude simples. Le modèle numérique utilisé pour représenter la centrale solaire thermique dans l'algorithme d'optimisation et la centrale virtuelle créée pour les essais sur la méthodologie sont présentés. La méthodologie de DRTO est ensuite décrite en détails, suivant les suggestions formulées dans le chapitre précédent. Des cas d'étude simples sont testés par la suite en temps-réel pour une journée seulement. Les données utilisées pour les conditions météorologiques et la demande en chaleur sont des données artificielles pour tester la méthodologie. Les résultats obtenus

sur la centrale virtuelle utilisant la DRTO sont comparés à des résultats obtenus avec une optimisation dynamique hors ligne. Les résultats montrent le potentiel de la DRTO pour améliorer l'exploitation des centrales solaires thermiques.

Le chapitre III se concentre sur la modélisation de la cuve de stockage. En effet, la cuve de stockage est un élément important de la centrale solaire thermique et la précision du modèle utilisé pour sa représentation a un impact direct sur les performances optimisées de la centrale. Malheureusement, l'utilisation d'un modèle précis pour représenter la cuve de stockage engendre des temps de calcul longs. Ce chapitre présente une alternative à la stratégie de résolution traditionnelle en 1D basée sur les volumes finis. La collocation orthogonale sur éléments finis (Orthogonal Collocation on Finite Elements, OCFE) est expliquée et les performances de ce schéma de discrétisation spatiale sont comparées à la stratégie de résolution classique utilisant les volumes finis. La solution avec l'OCFE est validée grâce à des données expérimentales. Enfin, des perspectives sur la modélisation de la convection naturelle dans une étude d'optimisation sont discutées.

Le chapitre IV présente des essais plus réalistes de la méthodologie de DRTO développée. Le modèle de cuve de stockage utilisé dans la centrale virtuelle pour tester la méthodologie a été amélioré suivant la méthode proposée dans le chapitre III. Ensuite, plusieurs scénarios ont été considérés dans l'étude de cas. Les données utilisées pour les prévisions et les mesures météorologiques en temp-réel sont des données réelles. La demande en chaleur est variable. Les tests sont menés sur 96 heures, et la DRTO utilise un horizon de temps glissant. La gestion du stockage dans la méthodologie de DRTO est étudiée, en utilisant les résultats issus de la planification. Les résultats pour les différents cas d'étude sont analysés et des lignes directrices pour la conduite optimale des centrales solaires thermiques sont formulées dans deux cas distincts : lorsqu'il y a un risque de surchauffe dans la centrale et lorsqu'il n'y en a pas.

Bibliography

Biegler, L. T. and Grossmann, I. E. (2004). Retrospective on optimization, *Computers & Chemical Engineering* **28**: 1169–1192.

Collier, U. (2018). Renewable Heat Policies - Delivering clean heat solutions for the energy transition, *Insights Series 2018 - International Energy Agency* .

Delubac, R., Sadr, M., Sochard, S., Serra, S. and Reneaume, J.-M. (2023). Optimized Operation and Sizing of Solar District Heating Networks with Small Daily Storage, *Energies* **16**(3): 1335.

Faninger, G. (2010). Potential of Solar Thermal Technologies1, *International Energy Agency, Solar Heating & Cooling Program* .

Gil, J. D., Topa, A., Álvarez, J., Torres, J. and Pérez, M. (2022). A review from design to control of solar systems for supplying heat in industrial process applications, *Renewable and Sustainable Energy Reviews* **163**: 112461.

Intergovernmental Panel on Climate Change (2023). Synthesis report, *6th Assessment Report (AR6)* .

Kadam, J. V., Schlegel, M., Marquardt, W., Tousain, R. L., Van Hessem, D. H., Van Den Berg, J. and Bosgra, O. H. (2002). A Two-Level Strategy of Integrated Dynamic Optimization and Control of Industrial Processes - a Case Study, *European Symposium on Computer Aided Process Engineering*, Vol. 12, Elsevier, The Hague, The Netherlands, pp. 511–516.

Koçak, B., Fernandez, A. I. and Paksoy, H. (2020). Review on sensible thermal energy storage for industrial solar applications and sustainability aspects, *Solar Energy* **209**: 135–169.

Pauschinger, T. (2016). Solar thermal energy for district heating, *Advanced District Heating and Cooling (DHC) Systems*, Elsevier, pp. 99–120.

Renewable Energy Directive (2018). Directive (EU) 2018/2001 of the European Parliament and of the Council of 11 December 2018 on the promotion of the use of energy from renewable sources, *OJ* **L328/82**.

Scolan, S. (2020). *Développement d'un outil de simulation et d'optimisation dynamique d'une centrale solaire thermique.*, thesis, Pau. Publication Title: http://www.theses.fr.

Weiss, W. and Biermayr, P. (2009). Potential of solar thermal in europe, *ESTIF* .

Weiss, W. and Spörk-Dür, M. (2021). Global Market Development and Trends in 2020 Detailed Market Data 2019, *Solar Heating and Cooling Programme - International Energy Agency* .

Chapter I

State of the art on solar thermal plants optimization

Contents

The introduction highlighted the potential of solar thermal energy to reduce the CO_2 emissions resulting from heat production. It also described the challenges associated with the operation of a solar thermal plant with storage, mostly due to the varying environmental conditions. As a promising solution to better operate such systems, mathematical optimization was introduced.

This chapter is a review article, published in *Solar Energy*, presenting the state of the art on the optimization of the operation of solar thermal plants (Untrau et al.; 2022). The system characteristics and its modeling are described. An analysis of the different optimization methodologies, especially those in real-time, is conducted. Details are provided on Dynamic Real-Time Optimization (DRTO) for solar systems as well as other applications in the field of chemical engineering and energy. Adaptations of the two-layer DRTO scheme, which includes the control layer, are presented, especially the coupling of DRTO with a planning phase. Then, the drawbacks and advantages of the different real-time optimization methodologies are discussed. Finally, perspectives on the application of Dynamic Real-Time Optimization to solar thermal plants are provided as it seems particularly suitable for such systems. The use of a planning phase to improve storage management is suggested. This chapter highlights the lack of studies on the DRTO applied to solar thermal plants and the potential of the methodology to improve the economic performances of such plants. It justifies the work carried out in the next chapters of the thesis. It also provides the general characteristics of the DRTO methodology developed in this thesis.

Article reference:

Untrau, A., Sochard, S., Marias, F., Reneaume, J.-M., Le Roux, G. A. and Serra, S. (2022). Analysis and future perspectives for the application of Dynamic Real-Time Optimization to solar thermal plants: A review, *Solar Energy* **241:** 275-291.

Analysis and Future Perspectives for the Application of Dynamic Real-Time Optimization to Solar Thermal Plants: A Review

Alix Untrau[a], Sabine Sochard[b], Frédéric Marias[c], Jean-Michel Reneaume[d], Galo A.C. Le Roux [e] and Sylvain Serra[f*]

[a,b,c,d,f] Universite de Pau et des Pays de l'Adour, E2S UPPA, LaTEP, Pau, France,

[*] sylvain.serra@univ-pau.fr

[e] Universidade de São Paulo, Escola Politécnica, São Paulo, Brazil

Published in *Solar Energy*, **241** (2022) 275-291

Abstract

This review provides a deep analysis of the different methodologies to improve the operation of solar thermal plants based on mathematical optimization. The various schemes found in the literature to determine the optimal operational strategy are classified depending on two criteria: time dependence (static or dynamic) and with feedback or not from the plant (real-time or offline). This review shows that offline dynamic optimization is performed on solar thermal plants in research papers but highlights the lack of real-time optimization studies. The analysis work conducted in this review, based on studies of the operation of solar systems but also on process engineering research articles, shows that dynamic real-time optimization seems capable of handling the intermittency of the solar radiation and well suited to improve the operation of a solar thermal plant. Indeed, the daily and seasonal variations of weather and heat demand associated with the uncertainty of their forecasts make the operation of such systems very challenging. This paper details the different ways to implement Dynamic Real-Time Optimization, and the possible improvements to the classical scheme. Perspectives on the application of Dynamic Real-Time Optimization in association with a planning phase to plan a smart use of storage are described. Although it has not been studied in depth in the literature, the Dynamic Real-Time Optimization of a solar thermal plant including storage should be investigated in order to maximize the benefits from the heat sold, extend the time period where the heat demand is met and reduce the consumption of back up fossil fuels.

Nomenclature

Abbreviations

ANN	Artificial Neural Network
BOA	Butterfly Optimization Algorithm
CSP	Concentrated Solar Power
DAE	Differential Algebraic Equations
DHN	District Heating Network
DRTO	Dynamic Real-time optimization
EMPC	Economic Model Predictive Control
FHI	Flexible Heat Integration
GA	Genetic Algorithm
HTF	Heat Transfer Fluid
ISCC	Integrated Solar Combined Cycle
MILP	Mixed-Integer Linear Programming
MPC	Model Predictive Control
NCO	Necessary Conditions of Optimality
PDE	Partial Differential Equations
PID	Proportional Integral Derivative
PSO	Particle Swarm Optimization
RTO	Real-time optimization
SRTO	Static Real-time optimization
TES	Thermal Energy Storage

Symbols

d	Disturbance
p	Parameter involved in the optimization
u	Vector of controlled variables
y	Vector of algebraic state variables
z	Vector of differential state variables

Subscripts

m	Measure of the variable
ref	Reference set-point or trajectory for the variable

I.1 Introduction

More than half of the final energy consumption in the world is in the form of heat (Collier; 2018). The production of heat contributes greatly to the global CO_2 emissions on the planet. Solar thermal energy uses a renewable source, the sun, to produce heat with very low greenhouse gases rejection while operating. According to the International Energy Agency, the use of all the installed solar thermal systems for heat production in 2020 led to savings of 43.8 million tons of oil and 141.3 million tons of CO_2 (Weiss and Spörk-Dür; 2021). Therefore, solar thermal energy acts as a good replacement for fossil fuels used for heat production in various applications and is a key element of a good energy transition.

In 2015, 196 countries signed the Paris Agreement which aims to limit global warming to well below 2°C and to pursue efforts to limit it to 1.5°C compared to pre-industrial levels (United Nations Framework Convention on Climate Change; 2015). Targets are fixed locally for the various sectors of greenhouse gases emissions. In Europe, the Revised Renewable Energy Directive (Renewable Energy Directive; 2018) fixed the target of a 1.3 % increase each year in the share of renewable energy for heating and cooling for every member state. In France, the Energy Transition Law for Green Growth (Loi de transition énergétique pour la croissance verte), adopted in 2015, aims at reaching 38 % of renewable heat in the final heat consumption of the country in 2030 (Loi française; 2015). Similar objectives are fixed in many countries around the world in order to reduce CO_2 emissions and mitigate climate change. In this context, developing efficient solar thermal plants and making the most out of them, through mathematical optimization for example, is crucial to achieve the objectives.

Optimization can be applied to the design of a solar thermal system, in order to size the elements and choose the layout of the process in a way that maximizes revenues while keeping the investments low. It can also be used to determine the best operation

strategies given a fixed design for the system. The optimization of the operation of a solar thermal plant including storage is the focus of this work.

It is worth mentioning that heat production for domestic or industrial use is only one purpose of solar thermal plants. Systems with concentration can achieve temperatures high enough for steam and electricity generation and are referred to as Concentrated Solar Power (CSP) plants. This review aims at providing solutions to improve solar heat production for domestic and industrial use. Nevertheless, heat is produced and stored in a solar thermal plant, regardless of the technology used or the final utilization of the heat generated. For this reason, both concentrating and non-concentrating solar thermal plants are considered in this paper, as long as the studies are focused on the solar field operation and storage management. Furthermore, the methodologies described in this paper could benefit to all types of solar thermal plants.

Figure I.1 presents the cumulated capacity in operation at the end of 2020, and the energy supplied that year, for solar thermal heat and other renewable energy technologies, including solar thermal power. This diagram shows that solar thermal plants for heat production are already an established technology for renewable energy production. The total collector area in the world is 715 million square meters and China is leading the market, with 48 % of the installed collector area for large-scale systems (Weiss and Spörk-Dür; 2021).

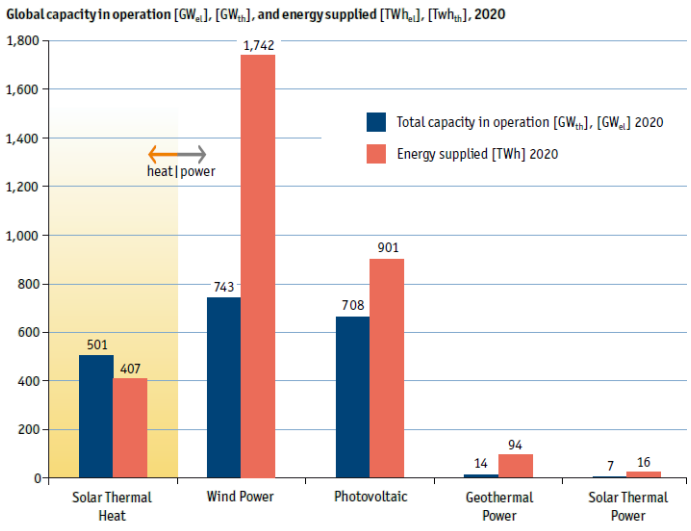

Figure I.1: Global capacity and energy supplied for solar thermal and other renewable energy technologies (Weiss and Spörk-Dür; 2021)

In a solar energy system, both the energy source and demand are time-varying. Thus, it is difficult to find the best operational strategy ensuring best economical performance of the system. A steady-state set point optimization, computing a constant value for the decision variables, would not be able to ensure optimal operation throughout time. Dynamic optimization computes optimal trajectories for the controlled variables on the complete time horizon chosen, by minimizing an objective function such as cost, and accounting for the dynamic behavior of the system (Biegler and Grossmann; 2004). In order to compute these reference trajectories, inputs such as solar irradiance, ambient conditions, heat demand and the complete initial state of

the solar thermal plant are necessary. The values of state variables could be measured directly on the solar plant and the complete initial state would then be inferred from the measurements using estimation techniques. However, the perfect knowledge of the meteorological data over the complete time horizon can not be acquired in advance. Weather forecasts, as well as load forecasts, need to be used even though they contain uncertainties. A way to remedy to these uncertainties is to use Dynamic Real-Time Optimization (DRTO) (Kadam et al.; 2002). This methodology, mainly used in process engineering research, could greatly improve the operation of a solar thermal plant. Dynamic optimizations are regularly performed to ensure that the plant continuously operates in optimal conditions (Kadam et al.; 2002) to maximize the benefits and meet the heat demand. Before each DRTO run, measurements are performed on the actual plant to determine the initial conditions and the disturbances affecting the system, and forecasts are updated. As the accuracy of forecasts increases when the time horizon shortens, the update reduces the error between the predicted and actual weather and load. On the other hand, a long time horizon ensures a better long term strategy as the solar radiation also varies between days and months.

Therefore, the continuous adaptation of the operation strategy to the current conditions could correct the forecasts uncertainties, and in association with the respect of a plan previously determined, it would help to find the optimal operation strategy for the solar thermal plant.

This paper gives a state of the art on dynamic optimization and control of solar thermal plants. It then provides detailed explanation of the methodology of DRTO with examples from the literature, highlighting the lack of studies focusing on the DRTO of solar systems. Finally, it provides ideas for future work on the DRTO of solar thermal plants. Such a comprehensive analysis of the application of DRTO to solar thermal plants has never been done before to the authors knowledge.

The first Section of this paper introduces the system studied and its modeling and defines the optimization problem considered. Section I.3 presents the state of the art on dynamic optimization and control of solar thermal plants. Real-time Optimization is then introduced in Section I.4. After a short presentation of the classical scheme for Static Real-Time Optimization (SRTO), the Dynamic Real-Time Optimization (DRTO) schemes are presented in Section I.5. Some adaptations to this methodology are provided in Section I.6. In Section I.7, the three main schemes for real-time optimization are compared and finally, in Section I.8, perspectives on the application of DRTO to solar thermal plants are presented.

I.2 Solar thermal plant modeling and optimization

I.2.1 Solar thermal plant modeling

A solar thermal plant is composed of several circuits with a Heat Transfer Fluid (HTF) flowing in them. The design of the solar thermal plant is different for each plant, depending on the solar collectors technology, HTF used and the application. Nonetheless, some features are common to all solar thermal plants. In the production loop, the HTF

is heated up in the solar field, made of solar collectors, and the heat collected is transferred to the storage circuit through a heat exchanger. Direct storage is also possible when the HTF and the stored fluid are the same. A by-pass pipe allows the HTF to flow through the solar field without supplying the heat in the heat exchanger during a warm up phase. The storage circuit is centered around a Thermal Energy Storage (TES) tank, which can be charged with hot fluid when solar irradiation is abundant and discharged when solar heat cannot be produced in sufficient quantity to satisfy the heat demand. The storage tank can also be by-passed to directly supply the heat produced to the consumer. In some CSP plants, two storage tanks, one for the cold fluid and one for the hot fluid are used (in (Casella et al.; 2014) for example), instead of a stratified single one (used in (Scolan et al.; 2020) for instance). The consumer circuit is generally connected to the storage circuit trough a heat exchanger, but the stored fluid can also be supplied directly. An example of the structure of a solar thermal plant is presented in Figure I.2. In order to optimize the operation of a solar thermal plant,

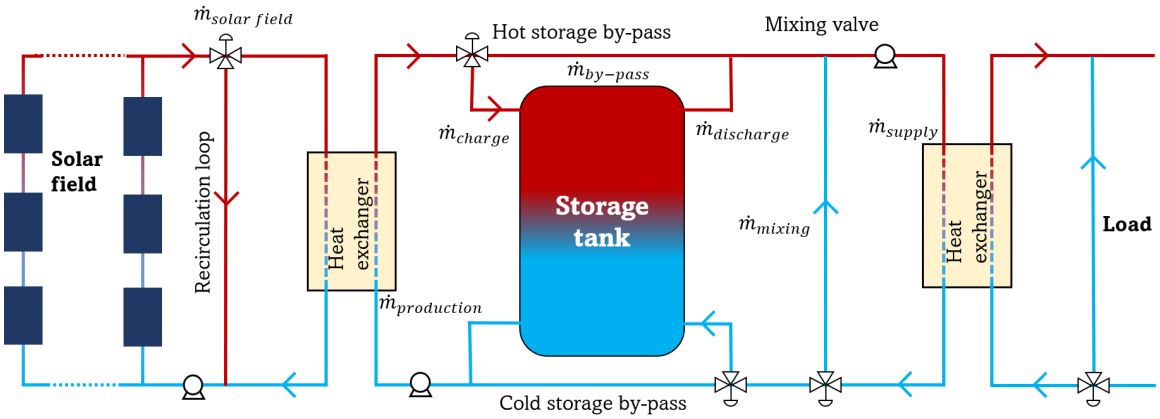

Figure I.2: General structure of a solar thermal plant

a model of the system needs to be developed. In a solar thermal plant, the quantity of energy produced, stored or supplied is as important as the temperature level of that energy. In contrary to electrical system with a fixed voltage, in a solar thermal system the temperature of the energy varies and affects the quality of the energy. For this reason, models of solar thermal plant are nonlinear, with power terms computed with a product between temperatures and flow rates. In order to keep the accuracy of the model, linearization should be avoided. When attempting to linearize the model, the difficulty of various operating points with different dynamics arises (Camacho et al.; 2007a). There are two types of models that can be used: first-principle models or data-based models. First-principle models are based on the equations of the conservation of mass and energy, an example can be found in (Pataro, Roca, Sanches and Berenguel; 2020). These models are based on Partial Differential Equations (PDE) that need to be discretised before the resolution. The equations can be developed for each element of a solar thermal plant to build a complete model. Nonlinear detailed models can provide accurate results but require more computational time. Thus, simplifications are often necessary. Data-based models are much faster to solve because they do not incorporate any differential equation or discrete-event based component. Historical data obtained from a real plant or a detailed, physical based, simulation model are used to build the empirical model. There are two categories of data-based models: parametric models

and data-driven models (Vasallo et al.; 2021). In the literature, data-based models are often used to represent the solar field of a solar thermal plant. In a parametric model, a parameterised function is used to represent the solar thermal plant and the values of parameters are determined with regression techniques. Such models are used in the literature in optimization studies to speed-up the calculations, in (Brodrick et al.; 2017) or (Rashid, Safdarnejad and Powell; 2019) for example. Linear models are easier to build with parameter identification. Grey-box models, based on first principles and tuned according to real measurements, can also be built (Gálvez-Carrillo et al.; 2009). Data-driven models are based on machine learning. They use historical data and a prediction algorithm to predict the solar thermal plant output, such as the outlet temperature of the solar field or the thermal power produced, based on a few inputs, such as ambient temperature, solar irradiance and inlet temperature. Artificial Neural Networks (ANN) are data processing systems inspired by human brain and have been used in recent years to model the solar field (Ghritlahre and Prasad; 2018). They present numerous advantages such as their simplicity, rapidity, capacity to represent complex and nonlinear relationship among the variables and input data. However, they require a large quantity of appropriate data to train the model, obtained from a real plant or a detailed simulation model. Elsheikh *et al.* reviewed the use of ANN for the modeling of solar energy systems and concluded that ANN models are much simplier and faster than theoretical models and require less experimental data than parametric models (Elsheikh et al.; 2019). Moreover, ANN models are able to represent changes such as plant degradation thanks to retraining with appropriate data. Farkas *et al.* trained an ANN model with simulation data from a physical model for flat-plate collectors. During the validation process, an average deviation of 0.9°C was achieved in the outlet temperature. This study shows that ANN model with an appropriate structure and a good training is accurate (Farkas and Géczy-Víg; 2003). A similar study was performed by Heng *et al.* for parabolic troughs collectors. In this paper, a transient model was developed to predict the parabolic trough collector tube exit temperature in Kuala Lumpur, Malaysia. In this location, the solar irradiation fluctuates a lot because of humidity and rarely stays at the same value for more than 1 minute. In such conditions, the accurate prediction of a solar thermal collector system performance is challenging and requires a transient model. The outlet temperature of the fluid during one day is obtained with a mean absolute deviation of 2K with the ANN model, and its calculation lasted only 1 minute on a personal computer, which is short compared to the Finite Element Method achieving the same accuracy (Heng et al.; 2019). This study confirms the rapidity of an ANN model to estimate the solar field performances compared to traditional models. Even though data-driven models might be less accurate than detailed first-principle models, the uncertainty in solar irradiance forecasts compensates for this disadvantage (Vasallo et al.; 2021). Machine learning techniques are also used to predict the weather conditions affecting solar thermal plants. For instance, Kumari *et al.* reviewed the deep learning models used for solar irradiance forecasting (Kumari and Toshniwal; 2021). Based on these studies, it seems that data-driven models are appropriate to model the solar field of a solar thermal plant in an optimization study. There are no data-based models representing the complete solar plant with the solar field, storage tank, pipes and heat exchangers found in the literature. A solar thermal plant is usually modeled with different sub-models for each element of the system. The remaining parts of this paper focus on the optimization of the operation of a solar

thermal plant, independently of the type of model used for the solar field and the other elements of the plant.

I.2.2 Generalities on optimization

Optimizing means finding the best solution to a problem among all the possible solutions respecting given constraints. The criterion to determine which one is the best solution is expressed through an objective function to be minimized or maximized. Generally, the minimization of cost or maximization of profit are used as objectives for the optimization, although non-economical objectives are sometimes employed, such as energy efficiency or exergy maximization or a target value for a variable (quality target as part of the objective function in (Ravi and Kaisare; 2020) or temperature target in (López-Alvarez et al.; 2018)).

The mathematical formulation of a dynamic optimization problem is presented in Equation I.1.

$$\begin{aligned} & \min_{\mathbf{u},\mathbf{z},\mathbf{y},p,t_f} \ \Phi(\mathbf{z},\mathbf{y},\mathbf{u},p,t_0,t_f) \\ s.t. \quad & 0 = f(\dot{\mathbf{z}},\mathbf{z},\mathbf{y},\mathbf{u},d,p,t),\ \mathbf{z}(t_0) = \mathbf{z}_0 \\ & 0 = g(\dot{\mathbf{z}},\mathbf{z},\mathbf{y},\mathbf{u},d,p,t), \\ & 0 \geqslant h(\dot{\mathbf{z}},\mathbf{z},\mathbf{y},\mathbf{u},d,p,t);\ t \in [t_0,t_f]. \end{aligned} \tag{I.1}$$

In this equation, Φ is the objective function to be minimized on the time span $[t_0, t_f]$, in which t_f itself can be an optimization variable. The objective function involves the differential state variables $\mathbf{z}(t)$, with initial conditions $\mathbf{z}_0$, the algebraic state variables $\mathbf{y}(t)$, the controlled variables $\mathbf{u}(t)$ and the parameters of the system p. The number of degrees of freedom in the optimization problem matches the number of optimization variables, which are some of the controlled variables, parameters and t_f if applicable. The minimization is subject to several constraints. Firstly, the process model is represented by the function f, which generally entails partial or ordinary differential equations as well as algebraic equations. In the model, $d(t)$ denotes the disturbances, including external disturbances, plant-model mismatch and measurement noise, and p are the time-independent parameters of the system, which might also be optimized. Finally, g and h contain the design and operational constraints formulated with equalities and inequalities respectively. The complete set of constraints forms a (Partial) Differential Algebraic Equations (DAE) system, in which the only derivatives appearing are those of the differential variables ($\mathbf{z}(t)$).

In Equation I.1, the time dependency of the problem denotes a dynamic optimization, which will compute optimal trajectories for the controlled variables. Simplification of this model to steady-state operation would lead to the computation of set-points (constant values) for the controlled variables. Various resolution algorithms may be used to solve a steady-state problem, depending on its characteristics: linear or not, made only of continuous variables or not. In the case of dynamic optimization, solving is more complex, due to the differential terms appearing in the model and constraints. Thus, discretization techniques are needed (Biegler and Grossmann; 2004). One way of solving complex optimization algorithms is to use stochastic algorithms, as opposed

to deterministic algorithms. Stochastic algorithms involve randomness and are often based on a biological or physical phenomenon. For example, Genetic Algorithm (GA) is inspired by natural selection and Particle Swarm Optimization (PSO) is inspired by the movement of organisms in a bird flock or fish school. One advantage of their use is a large search space which avoids local optimum but their main drawback is the need to evaluate the objective function many times until convergence is reached, which leads to long computational time. Stochastic algorithms require objective functions that can be evaluated quickly and are more often used for linear problems. ANN models or other data-based models are well-suited to be used with those algorithms, especially for real-time application (in (Blackburn et al.; 2020) for example) because of their fast computational time. Stochastic algorithms are particularly appropriate when the problem studied is complex and its physical modeling is not entirely known (Camacho et al.; 2007a), which is the case of a solar thermal plant since it uses an intermittent and hard to predict energy source.

If the optimization uses a deterministic algorithm, the application of the general optimization equation I.1 to the operation of a solar thermal plant, would involve the following variables and parameters:

- the differential state variables $\mathbf{z}$ are the temperatures in the system,
- the algebraic state variables $\mathbf{y}$ are the pressures in the system elements,
- the controlled variables $\mathbf{u}$ are flow rates, such as the flow rate through the solar panels $\dot{m}_{solarfield}$, the flow rate to collect the energy from the production loop $\dot{m}_{production}$, the flow rate to supply the energy to the consumer $\dot{m}_{supply}$ and the flow rates to charge, discharge or by-pass the storage tank $\dot{m}_{charge}$, $\dot{m}_{discharge}$ and $\dot{m}_{by-pass}$,
- the manipulated variables, not represented in equation I.1 because they are part of the control problem only, and not the open-loop optimization problem, are the valve openings and the pumps rotational speeds. The variable speed pumps and control valves are presented in Figure I.2,
- the disturbances d include the weather information (solar irradiance, ambient temperature, etc.), fouling of heat exchangers, plant-model mismatch, etc.,
- the model parameters p include characteristics such as size, heat transfer coefficients, etc. for solar collectors, thermal energy storage, pipes, heat exchangers and other parts of the plant. Some of these parameters are bound to evolve as disturbances affect the system. For example, the fouling of a heat exchanger has an impact of the heat transfer coefficient value.

It goes without saying that this description is highly model dependent and are chosen by the person in charge of developing the optimization scheme. If the system definition changes, so do the previous categories. Using these variables for a fixed design, the optimal trajectories for the flow rates could be determined with an economic objective function, taking into account the revenues due to the heat sold and the operating costs. More complex objective functions including several objectives could also be used (see subsection I.6.4). If a stochastic algorithm is used for the optimization, the problem

formulation would be adapted. Nonetheless, the variables and parameters involved would remain the same. Thus, this review includes both deterministic and stochastic optimizations, and details are given to explain the cited papers authors' choices.

The main difference between a solar thermal plant and a conventional fossil fuel plant is that the energy source is variable and cannot be manipulated. It then acts as a fast disturbance on the system. Several constraints are associated with the optimization of the operation of a solar thermal plant and are detailed hereafter (Camacho et al.; 2007a). The flow rate in the solar field must be above a minimum value to avoid overheating the fluid and to ensure that the pumps are working with a high efficiency. The outlet temperature is also limited to avoid overheating and phase change that would deteriorate the equipment. The temperature difference between the inlet and outlet of a solar field should also be kept under a maximum value to avoid a high pressure variation throughout the collectors. Compared to an electrical system, whose variations are almost instantaneous, there is a transport delay in the field and the pipes of a solar thermal plant. This leads to more complex dynamics. Furthermore, the dynamics of the system changes with the operating point making the optimization and control a solar thermal plant very challenging.

The next section will present a review on optimization and control of solar thermal plants, using a similar description of the system and the optimization problem.

I.3 Optimization and control of solar thermal plants

Most optimization studies on solar thermal plants aim at optimizing the design of the plant under standard operation strategies. It means that in Equation I.1, only the design parameters included in p are optimized. For example, the size of the solar field and its layout, the capacity of the storage tank, the capacity of the pumps, the pipes diameter, can be optimized in order to reduce investments while satisfying the production constraints. Research on the optimization of the design of the elements of solar thermal plants is still active, especially for the integration of solar heat in larger systems. For instance, several studies recently aimed at finding the optimal design for solar thermal systems integrated in District Heating Networks (DHN). Winterscheid *et al.* focused on the integration of solar energy into an existing DHN (Winterscheid et al.; 2017), while Hirvonen *et al.* analysed the feasibility of a solar DHN using seasonal storage in Finland (Hirvonen et al.; 2018). Furthermore, Tian *et al.* optimized the design of a hybrid solar plant supplying a DHN by minimizing the Levelized Cost Of Heat (LCOH) (Tian et al.; 2018). The use of solar heat for industrial processes is also under investigation ((Parvareh et al.; 2015), (Jannesari and Babaei; 2018)), the design of the solar system being economically optimized using standard control strategies. The optimization of the design of a solar thermal plant can also be an important step when studying the economic feasibility of a project. For example, Zubair *et al.* optimized the solar multiple and the size of the thermal energy storage of a parabolic trough concentrated solar thermal plant to assess the economic feasibility of a project for international electricity export (Zubair et al.; 2021). For the optimization of the design, stochastic algorithms are sometimes used. For example, a GA was used to find the optimal operating point of an evacuated tube solar collector system modeled with

an ANN (Dikmen et al.; 2014). PSO was used in multi-objective optimization based on a physical model to determine the best design and steady-state operating point ((Awan et al.; 2020), (Bahari et al.; 2021)). In these studies, no dynamic behavior was considered and the optimization only needed to be conducted once. Therefore, the use of a stochastic algorithm was possible.

Krause *et al.* outlined that the optimization of the design of a solar domestic hot water system greatly improves its performances, leading to a reduction of solar heat cost of about 18 % compared with the conventionally planned and installed system (Krause et al.; 2003). The authors concluded that, for a well-designed system, the improvements from the optimization of the operation strategy are smaller, only a few percents, but for a large system, this still leads to impactful savings. Camacho *et al.* explain that, because of the very expensive cost of solar thermal plants, any improvements in their performance, through better operation and control, would help to present them as a viable alternative to fossil fuels (Camacho et al.; 2007a). The optimization of the operation of the solar thermal plant is the main focus of this literature survey.

The optimization and control of a solar system can be divided into several levels of decision. The different levels are presented in Figure I.3, with the time step decreasing from top to bottom. In this diagram, LP stands for Linear Programming and QP for Quadratic Programming.

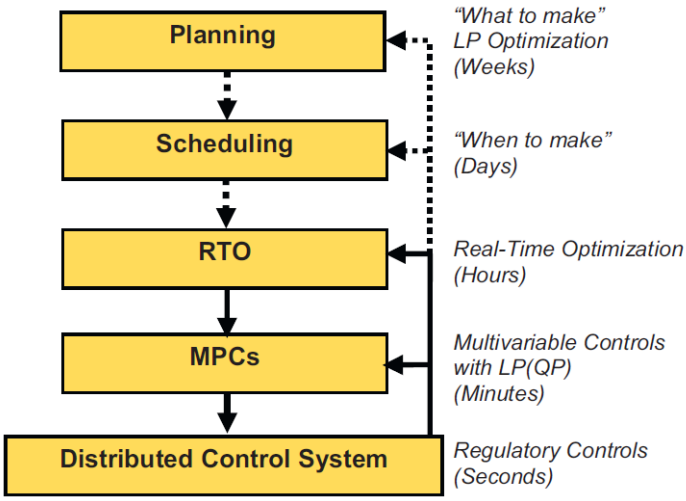

Figure I.3: General hierarchy for control and decision making in a plant (Darby et al.; 2011)

The two lower levels correspond to the control level, which aims at tracking a set-point or a trajectory for the controlled variables in the presence of disturbances by adjusting the values of the manipulated variables. The control strategy is an active area of research, especially for Concentrated Solar Power (CSP) plants, which are a particular type of solar thermal plants that produce solar heat at high temperature suitable for electricity or steam generation. In most control studies, the outlet temperature is maintained to a fixed level by adjusting the flow rate through the solar collectors, which presents several avantages (Camacho et al.; 2007a). This strategy ensures that the energy is always produced in a usable form with a temperature high enough for the consumer needs. It also avoids frequent shutdowns and startups by keeping the solar

field ready for full scale operation if the solar irradiance goes up. Finally, it allows the different parts of the solar thermal plant to work near design conditions with high efficiencies. Nowadays, the outlet temperature of the solar field in actual CSP plants is mainly controlled using basic control approaches to find the appropriate flow rate in the solar field, even though the system characteristics (nonlinear, various dynamics, changing environmental conditions) require a high order nonlinear controller (Camacho et al.; 2007a). In the last decades, numerous control methods have been studied and applied to CSP plants (Camacho et al.; 2007b), allowing a better disturbance rejection and uncertainties handling. For example, Gálvez-Carillo *et al.* used a nonlinear predictive controller with dead-time compensator to track the outlet fluid temperature from the solar field of a CSP plant in the presence of disturbances (Gálvez-Carrillo et al.; 2009). The authors found that this new controller can handle both significant nonlinear dynamics and variable dead-times. Csordas *et al.* compared several control strategies and highlight some drawbacks of the fixed outlet temperature control objective. This strategy leads to dump some solar energy when the solar irradiance is too low to reach the desired temperature. Moreover, if the inlet temperature is high in the solar field, a very high flow rate will be needed to avoid exceeding the target outlet temperature (Csordas et al.; 1992). The solar energy unused with this strategy could still be useful. If the consumer needs a precise temperature level, it can be adjusted by mixing the outlet HTF with colder fluid or heated up with a back-up fossil fuel burner. Csordas *et al.* recommended to fix the temperature raise in the solar field instead of the outlet temperature to waste less energy. However, this strategy also presents some drawbacks. The temperature at the outlet of the solar field becomes high when the inlet fluid is already warm. These high temperatures in the solar field lead to high thermal losses, reducing the benefits of avoiding the dumping of energy with a variable outlet temperature. Moreover, constraints on the maximum allowable temperature should be added in order to avoid exceeding the maximum temperature of the components. Some control strategies maximize the output power from the solar thermal plant by adjusting the flow rate in the solar collectors. For example, Amman *et al.* used a control algorithm based on ANN to detect the optimal power operating point of PhotoVoltaic Thermal Panels, maximizing both thermal and electrical powers (Ammar et al.; 2013). Ruiz-Moreno *et al.* developed a Model Predictive Control (MPC) to maximize the thermal power of a parabolic trough plant. The MPC needs to be run frequently, every few seconds or minutes. For a large-scale plant with a long time horizon, the computational time might exceeds the sampling time. To remedy to this issue, the authors developed an ANN model to represent the MPC and compute the control output. The computational time was reduced to only 3% of the tradiational MPC calculation time, and smoother outputs were generated with only slight violation of the constraints (Ruiz-Moreno et al.; 2021). Thus, control strategies based on ANN are a future direction for research. Allowing the outlet temperature to vary seems to help to meet the heat demand and increase the thermal energy produced. While advanced control strategies help to improve the solar field performances, the operation of a solar thermal plant could further be improved by dynamic optimization with a cost function. This will help to reduce the costs of the complete plant, by making a smart use of storage and running the pumps in order to avoid wasting electricity. This idea will be developed in the next sections.

The higher level of decision for the short term operation of the solar plant is the

offline dynamic optimization, also known as planning. In this level, the disturbances and initial state of the system are known inputs for the economic optimization. The time horizon comes from a compromise between long term optimal strategic vision and short term forecasts reliability. The optimal trajectories determined during this planning phase can be tracked by controllers only if the error between the forecasts and the actual measures is small. Delubac *et al.* used a dynamic multi-period approach to determine the best design and also the optimal operation strategy of a DHN using solar energy in association with a biomass plant and backup gas boilers (Delubac et al.; 2021). This planning determines the optimum energy mix and particularly the use of the solar thermal plant. It computes the optimal flow rate through the solar field but it does not model precisely the complete solar plant. Offline dynamic optimization has been performed on a non-concentrating solar thermal plant by Scolan *et al.* (Scolan et al.; 2020). In this study, the weather and the customer demand in solar heat were supposed to be perfectly known. Under such assumption of perfect forecasts, control was not included in the model since no disturbances were considered. Offline dynamic optimization was then performed to determine the best operation of the solar thermal plant including the heat storage, over a time horizon of 36 hours. Optimal trajectories for the flow rates in each part of the solar thermal plant were computed. The stored energy at the end of the time horizon was added to the objective function, with a weight, in order to give value to the stored energy and thus make the most out of the storage tank. Counterintuitive operating strategies were found to be optimal on this time horizon because of a smart use of storage. In this study, the solar heat provided to the consumer increased by 6.2%, the electricity consumption from the pumps decreased by 62.3% and finally, the economic profits increased by 2.1%. These gains could further be improved under less favorable weather conditions. This is, to the best of our knowledge, the only study referring to the offline dynamic optimization of the operation of a non-concentrating solar thermal plant, as most studies in this field focus on optimizing only the design of the plant.

The close field of concentrated solar power received slightly more attention recently. Several studies aiming at automatically finding the plant optimal operating point (maximizing the economic profit from electricity selling) can be found in the literature. Wittmann *et al.* developed a methodology to optimize the planning of power selling at the day ahead market for a CSP plant (Wittmann et al.; 2011), determining the optimal use of the backup fossil fuel burner and the storage tank. It takes into account meteorological and electricity market price forecasts to optimize the bidding strategy. Thermal Energy Storage (TES) transforms the intermittent solar power into a dispatchable power that can be sold when the electricity price is high and thus, increase revenue. Indeed, it is easier to store heat and then transform it into electricity when needed than to store electricity directly. The time horizon for such an optimization should be between one and two days to compromise between profit gains and forecasts quality. Similarly, Casella *et al.* optimized a Solar Tower Power Plant with TES (Casella et al.; 2014). The electricity generation schedule was optimized in terms of the Heat Transfer Fluid (HTF) flow rate to the power block. The other control variable of the problem was the power dumped by heliostat defocusing, which is needed in summer to avoid exceeding the maximum power that can be handled by the receiver. Their paper includes a detailed dynamic model and concludes that optimal control should be taken into account when estimating the potential plant revenue during the plant design

phase, as it can increase the revenue of about 7 % for a 10 days case study. Finally, Lizarraga-Garcia *et al.* conducted a similar study but added the possibility to recharge the TES using electric heaters and electricity from the grid (Lizarraga-Garcia et al.; 2013). This additional feature further increases the flexibility of the plant and its revenue by taking advantage of the high variability of electricity price. Their optimization variables were the initial temperatures of the hot tank, the cold tank, and the lid, the initial mass of salt in the hot tank, the start-up time, the shutdown time, the mass flow rates between the hot tank and the cold tank, and the electricity purchased from the grid. Offline dynamic optimization was also used by Lopez-Alvarez *et al.* to optimize start up policies of a CSP plant (López-Alvarez et al.; 2018). The objective was to reach the target operating temperature (control variable) in the shortest amount of time by manipulating the input water flow rate (water was the HTF used in this solar thermal plant). It is essential for such systems to achieve full operation from shut-down conditions in the minimal amount of time and using minimum energy requirements, in order to meet the power demand. In this study, TES was used after the Rankine cycle to store water warmer than fresh water and recycle it to speed-up the start-up policies of the CSP plant. Wagner *et al.* optimized the timing and rate at which electricity is generated by the power cycle (Wagner et al.; 2017) in a concentrated solar power tower plant with TES. They used a Mixed-Integer Linear Program (MILP) to maximize the electricity sales while avoiding frequent cycle start-ups. They used perfect forecasts from historical meteorological data to compute the solar power available, thanks to a simulation tool using design flow rates. Their methodology allows more production during highly priced hours and a smoother generation profile than heuristic control approach. The authors concluded that the Power Purchase Agreement price could improve by 10 to 15% for electricity markets with highly variable electricity prices or narrow windows of high revenues thanks to their optimization. The authors used the same approach in (Wagner et al.; 2018) and solved the optimization problem over a time horizon of 48h, applied the hourly dispatch schedule during 24h and then used a rolling horizon of 24h. The yearly results of this optimization show an improvement in the operating cost of the plant over its lifetime, with lower maintenance costs, compared to the standard algorithm that allocates the dispatch to hours of particularly high revenues. Finally, Hamilton *et al.* improved this methodology with a detailed model for off-design conditions for the electricity production (Hamilton et al.; 2020). The flexibility of CSP with TES can also help to alleviate negative effects of photovoltaic solar plants. Kong *et al.* optimized the scheduling for for a hybrid solar power plant comprising CSP and photovoltaic solar panels. They used a simplified linear model based on energy flows and optimized the day-ahead generation plan of the plant with a time step of one hour. A modified Butterfly Optimization Algorithm (BOA) was used because it is faster compared to GA and PSO. The use of a stochastic algorithm was possible because the system was simplified and the task is performed offline. The operation cost of the integrated system decreased by 10% with this methodology.

In addition to thermal energy storage, hybridization of a CSP plant with a back up fossil fuel system helps to harvest the maximal solar energy. Indeed, the hybrid system considered by Powell *et al.* led to a larger amount of solar energy collected, when optimizing the HTF flow rates through the solar field, through the bypass loop, and from the hot tank (Powell et al.; 2014). This is due to the hybrid mode which allows the solar field to operate at a lower temperature, reducing heat losses, the demand being com-

pleted by the fossil fuel. Such systems have been improved afterwards by Ellingwood *et al.* who added Flexible Heat Integration (FHI) to the hybrid plant (Ellingwood et al.; 2020a). They optimized dynamically a concentrated solar tower connected to a Rankine cycle and including three thermal storages. Brodrick *et al.* optimized the operation of an Integrated Solar Combined Cycle (ISCC), which included a parabolic trough solar thermal field and a gas turbine (Brodrick et al.; 2017). The hourly operation, in terms of part load of the gas turbine, solar focus rate and mass flow rate of the solar HTF, of representative days was optimized using different objective functions. A proxy model was used to recreate predicted solar output and no storage was considered in this study. The proxy model is a statistical model with fitting parameters determined thanks to a detailed simulation model. This is a data-based model, thus, the dynamics modeling was simplified compared to the previously mentioned studies based on first-principle models. The design and the operation of the same system were then optimized simultaneously for two conflicting objectives: the net present value (NPV) and the average CO_2 emissions intensity of the power produced (Brodrick et al.; 2018). Improvements over published designs were achieved and it shows that optimal operation should be considered when designing a system. Finally, an ISCC with storage was optimized in (Orsini et al.; 2021) and the benefits of using storage tanks were presented.

This literature review shows the benefits of using offline dynamic optimization and advanced control strategies to operate a solar thermal plant. There are many ways of implementing the optimization of the operation of a solar thermal plant, with their respective advantages and drawbacks. All of these methods are explored in this review: using a first-principle or a data-based model, employing a deterministic or a stochastic optimization algorithm. The implementation differs from one study to the other. This review is focused on the details of the optimization methodology (decision variables, time horizon, sampling time, hierarchical structure etc.) rather than the model construction or the optimization algorithm. The offline dynamic optimization is based on weather and load forecasts, and thus, cannot adapt the strategy to the current situation. If the uncertainty of the forecasts is too high, the optimal trajectories computed cannot be applied to the real plant. Besides, advanced control strategies are mostly used to track the target outlet temperature of the solar field. Some studies show the benefits of maximizing the output power of the field. Nevertheless, economic considerations are not included in most control strategies even though they might improve the operation of solar thermal plants. An intermediary level between control and planning is Real-Time Optimization (RTO). This method uses measurements of disturbances and state variables of the system to update the optimal set-points (Static Real-Time Optimization SRTO) or trajectories (Dynamic Real-Time Optimization DRTO) online. This ensures that the plant continually operates under optimal conditions, even in a variable and hard to predict environment. All the previously mentioned works would be improved by using a DRTO method, as mentioned in (Powell et al.; 2013), to adapt the optimal operation to the plant states, solar irradiation and updated forecasts. It is worth mentioning that data-based models and deterministic algorithms are faster to solve, based on the previous literature survey, and therefore constitute a good perspective for real-time optimizations where computational times are crucial. If DRTO has been widely studied in process engineering research, it is fairly new in the field of solar thermal plants, although it seems well-suited to such systems. The next sections will provide detailed explanations on DRTO, along with the few examples of application of

this method to solar systems found in the literature.

I.4 Generalities on Real-Time Optimization

In the aforementioned mathematical formulation of the optimization problem (Equation I.1), the disturbances $d(t)$ and the initial state $\mathbf{z}_0$ are not known in advance. If they are supposed to be perfectly known, offline optimization can be performed to compute the optimal set-points/trajectories until the end of the time horizon. In practical applications, disturbances and initial conditions are always unknown and online optimization, also called real-time optimization, has to be implemented. Measurements are then necessary to access to the initial conditions and disturbances values.

RTO is used in research articles in various fields, from electrical systems (Clarke et al.; 2018) to chemical processes. Among the latter category, batch reactors are the focus of many works ((Kadam et al.; 2002), (Hua et al.; 2004), (Alonso et al.; 2013), (Arpornwichanop et al.; 2005)). These systems are highly nonlinear, always in transient behavior, their process model is not generally well-known and finally only a few measurements are available (Arpornwichanop et al.; 2005). Those systems are then very challenging to optimize, explaining the numerous studies focusing on them. Their characteristics are similar to thermal systems such as solar thermal plants, in which both the energy source and the load are time varying. Solar systems are rarely optimized in real-time in the literature. Hence, batch chemical reactors constitute the major resource for this study. Other fields are seldom found in the optimization literature, such as waste water treatment (Elixmann et al.; 2010), thermal building (De Oliveira et al.; 2013) or district heating and cooling systems (Cox et al.; 2019). The next subsections will highlight the role of measurements in RTO, in subsection I.4.1, and the association of RTO and control in a plant, in subsection I.4.2.

I.4.1 Measurements

RTO takes process measurements to update the process model and the initial conditions and trigger a new optimization. Thus, it is able to reject unknown disturbances as they appear in the process. This applies even for large and slow disturbances which can have a high impact on the system, whereas controllers generally reject only fast disturbances because of their short time step.

In a RTO study, measurements are used before each optimization run. The measurements are performed directly on the facility to be optimized (Vettenranta et al.; 2006), but for research studies a prototype (Alonso et al.; 2013), or more often a simulation model, are used to represent the real process and provide feedback measurements. In the latter case, the simulation model may be different than the model used during the optimization step. For example, Hua *et al.* used a reduced model for the optimization and a detailed model for the simulation of their batch reactor because of their different computational costs (Hua et al.; 2004). Also, the measurements on the simulation model can include noise and sampling time delay to represent a real process more realistically (Arpornwichanop et al.; 2005). Most of the time, the measurements of the system state variables, although the values usually include noise,

provide the initial conditions of the optimization problem. In a solar thermal plant, the temperatures, pressures and flow rates could be measured on the plant and provide a feedback to the optimizer and also define the initial state of the plant. These online measurements allow the system to detect and take into account the disturbances. For a solar thermal plant, ambient temperature, wind speed and solar irradiation need to be measured in order to adapt the optimization and control accordingly. In addition, measurements can correct the plant-model mismatch resulting from simplifications in the model formulation due to computational limitations. Generally, the model used in the optimization algorithm includes uncertain parameters which can be estimated through measurements to limit the impact of the uncertainty on the optimum. The set of uncertain parameters to be estimated online is chosen based on the impact of each parameter value on the objective function. The selection of measurements to estimate those key parameters also has to be based on a sensitivity analysis. Indeed, a change in the measurement must accurately reflect a change in the parameter value. A method to choose the set of key parameters and measurements is presented by Krishnan *et al.* (Krishnan et al.; 1992).

There are several ways to take advantage of the measurements to correct parameter uncertainties and plant-model mismatch (Chachuat et al.; 2009). Estimation techniques are required to determine the parameters and states values from the noisy measurements. Various techniques exist with different minimization criteria (Zhang; 1997). Parameter and state estimation is an essential but complex topic, that could be the focus of a separate paper.

I.4.2 Economical and control objectives

Optimization is closely associated to control as both are necessary to ensure best economical performance and feasible operation of a process in the presence of disturbances and uncertainties. The objective of a controller is to track a set-point or a trajectory for the controlled variables in the presence of disturbances by adjusting the values of the manipulated variables. This is called a regulatory objective. Optimization tries to find the set-point (static optimization) or trajectory (dynamic optimization) for the controller to track which leads to the best economical performance for the system.

Tracking relies on the minimization of the quadratic error between the set-points determined by the optimization and the measurements performed on the actual system. The two tasks, economic optimization and tracking, can be done in one layer, called EMPC (Economic Model Predictive Control). However, they are generally performed in two distinct layers. On the upper layer, the economic optimization problem is solved, and the set-points/trajectories are sent to a lower layer controller which tracks them and rejects process disturbances. The lower layer can be composed of simple controllers such as PID (Proportional Integral Derivative) which are generally able to track the value of one output by adjusting one input. This is the case in a real-time optimization study of an evaporative cooling tower for example (Blackburn et al.; 2020). More advanced controllers include Model Predictive Control (MPC). These controllers use a dynamic model of the process inside their formulation in order to predict the future behaviour of the system and track the optimal trajectories more efficiently. The MPC system often constitutes a supervisory controller that communicates with the base

controllers (PID for example). Although not always necessary, the MPC ensures a better rejection of disturbances.

To summarize this Section, Figure I.4 presents the typical architecture of real-time optimization. State variables, y and z are measured on the system, and their measured values y_m and z_m are sent to the validation part of the algorithm. In the validation part, data reconciliation is performed to eliminate random and gross errors from the measurements and the estimated values for y and z, which are $\hat{y}$ and $\hat{z}$, are sent to the next step. The model updater takes the corrected data to estimate unknown model parameters. The new model is then used to update the optimization. The optimizer computes optimal set-points of trajectories for some variables, following a previously determined schedule or plan. If these new set-points or trajectories represent significant changes in optimization variables, which is tested in the condition part of this framework, the reference set-points or trajectories are sent to the controller. The controller compares the reference values to the measured ones and determines the appropriate control moves to track the optimal set-points or trajectories.

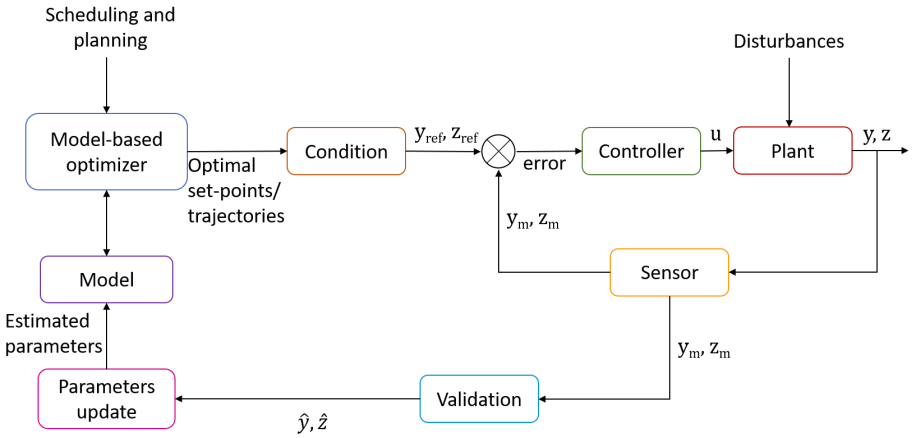

Figure I.4: Typical architecture of real-time optimization (based on (Shokri et al.; 2009))

Several schemes exist to implement RTO within the general framework of Figure I.4. After a short presentation of the original scheme SRTO, DRTO is explained in the next Section.

I.5 DRTO schemes

The classical scheme to optimize a process in real-time is based on a stationary model. This scheme, referred to as Static Real-Time Optimization (SRTO), allows the re-optimization of the process only when the system reaches steady-state. Measurements are performed at steady-state and the static model is updated before the next optimization is run. The optimal set-points are sent to the lower-level controller, which tracks the optimal constant values of the controlled variables until the next steady-state is reached. A downside of this approach is that the frequency of optimization runs can not be adjusted and is limited to the amount of times the process reaches steady-state.

Furthermore, detecting steady state in order to trigger the optimization is not trivial and requires complex detection algorithms (Darby et al.; 2011).

Rashid *et al.* performed a real-time optimization of a CSP plant hybridized with a back up fossil fuel burner using a steady-state model (Rashid et al.; 2018). The temperature exiting the parabolic trough collector and the split fraction of heat transfer fluid entering the steam generator and the pre-heater were optimized in real-time. The static model used for RTO was an empirical model based on data collected from a one year simulation. The nonlinear model was then complexified in (Rashid, Ellingwood, Safdarnejad and Powell; 2019). The detailed model used in simulation and the empirical model used in SRTO were different, introducing plant-model mismatch as in a real application. The data based models were able to predict accurately the total solar power collected for various solar irradiations and ambient temperatures. This nonlinear static model was used in (Rashid, Safdarnejad and Powell; 2019) to optimize the hybrid plant with flexible heat integration. It was shown that SRTO is able to improve the total solar power collected, and hence the solar fraction of the plant, especially when the irradiation is low. Adding Flexible Heat Integration and RTO increases the solar fraction by 18.2%, and the Leverage Cost Of Energy by 3.81% in comparison to the conventional hybrid plant. The CO_2 production also decreases by 4%. In these studies, the solar thermal plant used parabolic trough technology without storage, so the dynamics of the system were all fast (less than 10 minutes). By running the SRTO algorithm every 5 minutes, and adjusting the set-point in the simulation every optimization, the plant was able to stay near optimality.

Hybridization of natural gas with solar energy has also been studied for a Solar Power Tower system. Ellingwood *et al.* showed the improvement in solar energy utilization achieved with hybridization and FHI (Ellingwood et al.; 2020b) for a Solar Power Tower system including energy storage. In this study, the operation of the solar thermal plant was based on heuristic control. The preferred mode of operation was determined relative to the incident solar irradiation peaks on the receivers. Dynamic optimization was performed on the same system (Ellingwood et al.; 2020a), based on weather forecasts. The methodology is not able to adapt the operation of the plant as disturbances occur in the system, but it provides the optimal operation for known inputs. This study concluded that the heuristic control approach was reliable enough for design and optimization initialization. It also showed that optimization can lead to improved performance of the hybrid plant.

The systems in (Rashid, Safdarnejad and Powell; 2019) and (Ellingwood et al.; 2020a) are both hybridized solar-natural gas power plants, even though the solar collectors technologies are not the same. The main difference between the systems from (Ellingwood et al.; 2020a) and (Rashid, Safdarnejad and Powell; 2019) was the presence or not of thermal energy storages. TES allows the decoupling between the variable solar resource and the heat supply which aims to be as constant as possible. It can extend the use of solar energy at night and smooth the energy delivery during fluctuating weather conditions. In (Rashid, Safdarnejad and Powell; 2019), no storage was considered, so the dynamics of the different parts of the concentrated solar plant were all fast, allowing the plant to quickly reach steady-state. The use of a static model in a real-time optimization formulation was therefore possible. On the contrary, the three storage tanks in (Ellingwood et al.; 2020a), prevent the plant to reach steady-state

as the dynamics of the storages are slow while the other systems dynamics are fast. Offline optimization was then preferred, with supposedly perfect weather prediction.

These studies show that SRTO can improve the operation of a solar thermal plant. Since it uses a static model, it needs to be run regularly to adapt the operation to the changes happening in the transient system. A condition to make the use of a static model possible is to have a system with all fast dynamics. Indeed, with fast dynamics, the system will quickly reach steady-state. A disturbance affecting the system's inputs will immediately impact its outputs. Thus, a system with fast dynamics operates in quasi-static conditions with short transitions between steady-states. Computing constant set-point values for the optimization variables is possible. Those values will be optimal until a change occurs in the system or its environment, leading to a different steady-state and requiring a new optimization. On the contrary, if the solar thermal plant includes storage, there is accumulation/inertia in the system. There will be a delay before a disturbance on the system's inputs impacts its outputs. The slow dynamics of the storage and the fast dynamics of the solar collectors, pipes and heat exchangers will prevent the system to ever reach steady-state. It is therefore non-optimal to compute constant values for the controlled variables. Dynamic optimization, which will compute optimal trajectories for the decision variables in the system always operating in transient behavior, is more appropriate. When the inputs, such as solar irradiance, are not known in advance, a real-time scheme is required. Therefore, DRTO seems well-suited to such systems, as it can provide optimal trajectories taking into account process dynamics, while adapting the operation strategy online.

I.5.1 Single-layer scheme: EMPC

One approach to compute dynamic optimal trajectories in real-time is to perform the economic optimization and regulatory tasks on the same level (Engell; 2007). The economic objective is included into the formulation of the controller. This is generally called Economic Model Predictive Control (EMPC). In this method, the optimization algorithm is run at each sampling time of the controller, which depends on the distubance dynamics present in the system. With this single-layer method, a unique dynamic model is used, ensuring consistency between the economic optimization and the tracking task. The major drawback of EMPC is that the optimization is run very often, which might not be possible for a complete process with a complex model since the computational time would exceed the sampling time of the EMPC. Additionally, the EMPC is not able to handle systems with a wide range of dynamics because its very short sampling time might not be capable of dealing with slow disturbances, such as plant-model mismatch. Finally, stability issues might arise, ensuring best economic performance thanks to the controller is maybe not enough for stability. EMPC are used in some studies, when the process is well-suited for single-layer DRTO, and the model can be simplified without a large loss of accuracy. For instance, Clarke *et al.* used an EMPC to optimize an electrical system containing storage, such as microgrids or hybrid electric vehicles (Clarke et al.; 2018). The EMPC performs several tasks: it minimizes the short term economic cost and achieves a reasonable tracking of the storage state trajectories provided by a top-level controller in charge of planning. The use of an EMPC is here feasible because the dynamics of electric devices are very fast and

the model used for calculations can be simple. Amrit *et al.* used an EMPC to optimize an evaporation process and a William-Otto reactor (Amrit et al.; 2013). The use of a single-layer DRTO was made possible by only considering disturbances with similar dynamics. The sampling time of the controller was then chosen based on this common time constant, 1 minute was used in this study. Finally, Hotvedt *et al.* optimized a CO_2 capture facility with an EMPC (Hotvedt et al.; 2019). A reduced model allowed the EMPC to run faster than the sampling time chosen.

EMPC has already been used for solar systems. Serale *et al.* (Serale et al.; 2018) and Pintaldi *et al.* (Pintaldi et al.; 2019) developed an EMPC for solar systems with storage, with the objective of minimizing backup energy consumption. In (Serale et al.; 2018), the performance of a latent heat storage solar thermal system to be used in building is optimized with estimated weather forecasts to represent a real-time implementation. The control time step used in this study is one hour, and the problem is linearized, making the use of an EMPC possible. In (Pintaldi et al.; 2019), the system considered is a solar thermal cooling system with storage. A GA is used to solve the optimization problem, based on perfect weather forecasts. The control algorithm was adapted to be used in real-time since the resolution of a nonlinear system is too long. Only the state variables are computed in real-time by the simulation model. The layout of the EMPC is presented in Figure I.5, using identical models for the optimization and the simulation.

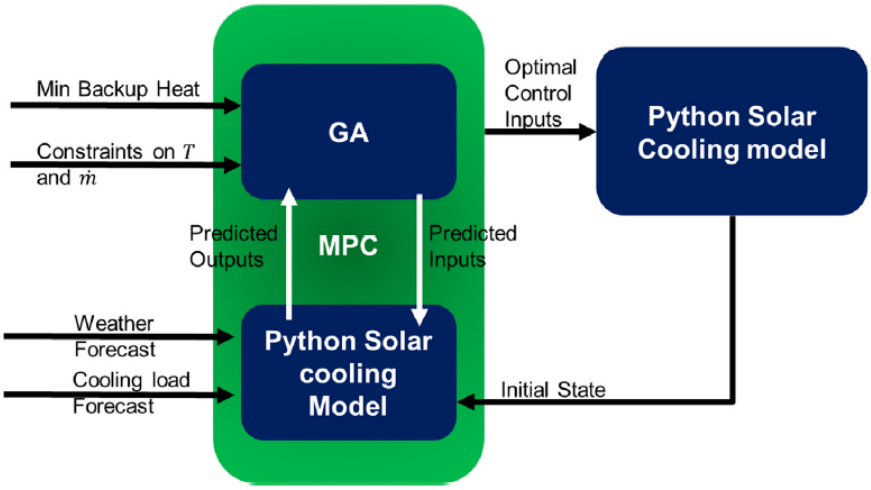

Figure I.5: Layout of the EMPC (Pintaldi et al.; 2019)

Pintaldi *et al.* highlight the necessity of using a well-tuned EMPC with a system with enough degrees of freedom in order to ensure an enhanced performance of the system thanks to the EMPC control. In their studies, fossil fuel burner energy was reduced by about 10% for the evaluated scenario using EMPC compared to a rule based controller. The authors state that a hierarchical MPC, including a lower layer of controllers, such as PID, to track the set-points, might improve the use of storage. Hierarchical methods with a decoupling of optimization and control will be presented in subsection I.5.2.

These were specific examples where the EMPC can solve the optimization problem. In most cases, the complex model involved, the wide range of dynamics in the

sub-systems and disturbances and the computational limitations make the single-layer DRTO impractical. In particular, a solar thermal plant including storage presents various time scales and includes highly nonlinear phenomena, so EMPC is not well suited for the optimization of their operation. This observation is bound to evolve with the recent and future computational developments such as methods that take into account the sparsity of the problem and can make the resolution run efficiently.

I.5.2 Two-layer scheme: DRTO and MPC

Based on the impracticability of the single-layer scheme for complex, large-scale processes, Kadam *et al.* suggested the decomposition of the economic optimization and the regulatory objective on two hierarchical levels (Kadam et al.; 2002). This methodology with two layers will be referred as two-layer DRTO in the following parts of the paper. The standalone acronym DRTO is used for the economic optimization on the upper layer. On the upper level, an economic DRTO is performed: optimal trajectories for the process variables are computed to minimize or maximize an economic objective function while satisfying all the process constraints. The DRTO problem is solved repeatedly to update the reference trajectories during the complete time span, taking into account slow disturbances. On the lower level, controllers, often MPC systems, track the reference optimal trajectories. The sampling time of the controllers, noted $\Delta\tilde{t}$, has to be small because the fast process disturbances are rejected at this level. On the other hand, the DRTO does not need to be executed that often and its sampling time, noted $\Delta\bar{t}$, can be larger. The dynamic models might differ between the 2 layers: a detailed model is required for the DRTO to achieve best performance, and a simplified model (sometimes linear) is more suited for the control layer as it has to be executed often and thus needs a short computational time. Since disturbances are rejected on both levels, a time-scale separation needs to be implemented and is schematized in Figure I.6, with $\mathbf{z}, \mathbf{y}, \mathbf{u}$ defined in Equation I.1. The circumflex accent represents estimates based on the measurements of some state variables $\mathbf{z}_m, \mathbf{y}_m$. The slow-varying and persistent disturbances, noted $\overline{d}$, such as parameter uncertainties, changes in price markets and slow physical disturbances which affect the economic objective are taken into account at the DRTO layer. The controller considers all types of disturbances in its process model, including the fast, stochastic disturbances, noted $\tilde{d}$. The switches in Figure I.6 represent the fact that the operations are not performed continuously but at every time step. The estimation of disturbances and parameters from the measurements, and the time-scale separation, can be performed in any order (Würth et al.; 2011).

The main advantage of the two-layer DRTO is that the DRTO is executed at a slower frequency, allowing larger computational time and hence, making it practical for real complex processes. A downside is that the models used in the two layers are different and inconsistencies might arise between the two objectives and strategies (Ravi and Kaisare; 2020). Using two layers is the current practice in chemical industries but usually with SRTO on the upper layer. This might change with the future improvements in computational performances.

Such a hierarchical control layout was used in (Gil et al.; 2020) to control the start-up procedure of a solar thermal field with storage, with the objective of maximizing the

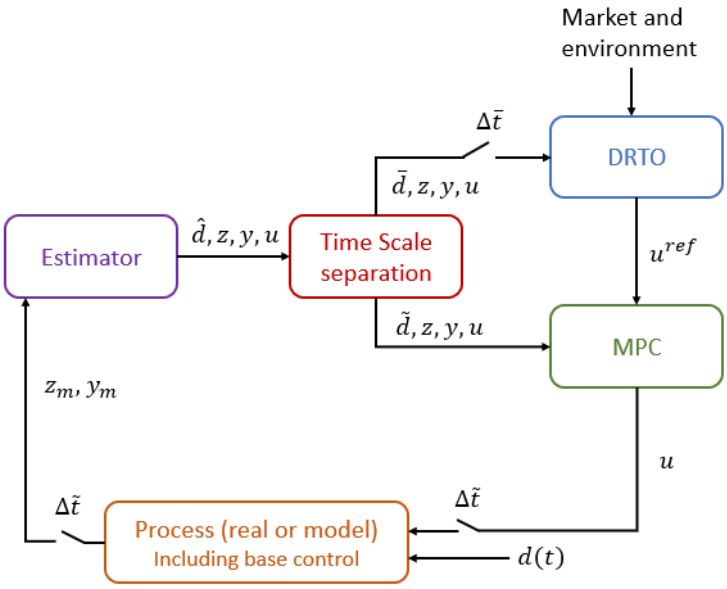

Figure I.6: Time-scale decomposition of the disturbances between the DRTO and the control layers (based on (Kadam et al.; 2002))

temperature at the top of the storage tank. However, no economic optimization was performed in this study. Berenguel *et al.* also used a hierarchical control architecture to optimize the electricity production of a CSP plant (Berenguel et al.; 2005). The set-point optimization layer used a static model and the control layer was based on classic control schemes. An upper layer consisted on a daily and seasonal operation optimization to determine the operating periods of the plant based on weather and electricity demand forecasts. These works, although not using an economic DRTO on the upper level, show that the hierarchical structure of the resolution allows the management of storage and a more complex model for the optimization layer. Thus, a two-layer DRTO approach, with a decoupling between the economic optimization and the tracking task, would improve the optimization and control of the solar systems.

Recently, Pataro *et al.* performed a two-layer DRTO of a parabolic concentrator collector field in order to maximize the thermal power energy delivered by the solar field (Pataro, Roca, Sanches and Berenguel; 2020). The economic objective function takes into account the thermal energy produced and the electricity consumption of the pumps. The DRTO algorithm uses measurements of the ambient temperature, solar irradiance and solar field inlet temperature to compute optimal trajectory for the inlet volumetric flow rate. This algorithm is solved repeatedly over a receding time horizon. The results in this paper are promising, the two-layer DRTO scheme seems to handle correctly disturbances and parameter uncertainties on the irradiance model parameter and the thermal losses coefficient. Even if a complete system with storage and customer load is presented in this paper, only the solar field was optimized in real-time. No other study focusing on the two-layer DRTO of a solar system was found in the literature, but this work confirms the interest of this methodology. The framework presented in (Wagner et al.; 2017), and tested in (Wagner et al.; 2018), then improved in (Hamilton et al.; 2020) seems able to perform the DRTO of the electricity

generation in a CSP plant. The methodology was only tested with perfect forecasts but it should be able to adapt the optimal dispatch as disturbances occur in the system. Indeed, the framework already include the CSP controllers and an optimizer, and uses a rolling time horizon. Future work based on these studies could add the possibility to handle uncertainty in weather and electricity pricing forecasts and permit intra-day adjustments to make sure this scheme can be applied on a real facility. For real-time applications, the optimization algorithm needs to run efficiently. One way to achieve that is to use a data-based model, such as in (Brodrick et al.; 2017), to model the solar field outputs. This reduces greatly computational time, allowing more frequent optimizations. The model could be adjusted online based on measurements on the real facility or a detailed simulation model.

I.6 Applications and adaptations of two-layer DRTO

The two-layer DRTO scheme is widely used in chemical engineering research papers and over the last decade, several adaptations have been made to the method presented in the last section, and are detailed in the following subsections I.6.1, I.6.2, I.6.3, I.6.4. The last subsection I.6.5 shows how to couple a planning phase to the DRTO methodology. This Section focuses on two-layer DRTO since this scheme seems to be the more complete and the more appropriate to optimize the operation of a solar thermal plant. Indeed, the dynamic optimization allows the computation of optimal trajectories, taking into account the various dynamics of the system's components. Additionally, the real-time aspect allows the adaptation of the operational strategy as disturbances occur in the system and can correct uncertainty in weather and demand forecasts. Furthermore, the two-layer scheme allows the rejection of small/fast disturbances that do not necessitate a new optimization. And it also corrects the plant-model mismatch arising from the difference between the simple model used for the frequent optimizations and the detailed model used to replace the real plant for research purposes. Finally, it allows the use of different time horizons and time step sizes in the optimization and the control layers. The methods presented hereafter are a good source of inspiration for future studies on the DRTO of solar systems. The features of the presented algorithms could also be used on studies based on SRTO or EMPC.

I.6.1 Fast updates and DRTO triggering

Although repetitive DRTO is widely used (in (Hua et al.; 2004), (Jamaludin and Swartz; 2016), (Remigio and Swartz; 2020) for example), re-optimization is not necessary at each time step. The previous reference trajectories might still be optimal at the end of the time step if no new significant disturbance appeared and a new DRTO would be computationally expensive and not really useful. A better way to trigger the optimization layer is based on the actual disturbances and is called conditional triggering. When a new optimization is not needed, fast updates of the previous trajectories are sufficient. In the case of small perturbations, linear updates of the solutions are performed and the DRTO is triggered only for large perturbations (Kadam et al.; 2003). The DRTO can be triggered based on disturbance sensitivity analysis, which indicates

when the Necessary Conditions of Optimality (NCO) are no longer fulfilled ((Würth et al.; 2011), (Pontes et al.; 2015)). Other studies suggested to re-optimize based on different conditions. Pataro *et al.* state that a new DRTO needs to be triggered when a large perturbation affects the values of the state variables or when a change in the optimization problem such as market prices, operational conditions, etc, appears (Pataro, da Costa and Joseph; 2020). Rohman *et al.* ran a new DRTO if the active constraint for the conversion of their final product was violated (Rohman et al.; 2019). Ochoa *et al.* listed three different ways of triggering the DRTO: based on a time step, on disturbance analysis and lastly on a value below a threshold for the economic objective function (Ochoa et al.; 2009). Finally, some studies mention detecting deviations between the predicted and real variables trajectories and trigger the DRTO when the deviation is too large (Alonso et al.; 2013).

I.6.2 Computational delay

The computational time, noted τ, necessary to obtain the reference trajectories at the DRTO upper level leads to a delay in the real-time implementation of the optimal trajectories by the MPC controllers on the lower level (Pontes et al.; 2015). Indeed, during the execution of the DRTO resolution, the state of the system is still under progress. The optimal trajectories computed based on the states measured at time t_n become sub-optimal when implemented in the process at time $t_n + \tau$. Pontes *et al.* suggested to anticipate the need of a new DRTO and predict the state of the system at the time of the new trajectories (Pontes et al.; 2015). The DRTO is triggered in advance and when the calculation is finished, the system has reached the predicted state so the reference trajectories implemented are optimal.

When the DRTO is not triggered in advance and there is some computational delay, the previous trajectories are applied during the calculation (Würth et al.; 2011). This is the common practice in the literature, but probably not the optimal one.

I.6.3 Closed-loop two-layer DRTO

Most two-layer DRTO approaches do not consider the presence of the Model Predictive Control (MPC) system in the DRTO problem formulation (Remigio and Swartz; 2020). This traditional scheme can be referred to as open-loop two-layer DRTO. A perfect control is assumed, the hypothesis is that the closed-loop response dynamics will follow the economically optimal trajectories of the DRTO layer. But it is not always the case, so closed-loop two-layer DRTO was introduced by Jamaludin *et al.* (Jamaludin and Swartz; 2016). In this new formulation, the future MPC control actions are included into the DRTO problem, which means that the control performance is considered when making economic decisions. The DRTO general problem includes MPC optimization subproblems, as presented in Figure I.7. In this Figure, a diagram provided in (Remigio and Swartz; 2020), u denotes the inputs of the system while y are the outputs. The entire DRTO prediction horizon N is divided into steps. At each step j, the predicted control moves from the previous step u_{j-1} are fed to the DRTO model in order to compute the actual trajectories for the outputs y_j^{DRTO}. The DRTO plant response provide disturbance estimates for the next MPC calculations. Economic optimization

is performed based on these disturbances predictions and new reference trajectories are determined y_j^{ref}. The disturbance estimates from y_j^{DRTO} along with the new trajectories y_j^{ref} are given to the MPC model to compute new corresponding control moves. At the end of the prediction horizon, the last outputs y_N^{DRTO} are used in the economic optimization to compute the set-point trajectories y^{SP} supplied to the plant MPC. The MPC will then determine the control moves to apply to the process u^{MPC}. Finally, the outputs of the process will be measured y^m and sent to the first step of the closed-loop prediction. In Figure I.7, scheduling decisions are also included in the DRTO framework.

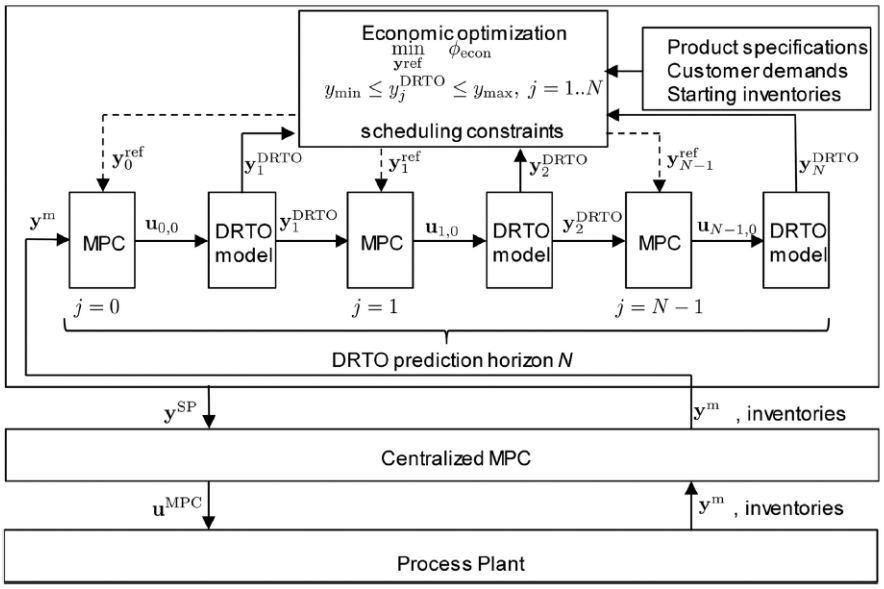

Figure I.7: The architecture of a closed-loop two-layer DRTO (Remigio and Swartz; 2020)

This closed-loop two-layer DRTO problem can be solved in different ways. In a sequential approach, the optimization determines updated trajectories and then a dynamic simulation generates the closed-loop plant response. These steps are performed iteratively until the minimum of the objective function is reached. This resolution method is used by Pataro *et al.* but they point out some stability and convergence difficulties (Pataro, da Costa and Joseph; 2020). The other method adopted in (Jamaludin and Swartz; 2016), (Remigio and Swartz; 2020) and (Li and Swartz; 2019) is the simultaneous approach. The MPC subproblems are transformed into complementary constraints using their conditions of optimality and are moved in the constraints set of the DRTO problem resulting in a single-level mathematical program with complementarity constraints (MPCC). This formulation was improved to include planning decisions (Remigio and Swartz; 2020) or distributed MPC systems for each subsystem of the plant (Li and Swartz; 2019). Although the closed-loop two-layer DRTO scheme performs slightly better than the open-loop two-layer DRTO, it is at the price of higher computational time. This method is still at an early stage of research and its application to a real system has never been tested. Thus, in this review, the focus is made on open-loop two-layer DRTO.

I.6.4 Multi-objective two-layer DRTO

In a few studies, multi-objective two-layer DRTO is performed. Ravi *et al.* had two hierarchical objectives: the tracking of the quality of their final product and the maximization of the overall profit on plant scale (Ravi and Kaisare; 2020). The tracking objective was formulated in the objective function as the minimization of the squared deviation between the reference and the actual qualities at the terminal point of the time step. The multi-objective problem was solved thanks to the Lexicographic method. The optimal solution for the priority quality objective was retained through an additional constraint for the economic optimization. The Pareto front was generated and the optimal solution was chosen to be the closest to the standalone optimal solution of the respective objective function. Kim *et al.* optimized an energy system with both economic and environmental objectives (Kim; 2020). As in the previous study, the two objectives are here conflicting: an improvement of one objective results in a decline of the second objective. A Tchebycheff weighted metric method was used to find the Pareto optimum without computing the complete Pareto front. Zhang *et al.* optimized the operation of an integrated energy system with several energy carriers (Zhang et al.; 2021). Their system included renewable energy sources and the associated uncertainty due to weather conditions. The two levels of optimization had a multi-objective function each: benefits maximization and customer satisfaction for the offline optimization and to limit the deviation from the offline trajectories and to ensure safe operation for the online optimization. An adapted GA was used to solve the multi-objective problems. These works show that it is possible to perform multi-objective two-layer DRTO.

I.6.5 Coupling between an offline planning and DRTO

The wide range of time scales in a problem sometimes imposes the use of distinct optimization layers. In Section I.3, the planning and the RTO levels were introduced. Although both optimization strategies have been applied to solar thermal systems in the literature, there was no coupling between them. Yet, the association of an offline and an online phase could benefit to the operation of a solar system and has been implemented previously for other processes.

For instance, Clarke *et al.* used an upper level planning controller to plan the storage levels of electric systems offline, on a slow time scale, and an EMPC on a lower level controlled the fast dynamics online while performing an economic optimization of the operation of the system (Clarke et al.; 2018). The time decomposition was necessary because storage has very slow dynamics compared to the other components of the system and the storage utilization has to be determined on a rather long time horizon to benefit from it. On the other hand, the system presents fast disturbances that need to be rejected on a small sampling time. The architecture of the two layers is presented in Figure I.8. In this Figure, $\bar{x}^B$ represents the storage state target set-point and u is the control input.

The upper layer is an offline planning while the lower layer is an EMPC. The storage state targets are the values passed from the offline optimization to the online optimization. Rossi *et al.* also had an offline and an online phases in their optimization

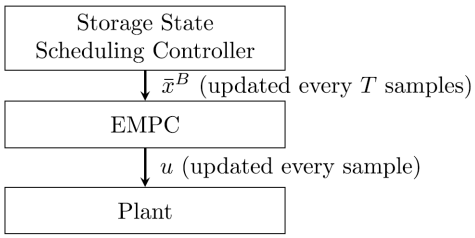

Figure I.8: Hierarchical control structure for a system with storage (Clarke et al.; 2018)

of multi-unit batch processes (Rossi et al.; 2017). Distinct objective functions were used in the two steps, with an economic objective present in each of the two layers. Some constant key parameters were passed from the offline to the online optimization steps, such as the number of batch cycles. During the second phase, the offline campaign schedule was updated in real-time and optimal control actions were generated. Zhang *et al.* optimized an integrated energy system (WE: We-Energy) including renewable energy sources (Zhang et al.; 2021), whose approach is shown in Figure I.9. A day-ahead planning was first performed offline, based on the daily energy prices, the renewable energy (RE) forecasts and the energy load. In order to maximize economic profit and customer satisfaction, the shifting of the flexible loads and the amount of energy traded with the networks were determined. Then, real-time optimization balances the renewable energy forecast error thanks to real-time information. A new operation strategy is determined, with some units following the day-ahead plan if they are not flexible enough to be adjusted in real-time. The goal in this step is to minimize the deviation between the day-ahead energy deal plan and the real-time deal.

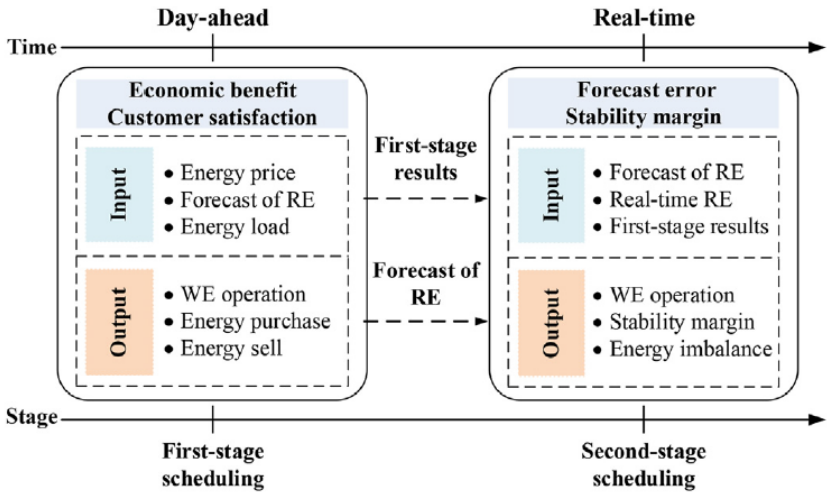

Figure I.9: The framework of the optimal planning of an integrated energy system (Zhang et al.; 2021)

Here, the uncertainty on the renewable energy forecast is corrected thanks to an online phase. Such a strategy seems perfectly adapted to solar systems.

I.7 Comparison of the different schemes

The three different real-time optimization schemes presented earlier are summarized in Figure I.10, based on a schematic in (Würth et al.; 2011), with a possible offline phase. The first scheme, SRTO, will not be studied much further as it only provides constant set-points values and is not well suited to a dynamic system, always in transient state and with various time scales. The advantages and disadvantages of the EMPC and the two-layer DRTO schemes have already been discussed. Caspari *et al.* compared the

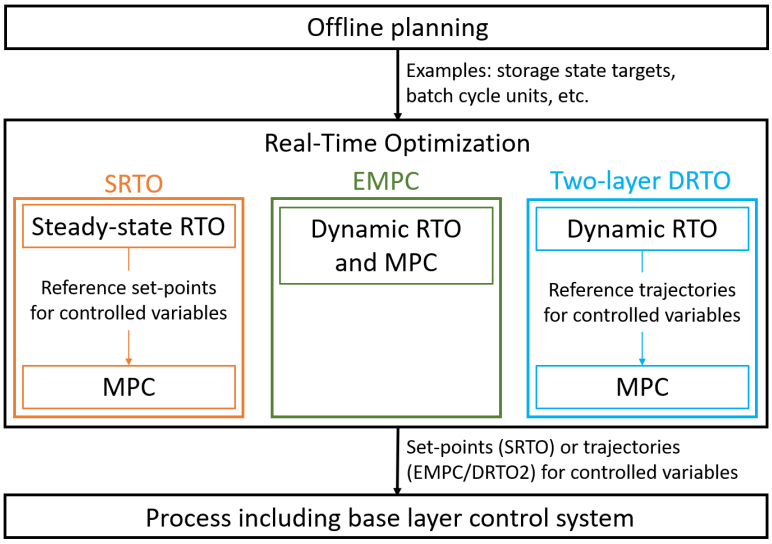

Figure I.10: The three different schemes in real-time optimization

two schemes for the optimization of a continuous air separation unit (Caspari et al.; 2020). The EMPC showed slightly better economic improvements even with a reduced model to decrease the computational requirements. It achieved 0.2 to 2.4 times higher economic performance compared to the improvements of the two-layer DRTO scheme. However, the authors outlined some downsides of choosing the EMPC scheme. First, it requires a new infrastructure to be installed on an existing plant. Also, the EMPC generated more aggressive control moves due to the smaller time step, which can lead to accelerated deterioration of the system components. Furthermore, the two-layer DRTO made a better use of the storage because of its longer time horizon. Given the current computational performances, the two-layer DRTO scheme seems more suitable for the optimization of a large-scale system despite its slightly lower economic improvements.

I.8 Perspectives on the application of DRTO to solar thermal plants

Based on this literature review, a lack of studies focusing on the DRTO of a complete solar thermal plant is noticed. Most authors performed offline dynamic optimization based on perfect weather forecasts and did not test their methodology online. These papers show the benefits resulting from dynamic optimization, but the methods presented are not readily applicable to a real plant. Indeed, the trajectories are computed

based on weather and load forecasts and are not updated online with plant measurements. Thus, the trajectories will probably become sub-optimal and the controllers might not even be able to track them. There are some studies using an EMPC scheme to optimize a solar system, but it required model simplifications and the use of storage was not optimal. A two-layer scheme, composed of a SRTO and controllers, has been used in (Rashid, Safdarnejad and Powell; 2019), but it was applied to a CSP plant without storage. There is only one study in which two-layer DRTO was performed, but it just optimized the operation of the solar field and not the complete solar plant including pipes and storage. Nevertheless, two-layer DRTO seems well-suited to improve the performances of solar thermal plants. Furthermore, if tested using a detailed simulation model, two-layer DRTO should be readily applicable to a real plant since it models both the optimization and the control layers.

The complete optimization strategy that could possibly be used to optimize the operation of a solar thermal plant is presented in Figure I.11 and entails a planning phase and a two-layer DRTO methodology. This hierarchical diagram clarifies the different time scales used for each step and the flow of information in the control structure.

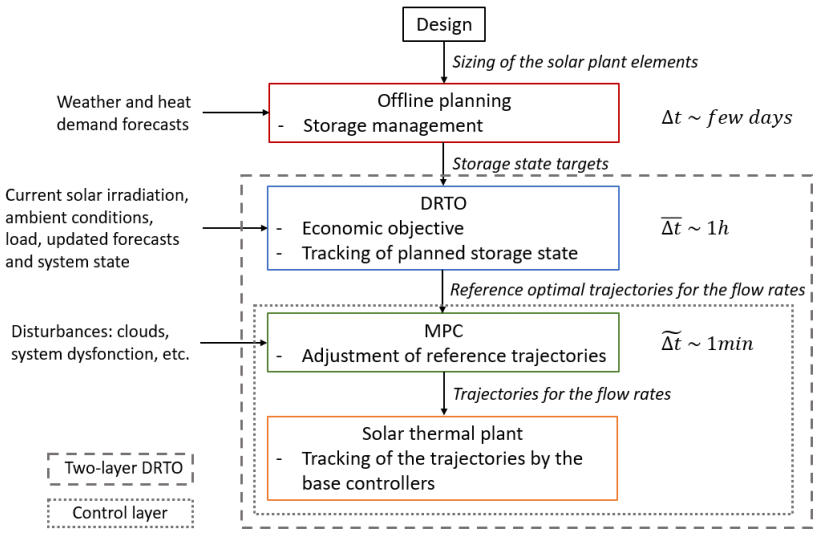

Figure I.11: Complete optimization strategy for a solar thermal plant

The design of the plant and the storage management could be determined offline using weather forecast and planned heat demand (as in subsection I.6.5) and sent to the DRTO level (as a market and environment information in Figure I.6). The storage planning should be made over a time period ensuring good strategic vision. It might be necessary to compute a new plan before the end of the current one if the forecasts are too inaccurate.

The DRTO layer could take into account the current solar irradiation and load measured on the system and updated forecasts. They would represent the slow disturbances $\overline{d}$ in Figure I.6. The optimal trajectories would therefore be adapted to changes in the weather or the load, on an hourly basis for example, or with other triggering methods (see subsection I.6.1). The solar irradiation and load forecasts used on the time horizon of the DRTO are updated forecasts. These forecasts will provide accurate but averaged values for the next few hours and they will not be able to predict

the actual weather and load with a very precise time step. Finally, the fast disturbances, $\tilde{d}$ in Figure I.6, such as cloud movements, would be handled at the MPC level. The averaged solar irradiation used in the DRTO level will be less variable than the actual irradiation, which is affected by clouds moving fast in the sky. Solar thermal plant could benefit from DRTO to correct weather forecast uncertainties and achieve a smoother and enhanced energy supply. To summarize the proposed methodology, Figure I.12 is the system diagram from Figure I.4 adapted to a solar thermal plant, given as an example of a possible scheme for the optimization of the operation of such systems. The measured outputs are the temperatures and flow rates in the system, as well as some environmental parameters, such as solar irradiation (noted DNI for Direct Normal Irradiation in Figure I.12). An example of an estimated parameter in this application is the heat transfer coefficient in the heat exchangers.

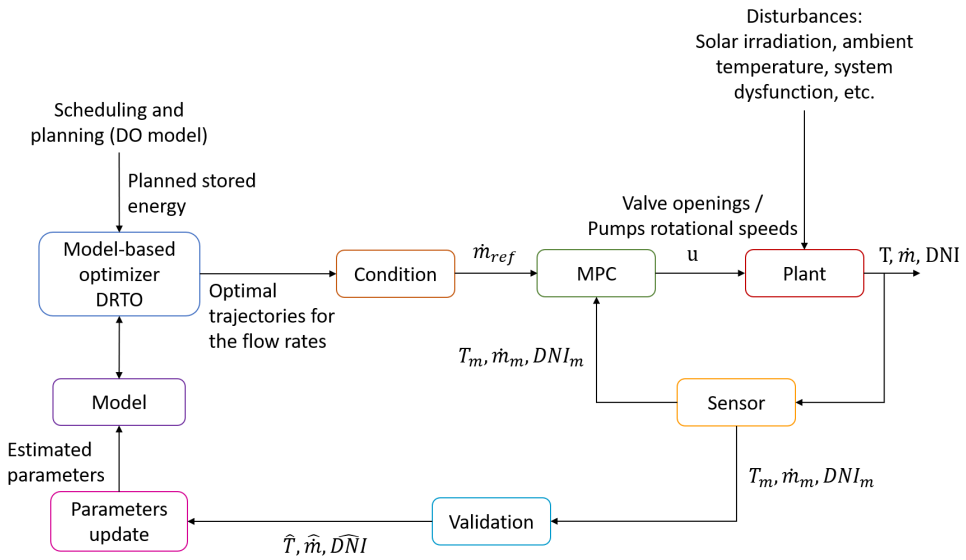

Figure I.12: Control diagram for the optimization of a solar thermal plant

Future works should focus on the two-layer DRTO of solar thermal plants and assess the benefits of using this methodology compared to standard control strategies or offline dynamic optimization. Since two-layer DRTO includes control, work could also be done to improve controllers, which track the optimal trajectories, in terms of uncertainty handling and disturbance rejection.

I.9 Conclusion

This review is focused on the mathematical optimization of the operation of a solar thermal plant, and particularly on the heat production and storage. It shows that dynamic optimization is often carried out in research papers to minimize the cost of the solar thermal plant operation. Optimal trajectories are computed for the decision variables in the system, taking into account the various dynamics of the components of the plant, such as the solar field and storage tank, and the variable environmental conditions. Improvements in the performance of the solar thermal plant, in terms of solar utilization and costs, are achieved thanks to dynamic optimization. However,

the uncertainty in weather and demand forecasts cannot be corrected with an offline optimization. Thus, the dynamic optimization methodologies are not readily applicable to real plants. This review then presents the different schemes of real-time optimization which appears to be a powerful tool to control a process and maximize its benefits. The measurements performed on the actual system allow the optimization algorithm to represent accurately the system and its environment at the current time and thus to provide regularly updated optimal set-points or trajectories. The control layer track these reference set-points or trajectories in the presence of disturbances. The analysis work conducted in this paper shows the potential of two-layer DRTO in association with a planning phase to optimize the operation of a solar thermal plant. The analysis is based on research articles in chemical engineering, where two-layer DRTO is studied in depth. This review provides perspectives on the application of two-layer DRTO to solar thermal plants with details on its possible implementation. Future research should focus on the DRTO of solar thermal plants, including control, in association with a planning phase, to reduce their operating cost, help to meet the heat load and cut down the fossil fuels consumption in heat production.

Acknowledgements

The project leading to this publication has received funding from Excellence Initiative of Université de Pau et des Pays de l'Adour – I-Site E2S UPPA, a French "Investissements d'Avenir" programme.

Bibliography

Alonso, A. A., Arias-Méndez, A., Balsa-Canto, E., García, M. R., Molina, J. I., Vilas, C. and Villafín, M. (2013). Real time optimization for quality control of batch thermal sterilization of prepackaged foods, *Food Control* **32**: 392–403.

Ammar, M. B., Chaabene, M. and Chtourou, Z. (2013). Artificial Neural Network based control for PV/T panel to track optimum thermal and electrical power, *Energy Conversion and Management* **65**: 372–380.

Amrit, R., Rawlings, J. B. and Biegler, L. T. (2013). Optimizing process economics online using model predictive control, *Computers & Chemical Engineering* **58**: 334–343.

Arpornwichanop, A., Kittisupakorn, P. and Mujtaba, I. (2005). On-line dynamic optimization and control strategy for improving the performance of batch reactors, *Chemical Engineering and Processing: Process Intensification* **44**: 101–114.

Awan, A. B., Chandra Mouli, K. V. and Zubair, M. (2020). Performance enhancement of solar tower power plant: A multi-objective optimization approach, *Energy Conversion and Management* **225**: 113378.

Bahari, M., Ahmadi, A. and Dashti, R. (2021). Exergo-economic analysis and optimization of a combined solar collector with steam and Organic Rankine Cycle using

particle swarm optimization (PSO) algorithm, *Cleaner Engineering and Technology* **4**: 100221.

Berenguel, M., Cirre, C. M., Klempous, R., Maciejewski, H., Nikodem, M., Nikodem, J., Rudas, I. and Valenzuela, L. (2005). Hierarchical Control of a Distributed Solar Collector Field, *EUROCAST 2005 - 10th International Conference on Computer Aided Systems Theory*, Vol. 3643, Springer, Las Palmas de Gran Canaria, Spain, pp. 614–620.

Biegler, L. T. and Grossmann, I. E. (2004). Retrospective on optimization, *Computers & Chemical Engineering* **28**: 1169–1192.

Blackburn, L. D., Tuttle, J. F. and Powell, K. M. (2020). Real-time optimization of multi-cell industrial evaporative cooling towers using machine learning and particle swarm optimization, *Journal of Cleaner Production* **271**: 122175.

Brodrick, P. G., Brandt, A. R. and Durlofsky, L. J. (2017). Operational optimization of an integrated solar combined cycle under practical time-dependent constraints, *Energy* **141**: 1569–1584.

Brodrick, P. G., Brandt, A. R. and Durlofsky, L. J. (2018). Optimal design and operation of integrated solar combined cycles under emissions intensity constraints, *Applied Energy* **226**: 979–990.

Camacho, E., Rubio, F., Berenguel, M. and Valenzuela, L. (2007a). A survey on control schemes for distributed solar collector fields. Part I: Modeling and basic control approaches, *Solar Energy* **81**(10): 1240–1251.

Camacho, E., Rubio, F., Berenguel, M. and Valenzuela, L. (2007b). A survey on control schemes for distributed solar collector fields. Part II: Advanced control approaches, *Solar Energy* **81**(10): 1252–1272.

Casella, F., Casati, E. and Colonna, P. (2014). Optimal Operation of Solar Tower Plants with Thermal Storage for System Design, *IFAC Proceedings volumes - 19th World Congress*, Cape Town, South Africa, pp. 4972–4978.

Caspari, A., Tsay, C., Mhamdi, A., Baldea, M. and Mitsos, A. (2020). The integration of scheduling and control: Top-down vs. bottom-up, *Journal of Process Control* **91**: 50–62.

Chachuat, B., Srinivasan, B. and Bonvin, D. (2009). Adaptation strategies for real-time optimization, *Computers & Chemical Engineering* **33**: 1557–1567.

Clarke, W. C., Manzie, C. and Brear, M. J. (2018). Hierarchical economic MPC for systems with storage states, *Automatica* **94**: 138–150.

Collier, U. (2018). Renewable Heat Policies - Delivering clean heat solutions for the energy transition, *Insights Series 2018 - International Energy Agency* .

Cox, S. J., Kim, D., Cho, H. and Mago, P. (2019). Real time optimal control of district cooling system with thermal energy storage using neural networks, *Applied Energy* **238**: 466–480.

Csordas, G., Brunger, A., Hollands, K. and Lightstone, M. (1992). Plume entrainment effects in solar domestic hot water systems employing variable-flow-rate control strategies, *Solar Energy* **49**(6): 497–505.

Darby, M. L., Nikolaou, M., Jones, J. and Nicholson, D. (2011). RTO: An overview and assessment of current practice, *Journal of Process Control* **21**: 874–884.

De Oliveira, V., Jaschke, J. and Skogestad, S. (2013). Dynamic online optimization of a house heating system in a fluctuating energy price scenario, *IFAC Proceedings Volumes - 10th International Symposium on Dynamics and Control of Process Systems*, Elsevier, Mumbai, India, pp. 463–468.

Delubac, R., Serra, S., Sochard, S. and Reneaume, J.-M. (2021). A Dynamic Optimization Tool to Size and Operate Solar Thermal District Heating Networks Production Plants, *Energies* **14**(23): 8003.

Dikmen, E., Ayaz, M., Ezen, H. H., Küçüksille, E. U. and Şahin, A. e. (2014). Estimation and optimization of thermal performance of evacuated tube solar collector system, *Heat and Mass Transfer* **50**(5): 711–719.

Elixmann, D., Busch, J. and Marquardt, W. (2010). Integration of model-predictive scheduling, dynamic real-time optimization and output tracking for a wastewater treatment process, *IFAC Proceedings Volumes - 11th International Symposium on Computer Applications in Biotechnology*, Vol. 43, Elsevier, Leuven, Belgium, pp. 90–95.

Ellingwood, K., Mohammadi, K. and Powell, K. (2020a). Dynamic optimization and economic evaluation of flexible heat integration in a hybrid concentrated solar power plant, *Applied Energy* **276**: 115513.

Ellingwood, K., Mohammadi, K. and Powell, K. (2020b). A novel means to flexibly operate a hybrid concentrated solar power plant and improve operation during non-ideal direct normal irradiation conditions, *Energy Conversion and Management* **203**: 112275.

Elsheikh, A. H., Sharshir, S. W., Abd Elaziz, M., Kabeel, A., Guilan, W. and Haiou, Z. (2019). Modeling of solar energy systems using artificial neural network: A comprehensive review, *Solar Energy* **180**: 622–639.

Engell, S. (2007). Feedback control for optimal process operation, *Journal of Process Control* **17**: 203–219.

Farkas, I. and Géczy-Víg, P. (2003). Neural network modelling of flat–plate solar collectors, *Computers and Electronics in Agriculture* **40**(1-3): 87–102.

Ghritlahre, H. K. and Prasad, R. K. (2018). Application of ANN technique to predict the performance of solar collector systems - A review, *Renewable and Sustainable Energy Reviews* **84**: 75–88.

Gil, J. D., Roca, L., Zaragoza, G., Normey-Rico, J. E. and Berenguel, M. (2020). Hierarchical control for the start-up procedure of solar thermal fields with direct storage, *Control Engineering Practice* **95**: 104254.

Gálvez-Carrillo, M., De Keyser, R. and Ionescu, C. (2009). Nonlinear predictive control with dead-time compensator: Application to a solar power plant, *Solar Energy* **83**: 743–752.

Hamilton, W. T., Newman, A. M., Wagner, M. J. and Braun, R. J. (2020). Off-design performance of molten salt-driven Rankine cycles and its impact on the optimal dispatch of concentrating solar power systems, *Energy Conversion and Management* **220**: 113025.

Heng, S. Y., Asako, Y., Suwa, T. and Nagasaka, K. (2019). Transient thermal prediction methodology for parabolic trough solar collector tube using artificial neural network, *Renewable Energy* **131**: 168–179.

Hirvonen, J., ur Rehman, H. and Sirén, K. (2018). Techno-economic optimization and analysis of a high latitude solar district heating system with seasonal storage, considering different community sizes, *Solar Energy* **162**: 472–488.

Hotvedt, M., Hauger, S. O., Gjertsen, F. and Imsland, L. (2019). Dynamic Real-Time Optimisation of a CO2 Capture Facility, *IFAC PapersOnLine* **52**: 856–861.

Hua, X., Rohani, S. and Jutan, A. (2004). Cascade closed-loop optimization and control of batch reactors, *Chemical Engineering Science* **59**: 5695–5708.

Jamaludin, M. Z. and Swartz, C. L. (2016). Closed-loop Formulation for Nonlinear Dynamic Real-time Optimization, *IFAC PapersOnLine* **49**: 406–411.

Jannesari, H. and Babaei, B. (2018). Optimization of solar assisted heating system for electro-winning process in the copper complex, *Energy* **158**: 957–966.

Kadam, J. V., Marquardt, W., Schlegel, M., Backx, T., Bosgra, O. H., Dünnebier, G., van Hessem, D., Tiagounov, A. and de Wolf, S. (2003). Towards integrated dynamic real-time optimization and control of industrial processes, *Proceedings Foundations of Computer-Aided Process Operations (FOCAPO2003)*, Coral Springs, Florida, pp. 593–596.

Kadam, J. V., Schlegel, M., Marquardt, W., Tousain, R. L., Van Hessem, D. H., Van Den Berg, J. and Bosgra, O. H. (2002). A Two-Level Strategy of Integrated Dynamic Optimization and Control of Industrial Processes - a Case Study, *European Symposium on Computer Aided Process Engineering*, Vol. 12, Elsevier, The Hague, The Netherlands, pp. 511–516.

Kim, R. (2020). A Tchebycheff-based multi-objective combined with a PSOSQP dynamic real-time optimization framework for cycling energy systems, *Chemical Engineering Research and Design* **156**: 180–194.

Krause, M., Vajen, K., Wiese, F. and Ackermann, H. (2003). Investigations on optimizing large solar thermal systems, *Solar Energy* **73**: 217–225.

Krishnan, S., Barton, G. and Perkins, J. (1992). Robust parameter estimation in on-line optimization—part I. methodology and simulated case study, *Computers & Chemical Engineering* **16**: 545–562.

Kumari, P. and Toshniwal, D. (2021). Deep learning models for solar irradiance forecasting: A comprehensive review, *Journal of Cleaner Production* **318**: 128566.

Li, H. and Swartz, C. L. (2019). Dynamic real-time optimization of distributed MPC systems using rigorous closed-loop prediction, *Computers & Chemical Engineering* **122**: 356–371.

Lizarraga-Garcia, E., Ghobeity, A., Totten, M. and Mitsos, A. (2013). Optimal operation of a solar-thermal power plant with energy storage and electricity buy-back from grid, *Energy* **51**: 61–70.

Loi française (2015). Loi n° 2015-992 du 17 août 2015 relative à la transition énergétique pour la croissance verte, *JORF n°0189 du 18 août 2015* .

López-Alvarez, M., Flores-Tlacuahuac, A., Ricardez-Sandoval, L. and Rivera-Solorio, C. (2018). Optimal Start-Up Policies for a Solar Thermal Power Plant, *Industrial & Engineering Chemistry Research* **57**: 1026–1038.

Ochoa, S., Repke, J.-U. and Wozny, G. (2009). Plantwide Optimizing Control for the Bio-ethanol Process, *IFAC Proceedings Volumes - 7th IFAC Symposium on Advanced Control of Chemical Processes*, Vol. 42, Elsevier, Istanbul, Turkey, pp. 42–51.

Orsini, R. M., Brodrick, P. G., Brandt, A. R. and Durlofsky, L. J. (2021). Computational optimization of solar thermal generation with energy storage, *Sustainable Energy Technologies and Assessments* **47**: 101342.

Parvareh, F., Milani, D., Sharma, M., Chiesa, M. and Abbas, A. (2015). Solar repowering of PCC-retrofitted power plants; solar thermal plant dynamic modelling and control strategies, *Solar Energy* **119**: 507–530.

Pataro, I. M., da Costa, M. V. A. and Joseph, B. (2020). Closed-loop dynamic real-time optimization (CL-DRTO) of a bioethanol distillation process using an advanced multilayer control architecture, *Computers & Chemical Engineering* **143**: 107075.

Pataro, I. M. L., Roca, L., Sanches, J. L. G. and Berenguel, M. (2020). An economic D-RTO for thermal solar plant: analysis and simulations based on a feedback linearization control case, *XXIII Congresso Brasileiro de Automática*, Virtual event.

Pintaldi, S., Li, J., Sethuvenkatraman, S., White, S. and Rosengarten, G. (2019). Model predictive control of a high efficiency solar thermal cooling system with thermal storage, *Energy and Buildings* **196**: 214–226.

Pontes, K. V., Wolf, I. J., Embiruçu, M. and Marquardt, W. (2015). Dynamic Real-Time Optimization of Industrial Polymerization Processes with Fast Dynamics, *Industrial & Engineering Chemistry Research* **54**: 11881–11893.

Powell, K. M., Hedengren, J. D. and Edgar, T. F. (2013). Dynamic optimization of a solar thermal energy storage system over a 24 hour period using weather forecasts, *Proceedings of the 2013 American Control Conference (ACC)*, Washington, DC, pp. 2946–2951.

Powell, K. M., Hedengren, J. D. and Edgar, T. F. (2014). Dynamic optimization of a hybrid solar thermal and fossil fuel system, *Solar Energy* **108**: 210–218.

Rashid, K., Ellingwood, K., Safdarnejad, S. M. and Powell, K. M. (2019). Designing Flexibility into a Hybrid Solar Thermal Power Plant by Real-Time, Adaptive Heat Integration, *Proceedings of the 9th International Conference on Foundations of Computer-Aided Process Design*, Elsevier, Copper Mountain, Colorado, USA, pp. 457–462.

Rashid, K., Safdarnejad, S. M. and Powell, K. M. (2019). Process intensification of solar thermal power using hybridization, flexible heat integration, and real-time optimization, *Chemical Engineering and Processing - Process Intensification* **139**: 155–171.

Rashid, K., Sheha, M. N. and Powell, K. M. (2018). Real-time optimization of a solar-natural gas hybrid power plant to enhance solar power utilization, *Proceedings of the 2018 American Control Conference (ACC)*, IEEE, Milwaukee, WI, USA, pp. 3002–3007.

Ravi, A. and Kaisare, N. S. (2020). A multi-objective dynamic RTO for plant-wide control, *IFAC PapersOnLine* **53-1**: 368–373.

Remigio, J. E. and Swartz, C. L. (2020). Production scheduling in dynamic real-time optimization with closed-loop prediction, *Journal of Process Control* **89**: 95–107.

Renewable Energy Directive (2018). Directive (EU) 2018/2001 of the European Parliament and of the Council of 11 December 2018 on the promotion of the use of energy from renewable sources, *OJ* **L328/82**.

Rohman, F. S., Sata, S. A. and Aziz, N. (2019). Online dynamic optimization studies of autocatalytic esterification in the semi batch reactor for handling disturbance and uncertainty, *Computers & Chemical Engineering* **129**: 106516.

Rossi, F., Casas-Orozco, D., Reklaitis, G., Manenti, F. and Buzzi-Ferraris, G. (2017). A computational framework for integrating campaign scheduling, dynamic optimization and optimal control in multi-unit batch processes, *Computers & Chemical Engineering* **107**: 184–220.

Ruiz-Moreno, S., Frejo, J. R. D. and Camacho, E. F. (2021). Model predictive control based on deep learning for solar parabolic-trough plants, *Renewable Energy* **180**: 193–202.

Scolan, S., Serra, S., Sochard, S., Delmas, P. and Reneaume, J.-M. (2020). Dynamic optimization of the operation of a solar thermal plant, *Solar Energy* **198**: 643–657.

Serale, G., Fiorentini, M., Capozzoli, A., Cooper, P. and Perino, M. (2018). Formulation of a model predictive control algorithm to enhance the performance of a latent heat solar thermal system, *Energy Conversion and Management* **173**: 438–449.

Shokri, S., Hayati, R., Marvast, M. A., Ayazi, M. and Ganji, H. (2009). Real time optimization as a tool for increasing petroleum refineries profits, *Petroleum and Coal* **51 (2)**: 110–114.

Tian, Z., Perers, B., Furbo, S. and Fan, J. (2018). Thermo-economic optimization of a hybrid solar district heating plant with flat plate collectors and parabolic trough collectors in series, *Energy Conversion and Management* **165**: 92–101.

United Nations Framework Convention on Climate Change (2015). Adoption of the paris agreement, *21st Conference of the Parties* .

Vasallo, M. J., Cojocaru, E. G., Gegúndez, M. E. and Marín, D. (2021). Application of data-based solar field models to optimal generation scheduling in concentrating solar power plants, *Mathematics and Computers in Simulation* **190**: 1130–1149.

Vettenranta, J., Smeds, S., Yli-Opas, K., Sourander, M., Vanhamäki, V., Aaljoki, K., Bergman, S. and Ojala, M. (2006). Closed loop dynamic optimization of production plants, *IFAC Proceedings Volumes - 1st IFAC Workshop on Applications of Large Scale Industrial Systems*, Vol. 39, Elsevier, Helsinki, Finland, pp. 161–166.

Wagner, M. J., Hamilton, W. T., Newman, A., Dent, J., Diep, C. and Braun, R. (2018). Optimizing dispatch for a concentrated solar power tower, *Solar Energy* **174**: 1198–1211.

Wagner, M. J., Newman, A. M., Hamilton, W. T. and Braun, R. J. (2017). Optimized dispatch in a first-principles concentrating solar power production model, *Applied Energy* **203**: 959–971.

Weiss, W. and Spörk-Dür, M. (2021). Global Market Development and Trends in 2020 Detailed Market Data 2019, *Solar Heating and Cooling Programme - International Energy Agency* .

Winterscheid, C., Dalenbäck, J.-O. and Holler, S. (2017). Integration of solar thermal systems in existing district heating systems, *Energy* **137**: 579–585.

Wittmann, M., Eck, M., Pitz-Paal, R. and Müller-Steinhagen, H. (2011). Methodology for optimized operation strategies of solar thermal power plants with integrated heat storage, *Solar Energy* **85**: 653–659.

Würth, L., Hannemann, R. and Marquardt, W. (2011). A two-layer architecture for economically optimal process control and operation, *Journal of Process Control* **21**: 311–321.

Zhang, N., Sun, Q. and Yang, L. (2021). A two-stage multi-objective optimal scheduling in the integrated energy system with We-Energy modeling, *Energy* **215**: 119121.

Zhang, Z. (1997). Parameter estimation techniques: A tutorial with application to conic fitting, *Image and Vision Computing pages* **15**: 59–76.

Zubair, M., Awan, A. B., Baseer, M. A., Khan, M. N. and Abbas, G. (2021). Optimization of parabolic trough based concentrated solar power plant for energy export from Saudi Arabia, *Energy Reports* **7**: 4540–4554.

I.10 Additional clarifications

- The distinction between parametric and data-driven models used in this paper was found in (Vasallo et al.; 2021) and more details between the two categories can be found in the mentioned paper. Other definitions can be found in the literature, please note that the analysis carried out in this paper is specific to the distinction chosen.

- *Stochastic algorithms* mentioned in Subsection I.2.2 should be replaced by *non-deterministic algorithms* to maintain as much generality as possible. Moreover, when describing their advantages and disadvantages compared to deterministic algorithms, the fact that non-deterministic algorithms do not guarantee the convergence to the global minimum should be mentioned.

- In subsection I.2.2, the variables and parameters that could be involved in the optimization of the operation of a solar thermal plant are presented. It should be highlighted that the description provided is an example and other choices are possible. For instance, the controlled variables could be the flow rates or the temperatures.

- In Section I.4, a comparison is made between batch reactors and solar thermal plants. They share similar challenges such as nonlinear phenomena, uncertain parameters in their model and constantly transient behavior. Thus, it is suggested that studies on batch reactors can be used for inspiration when developing a real-time optimization study on a solar thermal system. However, it should be mentioned that batch reactors have more challenges regarding measurements (species concentration, for instance).

- The single layer scheme presented in Subsection I.5.1 was first introduced by Gouvêa and Odloak in 1998.
  Reference: Gouvêa, M. and Odloak D. (1998). One-layer real time optimization of LPG production in the FCC unit: procedure, advantages and disadvantages, *Computers & Chemical Engineering* **22**: 191-198.

- The two-layer scheme presented in Subsection I.5.2 was first introduced by Jang, Joseph and Mukai in 1987.
  Reference: Jang, S.-S., Joseph, B. and Mukai, H. (1987). On-line Optimization of Constrained Multivariable Chemical Processes, *AIChE Journal* **33**: 26-35.

Chapter II

Application of DRTO in a simple case study

Contents

In the previous chapter, the potential of DRTO for the optimization of the operation of a solar thermal plant was discussed. Suggestions were provided for the optimization methodology. Especially, a planning phase should be used for storage management, as it benefits from a longer term strategic vision. The DRTO can then adapt the optimal trajectories of the controlled variables in real-time to the current disturbances and updated forecasts. The controllers of the plant will then follow the optimal trajectories despite new disturbances. The proposed methodology was tested in this chapter in a simple case study.

This chapter is an article published in *Computers & Chemical Engineering* (Untrau et al.; 2023a). The first part summarizes the context of the study and the state of the art on the optimization of the operation of solar thermal plants. This part is a shorter presentation of the analysis presented in the previous chapter and the hurried reader could skip it. Then, in Section II.2, the model developed for the solar thermal plant is presented. In the following section, the DRTO methodology is explained in details, following the suggestions from the previous chapter. The DRTO methodology is tested on a detailed simulation model representing the real solar thermal plant. To simplify, the controllers are not included in the detailed model and the optimal trajectories for the flow rates, obtained from the DRTO, are perfectly tracked. The methodology is tested in a simple case study, presented in Section II.4. Weather forecasts are used in the planning phase for 2 days. Then, the DRTO methodology is tested for the first day only, with an artificial disturbance introduced in the solar irradiation. The heat demand is constant and perfectly known. The economic objective function of the DRTO level includes a term tracking the planned stored energy at the end of the day. A new DRTO is run every hour, providing new optimal trajectories to the simulated plant. The first result presented is the adjustment of the weight on the storage state tracking term in the DRTO objective function. The impact of this weight on the optimization results are discussed and a weight offering a good compromise between the tracking and the economic performances for the day is chosen. Then, with the weight determined previously, an extended case study is carried out in Section II.6. Several disturbances scenarios are tested in 3 different seasons to analyze the performances of this DRTO methodology. The results are compared to simulations following the trajectories determined during the planning phase and without any real-time adaptation. The performances of the simulated solar thermal plant following trajectories determined with or without real-time adaptation are compared in terms of operating cost, solar fraction, excess heat delivered and final stored energy. The results show improvements in most performance indicators for all scenarios tested when using DRTO.

Article reference:

Untrau, A., Sochard, S., Marias, F., Reneaume, J.-M., Le Roux, G. A. C. and Serra, S. (2023a). Dynamic Real-Time Optimization of a solar thermal plant during daytime, *Computers & Chemical Engineering* **172:** 108184.

Dynamic Real-Time Optimization of a Solar Thermal Plant during daytime

Alix Untrau[a*], Sabine Sochard[b], Frédéric Marias[c], Jean-Michel Reneaume[d], Galo A.C. Le Roux [e] and Sylvain Serra[f]

[a,b,c,d,f] Universite de Pau et des Pays de l'Adour, E2S UPPA, LaTEP, Pau, France,

[*] alix.untrau@univ-pau.fr

[e] Universidade de São Paulo, Escola Politécnica, São Paulo, Brazil

Published in *Computers & Chemical Engineering*, **172** (2023) 108184

Abstract

This paper presents an economic Dynamic Real-Time Optimization (DRTO) of the operation of a solar thermal plant. The methodology includes a planning phase, used to improve storage management. A storage state target is included in the economic objective function of the DRTO, with a weight adjusted through a sensitivity analysis. The methodology is tested with a simulation model in a case study representing different seasons. The simulation results using the trajectories for the flow rates obtained with the DRTO algorithm or with the offline planning phase are compared, for several real-time scenarios. Thanks to our DRTO methodology, the operating cost and the excess energy delivered were reduced, the part of solar energy used to satisfy the heat demand was increased and a reasonable tracking of the storage state target was achieved. This study brings good perspectives for the implementation of our DRTO methodology on an actual plant.

Nomenclature

Abbreviations

OF_{eco} Economic Objective Function [€]
CFD Computational Fluid Dynamics
CSP Concentrated Solar Power
DAE Differential Algebraic Equation
DHN District Heating Network
DO Dynamic Optimization
DRTO Dynamic Real-Time Optimization
GHI Global Horizontal Irradiance $[W.m^{-2}]$
HRTO Hybrid Real-Time Optimization
MAPE Mean Absolute Percentage Error
MPC Model Predictive Control
NLP Nonlinear Programming
OCFE Orthogonal Collocation on Finite Elements
ODE Ordinary Differential Equation
OF Objective Function
PDE Partial Differential Equation
PID Proportional Derivative Integral
ROPA Real-time Optimization with Persistent Adaptation
RTO Real-Time Optimization
S-DO Simulation based on Dynamic Optimization
S-DRTO Simulation based on Dynamic Real-Time Optimization
SF Solar Field
TES Thermal Energy Storage

Greek Symbols

ΔP_{max} Pressure drop at the maximum flow rate $[Pa]$
Δz Height of a discretization layer in the storage tank $[m]$
η Overall efficiency of the pump
$\eta_{0,b}$ Optical Efficiency of a collector
η_{sh} Shading effect of a solar field loop onto the next loop
γ_{demand} Weight on the penalty term for the respect of the heat demand
γ_{var} Weight on the penalty term to smooth the flow rates trajectories
$\gamma_{var\ init}$ Weight on the penalty term to smooth the flow rates trajectories from one DRTO run to the next
ω Weight on the storage state tracking term
Φ_{demand} Penalty term for the respect of the heat demand
ϕ_i Excess in the consumer outlet temperature at the time step i
Φ_{var} Penalty term to smooth the flow rates trajectories
$\Phi_{var\ init}$ Penalty term to smooth the flow rates trajectories from one DRTO run to the next
ρ Fluid density $[kg.m^{-3}]$

Latin Symbols

$\dot{m}$ Mass flow rate $[kg.s^{-1}]$
$\dot{m}_{adjust}$ Mass flow rate in the recirculating pipe to adjust the supply temperature $[kg.s^{-1}]$
$\dot{m}_{charge}$ Mass flow rate to charge the storage tank $[kg.s^{-1}]$
$\dot{m}_{discharge}$ Mass flow rate to discharge the storage tank $[kg.s^{-1}]$
$\dot{m}_{max}$ Maximum flow rate allowed in the pump $[kg.s^{-1}]$
$\dot{m}_{production}$ Mass flow rate in the cold side of heat exchanger 1 $[kg.s^{-1}]$
$\dot{m}_{solarfield}$ Mass flow rate in the solar field $[kg.s^{-1}]$
$\dot{m}_{supply}$ Mass flow rate in the hot side of heat exchanger 2 $[kg.s^{-1}]$
$\dot{P}_{elec}$ Electric power $[W]$
$\dot{P}_{hydrau}$ Maximum pumping power $[W]$
$\dot{Q}_{gas}$ Power produced in the gas backup heater $[W]$
$\dot{Q}_{SF}$ Power transmitted from the sun to the heating fluid in the whole solar field $[W]$
A Tank cross sectional area $[m^2]$
A_{eq} Area of the equivalent surface panel representing the solar field $[m^2]$
c_1 Heat loss coefficient in the collector at $T_m = T_{amb}$ $[W.m^{-2}.K^{-1}]$
c_2 Temperature dependence of the heat loss coefficient $[W.m^{-2}.K^{-1}]$
c_5 Effective thermal capacity $[J.m^{-2}.K^{-1}]$
C_p Fluid specific heat capacity $[J.kg^{-1}.K^{-1}]$
E_{elec} Electricity consumed $[MWh]$
E_{excess} Excess heat delivered to the consumer, exceeding the heat demand $[MWh]$
E_{stored} Energy stored in the storage tank $[MWh]$
$E_{stored\ DRTO}$ Energy stored in the storage tank computed with the DRTO methodology $[MWh]$
$E_{stored\ planning}$ Energy stored in the storage tank predicted during the planning phase $[MWh]$
$E_{supplied}$ Heat supplied to the consumer $[MWh]$
$ElecPrice$ Price of electricity $[€/MWh]$
G_b Direct irradiation (beam) in the plane of a collector $[W.m^{-2}]$
G_d Diffuse irradiation in the plane of a collector $[W.m^{-2}]$
$GasPrice$ Price of gas $[€/MWh]$
$HeatPrice$ Price of heat $[€/MWh]$
k Fluid thermal conductivity $[W.m^{-1}.K^{-1}]$
k^* Effective thermal conductivity $[W.m^{-1}.K^{-1}]$
$K_b(\theta)$ Incidence angle modifier for the direct irradiation (beam)
K_d Incidence angle modifier for the diffuse irradiation
N Number of discretization layers in the storage tank
P Tank perimeter $[m]$
S_1 Exchanger surface between the bottom layer and the ambient $[m]$
S_l Lateral surface of a tank layer $[m^2]$
S_N Exchanger surface between the top layer and the ambient $[m]$
t Time $[s]$
$T(z,t)$ Fluid temperature inside the tank $[°C]$
T_m Mean temperature in a collector $[°C]$
$T_{amb}(t)$ Ambient temperature $[°C]$
T_{charge} Temperature of the charging fluid $[°C]$
$T_{consumer\ out}$ Temperature of the consumer stream after the solar energy is delivered $[°C]$
T_{demand} Target temperature of the heat demand $[°C]$
$t_{f\ DRTO}$ End of DRTO time horizon $[s]$
T_{return} Cold temperature returning to the storage tank $[°C]$
U Tank fluid to ambient overall heat transfer coefficient $[W.m^{-2}.K^{-1}]$
U_1 Tank fluid to ambient overall heat transfer coefficient in the bottom layer $[W.m^{-2}.K^{-1}]$
U_N Tank fluid to ambient overall heat transfer coefficient in the top layer $[W.m^{-2}.K^{-1}]$
z Tank height from the bottom of the tank $[m]$

II.1 Introduction

The Paris agreement signed by 196 countries in 2015 aims at keeping global warming below 2°C compared to pre-industrial levels (United Nations Framework Convention on Climate Change; 2015). Thus, it is necessary to reduce greenhouse gases emissions in every sector of our societies. Heat represents more than half of the final energy consumption (Collier; 2018). Hence, developing renewable heat production appears crucial and institutions are fixing local targets on the share of renewable heat. For example, the Revised Renewable Energy Directive (Renewable Energy Directive; 2018), fixed a target of 1.3% increase in the share of renewable energy for heating and cooling, each year, for each member of the European Union. One way to produce renewable heat is to use solar thermal energy. Different technologies of solar collectors exist but they share the same working principle: a fluid is flowing through collectors and is heated up by solar irradiation. That way, heat is produced without emitting CO_2 (Tian and Zhao; 2013). Depending on the technologies, various levels of temperatures can be reached (Kalogirou; 2004). Mirrors can be used to concentrate the solar radiations and reach temperatures of hundred of degrees Celsius, suitable for electricity or steam production or some industrial processes. Non-concentrating technologies, which are considered in this work, can be used for space heating, domestic hot water production and industrial processes requiring low temperatures. This is mostly the case in the food and beverage industries (Koçak et al.; 2020). In a solar thermal plant, solar thermal collectors are associated with heat exchangers and Thermal Energy Storage (TES), in order to supply heat to large systems such as industries or District Heating Networks (DNH). TES are necessary because the solar irradiance is highly intermittent, with daily and seasonal variations. TES helps to decouple the heat production and the heat supply, ensuring that, at each time instant, most of the heat demand (which also varies) is met with solar energy. Both daily and seasonal TES technologies exist, but only daily TES is considered in this study. The most common daily TES employed is a sensible storage tank, which will be used in this work (Tian and Zhao; 2013). The present work has been conducted in partnership with the French company NEWHEAT, specialized in solar heat and waste-heat recovery for large heat consumers. The system considered in the paper, whose design was provided by NEWHEAT and described in Subsection II.2.1, was chosen according to their research needs. In 2020, the use of all the installed solar thermal systems used to produce heat and replacing fossil fuel burners, led to savings of 43.8 million tons of oil corresponding to 141.3 million tons of CO_2 emissions, according to an annual report from the International Energy Agency published in 2021 (Weiss and Spörk-Dür; 2021). Thus, developing solar thermal plants and making the most out of them is a key element of the energy transition (Collier; 2018).

II.1.1 Optimization of solar thermal plants

In order to improve the performances of solar thermal plants, mathematical optimization can be used. In a general optimization problem, an objective function is minimized or maximized, by adjusting the value of some decision variables, while respecting physical and operational constraints. A common objective function is the minimization of the cost. Firstly, the design of the solar thermal plant can be optimized in order to

minimize the investment cost while satisfying the heat demand. In this case, the design is optimized, assuming the plant will follow standard operating strategies. A dynamic model is employed and the objective function generally involves integral terms, but the decision variables are only design parameters such as the size of the solar field, the size of the storage tank, etc. The optimization of the design of a solar thermal plant for its integration into a larger system is an active area of research. For example, some studies optimized the design of solar plants integrated in DHN ((Hirvonen et al.; 2018), (Tian et al.; 2018),(Winterscheid et al.; 2017)), other in industrial processes ((Jannesari and Babaei; 2018), (Parvareh et al.; 2015)). Krause *et al.* highlighted the benefits from design optimization for the performances of a solar domestic hot water system. The solar heat cost was up to 18% lower with the optimized design compared to the conventionally installed system (Krause et al.; 2003). The authors also investigated the optimization of the operation of a well-designed solar thermal system. A few percents reduction in solar heat cost was achieved, which can represent important savings for a large system. A solar thermal plant is a very expensive system. Thus, a better operation and control, reducing the heat production cost, makes them more competitive against fossil fuels (Camacho et al.; 2007a). The operation of a plant is usually decomposed into several hierarchical levels, as presented in Figure II.1.

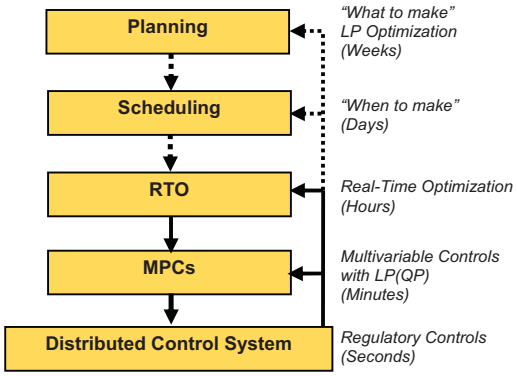

Figure II.1: Hierarchical layers for control and decision making in a plant (Darby et al.; 2011)

The two lower levels in this diagram are the control of the plant. Controllers are in charge of tracking a set point or trajectory for a controlled variable, in spite of disturbances, by adjusting the value of manipulated variables. For example, the temperature at the outlet of the solar field is generally kept constant during the standard operation of a solar thermal plant. Controllers are used to adjust the flow rate of fluid in the solar field, in order to maintain the outlet temperature at its set point. Basic controllers such as PID (Proportional Integral Derivative) controllers are often used in solar thermal plants. Nevertheless, the system characteristics are complex (nonlinear, various dynamics, changing environmental conditions) and a high order nonlinear controller would be better (Camacho et al.; 2007a). The research in this area is active, especially for concentrating solar thermal plants. Numerous advanced control methods have been developed in the last decade (Camacho et al.; 2007b) to ensure a better stability, disturbance rejection and uncertainty handling. For instance, a nonlinear predictive controller with deadtime compensator was developed to track the outlet fluid temperature of a concentrating solar field (Gálvez-Carrillo et al.; 2009). This new

controller was able to deal with highly nonlinear dynamics and variable dead-times. Maintaining a fixed temperature at the outlet of the solar field makes sure the system is run around design conditions. But it presents some drawbacks such as dumping of solar energy when the solar irradiance is not high enough to reach the target temperature. Thus, allowing a variable outlet temperature might improve the performances of the solar thermal plant (Csordas et al.; 1992). The appropriate temperature could be determined through the mathematical optimization of the operation of the plant. The optimal trajectory could then be sent to the controllers of the solar thermal plant to be tracked, as shown in Figure II.1. Offline dynamic optimization, which corresponds to the planning and scheduling levels in Figure II.1, has been applied to the operation of a solar thermal plant. Scolan *et al.* optimized the operation of a solar thermal plant including a storage tank over 36 hours during summer (Scolan et al.; 2020). Weather and load forecasts were used as inputs for the mathematical problem. The decision variables were the flow rates in the different parts of the solar thermal plant. The dynamic optimization allowed a better storage management, ensuring solar heat was used for the longer time period possible. The results in this paper were promising, with an increase in the energy provided to the consumer, a large decrease in electricity consumption, and finally an increase of 2.1% of the economic profits. The storage management might lead to counter-intuitive operating strategies when using a time horizon of several days, because it is based on a longer term strategic vision. For example, in (Scolan; 2020), the same solar thermal plant was optimized over 5 summer days. The association of high solar irradiation and low heat demand led to a risk of overheating in the solar field. To avoid overheating on day 4, the solar plant efficiency was deteriorated on day 3 to ensure an empty storage tank at the beginning of day 4. This counter-intuitive strategy was made possible by the longer term strategic vision and the use of weather forecasts. This is, to the best of our knowledge, the only works focusing on the dynamic optimization of the operation of a non-concentrating solar thermal plant. Delubac *et al.* studied the simultaneous optimization of the design and the operation of a DHN using solar energy in association with biomass and gas burners (Delubac et al.; 2021). They used a multi-period dynamic approach to determine the optimal energy mix. However, they did not model precisely the solar thermal plant. The dynamic optimization of the operation of concentrating solar thermal plants for electricity production is more commonly found in the literature (in (Casella et al.; 2014), (Lizarraga-Garcia et al.; 2013), (Wagner et al.; 2018), (Wittmann et al.; 2011) for instance). In these studies, the planning for electricity generation from the Concentrated Solar Power (CSP) plant was optimized using weather and electricity price forecasts. Thermal Energy Storage was used to store the hot fluid from the solar field for a future electricity production, allowing more degrees of freedom. In (Wittmann et al.; 2011), the planning of electricity selling was optimized in the day-ahead market, making a smart use of the backup fossil fuel burner and the TES to maximize economic profits. A time horizon between 1 and 2 days was advised to achieve a good compromise between profit gains and forecasts quality. In (Casella et al.; 2014), a detailed dynamic model for the optimal control approach is provided. Up to 7% increase in the plant revenues was achieved for a 10 day study using dynamic optimization instead of the standard control approaches. It was concluded that optimal control should be taken into account during the design phase. In (Lizarraga-Garcia et al.; 2013), the possibility to charge the TES with electric heaters and the electricity from the grid further increased the flexibility of the CSP

plant. Finally, in (Wagner et al.; 2018), a Mixed Integer Linear Program was used to maximize the electricity sales and avoid the cycle start-ups of a CSP plant. A rolling horizon of 24 hours was employed along perfect forecasts. Lower maintenance costs were obtained for the CSP plant. In these studies, dynamic optimization led to a better economic performance, exploiting the variable electricity price and the storage capacity of the plant. Dynamic optimization was also used for hybrid power plants with a solar field, a storage tank and a back up fossil fuel burner ((Powell et al.; 2014),(Brodrick et al.; 2018), (Ellingwood et al.; 2020)). In (Powell et al.; 2014), a larger amount of solar energy was collected when optimizing the flow rates in the hybrid CSP plant. This was possible because the solar field could be operated at lower temperature, leading to reduced heat losses, the target temperature being reached thanks to the backup fossil fuel burner. (Ellingwood et al.; 2020) improved the hybrid CSP plant by adding flexible heat integration. They performed dynamic optimization on their system including three TES and showed that flexible heat integration improves the performances of the plant. Finally, in (Brodrick et al.; 2018), the design and operation of a hybrid CSP plant were optimized simultaneously with two conflicting objectives: the average CO_2 emissions intensity of the electricity produced and the net present value. This study showed that optimal operation should be taken into account during the design phase of a system because it can improve the plant performances. In these studies, dynamic optimization was able to make the most out of the synergies between the two types of production. These studies showed the benefits of using dynamic optimization in order to improve solar thermal plants performances and economic profits from electricity selling for CSP plants. However, offline dynamic optimization is based on weather and load forecasts, which contain uncertainties. Indeed, the actual demand may differ from the forecasted load. But above all, solar irradiance is highly variable and the variations due to the weather are difficult to predict. The strategy determined offline may be unsuitable when new disturbances appear (such as a change in the cloud cover impacting the amount of solar radiation available) because these disturbances could not be taken into account in the offline planification. The trajectories determined offline become sub-optimal. Furthermore, too high uncertainties in the forecasts may lead to trajectories that the controllers fail to track. Therefore, offline dynamic optimization is not readily applicable to solar thermal plants. The intermediate level between offline optimization and control is Real-Time Optimization (RTO), as shown in Figure II.1. The optimization algorithm is run regularly, taking into account measurements of the plant states and the disturbances. The optimal setpoints, which will be tracked by the controllers, are updated regularly. Static RTO has been applied to a concentrating solar thermal plant without TES (Rashid et al.; 2019). In this approach, a new set point is computed when steady-state is reached. However, for a solar thermal plant with TES, static RTO cannot be applied because of the various dynamics of the subsystems, preventing the plant to reach steady-state (Matias and Le Roux; 2018). Modified RTO schemes have been proposed to avoid the steady-state wait and detection, such as ROPA (Real-time Optimization with Persistent Adaptation) (Matias and Le Roux; 2018) and HRTO (Hybrid RTO) (de Azevedo Delou et al.; 2021). These schemes were developed to avoid the steady state detection and the static parameter estimation step in RTO. However, they were still employed to improve the transient operation of systems eventually reaching steady state (Matias and Le Roux; 2018). In the case of a solar thermal plant with TES, the whole operation is dynamic with no steady state

ever reached because of the solar irradiation variability and the wide range of dynamics in the system. Thus, Dynamic RTO (DRTO) is more appropriate since it will compute new optimal trajectories, taking into account the different dynamics of the plant components. These trajectories will then be sent to the controllers of the plant to be tracked (Kadam et al.; 2002). DRTO has been widely studied in the field of chemical engineering, for instance, for a batch reactor (Arpornwichanop et al.; 2005) or a waste water treatment plant (Elixmann et al.; 2010). A thermal system has also been optimized in (De Oliveira et al.; 2013). In a context of a fluctuating energy price scenario, a house heating system was optimized with a moving horizon of 24 hours. Forecasts are used for the outside temperature and energy price. It was shown that DRTO can achieve substantial economic benefits. A simpler solution based on offline analysis and feedback control was then proposed to reduce the computational time of the online phase. In a solar thermal plant, the energy source itself is a disturbance, making its operation even more complex. However, there is only one study where DRTO was applied to a solar thermal plant (Pataro et al.; 2020). In this study, only the solar field was considered, without the TES. The flow rate in the solar field was optimized using measurements of the ambient conditions and an economic objective function. The results were promising, with a good uncertainty handling. In (Saloux and Candanedo; 2021), the primary energy use of a solar district heating system is minimized with a Model Predictive Control (MPC) approach. The system is composed of a solar field, a short term storage tank and a seasonal thermal energy storage, and simplified nonlinear models are employed. The flow rate between the two storage tanks is optimized in blocks of 4 hours, using weather forecasts for 48 hours. The MPC strategy with the flow rate defined in blocks is less dynamic than a DRTO approach computing trajectories for the decision variables. Nevertheless, it allows shorter computational time and thus a longer time horizon can be used for the online optimization. The methodology is tested online during 1 year in a simulation study using measured weather conditions. A new optimization is performed every 12 hours. The results were compared with the standard control strategy and with optimal reactive control. The MPC approach led to savings in primary energy and thus in energy cost and greenhouse gases emissions. This study brings good perspectives for the online optimization of the operation of a solar thermal plant. However, only one flow rate was optimized. The solar field operation was not optimized for example. To our knowledge, no study optimized the operation of a complete solar thermal plant with storage in real-time. Another way to perform RTO is to incorporate an economic objective in the controller (Engell; 2007). This was performed in two studies for solar systems ((Pintaldi et al.; 2019), (Serale et al.; 2018)). This approach presents some drawbacks. The computational time of the dynamic optimization must be shorter than the sampling time of the controller, which is based on the fastest dynamics in the system. Thus, the model needs to be simplified and the time horizon shortened in order to apply this approach. A hierarchical approach, with separate DRTO and control layers, might be easier to implement and better at handling various dynamics and important nonlinearities (Kadam et al.; 2002). Since the storage has a much slower dynamic than the rest of the system, a hierarchical approach might improve storage management (Caspari et al.; 2020). In (Clarke et al.; 2018), a hierarchical control structure is presented for microgrids and hybrid electric vehicles. The specificity of these electrical systems is the presence of storage, leading to the existence of a wide range of time-scales, similarly to a solar thermal plant. The

storage level, in the electrical system presented, varies on a relatively slow time scale compared to the other dynamics exhibited by the components in the system. Hence, a hierarchical control structure was developed with a top layer in charge of scheduling the storage level on a slow time scale and a lower layer controlling the fast dynamics. This hierarchical approach could be used for the optimization of the operation of a solar thermal plant. The storage tank used in our study has a storage capacity of about 2 days. In order to plan a smart use of storage taking advantage of weather forecasts, similarly to the work presented in (Scolan; 2020), a time horizon longer than 2 days is necessary. On the other hand, online optimization cannot be performed on a long time horizon because of the computational time. Moreover, the detailed optimal operation of the plant needs accurate forecasts, thus a shorter time horizon might be preferable. For example, a rolling horizon of 24 hours was used in (De Oliveira et al.; 2013) for the DRTO. In (Saloux and Candanedo; 2021), only one layer was used for the optimization because only one flow rate was optimized. This ensured short computational time even for the 48 hours rolling time horizon employed. For the optimization of the complete solar thermal plant, the decomposition of the optimization in two hierarchical layers could be more suitable. Based on this analysis, a hierarchical optimization framework, with a top layer in charge of storage management and a bottom layer in charge of optimizing the operation of the plant in real time seems appropriate.

Based on this literature review, presented in more details in (Untrau et al.; 2022), the DRTO of a complete solar thermal plant with short-term storage for heat production has never been studied. Thus, there is a need to test a DRTO approach to optimize the operation of a solar thermal plant. Furthermore, the optimization framework must ensure a good storage management during real-time operation. Indeed, the offline dynamic optimization offers an optimal strategy benefiting from a long term strategic vision but based on uncertain forecasts. The use of storage is well planned because the time horizon can be longer than the storage capacity. On the other hand, the DRTO approach uses more accurate inputs for the weather and load to determine the optimal operation of the plant. However, it comes at the expense of a good strategic vision because the time horizon has to be reduced to ensure a computational time allowing online optimization. Thus, there is a compromise to be found between the two optima, found offline (best storage management) and online (best operation based on corrected inputs). The objective of our work is to develop a methodology able to reconcile the two optimal solutions. Untrau *et al.* suggested to use a planning phase to determine the best storage management over a few days and to incorporate the storage state target into the economic objective function of the DRTO level (Untrau et al.; 2022).

II.1.2 New contributions of this work

Our paper presents a DRTO methodology coupling storage management and real-time adaptation. The method is tested on a simulation model in a case study using artificial test data. The method starts with a planning phase, performed offline based on weather and load forecasts, to plan a smart use of storage over two days. The DRTO is then run during daytime, since the disturbances considered are in the solar irradiation only. The DRTO objective function takes into account a storage state target ensuring that the plan is correctly followed, while still minimizing operating costs. Disturbances can

be handled by the DRTO algorithm since it is run regularly to compute new optimal trajectories for the flow rates in the solar thermal plant. Control is not included in this study, and we assume that the optimal trajectories computed are perfectly tracked. The new contributions of our work are:

- The DRTO of the complete operation of a non-concentrating solar thermal plant was tested in a simulation study considering disturbances in the solar irradiance.
- A planning phase (offline dynamic optimization) was used for storage management only, based on weather forecasts.
- The planned storage management policy was incorporated into the DRTO objective function.

The main results of our work are listed below and will be detailed in Section II.6:

- There is a compromise to be found between a good tracking of the planned storage state target and the minimization of the operating cost of the plant at the DRTO level.
- Our DRTO methodology in association with a planning phase for storage management led to an increase in the solar fraction of the plant and a reduction in the operating costs and the excess energy delivered.
- Our methodology was able to adapt to several real-time scenarios without deteriorating the storage management policy.

The remaining parts of the paper are organized as follows. Section II.2 presents the solar thermal plant layout and modeling. Section II.3 explains the optimization methodology. Section II.4 details the case study chosen to test the methodology. The results on storage management are presented in Section II.5 and a comparison with offline dynamic optimization is given in Section II.6 for different real-time scenarios.

II.2 Solar thermal plant description and modeling

II.2.1 Presentation of the system studied

According to the Task 49 of the International Energy Agency, a solar thermal plant is composed of 5 zones: the collector loop, the charge (including the solar heat exchanger), the storage, the discharge and the integration point where the solar heat is delivered to a consumer. Several architectures are possible to connect these essential elements (IEA; 2015). An example of the layout of a solar thermal plant is presented in Figure II.2. Each specific plant is different, depending on the application, the consumer needs, the technologies chosen for each sub-system, etc. The system presented hereafter is an example of a possible design for a solar thermal plant connected to a DHN, provided by our industrial partner NEWHEAT. This design will be the system studied for the remaining parts of the paper.

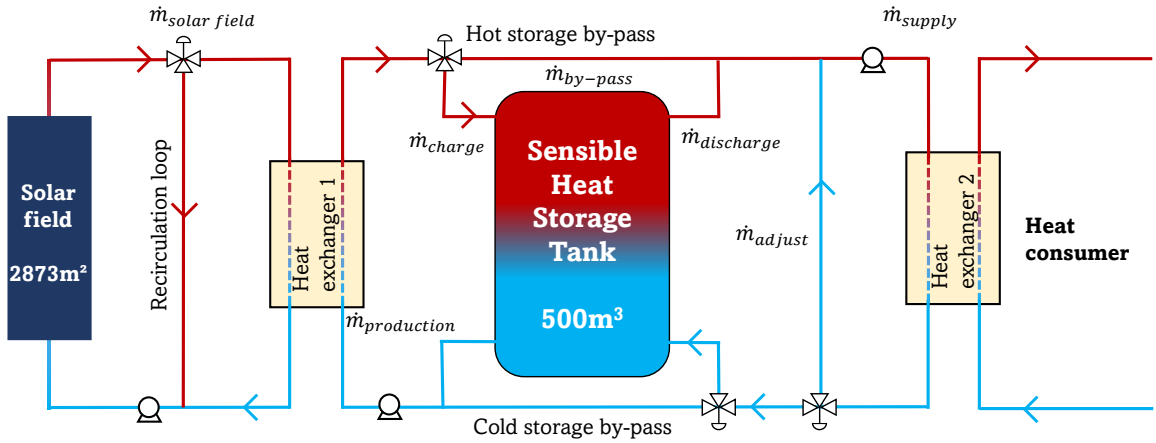

Figure II.2: Architecture of the solar thermal plant

It is composed of three different parts. The solar field is included in the production circuit and is made of 15 loops with 12 flat-plate collectors each. This represents a total collector area of $2873m^2$. The fluid, a mixture of 70% of water and 30% of glycol (volume) is heated up in the solar field. A recirculation pipe allows the fluid to circulate in a loop and by-pass the first heat exchanger during the warm up phase of the solar field. Once the temperature at the outlet of the solar field reaches a target value, the fluid flows through the heat exchanger to deliver the heat produced to the water of the secondary circuit. The heat exchanger is a plate heat exchanger with 97 plates of $1.5m^2$ each. Once the heat is transferred to the secondary circuit, it can be stored inside the $500m^3$ sensible heat storage tank, or directed towards the second heat exchanger, identical to the first one, to deliver it to the consumer. When not enough heat is produced in the solar field, at night or during a cloudy day for instance, the storage tank can be discharged. A mixing valve located before the second heat exchanger allows the adjustment of the supply temperature. If the incoming fluid from the solar field or the storage tank is too hot for the consumer needs, it can be diluted with some cold fluid exiting the heat exchanger. The last part of the solar thermal plant is the consumer side of the second heat exchanger. Variable speed pumps and three way control valves are used to move and direct the fluid in each part of the plant. Since there is the choice to charge, by-pass and discharge the storage tank, and the supply temperature can be adjusted thanks to a recirculation pipe, multiple operational modes are possible in the plant. Nowadays, most solar thermal plants are controlled with logic rules and basic controllers, such as PIDs, to track the set points (Camacho et al.; 2007a). Some typical logic control rules are listed below:

- the temperature at the outlet of the solar field is maintained constant by adjusting the flow rate in the solar field,
- the flow rates in each side of the heat exchangers are chosen to respect the equality of calorific fluxes $\dot{m}_{hot}Cp_{hot} = \dot{m}_{cold}Cp_{cold}$, with $\dot{m}_{hot}$ and $\dot{m}_{cold}$ the flow rates in the hot side and the cold side of the heat exchanger respectively and Cp_{hot} and Cp_{cold} the specific heat capacity of the hot and cold streams respectively,
- as long as the heat demand is not exceeded, all the solar heat produced is delivered to the consumer,

- the excess heat is stored and released as soon as the heat demand is not met.

The degrees of freedom in the operation of the solar thermal plant make the optimization of the system operation particularly promising. In case of a DHN, other heat sources are associated to the solar thermal plant, including a gas boiler. To simplify, the demand is completed with gas in this work but the gas power plant is not modeled.

II.2.2 Modeling of a solar thermal plant

In order to optimize the operation of the solar thermal plant, a model is needed. This model has to offer a good compromise between the accuracy of the results and the computational time. In this work, the DRTO methodology is tested on a simulation model instead of a real plant. Hence, both an optimization and a simulation models are needed. The models used are similar but some additional simplifying assumptions might be needed for the optimization model to further reduce the computational time. The models need to represent nonlinear phenomena. Indeed, in a solar thermal plant, both the quantity of energy and the temperature of that energy are important. The temperature directly affects the quality of the energy and is variable depending on the solar irradiation, thermal losses, efficiency of the elements. Thus, power terms written as the product between a flow rate and a temperature are involved. Linearization is difficult since there are multiple operating points (Camacho et al.; 2007a). Successive linearization could be explored in future work (such as in (Mendis et al.; 2019)) but has never been applied to a solar thermal plant to the best of our knowledge. Thus, a nonlinear model was considered in our work. Two opposing methods could be used to build a model for the solar thermal plant, leading to a first principle model or a data based model. A data based model requires a large quantity of historical data from a real plant or a detailed simulation model to be built. It does not incorporate differential equations or component representing discrete events. It is therefore faster to run. Data based models can be parametric or data driven (classification from (Vasallo et al.; 2021)). Both have been used to represent the solar field of a solar thermal plant, allowing faster simulations and optimizations of a solar thermal plant. For example, a parameterized model was used in (Brodrick et al.; 2018) and (Rashid et al.; 2019), and a data driven model based on an artificial neural network was developed in (Farkas and Géczy-Víg; 2003) and in (Heng et al.; 2019). In these studies, the data based models developed for the solar fields run faster than the corresponding first principle models, while still achieving a reasonable accuracy. In the literature, data based models are used to represent the solar field of a solar thermal plant, but not for the complete plant. Developing data based models for a complete solar thermal plant represents a good perspective for future research. Nevertheless, data based models require a large amount of data to be accurate, which are not easy to acquire. Moreover, the results cannot be extrapolated outside of the validity domain of the model, which depends on the data set used to built it. For these reasons, a first principle model was chosen in this work. Equations of conservation for the mass and the energy are developed for each sub-system of the plant. They form a system of equations with algebraic and Partial Differential Equations (PDE). The differential equations are discretized before resolution. The model used in the present paper was developed in (Scolan et al.; 2020). Only a few modifications have been made to the model, and will be explained

hereafter. The main assumptions and equations of the model are introduced below, and more details can be found in (Scolan et al.; 2020).

Solar Field

A simple model was chosen for the solar field, with a single equivalent solar panel whose area A_{eq} is equal to the area of all the collectors in the solar field. No spatial discretization of the solar collector is considered but the equivalent inertia of the flat plate collector is taken into account. In (Scolan et al.; 2020) the solar field was modeled with an equivalent loop, assuming a uniform distribution of the fluid between the loops and neglecting the heat losses between the collectors within a loop. The collected solar flux was obtained by multiplying the collected solar flux of the equivalent loop by the number of loops. Under the same assumptions, replacing the solar field by a single equivalent solar panel does not importantly deteriorate the accuracy of the model but leads to reduced computational time. Hence, the model from (Scolan et al.; 2020) was further simplified in the present work. The one node capacitance model employed can be written as follows (the time dependency of the variables is not written for conciseness):

$$\frac{\dot{Q}_{SF}}{A_{eq}} = \left(\eta_{0,b}(\eta_{sh} K_b(\theta) G_b + K_d G_d) - c_1(T_m - T_{amb}) - c_2(T_m - T_{amb})^2 - c_5 \frac{dT_m}{dt} \right) \tag{II.1}$$

This equation is used to determine the mean temperature of the fluid T_m inside the collector. $\dot{Q}_{SF}$ is the power transmitted from the sun to the heating fluid in the whole solar field and A_{eq} is the equivalent area of solar panels. $\eta_{0,b}$, c_1, c_2, c_5, $K_b(\theta)$ and K_d are provided by the collector's manufacturer and are defined as follows: $\eta_{0,b}$ is the optical efficiency of the collectors, c_1 is the heat loss coefficient in the collector at $T_m = T_{amb}$, c_2 is the temperature dependence of the heat loss coefficient, c_5 is the effective thermal capacity, $K_b(\theta)$ is the incidence angle modifier for the direct irradiation (beam) and K_d is the incidence angle modifier for the diffuse irradiation. Equation II.1 takes into account the direct irradiation in the plane of the collectors G_b and the diffuse irradiation from the sky and the ground in the plane of the collectors G_d, computed according to (Perez et al.; 1987). A shading effect from one loop to the next one is incorporated thanks to the efficiency η_{sh}. Finally, the heat losses are computed using the ambient temperature T_{amb}. Equation II.1 stems from standardization procedures and can include more phenomena if the technical characteristics of the collector are more detailed (ISO/FDIS 9806; 2017). It is an energy conservation equation with the heat gain from solar irradiance, heat losses to the ambient and an accumulation term. The temperature distribution inside the collector is considered linear in order to compute the outlet temperature (Close; 1967). This simplified model runs fast, but is still able to represent the transient behavior of the solar field.

Heat Exchanger

The two heat exchangers in the system are plate heat exchangers which are commonly used in solar thermal plants working at low temperatures (IEA; 2015). They have a

good efficiency, are compact and easily adaptable by adding or removing plates. In the first heat exchanger the hot side is glycol water while the cold side is water. In the second heat exchanger, the hot side is water and the cold side depends on the consumer and is here considered water as well. In order to keep the computational burden low, no spatial discretization is considered in the heat exchanger. The evolution of the temperatures between the plates is unknown but the simplified model does provide a good approximation for the outlet temperatures and the general behavior of the heat exchanger (Wang et al.; 2007). The model assumes no accumulation, no heat losses to the ambient and a uniform distribution of the fluid flow between the channels. All plates have the same area. Three equations are necessary to compute the three unknowns of the model: the two outlet temperatures and the exchanged heat. The ϵ-NUT model, detailed in (Wang et al.; 2007) for example, is used with the efficiency of the heat exchanger computed assuming a fixed global heat transfer coefficient of $4000 W.m^{-2}.K^{-1}$. This assumption does not clearly deteriorate the accuracy of the model, as shown in (Scolan; 2020), but reduces the nonlinearities, speeding up the calculations.

Pipes

The pipes connecting the elements of the plant are modeled, with the energy equation developed in 1D considering the fluid and wall inertia. Heat losses are computed, whether there is a flow circulating through the pipes or static fluid. A thermal resistance is computed involving external convection with the ambient air as well as conduction through the insulation layer. The heat transfer coefficient on the internal side is considered very large compared to the external convection coefficient. Thus, internal convection and conduction through the wall are neglected. The external convection coefficient is computed using Hilpert correlation (Incropera et al.; 2007). Mass and energy balances are written for each mixing valve or flow division in the plant, assuming no accumulation or heat losses.

Pumps

The electric consumption of the pumps is important to compute as it is part of the operational cost of the solar thermal plant. The pressure drop in the circuit at the maximum flow rate is compensated by the hydraulic power of the pump, as shown in Equation II.2. In this equation, $\dot{P}_{hydrau}$ is the maximum pumping power at the maximum flow rate allowed in the pump $\dot{m}_{max}$, leading to the maximum pressure drop ΔP_{max}. ρ is the fluid density. The electric power $\dot{P}_{elec}$ consumed depends on the actual flow rate $\dot{m}$ in the circuit according to Equation II.3, with η the overall efficiency of the pump.

$$\dot{P}_{hydrau} = \frac{\dot{m}_{max}}{\rho} \Delta P_{max}(\dot{m}_{max}) \tag{II.2}$$

$$\dot{P}_{elec} = \frac{\dot{P}_{hydrau}}{\eta} \left(\frac{\dot{m}}{\dot{m}_{max}} \right)^3 \tag{II.3}$$

Storage Tank

The storage tank is an essential part of a solar thermal plant. The solar irradiance varies daily and seasonally, with more solar radiation available in summer and only during daytime. Unfortunately, the heat demand does not follow the same trends. For an industrial process, the consumer needs can be constant for example. For a DHN providing heat to residential and office buildings, the demand is generally larger in winter and in the evenings. Thus, TES can help to decouple the production and the consumption of the heat. In this work, we only consider daily storage, that can help supplying solar heat at night or on cloudy days. Several technologies are developed to store the heat based on different working principles: latent, thermochemical or sensible TES (Guelpa and Verda; 2019). For a solar thermal plant working at low temperature, a sensible TES filled with water is generally preferred because it is cheaper and a more mature technology. Two tanks, one storing the hot water from the solar field and the other storing the cold return temperature can be used (Immonen and Powell; 2022). However, using a single tank requires less land space and construction material and, thus, is cheaper (He et al.; 2019). In the single tank, the hot fluid is charged from the top and the cold fluid from the bottom. Because of the difference in densities of the fluids, there is very limited mixing between the hot and cold zones in the stratified tank. A high temperature gradient characterizes the transition zone, also known as thermocline. Modeling the stratified storage tank remains a challenge because the model needs to accurately represent the thermocline region while running fast enough for dynamic simulation and optimization of a complete solar thermal plant. 3D CFD models are developed to study phenomena such as the effect of the diffusers on thermal stratification (Hosseinnia et al.; 2021). However, for simulation and optimization of stratified TES integrated into a larger energy system, one-dimensional models are preferred. Only the variations of temperature along the vertical axis are considered. The simpliest model is the fully mixed tank, neglecting thermal stratification, but it leads to an important exergy destruction (Campos Celador et al.; 2011). Ideally stratified models (Campos Celador et al.; 2011) or plug flow models (Kleinbach et al.; 1993) can provide a better approximation but do not represent all the thermal phenomena. The method chosen in this paper is based on the resolution of the energy conservation in 1D:

$$\rho C_p A \frac{\partial T(z,t)}{\partial t} + \dot{m} C_p \frac{\partial T(z,t)}{\partial z} = Ak \frac{\partial^2 T(z,t)}{\partial z^2} + UP(T_{amb}(t) - T(z,t)) \tag{II.4}$$

In this 1D model, the temperature variations are only considered along the vertical axis z, pointing upwards. The unknown variable in this equation is the temperature of the fluid inside the storage tank $T(z,t)$. In this equation, the fluid properties are ρ the fluid density, C_p the fluid specific heat capacity and k the fluid thermal conductivity. A is the tank cross sectional area and P is its perimeter. The heat losses are computed with a tank fluid to ambient overall heat transfer coefficient U and the ambient temperature $T_{amb}(t)$. Finally, $\dot{m}$ is the resulting flow rate from charging and discharging.

This Partial Differential Equation (PDE) entails an accumulation term, a convective term due to the charging and discharging, a conductive term and heat losses to the environment. This PDE can be vertically discretized using the finite volume approach, to transform it into a set of Ordinary Differential Equation (ODE). A uniform

temperature in each layer of fluid is assumed, layer 1 is located at the bottom and layer N at the top of the tank. Each layer has the same height Δz. The tank wall is considered in thermal equilibrium with the stored fluid in each layer because we assume that the thermal resistances for internal convection and conduction through the wall are zero. Hence, the multinode model can be written as follows, with the energy balance developed for each layer, composed of the stored fluid and the wall:

For the first layer at the bottom of the storage tank:

$$\begin{aligned}\rho C_p A \Delta z \frac{dT_1}{dt} &= U_1 S_1 * (T_{amb} - T_1) + \frac{4}{3}\frac{k^* A}{\Delta z}(T_2 - T_1) \\ &+ \dot{m}_{charge} C_p (T_2 - T_1) + \dot{m}_{discharge} C_p (T_{return} - T_1)\end{aligned} \tag{II.5}$$

For an intermediate layer i, for i varying from 2 to N-1:

$$\begin{aligned}\rho C_p A \Delta z \frac{dT_i}{dt} &= U S_l * (T_{amb} - T_i) + \frac{k^* A}{\Delta z}(T_{i-1} - 2T_i + T_{i+1}) \\ &+ \dot{m}_{charge} C_p (T_{i+1} - T_i) + \dot{m}_{discharge} C_p (T_{i-1} - T_i)\end{aligned} \tag{II.6}$$

For the last layer N at the top of the storage tank:

$$\begin{aligned}\rho C_p A \Delta z \frac{dT_N}{dt} &= U_N S_N * (T_{amb} - T_N) + \frac{4}{3}\frac{k^* A}{\Delta z}(T_{N-1} - T_N) \\ &+ \dot{m}_{charge} C_p (T_{charge} - T_N) + \dot{m}_{discharge} C_p (T_{N-1} - T_N)\end{aligned} \tag{II.7}$$

In this equation, $\dot{m}_{charge}$ and $\dot{m}_{discharge}$ are the flow rates associated with the charging and discharging fluxes respectively. The other inputs of the model are the temperature of the charging flow T_{charge} and the return temperature T_{return}. S_l is the lateral surface of the tank layer, exchanging energy with the ambient air. S_1 and S_N also take into account the top and bottom surfaces in contact with the ambient air. Thus, there are more heat losses through the top and bottom layers because of the larger exchange surface. Given the aforementioned assumptions, the overall heat transfer coefficient U accounts for the conduction through the insulation layer and the external convection with the ambient air. This coefficient can be different for the bottom layer (U_1) and the top layer (U_N). k^* is the effective conductivity of the fluid and the tank wall, as explained in (Newton; 1995). Despite a much smaller cross sectional area, conduction through the wall contributes to the homogenization of temperatures inside the storage tank because of the large conductivity of metal. The thermal capacity mC_p of the wall is neglected because the mass of metal is much smaller than the mass of water and the specific heat capacity Cp of the metallic wall is small compared to the one of water. Hence, only the thermal capacity of water is used in each layer. The assumption of a uniform temperature in each layer of fluid leads to the phenomenon of numerical diffusion, which smooths the vertical temperature profile (Powell and Edgar; 2013). The thermocline region is then modeled thicker than it should be. Adding more layers into the model helps to reduce this effect, as shown in Figure II.3. This figure represents the temperature profiles obtained at the same time instant during the charging of the storage tank for various numbers of layers in the model. However, adding layers

impacts the computational time: for 10, 100, 1000 and 2000 layers, the simulation of a complete charge of the storage tank took respectively 0.1s, 0.14s, 4.7s and 25.2s on a computer with the following characteristics: Intel Core i7-1065G7 1.3GHz, RAM 16Go. Other numerical strategies have been developed to eliminate numerical diffusion, such as in (Powell and Edgar; 2013), in which an adaptative grid was considered. The adaptative grid consists of a hot and a cold volumes separated by some layers of fluid representing the thermocline region. This allowed to use less layers in the tank to achieve the same accuracy, hence reducing computational time. However, this strategy is not easy to implement in an optimization model because it requires conditional structures to switch from the layers zone to the uniform volume zone while charging or discharging the storage tank. Another discretization scheme, orthogonal collocation on finite elements, has been tested to discretize the vertical axis of the storage tank in (Untrau et al.; 2023b). It reduced the numerical diffusion and provided more accurate results in a shorter time. However, a minimum number of collocation points was required to avoid oscillations in the vertical temperature profile. Thus, implementing this discretization scheme in an optimization study represents a good perspective for future work. In the present paper, the classic multinode model was implemented with a number of layers chosen to compromise between accuracy and computational time. For the optimization model, 10 layers are used, similarly to (Scolan et al.; 2020), even though the accuracy is low. This is necessary because optimizations, especially in real-time, require simplified models to run in a reasonable time. For the simulation model, which needs to converge only once, 1000 layers are chosen. It seems that adding even more layers does not greatly impact the results (as shown in Figure II.3). The MAPE (Mean Absolute Percentage Error) between each temperature profile from Figure II.3 and the profile with 2000 layers was computed. The results obtained were: 16.86% for 10 layers, 4.02% for 100 layers and 0.43% for 1000 layers. This shows the convergence of the results when more than 1000 layers are employed. In addition, adding more layers slows down the calculation (2000 layers takes more than 5 times longer than 1000 layers). Therefore, 1000 layers were chosen for the simulation model.

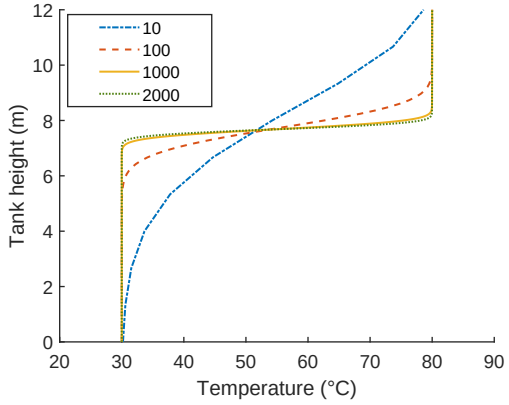

Figure II.3: Illustration of the phenomenon of numerical diffusion

An optimized solar thermal plant does not operate with a fixed temperature at the outlet of the solar field. For example, when solar irradiation goes down but is still high enough for the production of valuable heat for the consumer, the temperature might decrease compared to previous time instants. This lower temperature heat can

be charged inside the storage tank for latter use. In this situation, a temperature inversion will occur in the stratified storage tank since colder fluid will be charged on top of warmer fluid previously charged when solar irradiation was higher. Such a temperature inversion is corrected by buoyancy forces induced by natural convection. Indeed, the colder fluid will sink through the warmer fluid until temperature equilibrium is reached. The mixing induced by natural convection should be incorporated in the 1D storage tank model (Kleinbach et al.; 1993). Various models have been developed in the last decades to represent the correction of temperature inversions. The plume entrainment model (Pate; 1977) is based on physical equations. The discontinuities in the flow rates in this model make it not applicable to optimization studies. For simulations with continuous time integration, it requires events handling. Numerical artifices, that correct the inversion after its appearance, have also been studied. For example, the temperature profile can be reorganized (Franke; 1997) to have the hot temperatures at the top, or the temperature can be homogenized in the inversion region (Kleinbach et al.; 1993). These options cannot be incorporated in an optimization model because they are based on conditional structures. Injecting the fluid in the layer at the closest temperature also requires conditional structures and tends to overestimate the quantity of valuable energy stored by neglecting the mixing between the incoming and stored fluids (Saloux and Candanedo; 2019). Continuous formulations have been developed as well. They are based on an adjustable turbulent diffusion coefficient added before the diffusion term in Equation II.4 ((Hawlader et al.; 1988), (Nash et al.; 2017), (Powell and Edgar; 2013), (Viskanta et al.; 1977), (Zurigat et al.; 1988)). This additional term is only large when a temperature inversion appears. Thus, it is necessary to locate a temperature inversion, through a discontinuous function for a simulation model or a smooth approximation for optimization studies ((Lago et al.; 2019), (Soares et al.; 2022)). Nevertheless, the continuous and smooth models need tuning in the approximation functions. Moreover, the continuous formulations for natural convection slow down the calculations, as shown in (Untrau et al.; 2023b). Finally, Scolan *et al.* suggested to incorporate the correction of temperature inversions inside the optimization model, through the optimization of inversion flow rates (Scolan; 2020). Nonetheless, this approach is not based on physical theory and also requires tuning in the penalty term and the bounds of the inversion flow rates. In the present work, it was decided not to correct temperature inversions in the optimization model. Indeed, no available method seems appropriate for optimization studies, either because of the need of conditional structures or because of the tuning required based on experimental data. Inversions up to 6°C between layers are noticed in the results, and should be kept in mind for the analysis of the results. The correction of temperature inversions in an optimization model should be investigated in future work. For the simulation model, the temperature profile is regularly corrected. The reorganization of the temperatures to maintain a positive temperature gradient tends to overestimate the quantity of valuable energy inside the storage tank. On the other hand, the homogenization of the temperature profile around the inversion tends to underestimate the quantity of valuable energy (Pate; 1977). Indeed, the reality is probably in between the two approaches, with the cold fluid exchanging energy with the already stored fluid during its descent. In an attempt to model this effect, the reorganized temperature profile (Franke; 1997) and the homogenized profile (Kleinbach et al.; 1993) are both computed and the average between these two profiles is chosen as the corrected temperature profile in the storage

tank. The correction operation is done every 5 minutes during the simulation. Of course, an experimental validation of the model should be carried out. But the measurements need a high spatial and temporal resolution in order to accurately represent the appearance and correction of a temperature inversion inside the storage tank. A CFD model could be built to study the temperature inversions correction and compare the results with our simulation and optimization models. This could be explored in future work but is out of the scope of the present paper.

The models for the solar field, heat exchangers, pipes, pumps and storage tank are all connected to form the solar thermal plant optimization and simulation models. The gas burner used to complete the demand if the solar energy is not sufficient is modeled as a simple heater.

II.3 Dynamic Real-Time Optimization methodology

A new methodology was developed in order to optimize the operation of a solar thermal plant in real-time while ensuring a good storage management. The architecture of the methodology is schematized in Figure II.4. A planning phase, which is an offline economic dynamic optimization, is used to obtain the storage management policy and also provides the planned trajectories of the operational variables. The planning phase is an offline dynamic optimization, following the methodology developed in (Scolan et al.; 2020). It takes weather and load forecasts as inputs and provides the planned storage state throughout time to the next level. The next level developed in the present study, DRTO, updates the optimal operational strategy of the plant considering the planned storage state target and minimizing the operating costs. DRTO is regularly called by the simulation model representing the actual solar thermal plant. The simulation model gives measurements of state variables and disturbances to the DRTO, as a feedback, to ensure that the new trajectories are adapted in real-time. The different blocks are detailed hereafter.

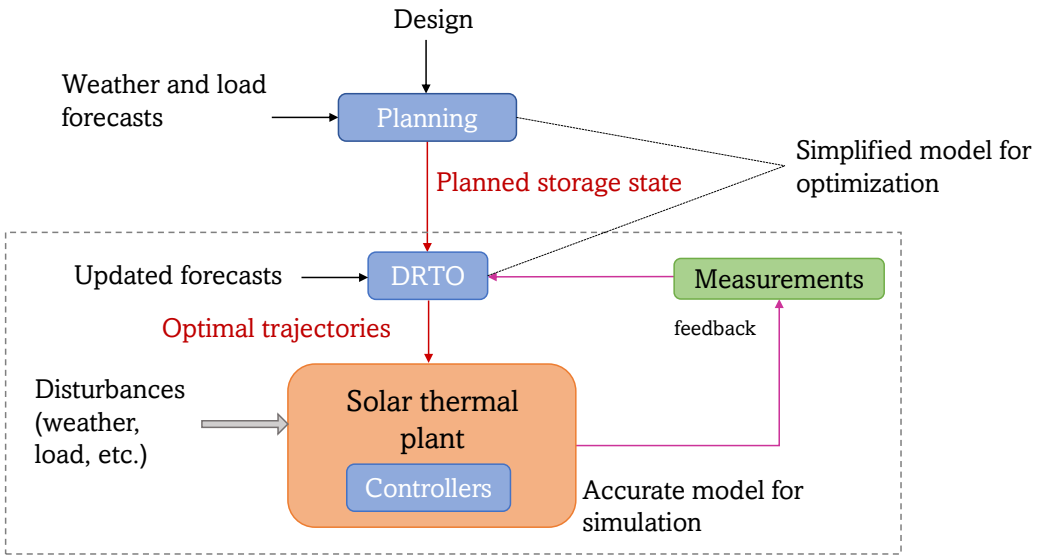

Figure II.4: Optimization algorithm

II.3.1 Planning

The first step is a planning phase, which corresponds to an offline dynamic optimization. This phase is used to plan a smart use of storage, taking advantage of a longer time horizon. Scolan *et al.* showed counter-intuitive operating strategies when optimizing the operation of a solar thermal plant over 36 hours, because the optimization algorithm made the most out of the storage tank (Scolan et al.; 2020). The storage management policy should ideally be obtained on a time horizon longer than the storage capacity, which is about 2 days for the system considered. Thus, 5 to 7 days seem to provide a good strategic vision. However, the accuracy of the weather forecasts decreases as the time horizon increases. The forecasts are usually given for the following 5 to 7 days, with high uncertainty after 2 days. Thus, 2 days seems a good compromise between forecast quality and strategic vision for this first study testing our methodology. A longer time horizon could be tested in future work.

Inputs and outputs

The optimization algorithm takes the design of the system and the weather and load forecasts as inputs and computes the optimal trajectories for the flow rates in the plant, similarly to the work in (Scolan et al.; 2020). There are 10 unknown flow rates in the plant (the consumer flow rate is an input of the problem). There are only 6 independent flow rates in the plant because of the mass conservation at the flow junctions and divisions. These 6 flow rates constitute the degrees of freedom of the optimization problem. Although these 6 flow rates are outputs of the optimization algorithm, they are not the variables of interest in this level of the optimization framework. The planning phase is used to obtain the storage management policy. Hence, the quantity of energy stored in the storage tank throughout time is the variable that will be kept for the next step of the method, the planned trajectories of the flow rates being updated on the other hand.

Constraints

Several operating constraints are added to the system. For security reasons, all temperatures should be below 95°C in order to avoid overheating and boiling, which would deteriorate the plant. The flow rates in the plant are constrained between their maximum value and 40% of it. Pumps cannot be turned on with a very small flow rate, a minimum value of 40% of the maximum flow rate ensures a reasonable efficiency. The minimum value is usually provided by the manufacturer. A pump has discontinuous operating modes: either it is turned off and the flow rate is zero or it is turned on and the flow rate is between two positive bounds. The discontinuous operating modes are approximated with a continuous function (sigmoid function) and inequalities based on Big M formulations are used to write the constraints on the minimum flow rates, as developed in (Scolan; 2020). The maximum flow rate in the solar field circuit is based on the collectors' manufacturer recommendations and is here $21 kg.s^{-1}$. The maximum flow rates in the secondary circuit are determined with the equality of the calorific fluxes in the two heat exchangers: $\dot{m}_{hot\ max} Cp_{hot} = \dot{m}_{cold\ max} Cp_{cold}$ (value of $19.6 kg.s^{-1}$). Finally, the solar thermal plant is here used to preheat the water for a

DHN, the demand being completed by gas if necessary. The heat demand is a power required at a certain temperature T_{demand}. The fluid on the consumer side flows at a fixed flow rate and the solar thermal plant is used to rise the temperature to $T_{consumer\ out}$, as close as possible to the target temperature. Therefore, even though the solar heat might not be sufficient to reach the target temperature, it is partially used to meet the heat demand. However, it is not permitted to exceed the target temperature. This can be written as: $T_{consumer\ out} \leq T_{demand}$. To facilitate the convergence of the optimization, this constraint on the temperature at the outlet of the cold side of the second heat exchanger is replaced by a penalty in the objective function, as will be explained in the next paragraph. To summarize, the operating constraints are:

- $T \leq 95°C$ for all temperatures T
- The flow rate in each pump is defined as follows:

$$\begin{cases} \dot{m} = 0 \text{ (corresponding to the pump turned off)} \\ \text{or} \\ 0.4\dot{m}_{max} \leq \dot{m} \leq \dot{m}_{max} \text{ (corresponding to the pump turned on)} \end{cases}$$

- $T_{consumer\ out} \leq T_{demand}$

Objective function

The objective of a heat producer for a DHN is to minimize the cost of the heat produced, namely minimize the operating cost of the plant. In this study, the operating costs are the electricity consumption of the pumps in the plant and the gas consumption of the backup heater. The costs considered are 130€/MWh for the electricity (ElecPrice) and 80€/MWh for the gas (GasPrice). An economic gain is associated with the energy stored E_{stored} at the end of the time horizon t_f. Indeed, the heat stored could be useful after the end of the time horizon. Scolan *et al.* considered a price of heat of 25€/MWh (HeatPrice) and performed a sensitivity analysis to determine the value to give to the stored heat (Scolan et al.; 2020), which is the price of heat affected by a weight. The quantity of heat provided to the consumer from the discharge of the storage tank will be lower than the quantity of heat originally stored because of heat losses and an imperfect transfer in the second heat exchanger. Thus, the price associated with the stored heat is lower than the price at which the heat would be sold. A weight of 0.7 was found appropriate in (Scolan et al.; 2020), thus we assumed economic gains of 17.5€/MWh associated to the stored energy at the end of the time horizon as a first approximation. Numerical penalty terms are added to the objective function. Firstly, as mentioned earlier, a penalty Φ_{demand} is associated to the respect of the heat demand. This term sums the cubed excess temperatures at the outlet of the consumer stream, as proposed in (Scolan; 2020). It is written as follows:

$$\Phi_{demand} = \sum_{i=0}^{f} \phi_i, \text{ with } \begin{cases} \phi_i \geq 0 \\ \phi_i \geq (T_{consumer\ out}(t_i) - T_{demand}(t_i))^3 \end{cases}$$

i varies between 0 and the final time step f and ϕ_i is the excess in the consumer outlet temperature at the time step i. Another penalty term Φ_{var} is used to smooth the

trajectories computed for the 6 free flow rates in the plant. This term sums all the quadratic differences in the flow rates between two consecutive time instants, as follows:

$$\Phi_{var} = \sum_{l=1}^{6} \sum_{i=1}^{f} \left(\frac{\dot{m}_l(t_i) - \dot{m}_l(t_{i-1})}{t_i - t_{i-1}} \right)^2$$

In this equation, l represents the 6 free flow rates, which are the 6 degrees of freedom in the system. This penalty term will help to avoid oscillatory behaviors in the optimal trajectories (Powell et al.; 2014) and to condition the optimization. The two penalty terms are affected by weights γ_{demand} and γ_{var} that need to be adjusted. A compromise between a good satisfaction of the constraints represented by these penalties and an optimal economic solution is to be found. The objective function can be written as follows:

$$\min_{free\ \dot{m}} OF_{eco} - \gamma_{demand}\Phi_{demand} - \gamma_{var}\Phi_{var} \tag{II.8}$$

with the economic objective function OF_{eco} detailed below:

$$\begin{aligned} OF_{eco} = & -GasPrice \int_0^{t_f} \dot{Q}_{gas}(t)\mathrm{d}t - ElecPrice \int_0^{t_f} \dot{P}_{elec}(t)\mathrm{d}t \\ & + 0.7 HeatPrice\ E_{stored}(t = t_f) \end{aligned} \tag{II.9}$$

$\dot{Q}_{gas}$ is the thermal power generated by the gas consumption and $\dot{P}_{elec}$ is the electric power consumed in the pumps.

Resolution

The model composed of the equations for the different sub-systems in the plant and the constraints forms a system of Differential Algebraic Equations (DAE). The system is transformed into a Nonlinear Programming problem (NLP) through the discretization of the ODEs. Consequently, the continuous algebraic equations are also replaced by a system of algebraic equations evaluated at each discretization point. The resolution method chosen is the equation oriented approach where all variables (controlled and state variables) are discretized. The time discretization is done through Orthogonal Collocation on Finite Elements (OCFE). The unknown variables are represented as Lagrange polynomials on each element and continuity is ensured at the boundary between elements according to the method developed in (Hedengren et al.; 2014). Elements are one hour long since the weather forecasts are generally provided with a 1 hour time step. 9 collocation points are chosen as the Gauss-Lobatto roots of Legendre polynomials shifted in [0,1]. A sensitivity analysis on the number of points in each element has been carried out in (Scolan; 2020) and 9 points seems to offer a good compromise between computational time and accuracy. The maximal time step is about 10 minutes. OCFE allows the transformation of the ODEs in the system, such as Equations II.1 and II.6 for example, into a set of algebraic equations. The original DAE system is thus approximated by a pure algebraic system, with each equation evaluated at each discretization point. The NLP problem obtained is then solved with the solver CONOPT in the GAMS software. CONOPT will provide a locally optimal solution after convergence. Thus, the initialization has an impact on the results. In order to initialize the

problem with a feasible solution as close as possible to the optimum, the engineering knowledge of the system is employed and standard operating strategies are utilized for the initialization. This ensures that the resolution starts from a satisfactory solution, currently used in real solar thermal plants, and converge to an optimal solution in a reasonable time. Our 2 day planning phase takes about 2 hours to converge to an optimal solution on a laptop using a processor with the following characteristics: Intel Core i7-1065G7 1.3GHz. Once this offline planning phase is completed, the next level of optimization, DRTO, can start. The quantity of energy stored inside the storage tank throughout time is sent to the next optimization level, as planning is here used for storage management only.

II.3.2 DRTO

Dynamic Real-Time Optimization (DRTO) constitutes the second level in the optimization framework developed in this work. The necessity for an online phase stems from the uncertainties in the weather and load forecasts. If the actual weather and load differ too much from the forecasts, the optimal trajectories computed during the planning phase are suboptimal and it might even be impossible for the controllers to track these trajectories. Hence, adapting the operational strategy online is crucial to optimize an actual solar thermal plant. The DRTO applied here follows the two-layers approach presented in (Kadam et al.; 2002), with the optimization and the tracking tasks performed separately. The optimization model needs to run fast in order to be employed in real-time. Indeed, it will be run regularly, ensuring that the optimal trajectories are adapted to new disturbances. The dynamic optimization algorithm for DRTO is built similarly to the planning phase, with the same model equations, operational constraints and resolution strategy. The specificities of this level are detailed hereafter.

Time horizon and discretization

The time horizon for the DRTO should be shorter than for the planning phase for two reasons. First, the updated forecasts fed into the algorithm should be as accurate as possible. Moreover, the DRTO needs to run fast to ensure that the computed trajectories are still optimal when the calculation is complete and these trajectories are sent to the controllers for tracking. In order to satisfy these two conditions, a time horizon no longer than one day seems appropriate, as suggested in (Wittmann et al.; 2011) and used in (Wagner et al.; 2018). In this study, the DRTO is tested during daytime of one day. Hence, a shrinking time horizon is chosen spanning from the current time to the end of the day when the sun goes down. Each new DRTO run is performed over a shorter time horizon than the previous run. Other options such as a rolling horizon could be explored in future work. Since the weather and load forecasts are updated, they are more precise. Thus, a finer temporal discretization is chosen, with elements of 15 minutes and the same 9 collocation points. The time step varies between 45 and 190 seconds approximately. Each DRTO run takes between 1 and 10 minutes to converge on the same laptop. The first DRTO, which uses the longest time horizon takes the most time to converge to an optimal solution.

The DRTO algorithm is regularly called to update the trajectories using the real-time measurements. In our study, DRTO was called every hour to ensure a good accuracy of the updated weather forecast. For future work, conditional triggering, based on a deviation from the reference trajectories for example (Alonso et al.; 2013), could be explored.

Storage management and objective function

The main difference between the planning and the DRTO algorithm is the storage management. In the DRTO objective function, the quantity of energy stored at the end of the time horizon is no longer an economic gain. Instead, costs are associated to the non-respect of the plan, which determined the optimal use of energy storage. Hence, the difference between the energy stored at the end of the day projected during the planning phase $E_{stored\ planning}$ and the stored energy achieved with DRTO at the same time instant $E_{stored\ DRTO}$ is minimized. The time instant for the storage evaluation corresponds to the end of the day and also to the end of the DRTO time horizon $t_{f\ DRTO}$. This energy difference is multiplied by the price of gas to obtain an order of magnitude of the cost of the non-respect of the plan. Indeed, the energy that has not been stored will be replaced by gas when the consumer will need it. A weight ω affects this term in the objective function and its effect on the performances of the solar thermal plant will be studied in Section II.5. Economic costs are minimized, similarly to the planning phase, with the same penalty terms. An additional penalty $\Phi_{var\ init}$ is added, ensuring that the first value computed for each flow rate at the initial time of the DRTO run does not differ too much from the current value of the flow rate in the plant. This makes sure that the complete trajectory for the day does not present harsh variations when updated trajectories are incorporated. The penalty term is adjusted with a weight $\gamma_{var\ init}$. The objective function for the DRTO is written as follows:

$$\min_{free\ \dot{m}} OF_{eco} - \gamma_{demand}\Phi_{demand} - \gamma_{var}\Phi_{var} - \gamma_{var\ init}\Phi_{var\ init} \tag{II.10}$$

with the economic objective function detailed below:

$$\begin{aligned} OF_{eco} = &-GasPrice \int_0^{t_f} \dot{Q}_{gas}(t)\mathrm{d}t - ElecPrice \int_0^{t_f} \dot{P}_{elec}(t)\mathrm{d}t \\ &+ \omega.GasPrice.|E_{stored\ planning}(t = t_{f\ DRTO}) - E_{stored\ DRTO}(t = t_{f\ DRTO})| \end{aligned} \tag{II.11}$$

New trajectories for the flow rates are computed and sent to the controllers for tracking, until a new DRTO is run. At the beginning of each DRTO run, the initial state of the system is retrieved from measurements on the plant, as presented in the next paragraph.

II.3.3 Simulation and feedback

An online methodology has to be tested on a real system or a digital twin. In this study, a simulation model is used to provide the plant feedback to the DRTO method. The

plant model is written in MATLAB and the time integration is done with the solver ode15s, suitable to solve a system of DAEs. In this study, the control is assumed perfect, controllers are not included in the simulation model. The trajectories determined at the DRTO level are perfectly tracked. The simulation model undergoes the actual weather and load. It can provide feedback measurement of the state variables, such as the temperatures in the plant, and the disturbances, such as solar irradiation. Since the methodology is tested on a simulation model, we assume that all the states are measured and no state estimation is employed. In a real application, a state estimation step should be added to the methodology to retrieve the state variables value from the noisy measurements. A future work could be to model this additional step to assess the performances of the methodology on a more realistic case study. In the present study, the optimization and simulation models differ for the storage tank: 10 layers are used in the optimization model employed for planning and DRTO while 1000 layers are used in the simulation model for the vertical discretization of the tank. Moreover, temperature inversions are corrected in the simulation model only. Feedback provided from the simulation model is used to correct the inaccuracy of the optimization model at the beginning of each DRTO run because the initial state of the system and the initial disturbances are known. That way, model error propagation is avoided because the system is updated with measurements. The methodology presented in this section has been tested in a case study presented hereafter.

II.4 Case study

In order to assess the performances of the optimization framework developed in the previous section, a case study with several scenarios for the weather was created.

II.4.1 Weather data for planning

Firstly, the planning phase was applied to 3 different time periods, representing three different seasons. The weather data was retrieved from a typical meteorological year in the city of Pau, France. The input solar irradiance for the chosen days is plotted on the graphics in Figure II.5 in terms of Global Horizontal Irradiance (GHI). The two summer days (August 8^{th} and 9^{th}) are sunny days, forcing the use of storage to avoid exceeding the heat demand. The two winter days chosen (February 2^{nd} and 3^{rd}) are also sunny days, otherwise the solar thermal plant would barely operate. The two days chosen to represent mid-seasons (May 5^{th} and 6^{th}) are characterized by a more variable solar irradiance. The ambient temperature and the wind speed are retrieved for the same days. They are used to compute the heat losses in the different parts of the plant. This artificial test data set is employed for this first study but real weather forecasts should be used in future work. For the remaining parts of the paper, the planning phase is also referred as DO (Dynamic Optimization), to distinguish it from DRTO.

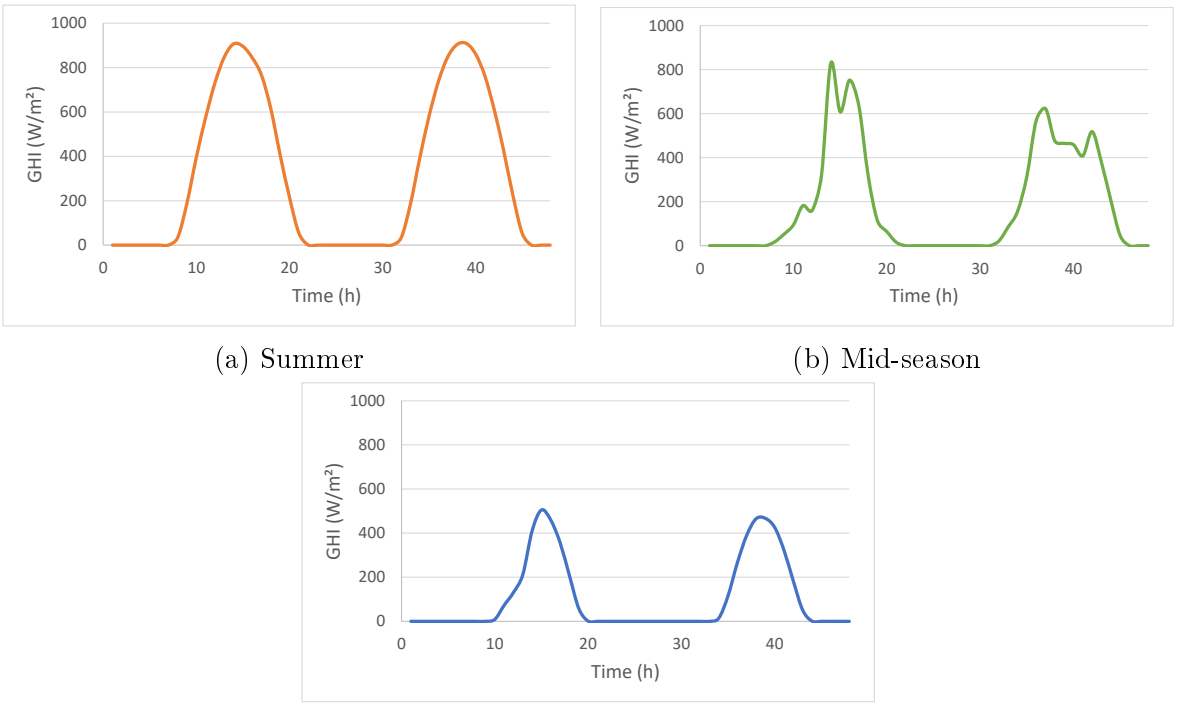

(a) Summer

(b) Mid-season

(c) Winter

Figure II.5: Solar irradiation for the planning phase

II.4.2 Weather data for DRTO

To test the DRTO methodology during daytime, disturbances in the weather for the first day of each season are introduced. In this work, the only disturbance considered is in the solar irradiance, the other inputs such as the heat demand are perfectly known. Since the only input disturbed is the solar irradiance, and it is zero at night, it is enough to perform the DRTO method during daytime only. The night, when no disturbance appears, acts as a reset before the DRTO method can be started again the next day. In this work, DRTO is tested only for one day, with a shrinking time horizon. 5 different scenarios are created, illustrated in Figure II.6 for the winter day, as an example. The solid blue line represents the forecast used during the planning phase and the dashed black line is the actual realization. Scenario 1 is a negative disturbance, there is 20% less solar irradiance actually available than predicted. Scenario 2 is a positive disturbance of maximum 20%. For the summer day, the positive disturbance is limited to the maximum GHI possible for the location. Scenario 3 is a random disturbance of $\pm$ 20%, representing clouds. There is a random value for each hour, and spline interpolation is used to create the rest of the curve, ensuring that the variations in the GHI are not faster than the DRTO time step. In reality, measured values for the GHI during a cloudy day present more variations. The disturbance considered here is a smooth profile. Finally, scenario 4 presents more solar irradiance in the morning and less in the afternoon, while scenario 5 is the opposite. Naturally, for a real application, these scenarios would be replaced by the actual weather. In order to correct the optimal operating strategy to take into account the disturbances, a new DRTO is performed every hour. The initial state of the solar thermal plant is retrieved from the plant model, which undergoes the actual weather and has a more precise storage tank model. In a real application, the

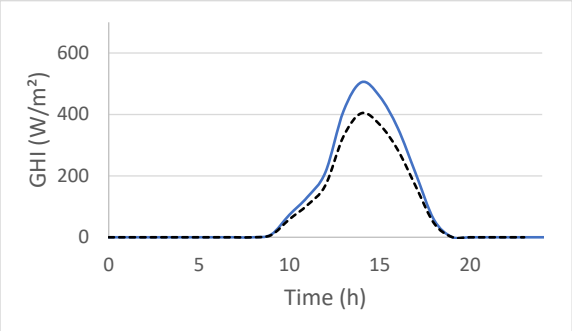

(a) Scenario 1: less

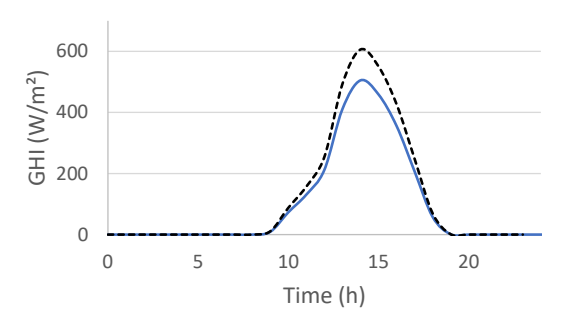

(b) Scenario 2: more

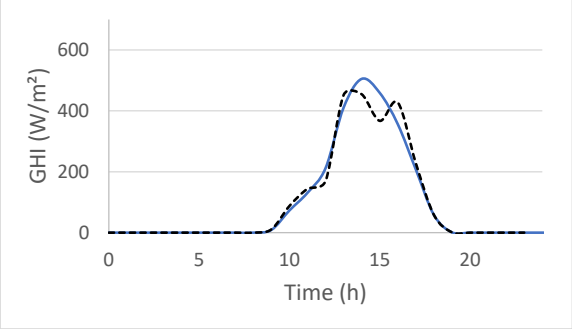

(c) Scenario 3: clouds

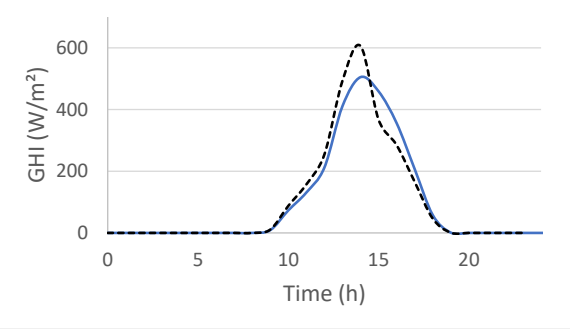

(d) Scenario 4: more then less

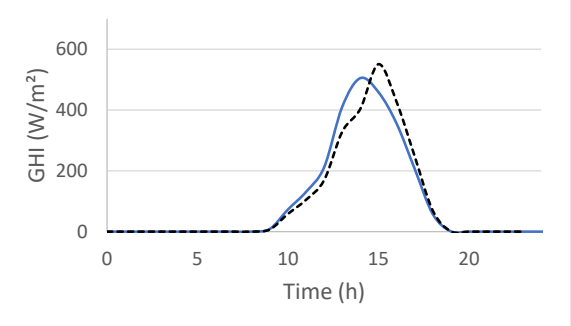

(e) Scenario 5: less then more

Figure II.6: Real-time solar irradiance scenarios: the solid blue line is the forecast and the dashed black line is the realization

initial state would be obtained from measurements on the plant. An additional step of state estimation and data reconciliation should be conducted to retrieve the initial state from the measured data and use it in the optimization model. The weather data fed into the DRTO algorithm should be a real and updated forecast for the time span of the DRTO. In this work, we built this data set with a simple numerical artifice using the planned weather data corrected by the real-time measurement. The different profiles for the GHI predicted, updated and realized are presented in Figure II.7, as an example, for the winter day with scenario 1. The numerical update should be replaced by an actual weather update from a specialist, or by a machine learning method (see (Fouilloy et al.; 2018) for example), to improve its accuracy for a real application.

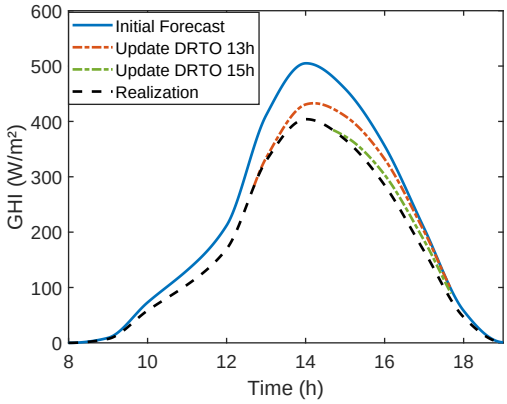

Figure II.7: Forecasted, Updated and realized weather data

II.4.3 Other inputs

The heat demand is considered constant for this case study. In a DHN, the heat demand is not constant and varies throughout the day and between seasons. The methodology developed could be applied to a variable heat demand but constant heat demand was chosen in first approach. The same heat demand is considered for the 3 seasons to facilitate the comparison between scenarios. The consumer stream arrives at 55°C with a flow rate of $8kg.s^{-1}$. The demand of thermal energy is 334kW and the target temperature for the consumer is 65°C. This represents a small heat demand, that could be the demand of a DHN in summer. In winter and mid-seasons, the heat demand cannot be met entirely while in summer, storage management is crucial to avoid exceeding the demand and overheating in the solar field. The initial temperatures at the beginning of the planning phase are equal to the ambient temperature. The planning phase starts at 0 hour, which is the middle of the night. Therefore, the solar field circuit is not used. The storage tank is initially half charged. The bottom half of the storage tank is at the return temperature of 55°C, which does not contain any value for the consumer. The top half is at 75°C, which is a temperature typically achieved in the solar field. The DRTO starts when solar irradiation is high enough to produce energy and the initial state of the first DRTO is retrieved from the planning. Then, the simulation will provide the initial conditions for the next DRTO runs.

II.4.4 Outputs

The free flow rates are optimized in the planning and the DRTO phases. However, the flow rate on the cold side of the first heat exchanger, $\dot{m}_{production}$ was fixed with the equality of the calorific fluxes in the heat exchanger. This is the common practice for the operation of solar thermal plants and it was found to facilitate convergence of the optimizations. During daytime, once the solar field is warm, the recirculation loop allowing the fluid to by-pass the first heat exchanger in the solar field circuit is not used anymore. To simplify the DRTO algorithm, this part was not modeled. In the real system, several warm up phases could happen during a day if the weather is highly variable. Thus, this limitation in our methodology could be improved in future work, if necessary.

The outputs obtained from the optimizations are the optimized flow rates in the different parts of the plant and the temperatures in each sub-system. The analysis of the results of the optimizations is not straightforward. Indeed, the thermal power terms are nonlinear, with the product of flow rate and temperature appearing. Thus, two distinct ways can increase the power: increase the flow rate or increase the temperature. For example in the solar field, if the flow rate is increased, the outlet temperature will decrease and reciprocally. Hence, there is an optimal strategy to be found in order to collect the maximum amount of useful energy. However, this optimal strategy is not intuitive and this is why mathematical optimization is used.

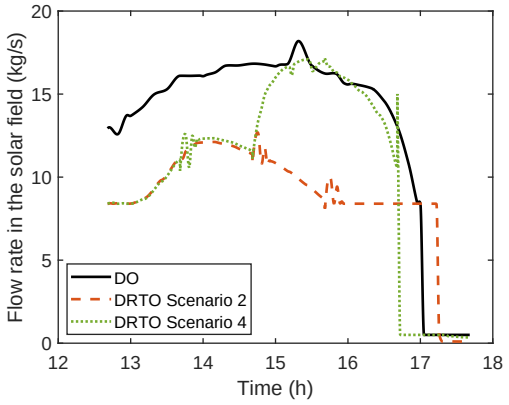

Figure II.8: Optimized flow rate in the solar field for planning and 2 DRTO scenarios in winter

Figure II.8 shows the optimized flow rates in the solar field for the winter day for the planning (DO) phase, the DRTO with scenario 2 and the DRTO with scenario 4. In this graphic, the trajectories for the flow rates are very different. In the case of scenario 2, with more solar irradiance than expected, the optimized flow rate is much smaller than the planned flow rate. This is because the additional solar irradiation allows the solar field to collect enough energy without using a high flow rate. Thus, we can save on electricity consumption, while still maintaining a good respect of the demand. We can also notice that the solar field is operated slightly longer because the solar irradiation decreases a little bit slower at the end of the day. For the scenario 4, with more and then less solar irradiance than expected, a similar analysis can be conducted. At first, the solar irradiation is larger than expected, hence the flow rate is

reduced. However, in the afternoon, the solar irradiation goes down and the flow rate is increased to ensure the collection of enough energy despite the lower irradiation. This energy will have a lower temperature than the one achieved the first half of the day but it is still valuable for the consumer. In this scenario, the solar irradiation goes down slightly earlier in the day, so the flow rate is zero earlier than in the planning phase. Based on these observations, we can see that DRTO adapts its operating strategy to the current disturbances and might even change the operating mode of the solar thermal plant to achieve the best performances. This shows the interest of our method, which only uses the flow rates determined at the DRTO level since the planning phase is employed for the storage management. The next sections will present detailed results and discussions on the performances of our DRTO methodology.

II.5 Storage management

As mentioned in Section II.3, the objective function of the DRTO involves a term for tracking the final storage state. The quantity of energy stored in the storage tank at the end of the day should be close to the one determined during the planning phase since it had a better strategic vision. Nevertheless, the operating costs during that day should still be minimized. Hence, the storage state tracking term is affected by a weight ω, as seen in Equation II.11. In order to assess the effect of the storage state tracking term on the performances of the solar thermal plant, a sensitivity analysis is conducted on the weight ω. This study is carried out in summer with a disturbance of -20% on the GHI for the real-time weather (Scenario 1). In summer, the storage tank is used the most whereas in winter or mid-season, the storage tank is more likely to be empty at the end of the day. Scenario 1 was chosen since it will easily show the interest of the storage state tracking term. With less solar irradiance than expected, the DRTO algorithm will tend to store less heat if no storage state tracking is included in the method. For the summer day, the heat demand during daytime is 3.344MWh and the objective on the storage state at the end of the day is 11.9MWh.

Table II.1: Effect of the weight ω on the simulated solar thermal plant performances

ω	**0**	**0.1**	**0.2**	**0.3**	**0.4**	**0.5**	**0.6**	**0.7**	**0.8**	**0.9**	**1**
E_{elec} (MWh)	0.025	0.023	0.030	0.036	0.041	0.045	0.049	0.052	0.054	0.057	0.057
E_{stored} (MWh)	6.85	7.56	7.85	7.98	8.06	8.13	8.18	8.23	8.26	8.40	8.56
$E_{supplied}$ (MWh)	3.23	3.23	3.22	3.22	3.22	3.22	3.22	3.22	3.20	3.11	2.94
Total cost (€)	12.4	12.4	13.8	14.5	15.3	15.8	16.1	16.8	18.3	25.9	40.0
Solar part (%)	96.6	96.5	96.3	96.3	96.3	96.3	96.3	96.2	95.8	93.1	87.8

The weight ω in the DRTO objective function was varied between 0 and 1, and for each weight chosen, the DRTO methodology was run, namely, the simulation was run for the complete day, with a new call to the DRTO algorithm every hour to obtain updated trajectories. Table II.1 shows the results achieved at the end of the simulation for each weight. Clear trends are visible in this table. Firstly, as expected, the quantity of energy in the storage tank at the end of the day, E_{stored}, increases with ω. This is done at the expense of a smaller amount of energy supplied to the consumer, $E_{supplied}$, and thus, a smaller fraction of the demand completed with solar heat (Solar

part). Moreover, the electricity consumption from the pumps tends to increase with ω. Therefore, with more gas used to complete the demand and more electricity consumed, the operating cost (true economic cost, without penalties) of the day increases with ω.

We can notice that the quantity of energy stored inside the storage tank at the end of the simulation is much lower than the objective, 11.9MWh, even when ω is close to 1. Although it is expected to store less energy when less solar irradiation is available, the difference seems too important to only result from the disturbance on the GHI. This will be explained in Section II.6.

In order to visualize the results from Table II.1 and help to find the best weight, two different performance criteria are plotted in Figure II.9 for the various values of ω. The solid orange line represents the difference between the stored energy at the end of the simulated day and the storage state target from planning. The difference decreases rapidly between 0 and 0.2 and then continues to decrease slowly. This shows that the chosen weight must be greater than 0.2 to ensure a reasonable storage state tracking. The dashed blue line shows the difference between the total operating cost achieved for the day and the cost achieved when no objective on the storage is considered ($\omega = 0$). The operating cost increases slowly for small weights, but for ω greater than 0.7, the operating cost increases rapidly, up to 225% of the cost for the weight 0, when ω is 1. The cost for a weight of 1 is visible in Table II.1, but is not represented in Figure II.9 because it is much larger than the other cost differences for the smaller weights. Based on Figure II.9 analysis, the chosen weight must be below 0.7 to avoid large operating costs. Thus, a compromise must be found between a good storage state tracking and small operating costs, the weight should be greater than 0.2 and lower than 0.7. This sensitivity analysis was carried out on a specific example. A different real-time scenario might lead to slightly different results, although the general trends described above should hold in most cases. A variable weight could be considered, adjusted according to the weather data. For example, for a much smaller solar irradiation than expected, the storage state target cannot be met. Thus, it seems more suitable to minimize the cost of the day without consideration for the planned stored energy. This could be explored in future work but in the current paper a fixed weight was chosen.

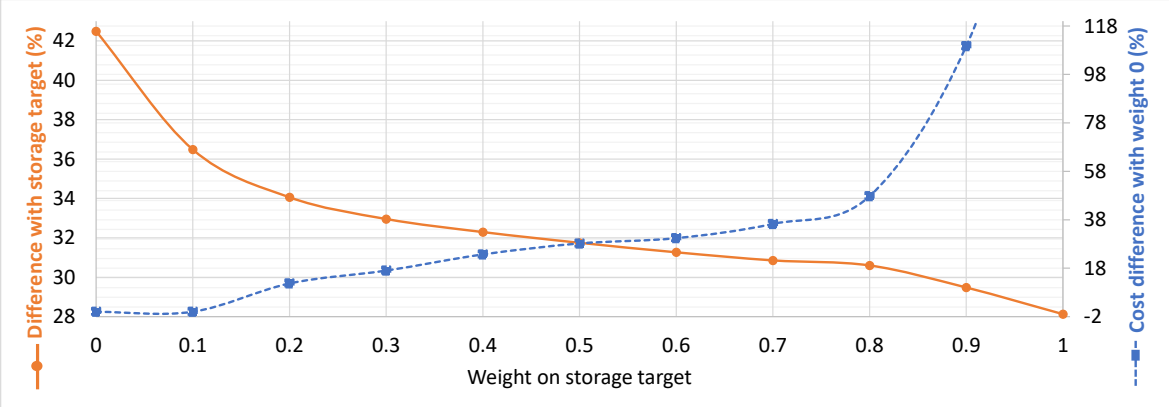

Figure II.9: Effect on the weight ω on the total cost and the following of the storage state target

Based on the analysis of Figure II.9, the best value for ω ensuring a reasonable storage state tracking and low operating costs is around 0.5. Thus, for the next section,

a weight of 0.5 is used in the DRTO objective function.

II.6 Comparison between DO and DRTO

In order to assess the performances of our DRTO methodology, we compared the results from a simulation following the trajectories determined during the planning phase (S-DO) to the results from the simulation regularly calling the DRTO algorithm (S-DRTO). Figure II.10 summarizes how this comparative study was carried out. For each season and each scenario, the following calculations were done. Firstly, the planning phase is ran for the corresponding season. For the real-time scenario, a simulation is ran, undergoing the actual weather, with the flow rate trajectories directly retrieved from the planning phase. This corresponds to the solar thermal plant performances if offline dynamic optimization is employed. This case is represented on the right hand side of Figure II.10. Another simulation, undergoing the same real-time scenario, is ran but using DRTO this time. The DRTO algorithm is called every hour, providing new flow rate trajectories for the simulation model. The DRTO algorithm takes into account a storage state tracking term in its objective function, as presented in Equation II.11, with the weight of 0.5 determined in Section II.5. It uses updated forecasts based on the real-time value to determine the optimal operation of the plant. Our methodology is presented on the left hand side of Figure II.10.

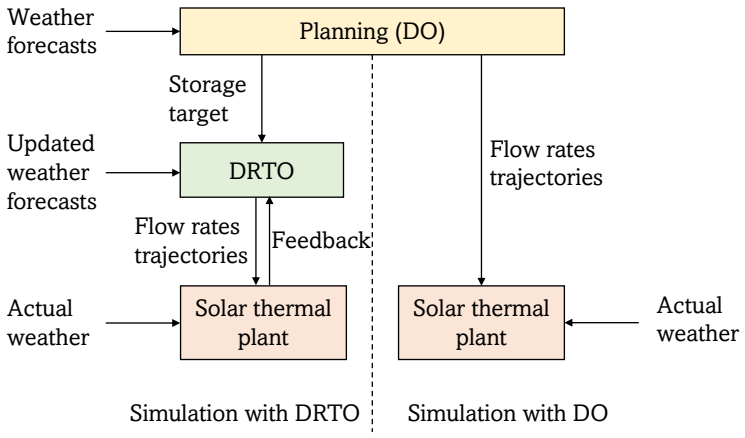

Figure II.10: Comparison of simulations based on DRTO or DO

The 5 scenarios presented in Figure II.6 for the real-time weather are tested, with an additional scenario 0 corresponding to no disturbance on the GHI. This scenario without disturbance allows us to compare the DO and DRTO methods when using the same inputs. The performance criteria studied in this comparison are:

- The quantity of energy stored in the storage tank at the end of the day E_{stored}. This number should be as close as possible to the target determined during planning.
- The excess heat E_{excess} which corresponds to the energy delivered to the consumer exceeding the heat demand. This should be minimal because exceeding the heat demand is generally forbidden by the consumer.

- The total operating cost summing the pumping cost and the cost of the gas used in the backup heater to complete the heat demand.
- The solar part (%) which is the percentage of the heat demand met by solar heat, either directly supplied, or thanks to the storage tank.

These four performance indicators are given for the summer day without any disturbance (scenario 0) in Table II.2. S-DO and S-DRTO refer to the simulation based on DO and the simulation based on DRTO respectively. That means that S-DO is the simulation employing the optimal trajectories determined during the planning (DO) phase, while S-DRTO is the simulation employing the optimal trajectories determined during the online (DRTO) phase. As a remainder, for the summer day, the heat demand during daytime is 3.344MWh and the objective on the storage state at the end of the day is 11.9MWh. Firstly, we can notice that the stored energy at the end of the day for both simulations is much lower than the target storage state from the planning phase. This shows that the target determined during planning is not feasible for the real system, here represented by the simulation model. In our methodology, the storage tank is modeled with a 1D model using finite volume discretization. The optimization model only uses 10 layers for the discretization scheme while the simulation model uses 1000 layers. Additionally, temperature inversions are corrected in the simulation model but not in the optimization model. Therefore, the optimization model for the storage tank is not accurate. During the planning phase, the storage tank is modeled with a low accuracy. The storage state target is computed at the end of the day, when the solar irradiation is going down. Thus, there are temperature inversions inside the storage tank, but no mixing is modeled to correct them. Because of this simplified model, the quantity of energy stored at the end of the day is over-estimated. When the simulation is carried out, using the trajectories determined during planning (S-DO) and with a more precise model for the storage tank, the quantity of energy actually stored differs from the target, even if the inputs of the problem are the same. Thus, the actual storage state target would be 10.63MWh, which corresponds to the energy actually stored at the end of the day for S-DO with no disturbance, as shown in Table II.2. This table allows us to compared the performance indicators for the simulation based on DO and the simulation based on DRTO. We observe that the results are similar, showing that the weight on the storage state tracking term in the objective function of the DRTO was correctly adjusted. Both the energy stored and the energy supplied are similar, with slightly better performances for S-DO in this example. In both simulations, the heat demand is slightly exceeded, even though no disturbance appears. We expect to exceed the heat demand in the case of S-DO with a positive disturbance on the GHI because the trajectories are planned for a lower solar irradiation and cannot be adapted. But even without a higher solar irradiation, a small excess energy appears. This is probably due to the difference in the storage tank models between the optimization and simulation models again. The fluid coming from the storage tank has a different temperature in both models, leading to the supply of an energy at a different temperature level. We notice that the excess heat is smaller in S-DRTO because the optimization regularly starts over with a corrected initial state. Based on this analysis, we notice that our DRTO methodology is able to correct the error made by the optimization model because the optimization algorithm regularly starts over with a corrected initial state, retrieved from the accurate simulation model

in our study. On the other hand, DO uses the simplified storage tank model for the entire time horizon. Thus, DO leads to a larger deviation from the simulated plant performances. In a real application, the optimization model cannot perfectly represent the actual plant and there will always be a plant-model mismatch. If DRTO is applied to an actual plant very well instrumented, with sensors to ensure a correct initial state at the beginning of each DRTO run, then our methodology can help to correct the plant-model mismatch. This verification part showed that our DRTO methodology is able to optimize the operation of a solar thermal plant without degrading the storage management and even reducing the plant-model mismatch impact. We will now test its ability to operate in an uncertain environment.

Table II.2: Results of the simulations based on DO and DRTO for a summer day without disturbance

	S-DO	S-DRTO
E_{stored} (MWh)	10.63	10.59
E_{excess} (MWh)	0.08	0.04
Total cost (€)	10.1	14.1
Solar part (%)	97.7	96.9

The four performance indicators for each real-time scenario are given in Tables II.3, II.4 and II.5 in the Appendix, for summer, mid-season and winter respectively. In order to visualize the results, the four criteria are plotted in Figure II.12 in terms of percentage of improvement for S-DRTO compared to S-DO. For each graphic, if the criteria is improved by DRTO, the value is positive and it appears in the green zone of the plot. Conversely, if the performance is deteriorated by DRTO, the percentage of difference is negative and it appears in the red zone of the plot. Figure II.12a presents the improvement in the solar part. It shows that S-DRTO leads to a better satisfaction of the demand with solar heat compared to S-DO, hence less gas used in the backup heater. The improvement is better for scenarios with less solar irradiation during a part of the day such as Scenario 1, 4 and 5. Such results were expected because S-DO follows trajectories computed for a higher solar irradiation. When the solar irradiation is lower than expected, but the same trajectories are used, it leads to a decrease in the solar heat delivery. Figure II.12b presents the improvement in the total operating costs, which are to be minimized. In mid-season and winter, S-DRTO always presented lower costs, due to lower electricity and gas consumption, compared to S-DO. For summer, 3 scenarios led to larger costs with DRTO. In summer, the operating costs tend to be lower than in other seasons because the solar irradiation is higher, allowing the demand to be entirely met. Thus, gas consumption is very low and the cost mostly generates from the electricity consumption. The 3 scenarios with an increased operating cost for S-DRTO correspond to scenarios with an equal amount or higher solar irradiation available in the real-time scenario compared to the forecast. Thus, the heat demand is met almost entirely and barely no gas is used. The cost only comes from the electricity consumption, which is small. Since the costs are low, a high relative difference between S-DO and S-DRTO actually corresponds to an absolute difference of a few euros, as can be seen in Table II.3. This is represented in Figure II.11, where the operating costs for each scenario are plotted for S-DO and S-DRTO. This figure shows that DRTO

largely reduced the operating costs when less solar irradiation was available. For the other scenarios, the operating costs for S-DO and S-DRTO are very similar. Thus,

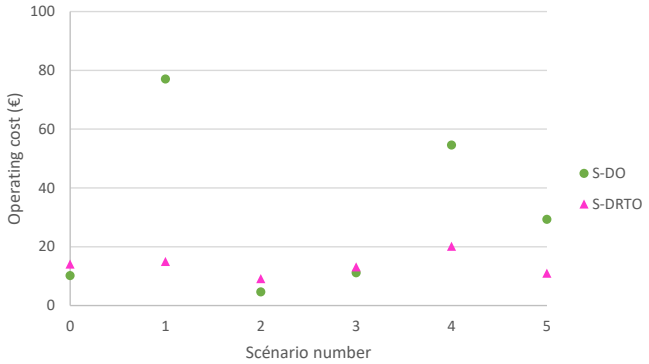

Figure II.11: Operating costs for each scenario in summer

DRTO seems to improve the cost of the solar thermal plant in most cases and, more importantly, when it makes the biggest impact. Figure II.12c shows the reduction of the excess heat, achieved thanks to DRTO. For scenario 1, where less solar irradiation during the whole day is considered, the heat demand is barely exceeded with both optimization methodologies. The excess heat is only due to a slight violation of the constraint on the respect of the heat demand, represented as a penalty term in II.11. Thus, the comparison between S-DO and S-DRTO in this case is not presented on figure II.12c because it is not relevant. For the other scenarios, DRTO always led to a better respect of the maximum amount of heat delivered. Since in S-DO the optimal operating strategy is not adapted in real-time, the heat demand is exceeded every time the solar irradiation is larger than predicted. Thanks to the online adaptation, S-DRTO is able to correct the trajectories and reduce the delivery of excess heat. Finally, Figure II.12d shows the difference in the amount of energy stored in the storage tank at the end of the simulated day. Since the objective determined during planning is not feasible and over-estimates the actual energy stored, as explained previously, the quantity of energy stored in S-DO and S-DRTO are directly compared. We can observe that the quantity of energy stored with S-DRTO does not differ much from the one stored with S-DO. The maximum difference is about -14%. Generally, S-DRTO tends to charge slightly less energy. Of course, the performances of the DRTO methodology depend on the weight chosen in Section II.5. The compromise of 0.5 determined in the sensitivity analysis seems to perform well, without deteriorating the storage management.

To conclude, our DRTO methodology presents some advantages over an offline dynamic optimization to operate a solar thermal plant. For most of our test cases, the solar part was increased, the operating costs were decreased and the excess heat was reduced thanks to the online adaptation. With our storage management strategy using the planning phase, we were able to achieve these improvements in the solar thermal plant performances only at the cost of a slight reduction of the quantity of energy stored. Therefore, our objective to reconcile accurate forecasts and long term strategic vision to find the best operational strategy for the solar thermal plant is met.

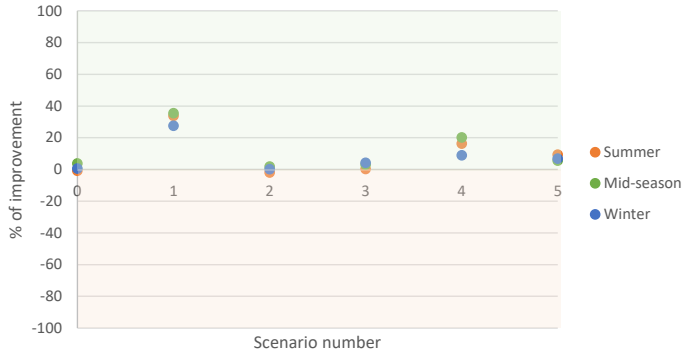

(a) Increase of the solar part

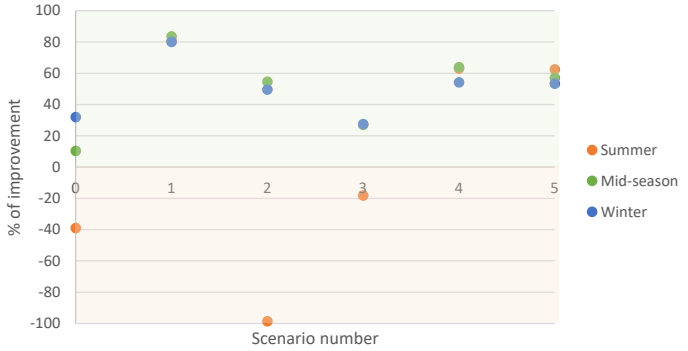

(b) Reduction of the operating cost

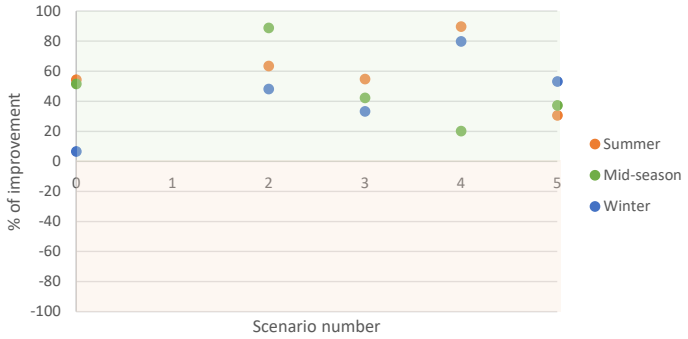

(c) Reduction of the excess heat

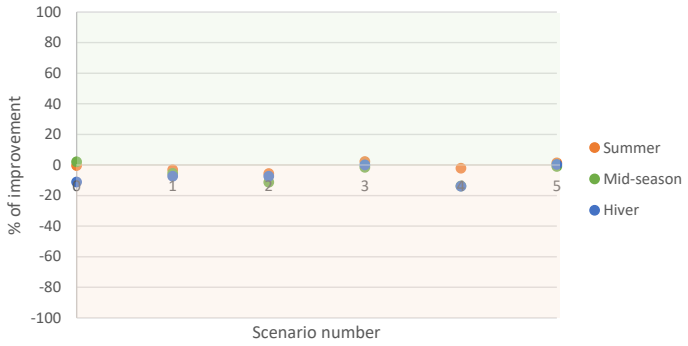

(d) Increase of the final energy stored

Figure II.12: Improvement of the solar thermal plant performances with DRTO compared to the simulation with DO

II.7 Conclusion and Perspectives

In this work, an economic DRTO methodology using a planning phase for storage management was developed for a solar thermal plant. A storage state target determined during the planning phase, thanks to its longer term strategic vision, was incorporated into the DRTO objective function. A weight associated with this term was adjusted with a sensitivity analysis to achieve a reasonable tracking of the storage target while minimizing the operating costs. A case study covering the different seasons of the year and with several real-time scenarios was conducted to assess the performances of our DRTO methodology. The results from simulations undergoing the actual weather, either following the optimal trajectories from the offline planning, or the regularly updated trajectories from the DRTO, were compared. We observed an improvement of the performances of the solar thermal plant thanks to our online optimization method. The solar part in the supplied energy was increased while the operating costs and excess energy were reduced. The storage state target was reasonably tracked. Thus, we were able to find a compromise between accurate forecasts and long term strategic vision in order to determine the optimal operation of the solar thermal plant. This brings good perspectives for the application of our DRTO methodology to a real system. Several directions could be taken for future work. Firstly, the models could be improved to offer a better compromise between accuracy and computational time, especially for the storage tank. Another discretization scheme such as orthogonal collocation on finite elements could help to speed up the calculations and represent more precisely the thermocline region. Moreover, the integration of natural convection in the tank model for an optimization study still needs to be investigated, with a validation step based on experiments or using a detailed CFD model. Different models could be used for the planning and for the DRTO. Indeed, the DRTO needs to run fast because of the real-time application, but the planning phase can take a bit longer, up to a night for example. Thus, the planning model could be more precise. Also, a convergence study on the time discretization could help to find an optimal solution faster. Secondly, the methodology should be tested over a longer time horizon and considering disturbances on all the inputs. In this case, a rolling time horizon for the DRTO could be more appropriate since disturbances could happen at any time. Then, the integration of the storage state target could be different, with the tracking of a trajectory for the storage state instead of a value at the end of the time horizon. These possibilities should be explored to assess the best way to improve the solar thermal plant performances with the best storage management. Finally, before its testing on an actual plant, the methodology should be tested with real weather and load data, and include a state estimation step.

Acknowledgements

The project leading to this publication has received funding from Excellence Initiative of Université de Pau et des Pays de l'Adour – I-Site E2S UPPA, a French "Investissements d'Avenir" programme.

CRediT authorship contribution statement

Alix Untrau: Conceptualization, Data curation, Formal analysis, Investigation, Methodology, Software, Validation, Visualization, Writing – original draft, Writing – review & editing. **Sabine Sochard:** Conceptualization, Funding acquisition, Methodology, Project administration, Resources, Supervision, Writing – review & editing. **Frédéric Marias:** Conceptualization, Funding acquisition, Methodology, Project administration, Resources, Supervision, Writing – review & editing. **Jean-Michel Reneaume:** Conceptualization, Funding acquisition, Methodology, Project administration, Resources, Supervision, Writing – review & editing. **Galo A.C. Le Roux:** Conceptualization, Methodology, Supervision, Writing – original draft, Writing – review & editing. **Sylvain Serra:** Conceptualization, Funding acquisition, Methodology, Project administration, Resources, Supervision, Writing – original draft, Writing – review & editing.

II.8 Appendix: Comparison between S-DO and S-DRTO

Tables II.3, II.4 and II.5 present the comparison of the performances of the simulated solar thermal plant optimized offline (S-DO) and online (S-DRTO), as explained in Section II.6, respectively for summer, mid-season and winter. The scenario numbers are explained in Figure II.6, and the additional scenario 0 corresponds to no disturbance in the GHI. A green color code is used for the cells where an improvement in the performance criteria is noticed with DRTO, compared to DO, and a red color code is applied when a deterioration of the performance is observed.

Table II.3: Summer

	0		1		2		3		4		5	
	S-DO	S-DRTO	S-DO	S-DRTO	S-DO	S-DRTO	S-DO	S-DRTO	S-DO	S-DRTO	S-DO	S-DRTO
E_{stored} (MWh)	10.63	10.59	8.49	8.22	11.23	10.61	10.82	11.06	9.21	9.01	10.13	10.27
E_{excess} (MWh)	0.08	0.04	0.00	0.02	0.28	0.10	0.25	0.11	0.15	0.02	0.09	0.06
Total cost (€)	10.1	14.1	77.0	15.0	4.6	9.1	11.1	13.1	54.6	20.2	29.3	11.0
Solar part (%)	97.7	96.9	72.7	97.3	99.8	97.9	97.4	97.7	81.1	94.4	90.5	99.0

Table II.4: Mid-season

	0		1		2		3		4		5	
	S-DO	S-DRTO	S-DO	S-DRTO	S-DO	S-DRTO	S-DO	S-DRTO	S-DO	S-DRTO	S-DO	S-DRTO
E_{stored} (MWh)	4.93	5.03	4.22	3.98	5.58	4.95	4.95	4.88	4.38	3.78	5.31	5.26
E_{excess} (MWh)	0.04	0.02	0.00	0.01	0.41	0.05	0.09	0.05	0.06	0.05	0.30	0.19
Total cost (€)	10.5	9.5	49.0	8.1	9.4	4.3	20.2	14.7	39.8	14.4	14.6	6.3
Solar part (%)	93.4	97.0	71.9	97.4	96.6	98.3	89.8	92.6	77.6	93.3	93.3	98.6

Table II.5: Winter

	0		1		2		3		4		5	
	S-DO	S-DRTO	S-DO	S-DRTO	S-DO	S-DRTO	S-DO	S-DRTO	S-DO	S-DRTO	S-DO	S-DRTO
E_{stored} (MWh)	4.93	4.38	4.22	3.90	5.44	5.04	4.90	4.90	4.48	3.86	4.99	5.01
E_{excess} (MWh)	0.04	0.03	0.00	0.00	0.31	0.16	0.09	0.06	0.10	0.02	0.16	0.07
Total cost (€)	5.9	4.0	34.6	6.9	4.2	2.1	12.0	8.7	21.0	9.6	13.4	6.2
Solar part (%)	98.0	98.6	76.5	97.6	99.3	99.5	93.4	97.3	86.7	94.5	92.4	98.7

Bibliography

Alonso, A. A., Arias-Méndez, A., Balsa-Canto, E., García, M. R., Molina, J. I., Vilas, C. and Villafín, M. (2013). Real time optimization for quality control of batch thermal sterilization of prepackaged foods, *Food Control* **32**: 392–403.

Arpornwichanop, A., Kittisupakorn, P. and Mujtaba, I. (2005). On-line dynamic optimization and control strategy for improving the performance of batch reactors, *Chemical Engineering and Processing: Process Intensification* **44**: 101–114.

Brodrick, P. G., Brandt, A. R. and Durlofsky, L. J. (2018). Optimal design and operation of integrated solar combined cycles under emissions intensity constraints, *Applied Energy* **226**: 979–990.

Camacho, E., Rubio, F., Berenguel, M. and Valenzuela, L. (2007a). A survey on control schemes for distributed solar collector fields. Part I: Modeling and basic control approaches, *Solar Energy* **81**(10): 1240–1251.

Camacho, E., Rubio, F., Berenguel, M. and Valenzuela, L. (2007b). A survey on control schemes for distributed solar collector fields. Part II: Advanced control approaches, *Solar Energy* **81**(10): 1252–1272.

Campos Celador, A., Odriozola, M. and Sala, J. (2011). Implications of the modelling of stratified hot water storage tanks in the simulation of CHP plants, *Energy Conversion and Management* **52**(8-9): 3018–3026.

Casella, F., Casati, E. and Colonna, P. (2014). Optimal Operation of Solar Tower Plants with Thermal Storage for System Design, *IFAC Proceedings volumes - 19th World Congress*, Cape Town, South Africa, pp. 4972–4978.

Caspari, A., Tsay, C., Mhamdi, A., Baldea, M. and Mitsos, A. (2020). The integration of scheduling and control: Top-down vs. bottom-up, *Journal of Process Control* **91**: 50–62.

Clarke, W. C., Manzie, C. and Brear, M. J. (2018). Hierarchical economic MPC for systems with storage states, *Automatica* **94**: 138–150.

Close, D. (1967). A design approach for solar processes, *Solar Energy* **11(2)**: 112–122.

Collier, U. (2018). Renewable Heat Policies - Delivering clean heat solutions for the energy transition, *Insights Series 2018 - International Energy Agency* .

Csordas, G., Brunger, A., Hollands, K. and Lightstone, M. (1992). Plume entrainment effects in solar domestic hot water systems employing variable-flow-rate control strategies, *Solar Energy* **49**(6): 497–505.

Darby, M. L., Nikolaou, M., Jones, J. and Nicholson, D. (2011). RTO: An overview and assessment of current practice, *Journal of Process Control* **21**: 874–884.

de Azevedo Delou, P., Curvelo, R., de Souza, M. B. and Secchi, A. R. (2021). Steady-state real-time optimization using transient measurements in the absence of a dynamic mechanistic model: A framework of hrto integrated with adaptive self-optimizing ihmpc, *Journal of Process Control* **106**: 1–19.

De Oliveira, V., Jaschke, J. and Skogestad, S. (2013). Dynamic online optimization of a house heating system in a fluctuating energy price scenario, *IFAC Proceedings Volumes - 10th International Symposium on Dynamics and Control of Process Systems*, Elsevier, Mumbai, India, pp. 463–468.

Delubac, R., Serra, S., Sochard, S. and Reneaume, J.-M. (2021). A Dynamic Optimization Tool to Size and Operate Solar Thermal District Heating Networks Production Plants, *Energies* **14**(23): 8003.

Elixmann, D., Busch, J. and Marquardt, W. (2010). Integration of model-predictive scheduling, dynamic real-time optimization and output tracking for a wastewater treatment process, *IFAC Proceedings Volumes - 11th International Symposium on Computer Applications in Biotechnology*, Vol. 43, Elsevier, Leuven, Belgium, pp. 90–95.

Ellingwood, K., Mohammadi, K. and Powell, K. (2020). Dynamic optimization and economic evaluation of flexible heat integration in a hybrid concentrated solar power plant, *Applied Energy* **276**: 115513.

Engell, S. (2007). Feedback control for optimal process operation, *Journal of Process Control* **17**: 203–219.

Farkas, I. and Géczy-Víg, P. (2003). Neural network modelling of flat–plate solar collectors, *Computers and Electronics in Agriculture* **40**(1-3): 87–102.

Fouilloy, A., Voyant, C., Notton, G., Motte, F., Paoli, C., Nivet, M.-L., Guillot, E. and Duchaud, J.-L. (2018). Solar irradiation prediction with machine learning: Forecasting models selection method depending on weather variability, *Energy* **165**: 620–629.

Franke, R. (1997). Object-oriented modeling of solar heating systems, *Solar Energy* **60**: 171–180.

Gálvez-Carrillo, M., De Keyser, R. and Ionescu, C. (2009). Nonlinear predictive control with dead-time compensator: Application to a solar power plant, *Solar Energy* **83**: 743–752.

Guelpa, E. and Verda, V. (2019). Thermal energy storage in district heating and cooling systems: A review, *Applied Energy* **252**: 113474.

Hawlader, M. N. A., Bong, T. Y. and Lee, T. S. (1988). A Thermally Stratified Solar Water Storage Tank, *International Journal of Solar Energy* **6**(2): 119–138.

He, Z., Qian, Y., Xu, C., Yang, L. and Du, X. (2019). Static and dynamic thermocline evolution in the water thermocline storage tank, *Energy Procedia* **158**: 4471–4476.

Hedengren, J. D., Shishavan, R. A., Powell, K. M. and Edgar, T. F. (2014). Nonlinear modeling, estimation and predictive control in APMonitor, *Computers & Chemical Engineering* **70**: 133–148.

Heng, S. Y., Asako, Y., Suwa, T. and Nagasaka, K. (2019). Transient thermal prediction methodology for parabolic trough solar collector tube using artificial neural network, *Renewable Energy* **131**: 168–179.

Hirvonen, J., ur Rehman, H. and Sirén, K. (2018). Techno-economic optimization and analysis of a high latitude solar district heating system with seasonal storage, considering different community sizes, *Solar Energy* **162**: 472–488.

Hosseinnia, S. M., Akbari, H. and Sorin, M. (2021). Numerical analysis of thermocline evolution during charging phase in a stratified thermal energy storage tank, *Journal of Energy Storage* **40**: 102682.

IEA, I. E. A. (2015). Integration guideline, solar process heat for production and advanced applications, *Task 49, Solar Heating and Cooling Program* .

Immonen, J. and Powell, K. M. (2022). Dynamic optimization with flexible heat integration of a solar parabolic trough collector plant with thermal energy storage used for industrial process heat, *Energy Conversion and Management* **267**: 115921.

Incropera, F., Dewitt, D., Bergman, T. and Lavine, A. (2007). Fundamentals of heat and mass transfer, *John Wiley, 6th edition* .

ISO/FDIS 9806 (2017). Énergie solaire - capteurs thermiques solaires - méthodes d'essai, *International Standard* .

Jannesari, H. and Babaei, B. (2018). Optimization of solar assisted heating system for electro-winning process in the copper complex, *Energy* **158**: 957–966.

Kadam, J. V., Schlegel, M., Marquardt, W., Tousain, R. L., Van Hessem, D. H., Van Den Berg, J. and Bosgra, O. H. (2002). A Two-Level Strategy of Integrated Dynamic Optimization and Control of Industrial Processes - a Case Study, *European Symposium on Computer Aided Process Engineering*, Vol. 12, Elsevier, The Hague, The Netherlands, pp. 511–516.

Kalogirou, S. A. (2004). Solar thermal collectors and applications, *Progress in Energy and Combustion Science* **30**(3): 231–295.

Kleinbach, E., Beckman, W. and Klein, S. (1993). Performance study of one-dimensional models for stratified thermal storage tanks, *Solar Energy* **50**(2): 155–166.

Koçak, B., Fernandez, A. I. and Paksoy, H. (2020). Review on sensible thermal energy storage for industrial solar applications and sustainability aspects, *Solar Energy* **209**: 135–169.

Krause, M., Vajen, K., Wiese, F. and Ackermann, H. (2003). Investigations on optimizing large solar thermal systems, *Solar Energy* **73**: 217–225.

Lago, J., De Ridder, F., Mazairac, W. and De Schutter, B. (2019). A 1-dimensional continuous and smooth model for thermally stratified storage tanks including mixing and buoyancy, *Applied Energy* **248**: 640–655.

Lizarraga-Garcia, E., Ghobeity, A., Totten, M. and Mitsos, A. (2013). Optimal operation of a solar-thermal power plant with energy storage and electricity buy-back from grid, *Energy* **51**: 61–70.

Matias, J. O. and Le Roux, G. A. (2018). Real-time Optimization with persistent parameter adaptation using online parameter estimation, *Journal of Process Control* **68**: 195–204.

Mendis, P., Wickramasinghe, C., Narayana, M. and Bayer, C. (2019). Adaptive model predictive control with successive linearization for distillate composition control in batch distillation, *2019 Moratuwa Engineering Research Conference (MERCon)*, pp. 366–369.

Nash, A. L., Badithela, A. and Jain, N. (2017). Dynamic modeling of a sensible thermal energy storage tank with an immersed coil heat exchanger under three operation modes, *Applied Energy* **195**: 877–889.

Newton, B. J. (1995). *Modelling of Solar Storage Tanks*, Master thesis, Unicersity of Wisconsin-Madison.

Parvareh, F., Milani, D., Sharma, M., Chiesa, M. and Abbas, A. (2015). Solar repowering of PCC-retrofitted power plants; solar thermal plant dynamic modelling and control strategies, *Solar Energy* **119**: 507–530.

Pataro, I. M. L., Roca, L., Sanches, J. L. G. and Berenguel, M. (2020). An economic D-RTO for thermal solar plant: analysis and simulations based on a feedback linearization control case, *XXIII Congresso Brasileiro de Automática*, Virtual event.

Pate, R. A. (1977). *A Thermal Energy Storage Tank Model for Solar Heating*, thesis, Utah State University.

Perez, R., Seals, R., Ineichen, P., Stewart, R. and Menicucci, D. (1987). A new simplified version of the perez diffuse irradiance model for tilted surfaces, *Solar Energy* **39(3)**: 221–231.

Pintaldi, S., Li, J., Sethuvenkatraman, S., White, S. and Rosengarten, G. (2019). Model predictive control of a high efficiency solar thermal cooling system with thermal storage, *Energy and Buildings* **196**: 214–226.

Powell, K. M. and Edgar, T. F. (2013). An adaptive-grid model for dynamic simulation of thermocline thermal energy storage systems, *Energy Conversion and Management* **76**: 865–873.

Powell, K. M., Hedengren, J. D. and Edgar, T. F. (2014). Dynamic optimization of a hybrid solar thermal and fossil fuel system, *Solar Energy* **108**: 210–218.

Rashid, K., Safdarnejad, S. M. and Powell, K. M. (2019). Process intensification of solar thermal power using hybridization, flexible heat integration, and real-time optimization, *Chemical Engineering and Processing - Process Intensification* **139**: 155–171.

Renewable Energy Directive (2018). Directive (EU) 2018/2001 of the European Parliament and of the Council of 11 December 2018 on the promotion of the use of energy from renewable sources, *OJ* **L328/82**.

Saloux, E. and Candanedo, J. (2019). Modelling stratified thermal energy storage tanks using an advanced flowrate distribution of the received flow, *Applied Energy* **241**: 34–45.

Saloux, E. and Candanedo, J. A. (2021). Model-based predictive control to minimize primary energy use in a solar district heating system with seasonal thermal energy storage, *Applied Energy* **291**: 116840.

Scolan, S. (2020). *Développement d'un outil de simulation et d'optimisation dynamique d'une centrale solaire thermique.*, thesis, Pau. Publication Title: http://www.theses.fr.

Scolan, S., Serra, S., Sochard, S., Delmas, P. and Reneaume, J.-M. (2020). Dynamic optimization of the operation of a solar thermal plant, *Solar Energy* **198**: 643–657.

Serale, G., Fiorentini, M., Capozzoli, A., Cooper, P. and Perino, M. (2018). Formulation of a model predictive control algorithm to enhance the performance of a latent heat solar thermal system, *Energy Conversion and Management* **173**: 438–449.

Soares, A., Camargo, J., Al-Koussa, J., Diriken, J., Van Bael, J. and Lago, J. (2022). Efficient temperature estimation for thermally stratified storage tanks with buoyancy and mixing effects, *Journal of Energy Storage* **50**: 104488.

Tian, Y. and Zhao, C. (2013). A review of solar collectors and thermal energy storage in solar thermal applications, *Applied Energy* **104**: 538–553.

Tian, Z., Perers, B., Furbo, S. and Fan, J. (2018). Thermo-economic optimization of a hybrid solar district heating plant with flat plate collectors and parabolic trough collectors in series, *Energy Conversion and Management* **165**: 92–101.

United Nations Framework Convention on Climate Change (2015). Adoption of the paris agreement, *21st Conference of the Parties* .

Untrau, A., Sochard, S., Marias, F., Reneaume, J.-M., Le Roux, G. A. C. and Serra, S. (2023b). A fast and accurate 1-dimensional model for dynamic simulation and optimization of a stratified thermal energy storage, *Applied Energy* **333**: 120614.

Untrau, A., Sochard, S., Marias, F., Reneaume, J.-M., Le Roux, G. A. and Serra, S. (2022). Analysis and future perspectives for the application of Dynamic Real-Time Optimization to solar thermal plants: A review, *Solar Energy* **241**: 275–291.

Vasallo, M. J., Cojocaru, E. G., Gegúndez, M. E. and Marín, D. (2021). Application of data-based solar field models to optimal generation scheduling in concentrating solar power plants, *Mathematics and Computers in Simulation* **190**: 1130–1149.

Viskanta, R., Behnia, M. and Karalis, A. (1977). Interferometric observations of the temperature structure in water cooled or heated from above, *Advances in Water Resources* **1**(2): 57–69.

Wagner, M. J., Hamilton, W. T., Newman, A., Dent, J., Diep, C. and Braun, R. (2018). Optimizing dispatch for a concentrated solar power tower, *Solar Energy* **174**: 1198–1211.

Wang, L., Sundén, B. and Manglik, M. (2007). Plate heat exchangers: Design, applications and performance, *WIT Press* .

Weiss, W. and Spörk-Dür, M. (2021). Global Market Development and Trends in 2020 Detailed Market Data 2019, *Solar Heating and Cooling Programme - International Energy Agency* .

Winterscheid, C., Dalenbäck, J.-O. and Holler, S. (2017). Integration of solar thermal systems in existing district heating systems, *Energy* **137**: 579–585.

Wittmann, M., Eck, M., Pitz-Paal, R. and Müller-Steinhagen, H. (2011). Methodology for optimized operation strategies of solar thermal power plants with integrated heat storage, *Solar Energy* **85**: 653–659.

Zurigat, Y., Ghajar, A. and Moretti, P. (1988). Stratified thermal storage tank inlet mixing characterization, *Applied Energy* **30**(2): 99–111.

II.9 Additional clarifications

- Boundary and initial conditions were missing for the storage tank model in Subsection IV.2.2. The two boundary conditions at the top and bottom of the tank are a zero thermal gradient. The initial condition can be provided as a given temperature profile inside the tank.
- The choice of 10 layers for the discretization of the height of the storage tank in the optimization model could be justified in more depth. Indeed, by looking at Figure II.3, we can see that using 10 layers deteriorates the accuracy of the model significantly compared to 100 layers. Moreover, the computational times for the charge of the storage tank alone are not too different: 0.1s for 10 layers and 0.14s for 100 layers. However, when looking at the computational times of the optimization of the operation of the complete solar thermal plant, the difference becomes more important. The computational time achieved when using 100 layers does not allow a real-time application. Therefore, 10 layers were used.

Chapter III

Storage tank modeling

Contents

In the previous chapter, the DRTO methodology in association with a planning phase was applied to a solar thermal plant in a simple case study. The results obtained on the simulated plant operated with DRTO were promising, with a reduction in the operating cost compared to the operation using dynamic optimization without real-time adaptation. The methodology was tested on a detailed simulation model representing the real solar thermal plant. As explained in subsection II.2.2, the storage tank is an element of the plant particularly challenging to model. As it is part of a complex system, the model employed should be simplified enough to ensure fast computational times, particularly for optimization purposes. Thus, a 1D model was chosen. The classical 1D model is based on finite volumes and requires a large number of cells in order to obtain a good accuracy in the temperature profile, especially in the thermocline region. Thus, a compromise has to be found between the accuracy of the results obtained and the computational times. In order to improve the DRTO methodology developed and its online testing, the model for the 1D storage tank was studied to improve the accuracy and reduce the computational time.

This chapter is an article published in *Applied Energy*, where another discretization scheme for the 1D model for the storage tank is proposed (Untrau et al.; 2023b). After a literature review on the modeling of stratified storage tanks, the classical 1D model is presented, along its advantages and drawbacks. Then, the new discretization scheme is introduced: orthogonal collocation. Results on the use of this scheme for modeling the vertical temperature profile inside a stratified storage tank are provided. They show that accurate results can be obtained with less discretization points than finite volumes. An adaptation of this scheme is then presented: orthogonal collocation on finite elements. This new scheme takes advantage of the fast convergence of orthogonal collocation and the fast resolution of finite volumes due to the sparsity of the matrices generated. Thus, this solution strategy is promising for the simulation of a complex system and for optimization purposes. The last solution based on orthogonal collocation on finite elements was then validated experimentally using data from the storage tank of a real solar thermal plant. Finally, the modeling of the natural convection taking place inside a stratified storage tank was discussed.

Article reference:

Untrau, A., Sochard, S., Marias, F., Reneaume, J.-M., Le Roux, G. A. C. and Serra, S. (2023b). A fast and accurate 1-dimensional model for dynamic simulation and optimization of a stratifed thermal energy storage, *Applied Energy* **333:** 120614.

A fast and accurate 1-dimensional model for dynamic simulation and optimization of a stratified thermal energy storage

Alix Untrau[a*], Sabine Sochard[b], Frédéric Marias[c], Jean-Michel Reneaume[d], Galo A.C. Le Roux [e] and Sylvain Serra[f]

[a,b,c,d,f] Universite de Pau et des Pays de l'Adour, E2S UPPA, LaTEP, Pau, France,

[*] alix.untrau@univ-pau.fr

[e] Universidade de São Paulo, Escola Politécnica, São Paulo, Brazil

Published in *Applied Energy*, **333** (2023) 120614

Abstract

As renewable energies are incorporated in larger shares in the electricity grid and district heating and cooling networks, the integration of storage solutions becomes more important. Thermal Energy Storage is an effective way to store heat and utilize the synergies between different energy carriers. Stratified storage tanks are a promising technology because of their low cost, simplicity and reliability. However, the modeling of the thermocline region in a stratified tank remains a challenge. There is a need to develop a fast and accurate 1D model for simulations and optimizations of TES. In this paper, a new discretization scheme is applied to the vertical axis of the storage tank. Orthogonal Collocation accurately represents the temperature profiles inside the storage tank with less points than the traditional multinode model, therefore running faster. Oscillations appear in the temperature profiles computed with orthogonal collocation if the thermocline represented is too steep and a low number of discretization points is used. But if a realistic thermocline is used as initial condition, the model performs well. Thus, it is appropriate to represent the real behavior of a storage tank, where uniform temperature conditions are avoided. Orthogonal Collocation on Finite Elements runs even faster and represents a good perspective for optimization studies. The model developed in this paper is validated with real data from a solar thermal plant with storage. A continuous and smooth model is also developed for natural convection inside the storage tank. The limitations of the model are discussed and perspectives on the modeling of natural convection for optimization models are given.

Nomenclature

Abbreviations

CFD	Computational Fluid Dynamics
DHCN	District Heating and Cooling Network
MAE	Mean Absolute Error
MAPE	Mean Absolute Percentage Error
OC	Orthogonal Collocation
OCFE	Orthogonal Collocation on Finite Elements
TES	Thermal Energy Storage

Symbols

β	Thermal expansion coefficient $[K^{-1}]$
Δz	Tank layer height in the multinode model $[m]$
$\dot{m}_c$	Mass flow rate to charge the storage tank $[kg.s^{-1}]$
$\dot{m}_d$	Mass flow rate to discharge the storage tank $[kg.s^{-1}]$
ρ	Storage fluid density $[kg.m^{-3}]$
A	Tank cross sectional area $[m^2]$
a_i	Coefficient associated with the trial function f_i^{trial}
A_{OCFE}	First derivative matrix in the OCFE method
A_{OC}	First derivative matrix in the OC method
B_{OCFE}	Second derivative matrix in the OCFE method
B_{OC}	Second derivative matrix in the OC method
C_p	Storage fluid heat capacity $[J.kg^{-1}.K^{-1}]$
D^2T	Column vector containing the second spatial derivative of the temperature at each collocation point in OC or OCFE
d_{insu}	Thickness of the insulation layer $[m]$
DT	Column vector containing the first spatial derivative of the temperature at each collocation point in OC or OCFE
E	Energy stored inside the tank $[J]$
f_i^{trial}	Trial function in the OC formulation
g	Gravitational acceleration $[m.s^{-2}]$
H	Tank height $[m]$
H_{ext}	Convection coefficient with the ambient air $[W.m^{-2}.K^{-1}]$
K	Von Karman constant
k	Storage fluid thermal conductivity $[W.m^{-1}.K^{-1}]$
k^*	Effective thermal conductivity $[W.m^{-1}.K^{-1}]$
k_{insu}	Thermal conductivity of the insulation layer $[W.m^{-1}.K^{-1}]$
k_{turb}	Turbulent diffusion coefficient $[W.m^{-1}.K^{-1}]$
k_{wall}	Thermal conductivity of the tank wall $[W.m^{-1}.K^{-1}]$
l_i	Lagrange polynomial
L_{el}	Length of an element in the OCFE method $[m]$
P	Tank perimeter $[m]$
R_{ext}	External radius of the storage tank $[m]$
R_{int}	Internal radius of the storage tank $[m]$
S_1	Exchange surface between the bottom layer and the environment $[m^2]$
S_l	Lateral surface of a tank layer $[m^2]$
S_N	Exchange surface between the top layer and the environment $[m^2]$
t	Time $[s]$
$T(z,t)$	Fluid temperature inside the tank $[°C]$
$T_{amb}(t)$	Ambient temperature $[°C]$
T_{charge}	Temperature of the charging fluid $[°C]$
T_{return}	Cold temperature returning to the storage tank $[°C]$
U	Tank fluid to ambient overall heat transfer coefficient $[W.m^{-2}.K^{-1}]$
U_1	Tank fluid to ambient overall heat transfer coefficient for the bottom layer $[W.m^{-2}.K^{-1}]$
U_N	Tank fluid to ambient overall heat transfer coefficient for the top layer $[W.m^{-2}.K^{-1}]$
z	Tank height from the bottom of the tank $[m]$

III.1 Introduction

In order to reduce the green house gases emissions of the energy sector, renewable energies will be incorporated in greater share into the electricity grid and District Heating and Cooling Networks (DHCN) (Renewable Energy Directive; 2018). Some of these renewable energies are intermittent, such as wind or solar energy. Thus, storage of the energy produced is required to ensure that the energy demand is met. Heat can be stored easily, unlike electricity (Argyrou et al.; 2018). Therefore, Thermal Energy Storage (TES) is an important technology to develop. TES can be used to store hot

fluid for space heating, domestic hot water or industrial processes. Moreover, if the temperature of the stored fluid is high enough, steam and electricity can be generated with the hot fluid. TES allows to exploit the synergies between heat and electricity (Ayele et al.; 2021). Thus, TES can be used in association with solar thermal plants or conventional thermal plants in order to store the heat produced. This will help to overcome the intermittency of renewable energies and will ensure that the energy demand is met.

There are three categories of TES based on different phenomena to store the heat: sensible, latent and thermochemical (Guelpa and Verda; 2019). The design, modeling and optimization of all types of technologies are studied actively nowadays. For example, a packed bed sensible heat storage was investigated in (Touzo et al.; 2020), a latent heat storage included in a solar system was optimized (Haillot et al.; 2013), and an adsorption heat storage was modeled in (Ferreira et al.; 2021). Hybrid storage solutions, such as a stratified storage tank with phase change emulsion in (Liang et al.; 2022), are also explored and simulation models are developed. Although latent and thermochemical storage technologies are promising, sensible heat storage is mostly used nowadays, because of its low cost, reliability and high level of maturity. There are two main ways to store the sensible heat in a thermal plant. It is possible to use two storage tanks, one for the hot fluid exiting the plant and one for the cold fluid returning to the plant, such as in (Immonen and Powell; 2022). The second option takes advantage of thermal stratification. It uses one single tank that is charged from the top with hot fluid while the cold fluid returning to the plant is charged from the bottom (Koçak et al.; 2020). Because the density of the storage fluid is lower at higher temperatures, there is no significant mixing taking place between the hot and cold zones. The temperature gradient between these two zones is very steep and this region is called the thermocline. The stratification inside the storage tank is illustrated in Figure III.1. This figure shows the thermocline region and the temperature profile inside the storage tank as an example.

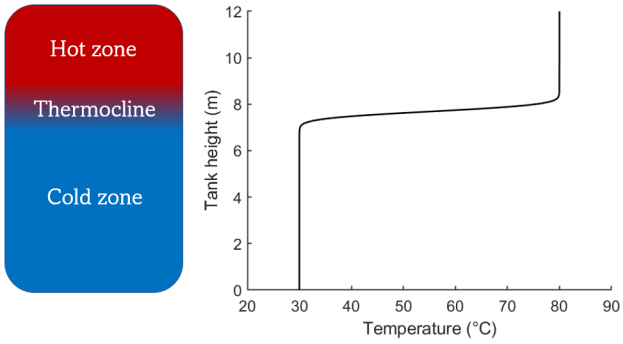

Figure III.1: The thermocline region and the temperature profile inside the tank

This single tank technology is cheaper to build because it requires less land space and construction materials, and is less complex (He et al.; 2019). For low temperatures, water is a commonly used storage fluid because of its availability and low cost. For application at higher temperatures, other fluids are chosen, such as molten salts for example, and packed bed materials, such as rocks, metals, ceramics or recycled materials are added (ELSihy et al.; 2021). Naturally stratified storage tanks and ther-

mocline storages with filler material share common features. In both technologies, a thermocline separates a cold and a hot zone, and can be thickened due to diffusion and convection (Stamps and Clark; 1992). However, the filler material plays a role in destratification. If idle periods are long, both water and bed conductivity lead to thermocline thickening (Sullivan et al.; 1984). Moreover, the limited heat transfer between the fluid and the filler material can also lead to thermal destratification. The present paper focuses on naturally stratified water storage tanks without any filler material. However, the model proposed in this work could be adapted to packed bed thermocline storages. The storage tank used for an energy system can be long-term, also called seasonal storage, to store heat between seasons. The other type of storage tank is short-term or daily, to store between days. This paper focuses on short term storage tanks, although the model developed in this work could also be applied to seasonal storage tanks. Developing fast and accurate simulation and optimization models of TES is crucial to accelerate their integration in smart grids or DHCN. Especially, TES models for real-time optimization and control of energy systems, such as solar thermal plants (Untrau et al.; 2022), are needed. Since they will be used online, they need to run even faster than offline optimization models. The modeling of thermocline TES requires spatial discretization, which can lead to complex and computationally expensive models. 3D and 2D approaches are useful to understand the phenomena taking place inside the storage tank but optimization studies or simulation studies of larger systems require a 1D model to speed up calculations. In the tank, a temperature inversion might arise if the storage is charged with a lower temperature, or because of heat losses for example. This is rapidly corrected by natural convection in the real system. However, the 1D model does not traditionally include a natural convection term. It needs to be added in order to correct temperature inversions. Adding the modeling of this 3D phenomenon in a 1D model remains a challenge. In this paper, a new discretization scheme for a 1D model, based on orthogonal collocation, is presented. This model is able to represent more accurately the thermocline region than the finite volumes discretization scheme that is traditionally used, and with reduced computational time. Some perspectives on the modeling of natural convection in a 1D model are also provided. This paper is divided as follows: Section III.2 presents the state of the art of TES modeling. Section III.3 details the traditional 1D model based on finite volumes and its drawbacks. Section III.4 introduces orthogonal collocation and its application for the spatial discretization of TES. Section III.5 shows the results obtained with the new discretization scheme. It also compares the two previously mentioned schemes, in terms of the estimation of the temperature profile in the storage tank as well as the valuable stored energy. Section III.6 introduces the adapted discretization scheme for optimization, Orthogonal Collocation on Finite Elements, and provides more results on the modeling of the TES in operation. Finally, Section III.7 is the validation of the model with real plant data and Section III.8 briefly discusses natural convection modeling.

III.2 Literature review on stratified TES modeling

In a thermocline storage tank, it is crucial to maintain the best degree of stratification possible, which means that the thermocline must remain as thin as possible. Indeed,

if there is some mixing between the hot fluid and the cold fluid, it will deteriorate the energy stored at the top of the tank by decreasing its temperature. Several phenomena lead to destratification inside the storage tank: the mixing induced during charging and discharging, the vertical diffusion between the hot and cold zones, natural convection due to charging and discharging at a variable temperature and to heat losses to the environment (Kleinbach et al.; 1993). He *et al.* (He et al.; 2019) analysed experimentally the thermocline evolution inside a storage tank during charging and discharging and also during the static mode. They observed that long periods of stand-by status should be avoided because the thermocline widens with diffusion. Also, the thermocline thickness is highly dependant on the flow rate during the charging and discharging phases. New technologies are developed to enable a better stratification inside the TES, focusing on the inlet design and location. For example, in (Al-Habaibeh et al.; 2018), a thin flexible tube, called water snake, delivers the incoming fluid in the TES at the position in the tank where the temperature and density of the stored fluid and the incoming fluid are the same. This minimizes mixing and turbulence inside the TES. Although promising, this design is still in the early stages of development.

Modeling a thermocline storage tank is challenging. The thermocline must be represented accurately because the temperature gradient in this region is very steep. On the other hand, the integration of a TES model into a thermal plant model or an energy network leads to long computational time. Therefore, it is necessary to find a compromise between computational time and accurate estimation of the valuable energy stored inside the storage tank. The compromise is even more necessary for real-applications, such as real-time optimization and control. Depending on the study objective, various modeling techniques have been developed, summarized in (Han et al.; 2009) for example, and explained below.

TES can be modeled in 3D, using Computational Fluid Dynamics (CFD) for example, in order to accurately represent all the phenomena taking place inside the tank. In such models, the mass, momentum and energy balance equations are solved on a 3D grid. These models allow to understand better the fluid movements around the diffusers for instance (Hosseinnia et al.; 2021), in order to improve their design and maintain a better stratification. Natural convection, taking place when temperature inversions appear inside the tank, can also be studied. Buoyancy forces due to natural convection correct these temperature inversions in a few minutes. For example, the transient cooling inside the storage tank and the natural convection movement induced by sidewall heat losses were investigated with CFD in (Paing et al.; 2019). 3D and 2D CFD models are very accurate but also computationally expensive. For storage tanks, a 2D simulation of the symmetry plane might help to reduce the computational burden, such as in (Liang et al.; 2022), but further reduction in computational time may be necessary for some applications. Thus, 2D and 3D models are usually employed to improve the design of TES (in (Ievers and Lin; 2009) for example) or to validate simplified models. Indeed, simplified models are needed for long term simulations, complex energy systems simulations or optimization studies. For instance, Johannes *et al.* (Johannes et al.; 2005) used a CFD model with 110,000 nodes to model a TES and noticed a bi-dimensional mass transfer leading to a non-uniform temperature along the radial axis of the tank. Their accurate model was used to validate a simplified 1D model along experimental measurements. They found a good agreement between the two models and the experiments for the vertical temperature profiles inside the storage

tank. Thus, they suggested to use the 1D model for the simulation of a global energy system.

2D zonal models allow the modeling of a temperature gradient in the radial direction with shorter computational times than CFD because they do not solve the momentum equation. Nevertheless, they can still be computationaly expensive and are used as references to validate 1D models (in (De Césaro Oliveski et al.; 2003) for example). De Césaro Oliveski *et al.* (De Césaro Oliveski et al.; 2003) concluded that their 1D model is much faster than the reference 2D model and the two models are in good agreement for the representation of the vertical temperature profiles inside the storage tank. Therefore, it is not necessary to use a 2D model for long-term simulations.

For optimization studies of energy systems, it is more common to use a 1D model for the TES. In this case, only the temperature variations along the vertical axis are considered. We assume that there is no temperature gradient in the radial direction. This assumption has been verified experimentally, in (Pate; 1977) for instance, in which the radial temperature gradients measured were below 1°C. The 1D model is a good approximation when the storage tank is cylindrical with its inlet and outlet located at the top and bottom surfaces on the axis of symmetry (Zachár; 2020). For other geometries, the 1D approximation is less accurate. The simpliest 1D model is the fully-mixed storage tank. The temperature is assumed uniform inside the whole storage tank, and there is no stratification. This model leads to an important exergy destruction (Campos Celador et al.; 2011). The ideally stratified storage tank considers two zones with fixed temperatures and variable volumes, one for the cold fluid and one for the hot fluid. The thermocline in considered having a zero thickness and moves up and down along the vertical axis of the tank. This model overestimates the valuable energy stored by considering a perfect stratification (Campos Celador et al.; 2011). In (Dickes et al.; 2015) two layers with variable volumes and temperatures were modeled and a hypothetical transition profile of the temperature, centered in the ideal separation line, was added to reproduce the thermocline. This model still runs fast but is more accurate than the ideally stratified storage tank model. The plug flow model uses a variable number of layers of fluid, each with a variable volume (Kleinbach et al.; 1993). A new layer is added when the incoming fluid temperature (during the charge or discharge) is too different from the closest layer temperature (more than 0.5°C difference). Otherwise, the incoming fluid is mixed with the fluid from the closest layer. The temperature profile is then shifted and the volume of fluid crossing the boundary of the storage tank is sent back to the heat source or sink. This 1D model is fast but does not rely on mass and energy balances and therefore, it is not very accurate. The last 1D model strategy is to solve the energy balance in the storage tank along an ascending vertical axis z. Assuming constant thermophysical properties for the storage fluid and no heat source inside the storage tank, the conservation of energy in 1D over a control volume of thickness dz leads to the following Partial Differential Equation (PDE):

$$\rho C_p A \frac{\partial T(z,t)}{\partial t} + \dot{m} C_p \frac{\partial T(z,t)}{\partial z} = Ak \frac{\partial^2 T(z,t)}{\partial z^2} + UP(T_{amb}(t) - T(z,t)) \qquad \text{(III.1)}$$

The first term is the energy accumulation, the second term represents the enthalpy fluxes due to the charge or discharge, the third term represents diffusion inside the

tank and the final term models the heat losses to the environment. In Equation III.1, the unknown variable is the storage fluid temperature $T(z,t)$ varying in space, along the vertical coordinate z, and in time t. ρ represents the stored fluid density, C_p the stored fluid heat capacity and k the stored fluid thermal conductivity. They are all assumed uniform and constant. A is the tank cross-sectional area, P is its perimeter. The enthalpy fluxes due to charge or discharge depend on the resulting flow rate $\dot{m}$ inside the storage tank. The thermal losses are computed based on an overall heat transfer coefficient U between the tank fluid and the ambient air at the temperature T_{amb}. Details on how we computed U in our model are given in Section III.3. The variables and parameters involved in Equation III.1 are listed in the nomenclature.

The initial condition for the temperature in Equation III.1 could be either a fully mixed condition, represented by a single uniform temperature, or a known temperature gradient (Hawlader et al.; 1988).

The boundary conditions at the top and bottom of the storage tank depend on its utilization ((Trevisan et al.; 2021), (Yang and Garimella; 2010)):

- Charge : $\left.\frac{\partial T(z,t)}{\partial z}\right|_{z=0} = 0$; $T_{z=H} = T_{charge}$
- Discharge : $T_{z=0} = T_{return}$; $\left.\frac{\partial T(z,t)}{\partial z}\right|_{z=H} = 0$
- Idle period : $\left.\frac{\partial T(z,t)}{\partial z}\right|_{z=0} = 0$; $\left.\frac{\partial T(z,t)}{\partial z}\right|_{z=H} = 0$

In these equations, $z = 0$ is the bottom of the storage tank, while $z = H$ is the top of the storage tank of height H. T_{charge} and T_{return} are the temperatures respectively of the charging flow and the return flow. When fluid is entering the tank, the temperature at the inlet of the storage is equal to the incoming fluid temperature. When fluid is leaving the tank, which corresponds to the bottom during charge and the top during discharge, a zero gradient is considered for the temperature. It means that the fluid at the outlet is at the same temperature on each side of the outlet (storage side and pipe side). During idle periods, the temperature gradient is also considered zero, which means that an adiabatic surface is assumed. A value could be given to the temperature gradient, equal to the heat losses to the environment through the top and bottom surfaces of the tank. Fixed boundary conditions can only be applied if a fixed working mode is determined for the simulation study. Otherwise, strategies need to be developed to represent the changing boundary conditions. This will be explored in III.4.3.

In order to solve this EDP, different discretization strategies along the space variable z can be used. They will allow the transformation of the EDP into a system of Ordinary Differential Equations (ODE). The traditional discretization scheme is based on finite volumes and is called the multinode model. It relies on the division of the storage vertical axis into several layers of fixed height and uniform temperature. An energy balance is written for each layer. Its implementation will be detailed in the next section of the paper. The multinode model has often been used in recent works for various applications. Firstly, the stratified storage tank alone has been studied. This allowed to better understand its stratification evolution (Mawire; 2013), assess its efficiency (Lake and Rezaie; 2018) and study the effect of the variation of important parameters

on the TES performances (Modi and Pérez-Segarra; 2014). Adaptations were made to the original formulation to incorporate immersed heat exchangers in (Rahman et al.; 2016). This new model was then used to size the storage tank using deep learning methods (Rahman and Smith; 2018). Furthermore, the multinode model has been used to model the storage tank in a more complex energy system such as a micro-combined heat and power system (Bird and Jain; 2020), a solar district heating system (Saloux and Candanedo; 2021) or a domestic hot water heat pump (Aguilar et al.; 2021). The authors sometimes implement the model themselves or directly use it within a software library, such as the TES implemented in TRNSYS used in (Lake and Rezaie; 2018), (Campos Celador et al.; 2011) and (Ryan et al.; 2022). The model was also adapted in 2D for a seasonal pit storage in (Dahash et al.; 2020) with segments of equal volumes instead of equal height. Finally, the multinode model has been compared to fully-mixed and ideally stratified models, showing a better estimation of the exergy stored (Campos Celador et al.; 2011). Also, it has been compared to a 2D zonal model in (De Césaro Oliveski et al.; 2003) and a CFD model in (Johannes et al.; 2005), showing sufficient accuracy in the vertical temperature profiles with a greatly reduced computational time. As this literature review shows, the multinode model has been extensively studied and used in the recent years. Nevertheless, it presents the issue of numerical diffusion, a smoothing effect on the vertical temperature profile when a reduced number of nodes is used (Powell and Edgar; 2013). To overcome this issue, a large number of nodes needs to be used, at least 100 according to (Dickes et al.; 2015), making the computational time prohibitive for some applications. For the simulation of a complex system or an optimization, a reduced number of nodes is used, leading to poor accuracy. For example 60 nodes were used in (Bird and Jain; 2020), 26 nodes in (Saloux and Candanedo; 2021), 15 nodes in (Ryan et al.; 2022) and 10 nodes in (Rahman et al.; 2016), (Rahman and Smith; 2018) and (Scolan et al.; 2020). These studies would benefit from a fast and accurate 1D model suitable for long-term simulations, global energy systems simulations and optimizations. A new discretization scheme, Orthogonal Collocation (OC), is introduced in Section III.4 to resolve the issue of numerical diffusion. OC has never been applied to discretize the vertical axis of the storage tank. Other discretization schemes for Equation III.1 have not been found in the literature. In (Muschick et al.; 2022), a 1D model with 5 layers of variable height but fixed temperatures was used for the incorporation of a TES in a MILP-based energy management system. In the present paper, no linearization is done and Equation III.1 is directly solved.

An important aspect of a storage tank model connected to a thermal plant that does not work with a constant outlet temperature is the correction of temperature inversions. This is needed when working with a solar thermal plant for example. At the end of the day, the solar irradiation goes down and the temperature at the outlet of the solar field might decrease a few degrees. Nevertheless, the temperature reached is still high enough for the consumer needs and it might be interesting to store this fluid. In this scenario, the incoming fluid is slightly colder than the stored fluid at the top of the storage tank. A temperature inversion appears. In the real system, this temperature inversion will be corrected by buoyancy forces induced by natural convection. This mixing phenomenon should be incorporated into the storage tank model (Kleinbach et al.; 1993). Another cause for a temperature inversion is the heat losses that are more important along the walls of the storage tank, and especially on the top surface, where the area is the

largest and the fluid is the hottest. The top section of fluid might cool down more rapidly than the rest of the stored fluid and therefore, a temperature inversion will appear (De Césaro Oliveski et al.; 2003). Temperature inversions are the main cause for destratification (Csordas et al.; 1992). Natural convection is a 3D phenomenon and its modeling requires the development of the momentum equation. The colder fluid entering the top of the tank will sink inside the tank because of its higher density. During its descent, it will exchange mass and energy with its surrounding, composed of warmer stored fluid. Thus, it will warm up and its downwards trajectory will stop once the temperature equilibrium is reached (Pate; 1977). Therefore, the incoming fluid will not mix perfectly with the fluid at the top of the tank and it will not go to the zone of storage with the same temperature without affecting the stored fluid either. Different numerical artifices have been developed to model natural convection in 1D, and have generally been incorporated into the multinode model. The first category of methods is to perform an operation after each time step, if a temperature inversion is spotted inside the storage tank. The first method is to reorganize the temperatures after each time step, making sure that the hottest temperature is at the top of the storage tank and that the coldest is at the bottom (Franke; 1997). This leads to an overestimation of the valuable stored energy because it neglects the mixing between the incoming fluid and the surrounding stored fluid. The other approach is to homogenize the temperatures around the inversion. A weighted mean temperature amoung the segments involved in the inversion is used (Kleinbach; 1990). These two methods provide good results (De Césaro Oliveski et al.; 2003) but require conditional structures to activate the operation only if needed. This is not easy to integrate into an optimization model because it only includes algebraic equations. Another method used in some studies is to inject the fluid inside the layer with the temperature closest to the charging temperature, thereby avoiding temperature inversions. Some actual systems provide several inlet ports to reproduce this behavior, but they are more expensive. Moreover, they do not completely prevent temperature inversions as small temperature differences will still occur because there are only a few inlet ports or because of the heat losses through the top and lateral walls during idle periods. If the actual system has only one inlet at the top of the tank, injecting at a variable height in the model neglects the mass and energy transfer between the incoming and the stored fluids. Thus, it overestimates the performances of the storage tank (Pate; 1977). Moreover, it requires the use of conditional structures and is not appropriate for optimization studies. Saloux *et al.* (Saloux and Candanedo; 2019) developed an advanced flow rate distribution method to reproduce the mixing between the incoming and stored fluid during the incoming fluid descent through the storage tank. The method is based on heuristics and not on physical models. Pate developed a 1D model based on physical equations to describe the natural convection inside the storage tank (Pate; 1977). It is called the plume entrainment model. Pate performed some experiments to visualize the trajectory of the incoming colder fluid. He observed that the colder fluid sinks inside the storage tank and some of the stored fluid is entrained with it. Some warmer stored fluid then rises inside the tank to replace the entrained fluid. Those turbulent movements are in 3D but the radial temperature gradient is negligible. From these observations, Pate developed a 1D plume entrainment model. Mass and energy balances are written for the plume and the bulk fluids. The plume stops its course when temperature equilibrium is reached. These differential equations have been solved with

finite volumes and led to good results, in agreement with experimental results (Pate; 1977). In order to solve the ODE system, the equations for the plume and the bulk were decoupled. The plume temperature was obtained from the previous bulk temperatures, and then the new bulk temperatures were computed using the plume depth ((Csordas et al.; 1992), (Kleinbach et al.; 1993)). Analytical solutions have also been developed, neglecting the diffusion term (Zachár; 2020). Although this model is promising since it is based on physics and is written in the form of ODEs, it is not appropriate for optimization studies because of the discontinuities in the flow rates computed inside the storage tank. Another approach is to model a turbulent diffusion coefficient that is large only when a temperature inversion appears ((Hawlader et al.; 1988), (Nash et al.; 2017), (Powell and Edgar; 2013), (Viskanta et al.; 1977), (Zurigat et al.; 1988)). The diffusion term in Equation III.1 is then replaced by:

$$(k + k_{turb})\frac{\partial^2 T(z,t)}{\partial z^2} \tag{III.2}$$

There are many formulations for the turbulent diffusion coefficient, based on physical models (Hawlader et al.; 1988) or not, which must be several order or magnitudes larger than k (Powell and Edgar; 2013). This formulation requires a conditional structure to determine if k_{turb} is zero or not, but it is a continuous formulation that does not need to be performed at the end of each time step. For this reason, it is easier to incorporate into a simulation model using an automatic integrator. It is possible to transform this model into a smooth model by using a continuous approximation of the condition (logistic function for example) or the max function. The development of a continuous and smooth model for a storage tank with temperature inversion correction is the topic of very recent works ((Lago et al.; 2019), (Soares et al.; 2022)). These formulations are appropriate for optimization studies but they require the tuning of the smooth functions parameters to find the best compromise between accuracy and convergence ease. Finally, a different approach was presented in (Scolan; 2020). Inversion flow rates are introduced as optimization variables in the optimization problem. They are activated to minimize the temperature inversion sum, that is included in the objective function. This method also requires some tuning for the bounds on these flow rates and on the weight associated with the temperature inversion sum in the objective function. This approach is easy to implement in an optimization study and does not cause convergence difficulties.

Based on this literature survey, there is still a need to develop a fast and accurate 1D model for simulation and optimization studies. Moreover, ways to correct temperature inversions in an easy way are needed, especially for optimization models. This paper presents the discretization of the 1D model with orthogonal collocation, which has never been applied to this problem before. The model proposed hereafter requires less discretization points than the traditional multinode model to achieve the same accuracy. It is therefore faster to run. A discussion on how to model natural convection for optimization studies is added at the end of the paper.

III.3 Traditional one-dimensional model

III.3.1 Mathematical Formulation

In the traditional multinode model, Equation III.1 is discretized with finite volumes, considering N layers of height Δz. Layer 1 is located at the bottom of the tank and layer N is located at the top. The unknown temperatures are located in the middle of each layer, and the temperature inside each layer is assumed uniform. This discretization scheme is illustrated in Figure III.2, with the vertical axis named x and pointing upwards.

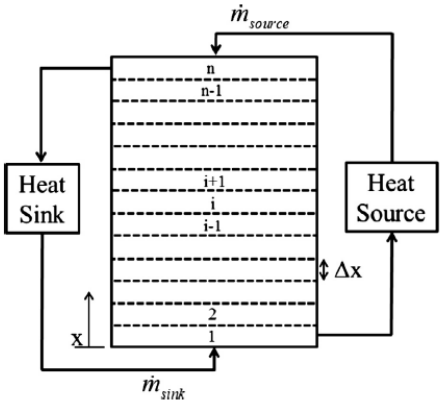

Figure III.2: Finite volumes discretization scheme for TES (Powell and Edgar; 2013)

Each layer is composed of the stored fluid and the wall, assumed in thermal equilibrium. The assumption stems from the large heat transfer coefficient between the stored water and the wall as well as the small thickness of the wall and its large conductivity. Thus, diffusion through the wall and convection in the water side are considered large, and the wall and the stored fluid are at the same temperature. In this discretization model, the first derivative with respect to z is approximated with finite differences of order 1 and used for the convective terms. The second derivative with respect to z is computed with centered finite differences, of order 2, and used for the diffusion term. For the top and bottom layers, the finite differences to approximate the second derivative are not centered but are computed using the wall temperature as one of the neighbor temperatures. We assumed that the wall temperature is equal to the fluid temperature. Since the wall is located at the distance $\frac{\Delta z}{2}$ from the top and bottom, a coefficient of $\frac{4}{3}$ appear in front of the diffusion term for the top and bottom layers. The equations used for the different layers i, at the temperature T_i, are presented hereafter:

For the first layer at the bottom of the storage tank:

$$\rho C_p A \Delta z \frac{dT_1}{dt} = U_1 S_1 (T_{amb} - T_1) + \frac{4}{3} \frac{k^* A}{\Delta z} (T_2 - T_1) + \dot{m}_c C_p (T_2 - T_1) + \dot{m}_d C_p (T_{return} - T_1) \tag{III.3}$$

For an intermediate layer i, for i varying from 2 to N-1:

$$\rho C_p A \Delta z \frac{dT_i}{dt} = U S_l (T_{amb} - T_i) + \frac{k^* A}{\Delta z}(T_{i-1} - 2T_i + T_{i+1}) + \dot{m}_c C_p (T_{i+1} - T_i) + \dot{m}_d C_p (T_{i-1} - T_i) \quad \text{(III.4)}$$

For the last layer N at the top of the storage tank:

$$\rho C_p A \Delta z \frac{dT_N}{dt} = U_N S_N (T_{amb} - T_N) + \frac{4}{3}\frac{k^* A}{\Delta z}(T_{N-1} - T_N) + \dot{m}_c C_p (T_{charge} - T_N) + \dot{m}_d C_p (T_{N-1} - T_N) \quad \text{(III.5)}$$

The time dependency of the variables in these equations is not written for conciseness. In these equations, $\dot{m}_c$ and $\dot{m}_d$ are the flow rates of charge and discharge respectively. The temperature of charge T_{charge} and the return temperature T_{return} are the other inputs of the system. S_1 and S_N are the surfaces of the layers 1 and N respectively in contact with the ambient temperature. They are composed of the lateral surface of the tank layer as well as the top or bottom surface. Therefore, the heat losses are more important for these layers than the interior ones, because the exchange surface is larger.

The overall heat transfer coefficient with the environment takes into account the diffusion through the insulation layer of the storage tank (with a depth d_{insu} and a thermal conductivity k_{insu}) and the convection with the ambient air:

$$\frac{1}{U} = \frac{1}{H_{ext}} + \frac{d_{insu}}{k_{insu}} \quad \text{(III.6)}$$

The heat transfer coefficient with the environment H_{ext} can be determined with an experimental correlation and depends on the environmental conditions (wind speed for example). Thus, this coefficient is variable and depends on the weather. This coefficient can be different for the top, bottom and lateral surface (hence the different names U_1, U and U_N in the above equations).

In this work, we consider the effective thermal conductivity k^* of the fluid and the wall, computed as follows:

$$k^* = k + k_{wall}\frac{R_{ext}^2 - R_{int}^2}{R_{int}^2} \quad \text{(III.7)}$$

In Equation III.7, R_{ext} is the external radius of the storage tank, including the wall, while R_{int} is the internal radius only considering the fluid. k and k_{wall} are the thermal conductivities of the fluid and the wall respectively. The effective conductivity represents the effect of diffusion in the tank wall on the destratification (Newton; 1995). Although the cross sectional area of the wall is much smaller than of the fluid, the large conductivity of the metallic wall contributes to the homogenization of the temperatures inside the storage tank. The thermal capacity mC_p is the one of the water only because the thermal capacity of the wall is neglected. Indeed, the specific heat capacity of the wall is small compared to the one of water and the mass of metal is much smaller than the mass of water.

III.3.2 Numerical Diffusion

One of the main assumptions in this model is the uniform temperature in each layer of fluid, which corresponds to an infinite thermal diffusion inside each layer. This generates an effect called numerical diffusion (Powell and Edgar; 2013), where the temperature profile along the vertical axis of the tank is smoothed. This effect is highly dependent on the number of layers used in the model. If a large number of layers is used, the thermocline region will be represented more accurately but the computational time will be longer. This is illustrated in Figure III.3 for 10, 100 and 1000 layers. In this example, a water storage tank of $500m^3$, initially at 30°C, was charged with hot fluid at 80°C at a flow rate of $10kg.s^{-1}$. The charge was performed over 26 hours in order to completely fill the storage tank. The computational times were 0.1s, 0.14s and 4.7s for 10, 100 and 1000 layers respectively, on a laptop with the following characteristics: Intel Core i7-1065G7 1.3GHz, RAM 16Go. The simulation was performed on MATLAB and the solver ode15s was used for the time integration.

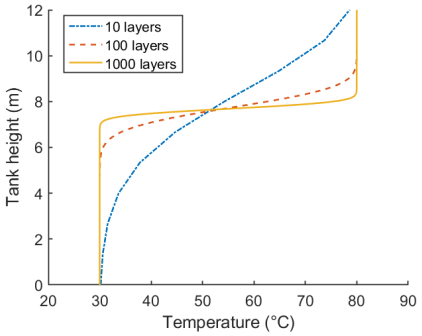

Figure III.3: Impact of the number of layers on the temperature profiles

Figure III.3 shows that the thermoclines are not well represented with a small number of layers. 1000 layers is not the converged solution yet and the thermocline continues to get thinner as the number of layers increases. Powell *et al.* (Powell and Edgar; 2013) tested up to 10,000 layers and showed an improvement compared to 1000 layers. However, the computational time greatly increases with the number of layers and the model with 1000 is already about 30 times slower than the model with 100 layers. Thus, it is needed to find a compromise between the accuracy of the model and the computational time for complex long-term simulations and optimizations. For a study on the storage tank only, a large number of nodes can probably be used without making the computational time prohibitive. The bad representation of the thermocline region with a low number of layers has a direct impact on the quantity of energy stored at a temperature high enough for its utilization. The stored energy $E(t)$ at each time instant compared to the initial state of the storage tank is defined as follows:

$$E(t) = \int_{z=0}^{z=H} \rho A C_p (T(z,t) - T(z,0))\,\mathrm{d}z \tag{III.8}$$

In this equation, $T(z,t)$ is the current temperature profile along the vertical axis inside the storage tank and $T(z,0)$ is the initial profile acting as a reference. For an energy system, the quantity of energy stored is not the only variable of interest, but also its

temperature. For example, if the consumer requires heat at a minimum temperature of 65°C, then it is the quantity of stored energy with a temperature higher than 65°C that matters. A bad representation of the thermocline region does not affect the quantity of stored energy but its quality.

Figure III.4 shows the cumulated energy at a temperature above 65°C stored throughout time during a charging phase, for different numbers of layers in the model. It can be observed that there is a large discrepancy between the cumulated energy profiles for 10 layers and for 100 or 1000 layers. A model with only 10 layers greatly underestimates storage utilization. Using 100 layers is a reasonable approximation, even if numerical diffusion still has an effect. A quantitative analysis shows that the maximal difference between the energy profile with 1000 layers and the one with 10 layers is 5.1MWh, while it is 1.3MWh for 100 layers. At the beginning of the charging phase, during the first hour, when the stored energy is small, the relative difference between the models with 1000 layers and 10 layers goes up to 100%, while it reaches 26% for 100 layers. This analysis shows that a bad representation of the thermoclines due to numerical diffusion with a model with few layers has a large impact on the estimation of the valuable stored energy. Furthermore, the time needed to completely charge the storage tank depends on its discretization. It takes 15 hours to completely charge the storage tank with the 1000 layers model while it takes 22 hours to do it with the 10 layers model. Therefore, using the multinode model with a small number of layers leads to an underestimation of the performances of the storage tank.

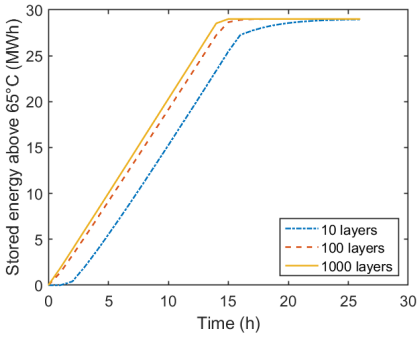

Figure III.4: Cumulated stored energy through time during charging

Modi *et al.* (Modi and Pérez-Segarra; 2014) chose to use 1500 layers after performing a grid convergence study for their packed bed storage tank. Their model was validated with experimental results. Mawire *et al.* (Mawire; 2013) used 200 layers to model their TES because no further improvement was observed with a finer spatial grid. Aguilar *et al.* (Aguilar et al.; 2021) used 100 layers and observed a deviation of 0.1% in the temperatures and energies computed compared to a model with 500 layers. These models used a large number of layers because they focused on the simulation of the storage tank only or on a simple system. The computational time was not an issue in these papers, and thus the authors were able to use enough discretization points to limit the numerical diffusion effect. For more complex systems, the number of layers needs to be reduced in order to achieve reasonable computational time. Thus, 60 layers were used for the TES in a micro-combined heat and power system (Bird and Jain; 2020), 15 layers were used for the TES associated with a ground source heat pump

(Ryan et al.; 2022) and 10 layers were used for the TES with two immersed heat exchangers, whose model was developed in (Rahman et al.; 2016). For the optimization of a complex energy system the number of layers must be further reduced to speed up the calculations. For instance, Scolan *et al.* (Scolan et al.; 2020) optimized the operation of a solar thermal plant including a storage tank. They used only 10 layers to model their storage tank. Similarly, Saloux *et al.* (Saloux and Candanedo; 2021) minimized the primary energy used in a solar district heating system with a 26 layers TES model. The TES size was optimized in (Rahman and Smith; 2018) with a model consisting of 10 layers. Although not very accurate, these models allowed the authors to obtain approximate results in a reasonable time. This highlights the need to develop a fast and accurate 1D TES model for complex long-term simulations or optimizations.

A first attempt to improve the results obtained was conducted in the present work. In the original method, the enthalpy fluxes associated with charging and discharging were computed with finite volumes in Equation III.4, as shown below for the interior points:

$$\dot{m}_c C_p(T_{i+1} - T_i) + \dot{m}_d C_p(T_{i-1} - T_i) \tag{III.9}$$

This corresponds to a finite difference of order 1 to approximate the first derivative with respect to z.

These terms were replaced by the following, based on finite differences with a centered scheme, which corresponds to a finite difference of order 2 to approximate the first derivative with respect to z:

$$\frac{\dot{m}_c C_p(T_{i+1} - T_{i-1})}{2} + \frac{\dot{m}_d C_p(T_{i-1} - T_{i+1})}{2} \tag{III.10}$$

The centered scheme for the computation of the first derivative of the temperature could lead to more accurate results since it involves two neighbors temperatures instead of one, and the order of the finite difference was increased by 1. A simulation with 100 discretization points is performed for the charging phase presented previously. For the boundary conditions, the temperature at the top of the storage tank is equal to the charging temperature and the temperature at the bottom of the tank, which is where the fluid exits during a charging phase, has a zero spatial derivative (Trevisan et al.; 2021). The temperature profiles obtained are plotted in Figure III.5, at four time instants. In this figure, the thermoclines are a bit steeper than the ones obtained with the traditional multinode model. Hence, numerical diffusion is slightly reduced compared to the previous discretization scheme. However, oscillations appear in the profiles above the thermoclines. The oscillations are increasing as the charging phase continues. This is also mentioned in (Baeten et al.; 2016), where the authors noticed spatial oscillations when a sharp gradient was represented with a higher order discretization scheme. Moreover, the computational time is the same for the two discretization schemes. Thus, changing the derivation scheme for centered finite differences does not appear to be a good approach.

In order to eliminate numerical diffusion, Powell *et al.* (Powell and Edgar; 2013) developed an intermediate model between the ideally stratified model and the multinode model. Two variable volumes represent the hot and the cold zones on each side of the thermocline. The thermocline itself is modeled with a fine 1D grid along the vertical axis. When the charging or discharging begins from a uniform temperature

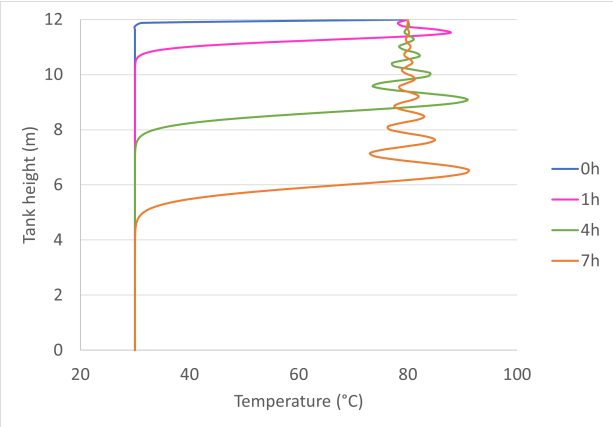

Figure III.5: Temperature profiles obtained with centered finite differences and 100 layers

storage tank, the thermocline is created while the fluid crosses the thin layers of the grid. Once the thermocline is established, it will move up and down the storage tank and only the hot and cold volumes will vary. With this approach, numerical diffusion is eliminated, the model runs faster than the traditional multinode model and does not overestimate the storage capacity as the ideally stratified model does. Thus, this model is accurate and fast enough for dynamic simulations. Unfortunately, conditional structures make it difficult to incorporate into an optimization model.

In this paper, a new discretization scheme is applied to the storage tank vertical axis in order to make numerical diffusion negligible and better represent the storage tank.

III.4 New spatial discretization scheme

III.4.1 General presentation of Orthogonal Collocation

Orthogonal Collocation (OC) approximates the unknown state variable involved in a differential equation with a sum of some selected trial functions of the integration variable. In this case, the unknown variable is the temperature inside the storage tank $T(z)$ and the integration variable is the space coordinate z. Equation III.11 shows the construction of the approximate temperature $\widetilde{T}(z)$ with the trial functions f_i^{trial}:

$$T(z) \approx \widetilde{T}(z) = \sum_{i=1}^{N} a_i f_i^{trial}(z) \tag{III.11}$$

With this method, the derivative of the temperature can be easily computed with the derivatives of the trial functions, which are known analytically. The satisfaction of the differential equation is imposed for N points carefully chosen and called collocation points. This method allows the transformation of a differential equation into a system of algebraic equations, whose unknowns are the coefficients a_i associated with each trial function in the sum. Generally, polynomials are used as trial functions. Collocation points are commonly chosen as the roots of orthogonal polynomials, hence the

name Orthogonal Collocation. The choice of the collocation points will impact the convergence and accuracy of the results. Moreover, orthogonal polynomial roots allow to use a quadrature method in order to compute the integral of the unknown variable. Polynomial interpolation ensures the continuous representation of the variable over the integration domain. On the contrary, finite volumes only provide the values for distinct discretization points. Linear interpolation can then be used to obtain a continuous solution. For the same degree of accuracy, less points are needed and thus less computational time, for OC. For these reasons, Equation III.1 was discretized with OC for the space variable z in the next subsections.

III.4.2 Implementation methodology

To the best of our knowledge, OC has never been applied to discretize the space dimension of a storage tank. This subsection presents the methodology developed. The unknown temperature along the z axis is represented by a linear combination of N interpolating Lagrange polynomials l_j (numbered from j=1 to N), which is a common choice for the trial functions of OC. The vertical axis is discretized with N collocation points z_i. The advantage of Lagrange polynomials is the following property: $l_j(z_i) = \delta_{ji}$, which is 1 if $j = i$ and 0 if $j \neq i$. Thus, the temperature can be written as follows:

$$T(z) \approx \widetilde{T}(z) = \sum_{i=1}^{N} T_i l_i(z) \tag{III.12}$$

The characteristics of Lagrange polynomials allow us to write: $T(z_i) = T_i$ for the temperature at each collocation point i. Thus, the coefficients involved in the linear combination used to approximate the temperature along the z axis are the temperatures in each collocation point. Diverse matrices formulations were developed for OC. An advantage of the matrix methods is that the matrices used to express the differential terms only depend on the collocation points. Therefore, once the points are chosen, the matrices can be computed once and then used in all the simulations and optimizations. That way, their construction does not participate in the computational time. One formulation takes advantage of the properties of Lagrange polynomials to build an accurate matrix method (Michelsen and Villadsen; 1972). Ebrahimzadeh *et al.* (Ebrahimzadeh et al.; 2012) detailed the following steps for the implementation of this method, here applied to the discretization of the height of the storage tank:

1. Normalise the domain (the height of the storage tank) between 0 et 1 : $z^* = \frac{z}{H}$
2. Choose N_{int} interior collocation points as roots of orthogonal polynomials. Shift then in [0,1] if necessary. The complete set of collocation points is composed of the N_{int} points and the boundary points 0 and 1
3. The interpolation polynomial representing the temperature along the z axis is passing through the $N_{int} + 2$ collocation points and has a degree of $N_{int} + 1$. It can be written as a linear combination of $N_{int} + 2$ Lagrange polynomials passing through the $N_{int} + 2$ collocation points:

$$T(z) \approx T_{N_{int}+1}(z) = \sum_{i=1}^{N_{int}+2} T_i l_i(z) \tag{III.13}$$

4. The interpolation polynomial can then be differentiated by using the expression of the derivatives of Lagrange polynomials:

$$\frac{\partial T(z)}{\partial z} \approx \frac{\partial T_{N_{int}+1}(z)}{\partial z} = \frac{1}{H} \sum_{i=1}^{N_{int}+2} \frac{\partial l_i(z)}{\partial z} T_i \tag{III.14}$$

   This Equation can be written for each collocation point, and the system can be put in matrix form: $DT = A_{OC}T$. The coefficients in matrix A_{OC} are $A_{OCij} = \frac{dl_j(z_i)}{dz}$ for i and j varying from 1 to $N_{int}+2$ and T is a column vector containing all the T_i values. DT is a column vector where each line $DT(i)$ corresponds to the first derivative of the temperature with respect to z at collocation point i and is expressed as a linear combination of all the temperatures T_j (with j varying from 1 to $N_{int}+2$).

5. The same method can be applied to the second derivative, with a matrix B_{OC} and a column vector D^2T containing the second derivatives $D^2T(i)$ of the temperature with respect to z for each collocation point i. If the domain has been normalized, we have $\frac{\partial T(z)}{\partial z} = \frac{1}{H}\frac{\partial T(z^*)}{\partial z^*}$, and similarly, $\frac{\partial^2 T(z)}{\partial z^2} = \frac{1}{H^2}\frac{\partial^2 T(z^*)}{\partial z^{*2}}$.

6. The differential terms in Equation III.1 can then be replaced by $\frac{A_{OC}T}{H}$ and $\frac{B_{OC}T}{H^2}$. This forms a system of N_{int} equations with $N_{int}+2$ unknowns which are the temperatures at each collocation point. Two boundary conditions complete the system (see subsection III.4.3)

With OC, Equation III.1 is transformed into a system of ODEs and the time integration is performed in MATLAB with the solver ode15s. The ODE equations are written as follows for each interior collocation point i:

$$\rho C_p A \frac{dT_i}{dt} = UP(T_{amb} - T_i) + k^* A \frac{D^2T(i)}{H^2} - (\dot{m}_c - \dot{m}_d) C_p \frac{DT(i)}{H} \tag{III.15}$$

The time dependency of the variables in this equation is not written for conciseness. The boundary conditions are those defined in Section III.2 and a new formulation able to adapt to the working mode of the storage tank is presented in III.4.3.

The collocation points associated with Gauss-Lobatto quadrature are chosen. This will allow an accurate calculation of the stored energy inside the storage tank, which requires the integration of the temperature profile over the height of the tank. For an interpolation polynomial of degree $N_{int}+1$, the collocation points are the two boundary points of the interval and the roots of the derivative of the orthogonal polynomial of degree $N_{int}+1$. In the simulations, the roots of Chebyshev polynomials were chosen as collocation points. They were found to perform better than Legendre polynomials.

III.4.3 Boundary Conditions

As mentioned is subsection III.4.2, to use OC with N collocation points ($N = N_{int}+2$) for the discretization of the space coordinate in the storage tank, two boundary conditions are needed in addition to the energy balance written for the interior collocation

points. In this case, Equation III.1 has a second derivative term for the space variable, therefore two boundary conditions are required: one at the bottom of the tank (point 1, $z = 0$) and one at the top (point N, $z = H$). For finite volumes discretization, the energy balance was written for the top and bottom layers, assuming that the derivative of the temperature with respect to space was zero at the boundary. With OC, no energy balance is written for the boundary points, and boundary conditions are directly added to the system of differential equations. The boundary conditions, which depend on the working mode of the storage tank, were presented in Section III.2. In the simulation or the optimization of an energy system including a storage tank, the model needs to switch to the appropriate boundary conditions automatically. Conditional structures would slow down the convergence of the calculations and should be avoided. In the multinode model, the energy balance written for the top and bottom layer involve the flow rates of charge and discharge. Thus, it is able to represent all the working modes. The idea detailed hereafter is to apply an energy balance on a small layer of fluid located at the top and at the bottom of the tank in order to compute the boundary temperatures. This is similar to the mixing zones mentioned in (Hawlader et al.; 1988). Pate also wrote an energy balance at the boundary points but neglected the accumulation term (Pate; 1977). This formulation did not require the construction of a small layer of fluid and was solved locally. However, since the inertia was neglected, it was found to generate oscillations in the boundary temperatures. Thus, mixing zones were preferred.

The boundary condition at the bottom of the tank, $z = 0$, is written as follows:

$$\rho C_p A \Delta z \frac{dT_1}{dt} = U_1 S_1 (T_{amb} - T_1) + \frac{4}{3}\frac{k^* A}{\Delta z}(T_2 - T_1) + \dot{m}_c C_p (T_2 - T_1) + \dot{m}_d C_p (T_{return} - T_1) \tag{III.16}$$

T_1 represents the temperature of the boundary and T_2 is the temperature of the first interior collocation point.

The boundary condition at the top of the tank, $z = H$, is written as follows:

$$\begin{aligned} \rho C_p A \Delta z \frac{dT_N}{dt} = {} & U_N S_N (T_{amb} - T_N) + \frac{4}{3}\frac{k^* A}{\Delta z}(T_{N-1} - T_N) \\ & + \dot{m}_c C_p (T_{charge} - T_N) + \dot{m}_d C_p (T_{N-1} - T_N) \end{aligned} \tag{III.17}$$

T_N represents the temperature of the boundary and T_{N-1} is the temperature of the last interior collocation point. The time dependency of the variables in these equations is not written for conciseness. The impact of the thickness Δz of this mixing zone was assessed. It appeared that using the distance between the boundary point and the closest collocation point as the layer thickness was appropriate. The temperature profiles obtained during the charging phase were in total agreement with the ones obtained with fixed boundary conditions corresponding to a charge. The computational times were also similar. When the fixed boundary conditions are used, the temperature at the top of the storage tank is the temperature of the charged fluid. However, with the mixing zone, an energy balance is used, so the temperature is not immediately equal to the charging temperature. Figure III.6 shows the variations of temperature

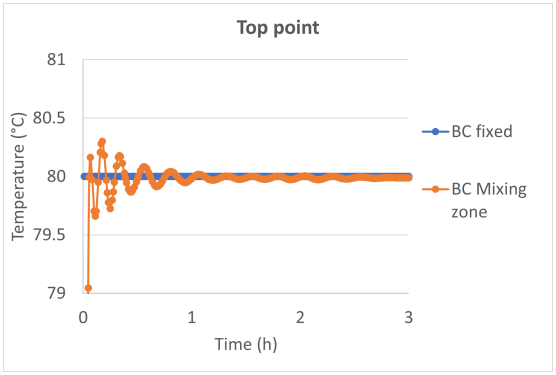

Figure III.6: Temperature evolution at the top of the tank during charging

at the top point during the charging of the storage tank for fixed boundary conditions and mixing zones. The temperature at the very beginning of the simulation is not included in Figure III.6 for the mixing zone because it is much smaller than the charging temperature. During the first time instants, there is some mixing between the charged fluid and the stored fluid, which seems realistic. We observe that the top temperature quickly reaches the charging temperature and slightly oscillates around it during the first hours. However, these oscillations are small, less than 0.4°C. The model with mixing zones to represent the changing boundary conditions is therefore validated.

III.4.4 Importance of the diffusion term

In some studies, the diffusion term in Equation III.1, $Ak\frac{\partial^2 T(z,t)}{\partial z^2}$, is neglected ((Campos Celador et al.; 2011),(Modi and Pérez-Segarra; 2014), (Csordas et al.; 1992), (Saloux and Candanedo; 2019)). Nevertheless, He *et al.* (He et al.; 2019) showed in an experimental study the expansion of the thermocline during the stand-by status. They highlighted the importance of reducing the duration of those idle periods in order to preserve the quality of the stored energy. First, the impact of the diffusion term during the idle periods was assessed in a simulation in MATLAB. A stand-by period of 48 hours was considered, which corresponds to a long idle period for a daily storage tank. Heat losses to the environment are included in the model. The storage tank is initially half charged and the vertical axis is discretized with 200 collocation points. Two simulations are run, one considering the diffusion term and the other neglecting it.

Figure III.7 presents the initial and final profiles with and without the diffusion term. First, we can notice that the hot temperature in the tank decreases slightly due to heat losses for the two simulations. When diffusion is considered, the thermocline thickens over time, but the effect is rather small. The computational times for these two simulations are similar (0.12s without diffusion and 0.15s with diffusion). A quantitative comparison of the stored energy inside the tank was performed. Here, the energy is valuable above 65°C. The initial valuable energy stored is 18.54MWh. After 48 hours, this value is 18.45MWh when diffusion is neglected, which represents a drop of 0.49% due to heat losses. When the diffusion is modeled, the valuable stored energy after 48 hours is 18.23MWh, which is a decrease of 1.67% compared to the initial state. Thus, in this model, diffusion does lead to a slight destratification but the effect is

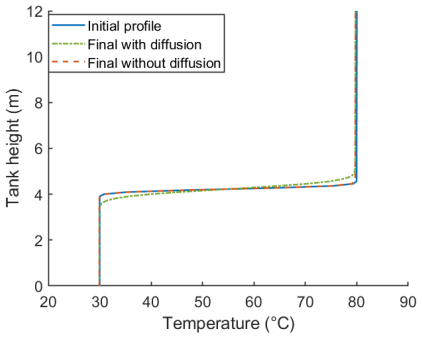

Figure III.7: Effect of the diffusion term during idle periods

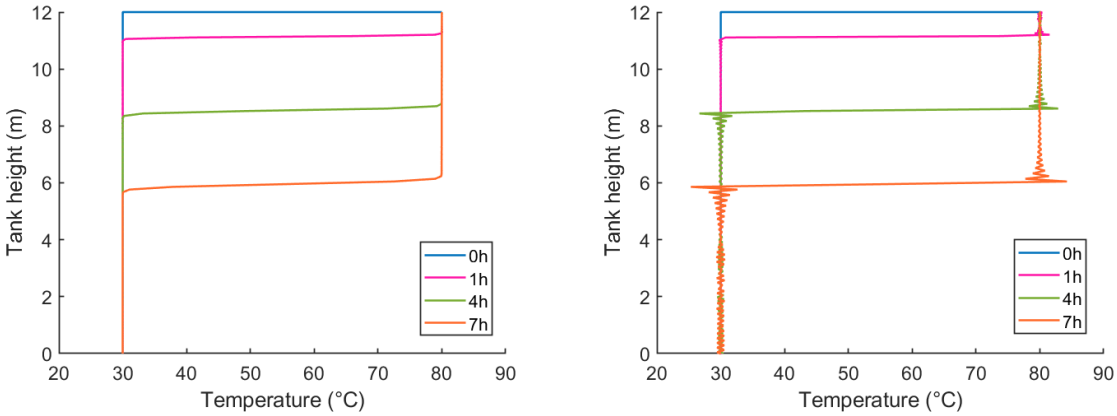

(a) With diffusion

(b) Without diffusion

Figure III.8: Effect of the diffusion term during the charging phase

small. Experimental studies showed a larger impact of diffusion on energy degradation (He et al.; 2019). Other effects than diffusion can lead to some mixing. For instance, the heat losses are larger along the tank walls. The fluid close to the walls is cooled down and sinks along the wall, generating convection movement that mixes the stored fluid. Diffusion is probably negligible compared to these convection movements and the destratification is mostly due to these 3D convection movements. Unfortunetaly these 3D phenomena are difficult to model in 1D.

So these simulations showed that the diffusion term does not have a great impact on the temperature profiles inside the storage tank during idle periods. A second test has been conducted to assess the importance of the diffusion term during charging or discharging. Figure III.8 shows the temperature profiles in the tank at 4 time instants during the charging phase of the storage tank for the models neglecting or not the diffusion term. It can be observed that oscillations appear on each side of the thermocline region when diffusion is neglected. Therefore, it is a good practice to keep the diffusion term when discretizing the storage tank with orthogonal collocation. This term has a stabilizing behavior.

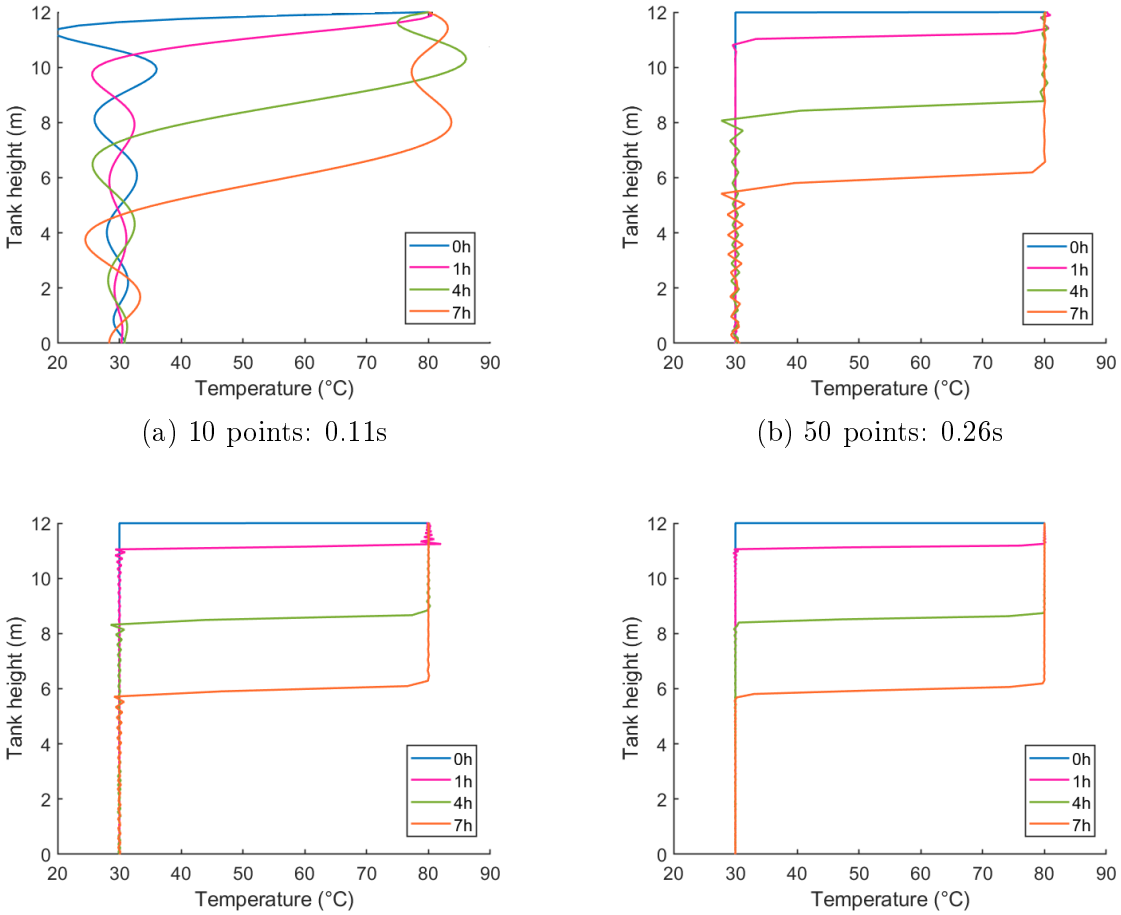

(a) 10 points: 0.11s

(b) 50 points: 0.26s

(c) 100 points: 0.44s

(d) 150 points: 0.90s

Figure III.9: Impact of the number of collocation points on the temperature profiles

III.5 Orthogonal Collocation: results and discussion

The methodology explained in the previous section was applied to discretize the vertical axis of the storage tank during a simulation of a charging phase. The storage tank is initially at a uniform temperature of 30°C and is charged with a hot fluid at 80°C with a flow rate of $10 kg.s^{-1}$. A sensitivity analysis on the number of collocation points is conducted to assess its effect on the temperature profiles. Figure III.9 shows the temperature profiles at 4 times instants during a charging phase, with 10, 50, 100, 150 collocation points, along with the computational times required to perform the 26 hours charge. Firstly, it can be observed that the temperature profiles with a model with few collocation points are not smooth and present oscillations in the temperature, especially around the thermocline region. These oscillations fade away when the number of points is increased. It can be noticed that the slope of the thermoclines is correctly estimated with only 50 points. As expected, the computational time increases with the number of points but they stay reasonable for simulations.

The impact of the number of points on the valuable stored energy over time was also assessed. Figure III.10 represents the cumulated stored energy at a temperature above 65°C for different numbers of collocation points. It can be observed that the

energy computed with the model with 10 points differs from the other energy profiles. For 50 and 200 collocation points, the energy profiles are the same. This shows that the oscillations in the temperature profiles do not impact the stored energy estimation. The oscillations probably compensate along the temperature profile. However, the thermocline slope needs to be accurately represented in order to estimate correctly the stored energy. A quantitative analysis was performed. The maximal difference between the energy computed with the 200 points model and the 10 points model is 1.1MWh and for the 50 points model it is 0.14MWh. The maximal relative difference is reached at the beginning of the charging phase when the energy is small. It is 27% for the 10 points model and 2.8% for the 50 points model compared to the 200 points model.

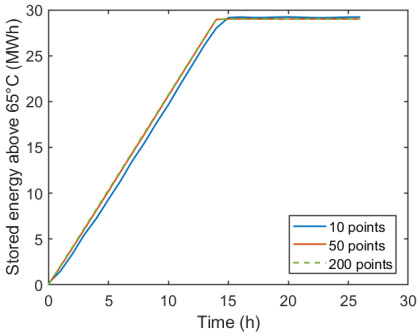

Figure III.10: Cumulated stored energy throughout time during charging

The results obtained are compared with the multinode model (see subsection III.3.2). The chosen reference is OC with 200 collocation points because the results converge towards the same solution with a larger number of collocation points. The multinode model with 1000 layers underestimates the stored energy by up to 0.46MWh, and up to 8% at the beginning of charge. The difference is small but still more important than the difference between the stored energy with 50 points with OC and 200 points. This confirms that OC gives a better estimation of the temperature gradient, despite some oscillations around the thermocline, which do not impact the stored energy much. With 5000 layers in the multinode model, the relative difference with the reference is 2.9% and the absolute difference is 0.16MWh. These differences are similar to the ones observed with 50 collocation points. In terms of temperature profiles, 5000 layers in the multinode model and 200 collocation points lead to similar results, plotted in Figure III.11. In this figure, a temperature profile is plotted every hour until the charge is complete, with solid black line for OC with 200 collocation points and dashed red lines for the multinode model with 5000 layers. Both models give similar results, although the multinode model still presents slight numerical diffusion. The largest difference between the temperatures from the two models at the same height is 5.9°C, and the maximal relative difference is 17%. These differences are not negligible but even more layers would be necessary in the multinode model in order to find the same results as OC. The computational times are very different: 0.85s for OC and 330s for multinode. This clearly shows the advantage of using OC over finite volumes to discretize the storage tank.

This study showed that OC greatly reduces numerical diffusion and is able to accurately represent the steep temperature gradient in the thermocline region even with a

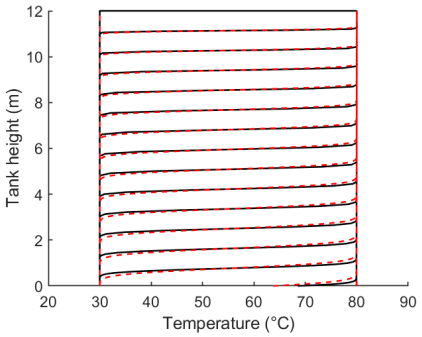

Figure III.11: Comparison of the temperature profiles throughout time with 200 collocation points (solid black lines) and 5000 layers (dashed red lines)

small number of collocation points. However, oscillations appeared in the spatial temperature profiles around the thermocline for a smaller number of collocation points. The reason for these oscillations is that a low-degree polynomial is not able to represent a very steep gradient. By increasing the number of collocation points, hence the degree of the temperature polynomial, the oscillations fade away.

For a simulation model, OC with 100 to 200 collocation points seems to provide accurate and fast results. Thus, the problem of oscillations will not arise because the number of collocation points is large enough. However, for an optimization model, computational times might be too long. The number of points should probably be reduced. The next section will introduce Orthogonal Collocation on Finite Elements (OCFE), which present some advantages over OC and might be more suited for an optimization study.

III.6 Orthogonal Collocation on Finite Elements

When the discretization domain is large or when an important number of collocation points is required, Orthogonal Collocation on Finite Elements (OCFE) is generally more appropriate (Carey and Finlayson; 1975). The domain is divided into elements and OC is applied in each element. The continuity of the differential variable and its first derivative (in the case of a 2^{nd} order differential equation) is imposed at the boundaries between elements. This method gathers the advantages of the two previously mentioned discretization techniques. The convergence is fast, as in OC, which allows to use a smaller number of discretization points. The resolution is fast as for the finite volumes method. OCFE involves sparse matrices, while OC involves full matrices. Thus, OCFE is faster to solve than OC. Carey and Finlayson recommend using OCFE when there is a zone with a steep gradient in the solution, by adapting the size and position of the elements to the expected solution (Carey and Finlayson; 1975). For example, OCFE is particularly well suited to model boundary layers. In the storage tank, there is indeed a zone with a steep gradient, the thermocline. Unfortunately, its position moves inside the storage tank. It is therefore not possible to use fixed smaller elements around the thermocline. Moving elements could be a good direction for future works but it is more complex to implement in an optimization study than fixed elements.

Yet, OCFE presents promising advantages over OC, such as its fast resolution. Therefore, it might be more appropriate than OC for optimization studies. In order to assess OCFE performances for optimization studies, a simulation model for the storage tank was built in an optimization environment. The software GAMS was used and the model was solved with the optimization solver IPOPT. The simulation model developed can be directly incorporated into an optimization model in GAMS. The model is built similarly to the OC model explained in III.4.2. We consider N the total number of collocation points in each element. The energy balance can be written for each interior point i of each element j. This is represented by the following equation:

$$\rho C_p A \frac{dT_{j,i}}{dt} = UP(T_{amb} - T_{j,i}) + k^* A \frac{D^2T(j,i)}{L_{el}^2} - (\dot{m}_c - \dot{m}_d) C_p \frac{DT(j,i)}{L_{el}} \quad \text{(III.18)}$$

The time dependency of the variables in this equation is not written for conciseness. The first and second derivatives of the temperature with respect to z, $DT(j,i)$ and $D^2T(j,i)$ respectively, are expressed as a linear combination of all the temperatures $T_{j,l}$ in the l collocation points (from 1 to N) of the corresponding element j. The matrices A_{OCFE} and B_{OCFE}, computed with the Lagrange polynomials derivatives evaluated in each collocation point inside an element, as explained in III.4.2, are used to express the linear combination. L_{el} is the length of each element. The continuity equations between elements for the temperature and its first derivative with respect to time are written as follows:

$$T_{j-1,N} = T_{j,1} \quad \text{(III.19)}$$

$$\frac{dT_{j-1,N}}{dt} = \frac{dT_{j,1}}{dt} \quad \text{(III.20)}$$

One major difference between MATLAB and GAMS is the time integration. In MATLAB, the simulation model was solved with the solver ode15s, using a variable time step. In GAMS, the time discretization must be explicitly written by the user. We chose orthogonal collocation on finite elements for the time discretization. The time step does not adapt to the simulation but is fixed in advance. Elements of 15 minutes are chosen, with 5 collocation points in each element, including the boundary points. The collocation points are the Gauss-Lobatto Legendre points. The matrix method implemented for the time discretization is based on (Hedengren et al.; 2014) and detailed in (Scolan; 2020). This method is particularly suited for initial value differential equations. The length of the time elements needs to be chosen carefully to respect the convergence criteria even though the spatial grid is non-uniform. Indeed, numerical instabilities might arise if the time step is too large compared to the space discretization (Scolan; 2020). Generally, it is recommended to ensure that the fluid does not flow through several space discretization points during a single time step. Of course, with OCFE, both time and space discretization are non-uniform. It is necessary to ensure that the recommendation is followed for every time and space steps. This is only a general recommendation and a time step 2 or 3 times larger might not generate numerical instabilities. OC was used to discretize the vertical axis of the storage tank to provide a comparison in this study. Figure III.12 shows the temperature profiles obtained during a charging phase for OC and OCFE with the same total number of

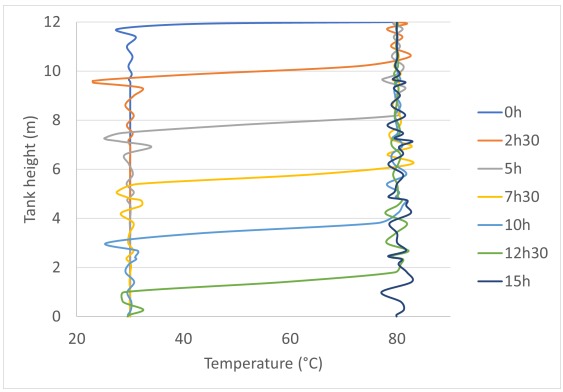

(a) 5 elements, 10 points (10 s)

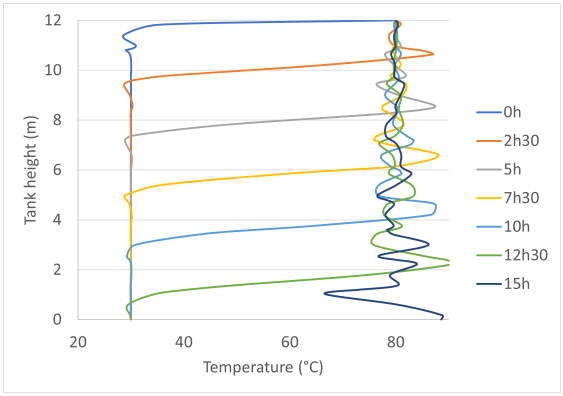

(b) 10 elements, 5 points (7 s)

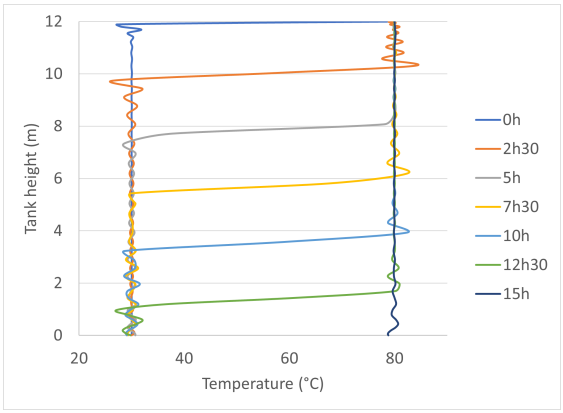

(c) 50 points (34 s)

Figure III.12

points, along with the computational times for the complete charge. This figure shows that OC is the most accurate but its resolution takes the longest. OCFE results depend on the number of elements and points. The more elements are used for the same total number of points, the less accurate the solution is. That is expected because the energy balance in Equation III.1 is only performed on the interior points. At the boundary points between elements, continuity equations are derived. Based on these results, it is recommended to use OCFE in an optimization code because it is much faster to solve. However, a sufficient number of collocation points should be used in each element to ensure a good accuracy in the results.

Unfortunately, a very large number of elements or collocation points cannot be used in an optimization study because it would increase the computational time too much. Thus, oscillations in the temperature profiles will not be avoided by increasing the number of points (see Section III.5). These oscillations are due to the representation of very thin thermoclines with polynomials. The steepness of the temperature gradient in the thermocline is actually unknown. A validation with a real system will be conducted in Section III.7. It is possible that the thermocline representation obtained with the accurate resolution of Equation III.1 for a charging phase starting with a uniform storage tank is too steep and not realistic. The next study conducted was the assessment of the performances of OCFE when the initial condition of the storage tank is not a uniform

temperature, but rather a thermocline. This initial condition is more likely to happen in an energy system, since it is avoided to completely empty or fill up a storage tank in a real system. This strategy is used because the beginning of charging is when the thermocline thickens the most (He et al.; 2019). It is then better to create the thermocline carefully, by using a small flow rate for example, and then try to keep it inside the storage tank. For this calculation, OCFE was used and the charging phase was simulated in GAMS in anticipation for future optimization studies using this software. The solver IPOPT was used. As mentioned above, it is much faster to use OCFE in GAMS than OC for the same total number of collocation points. In the simulations performed, an initial thermocline exists in the middle of the storage tank. The charging phase starts, with a flow rate of $10 kg.s^{-1}$ and a temperature equal to the hot section of the storage. Two cases were tested: a multinode model with 500 layers and an OCFE model with 5 elements and 10 collocation points each. The results are plotted in Figure III.13. Firstly, there are no major oscillations visible in the OCFE temperature profiles even though only 50 discretization points were used. This is because the initial thermocline is not too steep and therefore, a low degree polynomial representation can approximate it accurately. Moreover, a slight numerical diffusion can be observed for the multinode temperature profiles. The thermocline thickens slightly during the charging phase. On the other hand, the thermocline thickness remains unchanged with OCFE. Therefore, OCFE was able to greatly reduce numerical diffusion. Finally, the computational times are very different: 7s for OCFE and 1000s for the multinode model to complete the charge of the storage tank.

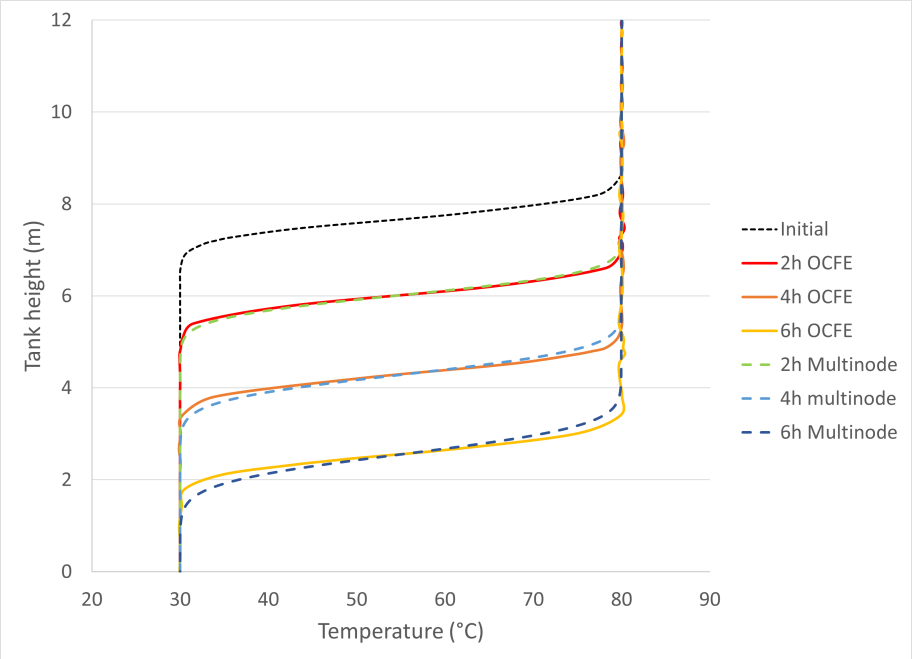

Figure III.13: Comparison of the temperature profiles for the multinode model and OCFE during a charging phase from a half charged tank

We showed that a small number of collocation points is able to accurately represent the temperature profiles in the tank when the thermocline is already created. OCFE runs much faster than the multinode model to achieve comparable accuracy.

In this section, the results obtained with the multinode model and OC/OCFE were compared. With a sufficiently large number of discretization points, a convergence in the results is achieved. Therefore, we have access to the solution of Equation III.1. We showed that OC performs better than the multinode model in order to solve this equation accurately and rapidly. However, Equation III.1 might not be an accurate representation of the reality. Therefore, the next section will present a validation of our OCFE model with real plant data.

III.7 Validation with a real system

III.7.1 Condat-Sur-Vézère, France, Solar Thermal Plant

NEWHEAT is a French company specialized in solar thermal plants, taking part in each stage of their life: design, financing, building and operation. Their solar thermal plants are providing heat at a competitive price to industrial processes or district heating networks. In June 2019, NEWHEAT inaugurated a solar thermal plant in Condat-Sur-Vézère, in the South-West of France. At the time, it was the largest solar thermal plants with flat plate collectors in France and the first in the world to use a 1-axis solar tracking system. The heat produced by this plant is delivered to a paper mill. A water storage tank of $450m^3$, with a height of 11.25m, allows the decoupling between the heat production and consumption. The solar plant has been instrumented for accurate measurements of flow rates and temperatures. Especially, 11 thermocouples are measuring the temperatures along the vertical axis of the storage tank. The flow rates and temperatures for the charging and return flows are also measured. It was therefore possible to use real plant data to validate our storage tank model.

III.7.2 Validation

In order to validate the OCFE model presented above, a simulation is performed over a charging cycle and compared to real plant data. The initial temperatures inside the storage tank at the beginning of the charging phase, as well as the charging flow rate and temperature are used as inputs to the simulation model. The data were acquired on June 3^{rd}, 2019, with a time resolution of 10 minutes. The charging phase begins at 2pm. The multinode model as well as the OCFE model presented in Section III.6 were compared to the experimental data. The simulations were performed in GAMS with the IPOPT solver. For the multinode model, a simplified simulation with 10 layers was first conducted. The time discretization uses elements of 1 hour and 9 collocation points. The results are plotted in Figure III.14a, and the charging phase simulation lasted 2 seconds. The temperature profiles at 3pm, 6pm and 9pm for the experimental data and for the model are plotted. The uncertainty in the temperature measurement is ± 0.5 °C, which is too low to be represented on the plot. We observe that numerical diffusion has an important impact on the numerical temperature profiles and that there is a poor agreement between the experimental and modeled values. Another simulation with 100 layers was then run, with a finer time discretization. Elements of 30 minutes were used in order to avoid numerical instabilities due to the smaller space

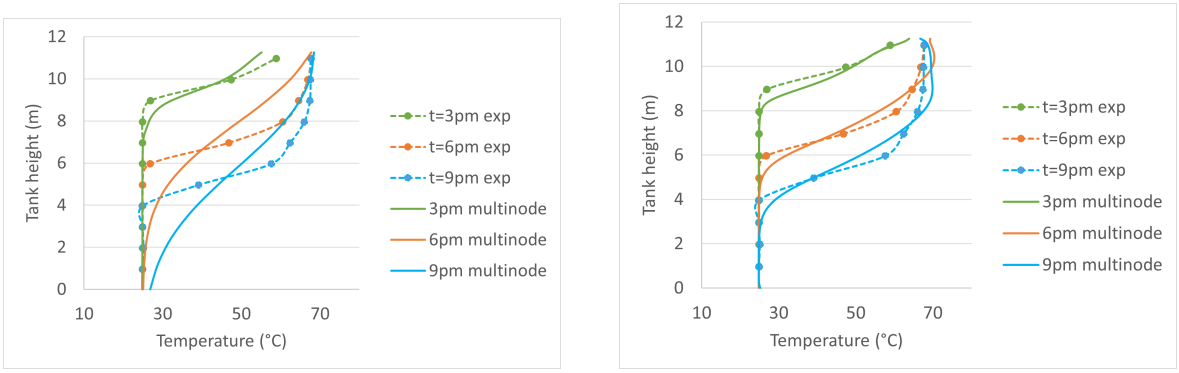

(a) 10 layers (2 s)

(b) 100 layers (15 s)

Figure III.14: Comparison of the experimental and multinode model temperature profiles during a charging phase

elements. The results are presented in Figure III.14b. The effect of numerical diffusion is less visible in this plot. A better agreement is noticed between the experimental and modeled temperature profiles. However, the simulation lasted 15 seconds, which is 7 times longer than the simulation with 10 layers. For this simple system, with only the storage tank, and a short time horizon, the computational times are short in both cases. Nevertheless, for the simulation of a more complex system including storage or for an optimization study, the computational time might become too long with 100 layers. This is even more important for real-time optimization.

The OCFE model developed in this paper was then compared to the experimental results. The model in GAMS validated for optimization studies uses 3 elements and 8 collocation points. The time discretization uses elements of 1 hour and 9 collocation points, which is the same as the multinode model with 10 layers. The results are plotted in Figure III.15, and the computational time for the charging phase is 3 seconds. This is very close to the computational time for the multinode model with 10 layers, and 5 times faster than the model with 100 layers. Moreover, as shown in Figure III.15, the thermoclines are here well represented. There is a good agreement between the numerical and experimental profiles.

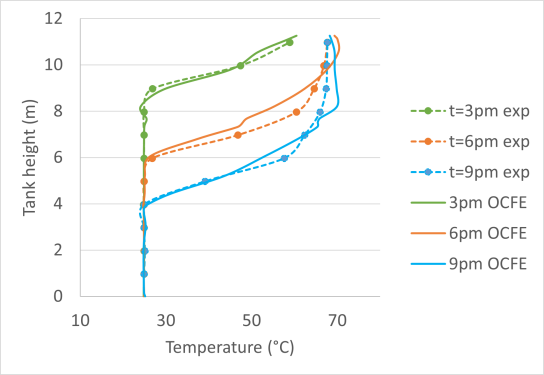

Figure III.15: Comparison of the experimental and OCFE model temperature profiles during a charging phase

The error made by the models was quantified with two indicators: Mean Absolute

	10 layers			100 layers			3x8 OCFE		
Time	3pm	6pm	9pm	3pm	6pm	9pm	3pm	6pm	9pm
MAE (°C)	1.1	4.4	5.3	1.1	1.6	1.9	0.7	1.9	1.5
MAPE (%)	3.1	11.5	15.9	3.5	3.7	4.2	1.8	3.8	2.8

Table III.1: Validation of the numerical models

Error (MAE) and Mean Absolute Percentage Error (MAPE). These are defined as follows:

$$MAE(°C) = \frac{1}{k}\sum_{i=1}^{k}|x_i - y_i| \tag{III.21}$$

$$MAPE(\%) = \frac{1}{k}\sum_{i=1}^{k}\left|\frac{x_i - y_i}{x_i}\right| \tag{III.22}$$

In these Equations, k is the number of comparison points, x_i are the experimental points and y_i are the numerical points. To ensure that x_i and y_i are taken at the same height in the storage tank, the numerical profile obtained is interpolated. The results for these two indicators are presented in Table III.1 for the three models tested.

Table III.1, confirms that the model with 10 layers is not accurate with MAPE going up to 15.9%. The two other models have a MAPE below 5% for 100 layers and 4% for OCFE. The MAE is below 2°C, which is small compared to the accuracy of the temperature measurements. Therefore, these models are considered valid. With OCFE, we were able to use less points and achieve a better accuracy than the multinode model. Thus, the OCFE model presented in this study is validated and should be used to discretize a TES for simulation and optimization studies.

This validation study was conducted for a charge cycle, starting once the thermocline inside the storage tank is created. The beginning of charge from an empty storage is not well represented by Equation III.1. Indeed, there is some mixing happening when the fluid enters the storage tank, leading to a thicker thermocline than the one predicted by the model. Developing diffusers that prevent this effect is still an active area of research ((Parida et al.; 2022), (Xu et al.; 2022) for example). To accurately represent this phenomenon in a 1D model, data reconciliation should be performed and an additional diffusion term should be introduced in the model to account for the mixing due to injection. This has been done for reactors modeling to represent non-ideal flow patterns (Gilbert F. Froment and Kenneth B. Bischoff; 1990). This would require a large amount of data with a fine spatial and temporal resolution. In real applications, it is avoided to completely empty or fill up the storage tank. Therefore, the model presented in this paper is accurate to represent the real conditions inside the storage tank.

III.8 Perspectives on natural convection modeling

As mentioned in Section III.2, the correction of temperature inversions inside the storage tank is an important aspect of TES modeling. It is particularly challenging to

incorporate natural convection in a 1D model appropriate for optimization studies. Indeed, a continuous and smooth model is required for optimization. Such a model was developed based on the physical model suggested in (Hawlader et al.; 1988). A turbulent diffusion coefficient was added to correct the temperature inversions, and had the following value:

$$\epsilon_{turb} = \frac{k_{turb}}{\rho C_p} = \begin{cases} (K\delta l)^2 \sqrt{g\beta \frac{\partial T(z,t)}{\partial z}}, & \text{if } \frac{\partial T(z,t)}{\partial z} < 0 \\ 0, & \text{otherwise.} \end{cases} \tag{III.23}$$

In this equation, K is the Von Karman constant, whose value is 0.4, g is the gravitational acceleration which is 9.81 $m.s^{-2}$ and β is the thermal expansion coefficient of water, which is about $2.6e^{-4}K^{-1}$. The characteristic length δl is chosen to be the tank height.

Such inversions correspond to a reversed temperature gradient. With z axis pointing upwards, the gradient in normal conditions is positive, and in case of temperature inversion it is negative. It is thus possible to spot a temperature inversion thanks to the max function, with the turbulent coefficient written as:

$$k_{turb} = \rho C_p (KH)^2 \sqrt{g\beta \mathbf{max}(-\frac{\partial T(z,t)}{\partial z}, 0)} \tag{III.24}$$

This formulation can be incorporated into an OCFE model for TES simulation. The boundary conditions used are presented in Subsection III.4.3. 100 collocation points are used in this study. Figure III.16 presents the results of a simulation with an inversion correction. In this study, the hot zone of the storage tank is initially at 80°C. The storage tank is charged during 1h with fluid at 75°C, and then the charging fluid goes back to 80°C and the simulation runs for 5 more minutes. With this model, the temperature inversion persists as long as the charging with fluid at 75°C is still in progress, as shown in Figure III.16. However, after the charging temperature goes back to 80°C, temperature inversions are corrected. The inlet of the storage tank is at 80°C while the rest of the hot zone is at a homogeneous temperature resulting from the mixing between the fluid already present at 80°C and the charged fluid at 75°C. This behavior seems realistic, but the model is much slower than a model without natural convection, about 150 times slower. Unfortunately, no validation with real plant data could be conducted for the natural convection modeling. This would require data from thermocouples that are close to each other and with a small time resolution. Such data were not available in the plant used for the validation.

For a simulation model, this works fine with the max function, although it is much slower than a model without the inversion correction. For an optimization model, a smooth approximation of the max function needs to be used, such as in (Lago et al.; 2019) and (Soares et al.; 2022). The parameter determining the steepness of the max function needs to be adjusted to offer a compromise between the accurate representation of the max function and the ease of convergence. This will slow down even more the calculations. For example, the following approximation was used to determine the maximum between two values x_1 and x_2:

$$\text{smoothMax}(x_1, x_2, d) = 0.5(x_1 + x_2 + \sqrt{(x_1 - x_2)^2 + d^2}) \tag{III.25}$$

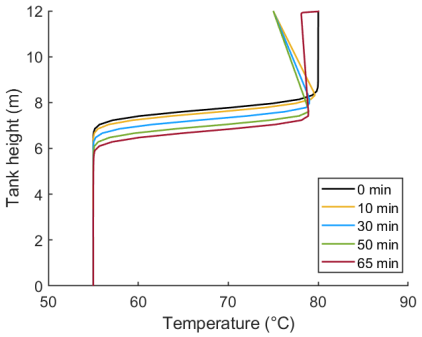

Figure III.16: Correction of temperature inversions with a continuous model

In this formulation, parameter d needs to be adjusted to adapt the steepness of the function. If d is large, the function varies smoothly and temperature inversions are not spotted accurately. This leads to the thickening of the thermocline due to a large diffusion coefficient, even when it is not needed. On the contrary, if d is small, the approximate function better represents the max function and the computation of k_{turb} is more accurate. However, convergence is not ensured.

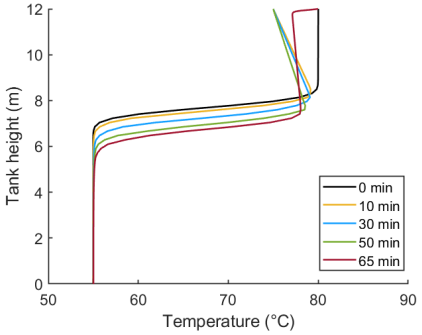

Figure III.17: Correction of temperature inversions with a smooth model

Figure III.17 shows the results obtained with $d = 1e^{-4}$. The results are slightly different from the ones obtained in Figure III.16, with a maximum difference of 2.5% in the final profiles. We notice that the average temperature in the hot zone after the correction of the temperature inversion is about 1°C lower with the smooth function. This happens because the turbulent coefficient is not 0 in the thermocline region, even though the temperature gradient is not reversed. Thus, there is a large diffusion at the ends of the thermocline, introducing some mixing between colder fluid from the thermocline and hot fluid in the hot zone. Overall the results are in good agreement with the ones obtained with the discontinuous max function. The computational time is about 32 times longer than the model with the max function. If parameter d is smaller, the simulations do not converge.

To conclude, it is possible to build a continuous and smooth model to represent natural convection inside a storage tank. However, this model needs some tuning in the smooth function. The physical basis of the model is therefore deteriorated by these tuning parts. Moreover, the computational time is largely increased when using this model. Based on these observations, it is recommended to choose another solution

for the modeling of natural convection in an optimization model. For example, the inversion flow rates presented in (Scolan; 2020) appear to be a good solution to correct temperature inversions in an optimization framework. An experimental study should be conducted to validate this model.

III.9 Conclusion and perspectives

The increasing share of intermittent renewable energies into the electricity grid or heating and cooling district networks requires the development of storage solutions to ensure that the energy demand is met. Thermal Energy Storage (TES) is an effective way to store energy in the form of heat, that can be latter used, employing the synergies between various energy carriers. In order to expand the use of stratified TES in energy systems, a good model for it needs to be developed. Especially, a fast and accurate model, that can be used for complex dynamic simulations and optimizations is required. A short computational time is even more crucial for real-time optimization and control. The challenge in modeling a thermocline TES is the representation of the steep temperature gradient between the hot and cold zones. The discretization scheme presented in this paper, Orthogonal Collocation on Finite Elements (OCFE), is able to reduce numerical diffusion and therefore estimates accurately the temperature profile inside the tank as well as the valuable energy stored. This model uses less discretization points and runs faster than the multinode model in order to achieve the same accuracy. This discretization method can generate oscillations in the temperature profiles if the storage is initially at a uniforme temperature. The thermoclines estimations are too steep, and thus a low degree polynomial is not able to represent them. Adding a term in the energy balance inside the tank to represent the mixing at the injection point could solve the problem. However, in a real plant, the storage tank is very rarely at a uniform temperature. Therefore, the model presented in the paper is appropriate to represent the actual behavior of a storage tank. This has been validated with real plant data. Thus, the model developed in this work can be used in simulation and optimization, including real-time applications. Finally, a continuous model for the correction of temperature inversions was presented, based on a turbulent diffusion coefficient. The model was able to correct temperature inversions effectively in a simulation. However, the computational time was greatly increased. Transforming it into a smooth model for optimization is even slower, making it not computationally effective. Other ways to model natural convection, as part of the optimization framework, could be better. Future work should focus on the integration of natural convection in a 1D optimization model. Furthermore, the validation of the correction of temperature inversion should be performed with an experimental set up or a real plant.

Acknowledgements

The project leading to this publication has received funding from Excellence Initiative of Université de Pau et des Pays de l'Adour – I-Site E2S UPPA, a French "Investissements d'Avenir" programme.

III.10 CRediT authorship contribution statement

Alix Untrau: Conceptualization, Data curation, Formal analysis, Investigation, Methodology, Software, Validation, Visualization, Writing – original draft, Writing – review & editing. **Sabine Sochard:** Conceptualization, Funding acquisition, Methodology, Project administration, Resources, Supervision, Writing – review & editing. **Frédéric Marias:** Conceptualization, Funding acquisition, Methodology, Project administration, Resources, Supervision, Writing – review & editing. **Jean- Michel Reneaume:** Conceptualization, Funding acquisition, Methodology, Project administration, Resources, Supervision, Writing – review & editing. **Galo A.C. Le Roux:** Conceptualization, Methodology, Supervision, Writing – original draft, Writing – review & editing. **Sylvain Serra:** Conceptualization, Funding acquisition, Methodology, Project administration, Resources, Supervision, Writing – original draft, Writing – review & editing.

Bibliography

Aguilar, F., Crespí-Llorens, D., Aledo, S. and Quiles, P. V. (2021). One-Dimensional Model of a Compact DHW Heat Pump with Experimental Validation, *Energies* **14**(11): 2991.

Al-Habaibeh, A., Shakmak, B. and Fanshawe, S. (2018). Assessment of a novel technology for a stratified hot water energy storage – The water snake, *Applied Energy* **222**: 189–198.

Argyrou, M. C., Christodoulides, P. and Kalogirou, S. A. (2018). Energy storage for electricity generation and related processes: Technologies appraisal and grid scale applications, *Renewable and Sustainable Energy Reviews* **94**: 804–821.

Ayele, G. T., Mabrouk, M. T., Haurant, P., Laumert, B. and Lacarrière, B. (2021). Optimal heat and electric power flows in the presence of intermittent renewable source, heat storage and variable grid electricity tariff, *Energy Conversion and Management* **243**: 114430.

Baeten, B., Confrey, T., Pecceu, S., Rogiers, F. and Helsen, L. (2016). A validated model for mixing and buoyancy in stratified hot water storage tanks for use in building energy simulations, *Applied Energy* **172**: 217–229.

Bird, T. J. and Jain, N. (2020). Dynamic modeling and validation of a micro-combined heat and power system with integrated thermal energy storage, *Applied Energy* **271**: 114955.

Campos Celador, A., Odriozola, M. and Sala, J. (2011). Implications of the modelling of stratified hot water storage tanks in the simulation of CHP plants, *Energy Conversion and Management* **52**(8-9): 3018–3026.

Carey, G. and Finlayson, B. A. (1975). Orthogonal collocation on finite elements, *Chemical Engineering Science* **30**(5-6): 587–596.

Csordas, G., Brunger, A., Hollands, K. and Lightstone, M. (1992). Plume entrainment effects in solar domestic hot water systems employing variable-flow-rate control strategies, *Solar Energy* **49**(6): 497–505.

Dahash, A., Ochs, F., Tosatto, A. and Streicher, W. (2020). Toward efficient numerical modeling and analysis of large-scale thermal energy storage for renewable district heating, *Applied Energy* **279**: 115840.

De Césaro Oliveski, R., Krenzinger, A. and Vielmo, H. A. (2003). Comparison between models for the simulation of hot water storage tanks, *Solar Energy* **75**(2): 121–134.

Dickes, R., Desideri, A., Lemort, V. and Quoilin, S. (2015). Model reduction for simulating the dynamic behavior of parabolic troughs and a thermocline energy storage in a micro-solar power unit, *Proceedings of ECOS 2015 - The 28th international conference on Efficiency, Cost, Optimization, Simulation and environmental impact of energy systems* p. 13.

Ebrahimzadeh, E., Shahrak, M. N. and Bazooyar, B. (2012). Simulation of transient gas flow using the orthogonal collocation method, *Chemical Engineering Research and Design* **90**(11): 1701–1710.

ELSihy, E. S., Liao, Z., Xu, C. and Du, X. (2021). Dynamic characteristics of solid packed-bed thermocline tank using molten-salt as a heat transfer fluid, *International Journal of Heat and Mass Transfer* **165**: 120677.

Ferreira, S., Sochard, S., Serra, S., Marias, F. and Reneaume, J.-M. (2021). Modelling of an Adsorption Heat Storage System and Study of Operating and Design Conditions, *Processes* **9**(11): 1885.

Franke, R. (1997). Object-oriented modeling of solar heating systems, *Solar Energy* **60**: 171–180.

Gilbert F. Froment and Kenneth B. Bischoff (1990). *Chemical Reactor Analysis and Design - Second Edition*, Wiley Series in Chemical Engineering, John Wiley and Sons, Inc, New York.

Guelpa, E. and Verda, V. (2019). Thermal energy storage in district heating and cooling systems: A review, *Applied Energy* **252**: 113474.

Haillot, D., Franquet, E., Gibout, S. and Bédécarrats, J.-P. (2013). Optimization of solar DHW system including PCM media, *Applied Energy* **109**: 470–475.

Han, Y., Wang, R. and Dai, Y. (2009). Thermal stratification within the water tank, *Renewable and Sustainable Energy Reviews* **13**(5): 1014–1026.

Hawlader, M. N. A., Bong, T. Y. and Lee, T. S. (1988). A Thermally Stratified Solar Water Storage Tank, *International Journal of Solar Energy* **6**(2): 119–138.

He, Z., Qian, Y., Xu, C., Yang, L. and Du, X. (2019). Static and dynamic thermocline evolution in the water thermocline storage tank, *Energy Procedia* **158**: 4471–4476.

Hedengren, J. D., Shishavan, R. A., Powell, K. M. and Edgar, T. F. (2014). Nonlinear modeling, estimation and predictive control in APMonitor, *Computers & Chemical Engineering* **70**: 133–148.

Hosseinnia, S. M., Akbari, H. and Sorin, M. (2021). Numerical analysis of thermocline evolution during charging phase in a stratified thermal energy storage tank, *Journal of Energy Storage* **40**: 102682.

Ievers, S. and Lin, W. (2009). Numerical simulation of three-dimensional flow dynamics in a hot water storage tank, *Applied Energy* **86**(12): 2604–2614.

Immonen, J. and Powell, K. M. (2022). Dynamic optimization with flexible heat integration of a solar parabolic trough collector plant with thermal energy storage used for industrial process heat, *Energy Conversion and Management* **267**: 115921.

Johannes, K., Fraisse, G., Achard, G. and Rusaouën, G. (2005). Comparison of solar water tank storage modelling solutions, *Solar Energy* **79**(2): 216–218.

Kleinbach, E., Beckman, W. and Klein, S. (1993). Performance study of one-dimensional models for stratified thermal storage tanks, *Solar Energy* **50**(2): 155–166.

Kleinbach, E. M. (1990). *Performance Study of One-Dimensional Models for Stratified Thermal Storage Tank*, Master's thesis, University of Wisconsin-Madison.

Koçak, B., Fernandez, A. I. and Paksoy, H. (2020). Review on sensible thermal energy storage for industrial solar applications and sustainability aspects, *Solar Energy* **209**: 135–169.

Lago, J., De Ridder, F., Mazairac, W. and De Schutter, B. (2019). A 1-dimensional continuous and smooth model for thermally stratified storage tanks including mixing and buoyancy, *Applied Energy* **248**: 640–655.

Lake, A. and Rezaie, B. (2018). Energy and exergy efficiencies assessment for a stratified cold thermal energy storage, *Applied Energy* **220**: 605–615.

Liang, H., Liu, L., Zhong, Z., Gan, Y., Wu, J.-Y. and Niu, J. (2022). Towards idealized thermal stratification in a novel phase change emulsion storage tank, *Applied Energy* **310**: 118526.

Mawire, A. (2013). Experimental and simulated thermal stratification evaluation of an oil storage tank subjected to heat losses during charging, *Applied Energy* **108**: 459–465.

Michelsen, M. and Villadsen, J. (1972). A convenient computational procedure for collocation constants, *The Chemical Engineering Journal* **4**(1): 64–68.

Modi, A. and Pérez-Segarra, C. D. (2014). Thermocline thermal storage systems for concentrated solar power plants: One-dimensional numerical model and comparative analysis, *Solar Energy* **100**: 84–93.

Muschick, D., Zlabinger, S., Moser, A., Lichtenegger, K. and Gölles, M. (2022). A multi-layer model of stratified thermal storage for MILP-based energy management systems, *Applied Energy* **314**: 118890.

Nash, A. L., Badithela, A. and Jain, N. (2017). Dynamic modeling of a sensible thermal energy storage tank with an immersed coil heat exchanger under three operation modes, *Applied Energy* **195**: 877–889.

Newton, B. J. (1995). Modelling of solar storage tanks.
URL: *http://digital.library.wisc.edu/1793/7803*

Paing, S. T., Anderson, T. and Nates, R. (2019). Modelling and experimental validation of natural convection heat loss from a solar hot water storage tank, *Asia Pacific - Solar Reaseach Conference* .

Parida, D. R., Advaith, S., Dani, N. and Basu, S. (2022). Assessing the impact of a novel hemispherical diffuser on a single-tank sensible thermal energy storage system, *Renewable Energy* **183**: 202–218.

Pate, R. A. (1977). *A Thermal Energy Storage Tank Model for Solar Heating*, thesis, Utah State University.

Powell, K. M. and Edgar, T. F. (2013). An adaptive-grid model for dynamic simulation of thermocline thermal energy storage systems, *Energy Conversion and Management* **76**: 865–873.

Rahman, A. and Smith, A. D. (2018). Predicting heating demand and sizing a stratified thermal storage tank using deep learning algorithms, *Applied Energy* **228**: 108–121.

Rahman, A., Smith, A. D. and Fumo, N. (2016). Performance modeling and parametric study of a stratified water thermal storage tank, *Applied Thermal Engineering* **100**: 668–679.

Renewable Energy Directive (2018). Directive (EU) 2018/2001 of the European Parliament and of the Council of 11 December 2018 on the promotion of the use of energy from renewable sources, *OJ* **L328/82**.

Ryan, E., McDaniel, B. and Kosanovic, D. (2022). Application of thermal energy storage with electrified heating and cooling in a cold climate, *Applied Energy* **328**: 120147.

Saloux, E. and Candanedo, J. (2019). Modelling stratified thermal energy storage tanks using an advanced flowrate distribution of the received flow, *Applied Energy* **241**: 34–45.

Saloux, E. and Candanedo, J. A. (2021). Model-based predictive control to minimize primary energy use in a solar district heating system with seasonal thermal energy storage, *Applied Energy* **291**: 116840.

Scolan, S. (2020). *Développement d'un outil de simulation et d'optimisation dynamique d'une centrale solaire thermique.*, thesis, Pau.
URL: *https://theses.hal.science/tel-03725400/document*

Scolan, S., Serra, S., Sochard, S., Delmas, P. and Reneaume, J.-M. (2020). Dynamic optimization of the operation of a solar thermal plant, *Solar Energy* **198**: 643–657.

Soares, A., Camargo, J., Al-Koussa, J., Diriken, J., Van Bael, J. and Lago, J. (2022). Efficient temperature estimation for thermally stratified storage tanks with buoyancy and mixing effects, *Journal of Energy Storage* **50**: 104488.

Stamps, D. W. and Clark, J. A. (1992). Thermal destratification in a cylindrical packed bed, *International Journal of Heat and Mass Transfer* **35**(3): 727–737.

Sullivan, H., Hollands, K. and Shewen, E. (1984). Thermal destratification in rock beds, *Solar Energy* **33**(2): 227–229.

Touzo, A., Olives, R., Dejean, G., Pham Minh, D., El Hafi, M., Hoffmann, J.-F. and Py, X. (2020). Experimental and numerical analysis of a packed-bed thermal energy storage system designed to recover high temperature waste heat: an industrial scale up, *Journal of Energy Storage* **32**: 101894.

Trevisan, S., Jemmal, Y., Guedez, R. and Laumert, B. (2021). Packed bed thermal energy storage: A novel design methodology including quasi-dynamic boundary conditions and techno-economic optimization, *Journal of Energy Storage* **36**: 102441.

Untrau, A., Sochard, S., Marias, F., Reneaume, J.-M., Le Roux, G. A. and Serra, S. (2022). Analysis and future perspectives for the application of Dynamic Real-Time Optimization to solar thermal plants: A review, *Solar Energy* **241**: 275–291.

Viskanta, R., Behnia, M. and Karalis, A. (1977). Interferometric observations of the temperature structure in water cooled or heated from above, *Advances in Water Resources* **1**(2): 57–69.

Xu, C., Liu, M., Jiao, S., Tang, H. and Yan, J. (2022). Experimental study and analytical modeling on the thermocline hot water storage tank with radial plate-type diffuser, *International Journal of Heat and Mass Transfer* **186**: 122478.

Yang, Z. and Garimella, S. V. (2010). Molten-salt thermal energy storage in thermoclines under different environmental boundary conditions, *Applied Energy* **87**(11): 3322–3329.

Zachár, A. (2020). Analytic solution for convection dominant heat transport induced by buoyant jet entrainment inside hot fluid storage tanks, *Solar Energy* **195**: 239–248.

Zurigat, Y., Ghajar, A. and Moretti, P. (1988). Stratified thermal storage tank inlet mixing characterization, *Applied Energy* **30**(2): 99–111.

III.11 Additional clarifications

- The fully-mixed model for the storage tank mentioned in Section III.2 is a 0D model and not a 1D model since no spatial discretization is used.
- The resulting flow rate $\dot{m}$ from charging and discharging inside the storage tank introduced in Section III.3 is equal to $\dot{m}_c - \dot{m}_d$.

- Orthogonal Collocation on Finite Elements has been applied to discretize the spatial axis of a storage tank in the literature before, in the following paper: Klein *et al.*, 2010. The discretization scheme also used Gauss-Lobatto quadrature and Chebychev polynomials to determine the collocation points. However, the model used was a 2D model for a packed-bed tank with filler material. For a stratified water tank, there is no study using OCFE for spatial discretization inside the tank, to the best of our knowledge.
  Reference: Klein, P, Roos, T, and Sheer, J. (2010). Numerical simulation of a high temperature thermal storage unit for solar gas turbine applications. *16th SolarPACES2010 Conference*, Perpignan, France, 21-24 September 2010, pp. 8.

- A Gauss quadrature (or a Gauss-Radau quadrature) instead of the Gauss-Lobatto quadrature chosen in Subsection III.4.2 could probably improve the results obtained for the OCFE inside the tank by increasing the accuracy and reduce the computational time.

- Chebychev and Legendre polynomials were compared using the Gauss-Lobatto quadrature points, in a simulation of the charging phase of the storage tank. Legendre polynomials led to larger oscillations in the temperature profiles obtained compared to Chebychev polynomials, using the same number of collocation points and leading to similar computational times. Thus, Chebychev polynomials were chosen, as mentioned in Subsection III.4.2.

- In Section III.8, the natural convection inside the tank is studied with a discretization using 100 collocation points and a single element. The smooth approximation of the maximum is done with a hyperbolic approximation function.

Chapter IV

Storage management in DRTO: A realistic case study

Contents

In Chapter II, a DRTO methodology with a planning phase was developed and tested on a virtual plant in a simple case study. The performances of the simulated plant following optimal trajectories determined with the DRTO methodology were compared with the performances of a simulation following trajectories determined during the planning phase, without real-time adaptation. The case study carried out was simple, with the DRTO tested for only one day with a shrinking time horizon. A term for tracking the planned storage state was adjusted in the economic objective function, to take advantage of the planning long term strategic vision for a good storage management policy. The disturbance in the solar irradiation introduced was artificial and the heat demand was constant. The results obtained were promising, with a reduction in the operating cost, an increase in solar fraction and only a small reduction in final stored energy compared to dynamic optimization without real-time adaptation. These promising results will be confirmed in a more realistic case study in the present chapter.

In Chapter II the 1D storage tank model used was the multinode model. 10 layers were used for optimization to ensure fast computational times. 1000 layers were used in the detailed simulation model to mitigate numerical diffusion. Chapter III presented another discretization scheme for the spatial discretization of the storage tank. It was shown that orthogonal collocation requires less discretization points to obtain an accurate representation of the vertical temperature profile in the tank, thus leading to reduced computational time when an accurate solution is needed. So orthogonal collocation converges rapidly, with few discretization points, towards the actual solution of the differential equation. However, for the same number of discretization points, finite volumes run faster due to the sparsity of the matrices generated. Orthogonal collocation on finite elements offers a good compromise between the fast convergence of orthogonal collocation and the fast resolution of finite volumes. Thus, it can be a good alternative to the multinode model for complex simulation models or optimization studies. Additionally, the modeling of natural convection in the storage tank was discussed. This work will be used in the following chapter to choose the storage tank model offering the best compromise between accuracy and computational time for the simplified optimization model and the detailed simulation model.

This chapter is an article submitted to *Applied Energy*, presenting the DRTO methodology and its testing in realistic case studies. After presenting the context and objective of the paper, the solar thermal plant and its modeling is described. In particular, the storage tank models for optimization and simulation purposes are chosen. The hurried reader could skip these sections since the literature review and the modeling assumptions were presented in previous chapters. Then, in Section IV.3, the input data used in the method are presented. Real data are used for the weather forecasts and real-time measurements. The heat demand is a varying daily profile. In Section IV.4, the DRTO methodology is explained. It uses a rolling time horizon in this paper. Several possibilities to integrate storage management into the DRTO objective function, using the planning phase or not, are considered and compared. In this chapter, the DRTO methodology is tested on a virtual plant for 96 hours. Case studies have been carried out to determine guidelines regarding storage management in the DRTO methodology and detailed results are provided and discussed. The case studies allow the formulation of guidelines in two distincts cases: when the solar irradiation does not lead to a potential overheating in the system, and when there is a risk of overheating due to high solar irradiation and low heat demand or both.

Storage management in a rolling horizon Dynamic Real-Time Optimization of a solar thermal plant

Alix Untrau[a*], Sabine Sochard[b], Frédéric Marias[c], Jean-Michel Reneaume[d], Galo A.C. Le Roux [e] and Sylvain Serra[f]

[a,b,c,d,f] Universite de Pau et des Pays de l'Adour, E2S UPPA, LaTEP, Pau, France,

[*] alix.untrau@univ-pau.fr

[e] Universidade de São Paulo, Escola Politécnica, São Paulo, Brazil

Submitted to *Applied Energy*, 2023

Abstract

The intermittency and uncertain forecasts of solar irradiation complicates the operation of a solar thermal plant for heat production. Thermal energy storage helps to decouple the heat production from the heat supply but further increases the complexity of the operation of the plant by adding more degrees of freedom. In this work, a rolling horizon Dynamic Real-Time Optimization (DRTO) methodology is proposed to determine the economic optimal operation of the solar thermal plant. The methodology is tested online on a detailed simulation model representing an industrial plant for 96 hours. Several case studies are considered, using variable heat demand and real data for the weather forecasts and measurements. It was shown that DRTO performs better than offline dynamic optimization thanks to the use of updated weather forecasts and the regular re-initialization of the system state using measurements. The main objective of the present paper is to formulate guidelines on storage management in a DRTO methodology. An important step of the methodology is the planning phase, determining the best operational strategy for the solar thermal plant a few days in advance, based on weather forecasts. The best storage management policy depends on the risk of overheating predicted in the planning, which happens when the storage tank is full and the solar energy collected is larger than the heat demand. While storing the maximum energy possible for later use is the best option when overheating is not a risk, following the planned storage state helps to prevent overheating when the solar irradiation is high.

Nomenclature

Abbreviations

CSP Concentrated Solar Power
DAE Differential Algebraic Equation
DHN District Heating Network
DO Dynamic Optimization
DRTO Dynamic Real-Time Optimization
DRTO E DRTO Economic
DRTO P DRTO Planning
DRTO S DRTO Storage
GHI Global Horizontal Irradiance $[W.m^{-2}]$
MAPE Mean Absolute Percentage Error
MPC Model Predictive Control
NLP Nonlinear Programming
NTU Number of Transfer Units
OCFE Orthogonal Collocation on Finite Elements
OF Objective Function
OF_{eco} Economic Objective Function [€]
PDE Partial Differential Equation
PID Proportional Derivative Integral
RTO Real-Time Optimization
TES Thermal Energy Storage

Greek Symbols

β Scalar characterizing the steepness of the sigmoid function
ΔP_{max} Pressure drop at the maximum flow rate $[Pa]$
Δz Height of a discretization layer in the storage tank $[m]$
δ Threshold for the sigmoid function
ϵ_{HX} Effectiveness of a heat exchanger
η Overall efficiency of the pump
$\eta_{0,b}$ Optical Efficiency of a collector
η_{sh} Shading effect of a solar field loop onto the next loop
γ_{var} Weight on the penalty term to smooth the flow rates trajectories
λ Scalar used in a soft constraint
ω Weight on the storage state tracking term
Φ_{var} Penalty term to smooth the flow rates trajectories
ρ Fluid density $[kg.m^{-3}]$

Subscripts and superscripts

amb Ambient
cold Cold side of a heat exchanger
consumer Consumer stream
demand Heat demand
elec Electric
hot Hot side of a heat exchanger
HX Heat Exchanger
in Inlet of the element
mean Mean value
out Outlet of the element
s Storage
SF Solar Field

Latin Symbols

$\dot{m}$ Mass flow rate $[kg.s^{-1}]$
$\dot{m}_{max}$ Maximum flow rate allowed in the pump $[kg.s^{-1}]$
$\dot{P}$ Power $[W]$
$\dot{Q}$ Heat flow $[W]$
A Area $[m^2]$
c_1 Heat loss coefficient in the collector at $T_{mean} = T_{amb}$ $[W.m^{-2}.K^{-1}]$
c_2 Temperature dependence of the heat loss coefficient $[W.m^{-2}.K^{-1}]$
c_5 Effective thermal capacity $[J.m^{-2}.K^{-1}]$
C_p Fluid heat capacity $[J.kg^{-1}.K^{-1}]$
C_{tot} Total operating costs (electricity and gas) for a simulation [€]
E Energy $[MWh]$
$E_{stock\ final}$ Energy stored in the storage tank at the end of the simulation $[MWh]$
E_{stored} Energy stored in the storage tank $[MWh]$
$E_{supplied}$ Energy supplied to the consumer $[MWh]$
$ElecPrice$ Price of electricity $[€/MWh]$
G_b Direct irradiation (beam) in the plane of a collector $[W.m^{-2}]$
G_d Diffuse irradiation in the plane of a collector $[W.m^{-2}]$
$GasPrice$ Price of gas $[€/MWh]$
$HeatPrice$ Price of heat $[€/MWh]$
k Fluid thermal conductivity $[W.m^{-1}.K^{-1}]$
$K_b(\theta)$ Incidence angle modifier for the direct irradiation (beam)
K_d Incidence angle modifier for the diffuse irradiation
M Fixed scalar used in inequalities representing discontinuities
N Number of discretization layers in the storage tank
P Perimeter $[m]$
R Heat capacity ratio
R_{th} Thermal resistance $[K.W^{-1}]$
S_l Lateral surface of a tank layer $[m^2]$
T Temperature $[°C]$
t Time $[s]$
U Overall heat transfer coefficient $[W.m^{-2}.K^{-1}]$
z Tank height from the bottom of the tank $[m]$

IV.1 Introduction

The energy transition is necessary to mitigate climate change and keep the global warning below 2°C as aimed by the Paris agreements (United Nations Framework Convention on Climate Change; 2015). Heat represents more than 50% of the final energy consumption in the world, and its production mostly relies on fossil fuels nowadays (Collier; 2018). Therefore, increasing the part of renewable heat is crucial to achieve the energy transition objectives fixed worldwide and locally. For example, in Europe, the Revised Renewable Energy Directive (Renewable Energy Directive; 2018) targets an increase of 1.3% per year in the share of renewable energy in the heating and cooling sectors for each state member. Solar thermal energy represents a good alternative to fossil fuels for the production of heat, especially at low temperatures. Indeed, it uses a renewable source of energy, the sun irradiation, to produce heat without direct CO_2 emissions (Tian and Zhao; 2013).

IV.1.1 Solar thermal plant potential and challenges

In a solar thermal plant, a fluid flows through solar collectors and it heated up by solar irradiation (Tian and Zhao; 2013). Mirrors can be added to concentrate the solar radiation and increase the temperature that can be reached in the solar collectors whose technology depends on the application (Kalogirou; 2004). In this work, non-concentrating solar thermal plants are considered, which are used for low temperature heat production ($< 110°C$). The heat can be supplied to district heating networks for domestic use or to industries requiring low temperature heat such as the food and beverage industries (Koçak et al.; 2020). The use of the existing solar thermal systems for heat production in 2020 led to savings of 43.8 million tons of oil corresponding to 141.3 million tons of CO_2 emissions, according to the annual report from the International Energy Agency (Weiss and Spörk-Dür; 2021). This shows that using solar thermal energy instead of fossil fuels for heat production is a promising alternative to achieve the necessary energy transition. Steam and electricity can be generated in concentrating solar thermal plants. Even though these technologies are not the focus of the present paper, the methodology presented could be applied to such solar power plants as well. The challenge with solar thermal energy is its intermittency, with daily and seasonal variations, that are difficult to predict accurately. Moreover, the heat demand is also variable in most cases. In order to decouple the solar heat production from the heat consumption, Thermal Energy Storage (TES) is used. That way, with a daily storage, the solar heat produced during the day can be supplied at night or during the next day if the solar irradiation is too low. Seasonal storage can also be added, to store the solar heat produced during summer, to supply it in the winter when the production is lower and the consumption often higher because of the need of space heating. Seasonal TES will not be considered in the present work. In a low temperature solar thermal plant, the most common daily storage technology is the stratified water tank, because of its low cost and simplicity (Tian and Zhao; 2013). This is the TES chosen in this study. The association of the solar field and the TES makes the operation of the solar thermal plant complex. Indeed, there are different operational modes: direct supply of the solar heat, charge or discharge of the storage tank or shut down of heat supply if there is

no solar heat available. Optimization methodologies appear particularly promising for solar thermal plants because of their various degrees of freedom.

IV.1.2 Solar thermal plant optimal operation

Mathematical optimization is used to find the best solution to a problem with degrees of freedom, that can be subject to some constraints, by minimizing an objective function. The design of a solar thermal plant, such as the solar collectors total area and storage tank capacity, can be optimized to minimize the investment cost while satisfying the heat demand when using standard operating strategies. For example, the design of a solar thermal plant supplying heat to a District Heating Network (DHN) has been optimized in ((Hirvonen et al.; 2018), (Tian et al.; 2018) and (Winterscheid et al.; 2017)), while similar work was conducted in ((Jannesari and Babaei; 2018) and (Parvareh et al.; 2015)) with solar heat for industrial processes. Krause *et al.* optimized the design of a solar domestic hot water system and achieved a reduction of 18% of solar heat cost thanks to a lower investment cost and an increase in the solar gain (Krause et al.; 2003). For a correctly designed system, the optimization of the operation can also improve performances of the solar thermal plant. For example, Krause *et al.* also showed a reduction of 0.6% in the cost of solar heat thanks to dynamic optimization of the operation of a well-designed system. Although the improvement seems small, given the large cost of a solar thermal plant, it can still lead to important savings, making solar heat more competitive against fossil fuels (Camacho et al.; 2007a). The optimization of the transient operation of a solar thermal plant is the focus of the present paper.

The operation of a system is decomposed into several hierarchical layers. The bottom layer corresponds to the control. In a solar thermal plant, the operation is usually determined by logic rules which are tracked by basic controllers such as Proportional Integral Derivative (PID) (Camacho et al.; 2007a). Nevertheless, a solar thermal plant is a complex system, showing highly nonlinear behavior, undergoing variable energy source and demand, and composed of elements with various dynamics. Thus, advanced controllers are more suitable to such systems and have been the focus of many works, as summarized in (Camacho et al.; 2007b). The advanced controllers show better uncertainty handling and stability, as shown in (Gálvez-Carrillo et al.; 2009) for example, but are still used to follow the logic control rules to operate the solar thermal plant. An example of such control rules is to maintain a constant temperature at the outlet of the solar field. It has been shown in (Csordas et al.; 1992) that allowing a variable outlet temperature could reduce the dumping of solar energy when the solar irradiation is not high enough to reach the target temperature but still allows the production of valuable solar heat.

Thus, replacing the logic control rules by optimized trajectories can improve the solar thermal plant operation. Trajectories are here defined as transient set points, with a value at each discretization point chosen, to be tracked by controllers. A first possibility is to integrate an economic objective into the controllers, as introduced by (Engell; 2007). Instead of tracking trajectories determined by heuristics, the advanced Model Predictive Controller (MPC) minimizes the operational cost of the solar thermal plant. This has been applied to solar systems in (Pintaldi et al.; 2019) and (Serale

et al.; 2018) for instance, to reduce the need of auxiliary energy to satisfy the demand. Although the performances of the solar systems were improved in these two studies, the methodology presents a major drawback: the computational time of the economic optimization has to be shorter than the control sampling time. Thus, a short time horizon is required, along important simplifying assumptions in the control model. This can deteriorate the solar thermal plant operation, especially the storage management policy which requires a longer term strategic vision (Caspari et al.; 2020). Decoupling the control task and the economic optimization might help to overcome these challenges. The top layer in the hierarchical optimal operation of a system is planning. This layer is an economic Dynamic Optimization (DO) using a longer time horizon to plan the optimal operation of the solar thermal plant. The optimal trajectories could then be sent to the controllers of the plant in terms of transient set-points for further tracking. Offline dynamic optimization has been studied in (Scolan et al.; 2020) and optimal trajectories for all the flow rates in the different parts of a non-concentrating solar thermal plant were determined. Weather forecasts were used to plan the operation. Thanks to this methodology, the operating costs of the plant were reduced by 2.1%, mostly thanks to a decrease in pumping power. In (Delubac et al.; 2021), the energy mix of a solar DHN was optimized and an increased share of renewable energy was obtained. However, the solar thermal plant used was not modeled precisely. Dynamic optimization has been more often studied for Concentrated Solar Power (CSP) plants. In this case, the solar heat produced is at a temperature high enough for electricity generation and TES is used to shift the electricity production depending on the demand and the variable electricity price throughout the day. The optimal operation of a CSP plant was determined a day ahead using weather and electricity price forecasts in ((Lizarraga-Garcia et al.; 2013), (Wagner et al.; 2018) and (Wittmann et al.; 2011)) with increased revenues from electricity selling. Similarly, the backup fossil fuel consumption of a hybrid gas and solar power plant was reduced with DO in some studies ((Brodrick et al.; 2018), (Ellingwood et al.; 2020), (Powell et al.; 2014)). All these works improved the solar thermal plant operation with DO, using forecasts. However, the methodology was not tested on a real system undergoing actual environmental conditions in these studies. Indeed, the forecasts were never compared to the actual conditions, even though weather and load forecasts can be inaccurate. DO does not adapt the optimal operational strategy to the actual environmental conditions. The optimal operation determined offline, can become sub-optimal and the controllers might even fail to track the optimal trajectories if the real-time values differ too much from the forecasts.

An intermediate level in the hierarchical operation of a system is Real-Time Optimization (RTO). This methodology takes into account a planning and adapts the optimal operation to the current disturbances, measured on the plant along the state of the system, and passes the optimal trajectories to the controllers of the plant. Static RTO is the original methodology, based on a static model of the system and regular re-optimization every time a new steady state is reached by the system. This has been tested for a CSP plant in (Rashid et al.; 2019) with no storage. Although the system is transient since the energy source is variable, the lack of storage and the fast dynamics of the solar field made it possible to apply static RTO regularly. Modified RTO methods have been developed to avoid the necessary steady-state wait and detection steps, such as Real-Time Optimization with Persistent Adaptation (ROPA)

(Matias and Le Roux; 2018) or Hybrid RTO (de Azevedo Delou et al.; 2021). However, these strategies are employed to optimized the operation during the transient phases of systems eventually reaching steady-state. For true dynamic systems, Dynamic RTO (DRTO) can be applied (Kadam et al.; 2002). This is more suitable for solar thermal plants with TES since the elements in the plant have various dynamics preventing the system to ever reach steady-state. DRTO has been widely studied in the last decades for various processes such as a batch reactor (Arpornwichanop et al.; 2005), a waste water treatment system (Elixmann et al.; 2010) or a house heating system with storage (De Oliveira et al.; 2013). In all of these applications, the optimization methodology needs to adapt to disturbances (for example the outdoor temperature and the energy price in (De Oliveira et al.; 2013)) while minimizing the operating cost. In the case of a solar thermal plant, the energy source itself is a distubance for the system, so the operation is very complex. DRTO has been applied to the solar field of a CSP plant in (Pataro et al.; 2020). Only the flow rate in the solar field was optimized, and no storage was included in the study. But it showed promising performances, with a good uncertainty handling. In another study, the flow rate between a short term and a long term storages in a solar DHN system was optimized in real-time using weather forecasts (Saloux and Candanedo; 2021). The economic optimization was tested over a year, with a rolling time horizon of 48 hours. The optimal trajectories for the flow rate were discretized in blocks of 4 hours with a single value, which speeds-up the calculations but makes the operation less dynamic. A simple nonlinear model was used for the optimization, which, along with the flow rate defined in blocks, allowed a real-time application with fast computations. The methodology led to a reduction in electricity consumption of the pumps and thus to lower operating costs. These last two studies had only one flow rate in the solar thermal plant as optimization variable. Optimizing the operation of the complete solar thermal plant including the storage tank in real-time involves longer computational time. In order to make it reasonable for a real-time application, the time horizon should be reduced. However, this would deteriorate the storage management policy, which needs a longer term strategic vision. Hence, it might be better to decompose the optimization in two hierarchical levels to improve storage management (Caspari et al.; 2020). This was done in (Clarke et al.; 2018) for an electric system with storage. The first optimization layer is in charge of planning the storage management policy over a longer time horizon and passes the storage state of charge to a lower layer optimizing the operation of the system in real-time. In (Untrau et al.; 2023a), this hierarchical optimization methodology was applied to a solar thermal plant. A planning phase is used for storage management, benefiting from a longer term strategic vision and using weather forecasts, and passes the planned stored energy to a DRTO level optimizing the flow rates in the different parts of the plant. The DRTO objective function is to minimize the operating costs of heat production in real-time while tracking the storage state determined during planning. This methodology has been tested in a simple case study with artificial disturbances and constant heat demand, over only one day, using a shrinking time horizon for the DRTO. The methodology showed improved performances (lower operating costs, increase in solar share) for the solar thermal plant compared to DO, without deteriorating the storage management policy significantly. This is, to the best of our knowledge, the only study where the DRTO of a complete solar thermal plant with storage was investigated.

IV.1.3 Paper contributions and organization

This literature review, which is presented in more details in (Untrau et al.; 2022), shows a lack of studies focusing on the DRTO of a complete solar thermal plant. Most studies in this field were carried out using DO, with no online testing. Two studies only focused on the DRTO of one flow rate in the plant ((Pataro et al.; 2020), (Saloux and Candanedo; 2021)). Another study presented a DRTO methodology with storage management, but in a simple and theoretical case study (Untrau et al.; 2023a). The present paper aims at continuing the work conducted in (Untrau et al.; 2023a) by applying the DRTO methodology with storage management to a more realistic case study. Hereafter are some new features of the research conducted in this paper:

- All independent flow rates in the different parts of the plant are optimization variables, with a value at each time discretization point (no flow rate defined in blocks).
- A variable daily heat demand is considered.
- Real data are used for the weather forecasts and disturbances, allowing a realistic online testing of the methodology.
- The method is tested in simulations over 96 hours.
- A planning phase is used for storage management.
- A rolling time horizon of 12 hours is used for the DRTO.

The main objective of this study is to determine the best way to integrate storage management in the DRTO objective function for different scenarios. Some guidelines regarding this question will be provided. The remaining parts of the paper are organized as follows. Section IV.2 presents the solar thermal plant considered and its numerical model. Section IV.3 presents the input data used in the methodology. Section IV.4 explains the hierarchical optimization methodology developed. Section IV.5 details the case studies used to test the methodology. Section IV.6 presents the results obtained for the various case studies and analyzes the storage management strategies for each case. Finally, Section IV.7 provides some guidelines regarding storage management in a DRTO methodology for a solar thermal plant. It also gives some perspectives for future work.

IV.2 Solar thermal plant description and modeling

IV.2.1 Presentation of the system studied

The solar thermal plant layout considered in this work is presented in Figure IV.1. It corresponds to the initial design of a solar thermal plant provided by our industrial partner NEWHEAT.

There are 3 distinct loops in the plant: the production loop, the secondary one including the storage tank, and the consumer loop. The standard operating strategies

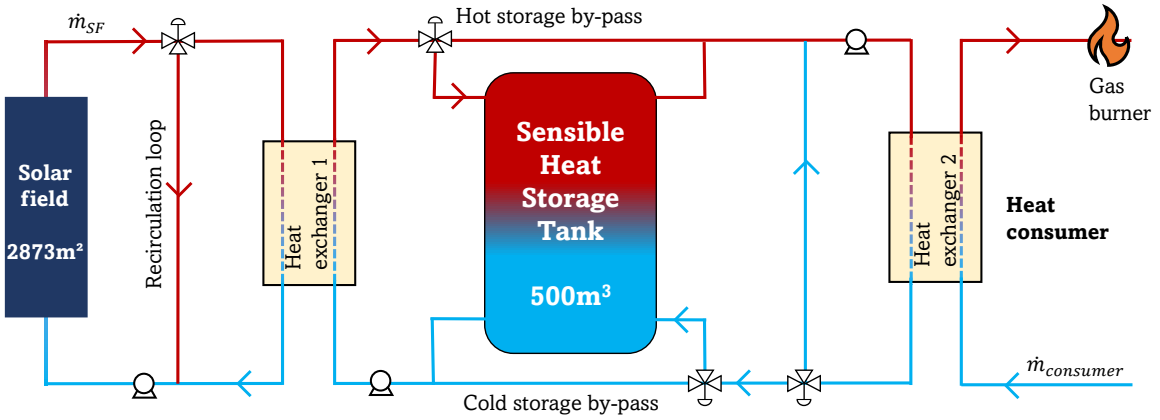

Figure IV.1: Architecture of the solar thermal plant

generally used to operate a solar thermal plant will be presented along the description of the elements of the plant. First, the production circuit is composed of the solar field, made of 15 loops with 12 flat-plate collectors each, representing a total area of 2873m^2. The fluid, composed of 70% of water and 30% of glycol, is heated up by the solar irradiation. Generally, the solar field operation starts when the solar irradiation exceeds a threshold, $200W.m^{-2}$ for instance. The recirculation loop accelerates the warm-up phase of the solar circuit by by-passing heat exchanger 1. Once the temperature at the outlet of the solar field is high enough, the hot fluid is directed to heat exchanger 1 to transfer the heat to the secondary loop, filled with water. When the production loop is in operation, the temperature at the outlet of the solar field is generally maintained constant by adjusting the flow rate in the solar field. The main part of the secondary circuit is the storage tank, which is a stratified water tank of 500m^3 which can be charged, discharged and by-passed. The storage tank is by-passed when the heat production and consumption coincide. Any excess heat can be directed to the storage tank. As soon as the demand is not met directly by the heat coming from the solar field, the storage tank is discharged. The discharge can continue as long as some energy remains inside the storage tank. The temperature of the fluid coming from the production circuit or the storage tank can be adjusted before it enters the second heat exchanger by diluting it with colder fluid exiting heat exchanger 2. That way, the consumer demand will not be exceeded when the solar heat is transferred in heat exchanger 2. Both heat exchangers are plate exchangers, which are a common choice in solar thermal plants working at low temperatures because of their compactness, efficiency and adaptability (International Energy Agency; 2015). They share the same design: 97 plates of 1.5m^2 each. The flow rates in each side of the heat exchangers are generally chosen to respect the equality of calorific fluxes $\dot{m}C_p$. Variable speed pumps are used to move the fluid at a chosen flow rate and three-way valves direct the fluid in the different parts of the plant. As explained above, there are different operational modes in the solar thermal plant depending on the storage utilization (charge, discharge, by-pass) and the temperature adjustment through the recirculation pipe and dilution pipe. Thus, the solar thermal plant operation presents various degrees of freedom which is promising for optimization. Replacing the logic rules detailed previously by an optimal operation might improve the solar thermal plant operation by extending the supply of solar heat for example. Finally, the consumer needs a back-

up heater in case the solar energy can not meet the heat demand. This is generally a gas boiler, placed after the solar thermal plant in the consumer circuit. The gas consumption should be as low as possible to reduce the cost of heat production but also the CO_2 emissions. The gas boiler is modeled very simply in this work. The power needed to raise the consumer stream temperature to the target temperature after it collected the solar heat is computed. The gas consumption associated is then calculated.

IV.2.2 Modeling of the solar thermal plant

The solar thermal plant undergoes variations in both the energy source and the heat demand. Thus, the system is intrinsically dynamic. Moreover, the characteristic times of the elements of the system are different: the solar irradiation varies rapidly while the storage state varies on a slow time scale. Therefore, we chose a transient model to represent the solar thermal plant. Furthermore, nonlinear phenomena take place in the system. For instance, both the energy transferred and the temperature level of that energy are important to characterize the solar thermal plant operation. Hence, temperature and flow rates appear together in power terms. Linearization of the model would be difficult because there are several operating points (Camacho et al.; 2007a). Thus, the model chosen is nonlinear. The model used was originally developed in (Scolan et al.; 2020). An experimental validation of the models was also conducted in the above mentioned paper, using data from a real solar thermal plant in operation. A few changes have been made to the original model, in the solar field and the storage tank, and will be explained below. The optimization methodology developed is for a real-time application so it requires a real system to test it. In this work, the method will be tested on a detailed simulation model set up to represent the real unit. Therefore, both a detailed model and a simplified model for optimization are required. The differences in the two models will be detailed below. The next subsections present the main assumptions and equations used for each element of the solar thermal plant. More details are available in (Scolan et al.; 2020) and (Untrau et al.; 2023a).

Solar field

The solar field is composed of 15 loops with 12 flat plate collectors in each loop. The chosen model is the one-node capacitance model and is based on the following assumptions: there is no spatial discretization of the temperature inside a collector, no heat losses between the collectors within a loop and the distribution of the fluid between the loops is uniform. The original model represented the solar field with a single equivalent loop (Scolan et al.; 2020). But in (Scolan; 2020), it was shown that considering an equivalent solar panel does not deteriorate the accuracy of the model significantly but speeds up the calculations. Therefore, the solar field is here represented by a single solar panel with an area A_{SF} equal to the total area of all the solar collectors. The mean temperature T_{SF}^{mean} in the solar field is computed with the

following equation (ISO/FDIS 9806; 2017):

$$\frac{\dot{Q}_{SF}}{A_{SF}} = \left(\eta_{0,b}(\eta_{sh}K_b(\theta)G_b + K_dG_d) - c_1(T_{SF}^{mean} - T_{amb}) - c_2(T_{SF}^{mean} - T_{amb})^2 - c_5\frac{dT_{SF}^{mean}}{dt}\right) \tag{IV.1}$$

This is an energy balance equation, the power collected by the heating fluid $\dot{Q}_{SF}$ in the collectors stems from the solar irradiation, both direct G_b and diffuse G_d, the heat losses to the environment at the temperature T_{amb} and the equivalent inertia of the collector at the mean temperature. The collectors manufacturer provides values for the following parameters: $\eta_{0,b}$, c_1, c_2, c_5, $K_b(\theta)$ and K_d, which correspond to the collector optical efficiency, resistance to heat losses, thermal capacity and direct and diffuse irradiation angle modifiers. η_{sh} represents the reduction in efficiency due to the shading effect. Inside the collectors, a linear temperature distribution is assumed:

$$T_{SF}^{mean} = \frac{T_{SF}^{in} + T_{SF}^{out}}{2} \tag{IV.2}$$

This simplified dynamic model is able to represent the fast variations in the solar field temperature accurately with a reduced computational time.

Heat exchangers

The two plate heat exchangers of the solar thermal plant are the same, with 97 plates of 1.5m^2 each. A simple model is used to keep the computational time low while still achieving a good accuracy in the calculation of the exchanged power $\dot{Q}_{HX}$ and outlet temperatures T_{hot}^{out} and T_{cold}^{out}, respectively for the hot side and the cold side. No spatial discretization is considered, so the evolution of the temperatures between the plates is unknown. The other main assumptions are:

- no heat losses to the environment,
- no accumulation,
- a uniform distribution of the fluid flow between the channels,
- the same exchange area for every pass,
- a perfect mixing at the end of a pass.

The effectiveness-NTU model is chosen, as described in (Wang et al.; 2007) for example. The three main equations of the model are hence the following:

$$\dot{Q}_{HX} = (\dot{m}C_p)_{cold}(T_{cold}^{out} - T_{cold}^{in}) \tag{IV.3}$$

$$\dot{Q}_{HX} = (\dot{m}C_p)_{hot}(T_{hot}^{in} - T_{hot}^{out}) \tag{IV.4}$$

$$\dot{Q}_{HX} = \epsilon_{HX}(\dot{m}C_p)_{min}(T_{hot}^{in} - T_{cold}^{in}) \tag{IV.5}$$

Here, $(\dot{m}C_p)_{min}$ represents the minimum heat capacity between the two sides of the heat exchanger: $(\dot{m}C_p)_{min} = min((\dot{m}C_p)_{hot}, (\dot{m}C_p)_{cold})$. Similarly, $(\dot{m}C_p)_{max}$ can be defined for the maximum heat capacity. The effectiveness ϵ_{HX} can be computed with the following equations:

$$R = \frac{(\dot{m}C_p)_{min}}{(\dot{m}C_p)_{max}} \tag{IV.6}$$

R is the heat capacity ratio.

$$NTU = \frac{U_{HX}A_{HX}}{(\dot{m}C_p)_{min}} \tag{IV.7}$$

NTU is the number of transfer units, computed here with the total exchanged surface A_{HX} of the heat exchanger and a global heat transfer coefficient considered constant in this work $U_{HX} = 4000W.m^{-2}.K^{-1}$. This simplifying assumption does not deteriorate the accuracy of the model significantly but it reduces the nonlinearities, which helps to speed up the calculations (Scolan; 2020). The effectiveness for a counter-current flow heat exchanger is then defined as follows:

$$\begin{cases} \epsilon_{HX} = \frac{1-exp(-NTU(1-R))}{1-Rexp(-NTU(1-R))} \text{ if } R < 1 \\ \text{or} \\ \epsilon_{HX} = \frac{NTU}{1+NTU} \text{ if } R > 1 \end{cases}$$

Storage tank

The storage tank considered is a 12 meters high vertical cylinder with a volume of $500m^3$. It is a stratified water tank. In this system, the hot fluid coming from heat exchanger 1 after collecting the solar heat is charged at the top of the tank. When the storage tank is discharged, the return cold fluid enters at the bottom of the tank. That way, there is limited mixing between the hot zone at the top of the tank and the cold zone at the bottom of the tank (Koçak et al.; 2020). This single tank solution is cheaper than having a hot tank and a cold tank (He et al.; 2019). Between the hot and cold zones, there is a high temperature gradient region, also known as thermocline. The thermocline should be as thin as possible to maximize the solar thermal plant efficiency but destratification can occur due to the injection of fluid inside the tank, conduction in the fluid or heat losses for example (Kleinbach et al.; 1993). It is particularly challenging to model a stratified storage tank because it needs a very accurate model to represent the thermocline region. However, such a detailed model can lead to long computational time. Although 2D and 3D models are developed to better understand the fluid dynamics inside the tank (Hosseinnia et al.; 2021), a 1D model was chosen in this work to reduce the calculation time. Only the variations of the temperature along the vertical axis of the storage tank are considered. There are several approaches to model a storage tank in 1D, listed in (Untrau et al.; 2023b) for example, but the solving of the energy balance is more accurate because it is based on physical phenomena. The conservation of energy in 1D, along an ascending vertical axis z and over a control volume of thickness dz can be written as follows, assuming constant thermophysical

properties for the stored fluid and no heat source inside the storage tank:

$$\rho C_p A_s \frac{\partial T_s(z,t)}{\partial t} + \dot{m} C_p \frac{\partial T_s(z,t)}{\partial z} = A_s k \frac{\partial^2 T_s(z,t)}{\partial z^2} + U_s P (T_{amb}(t) - T_s(z,t)) \quad \text{(IV.8)}$$

This Partial Differential Equation (PDE) represents the variations of the fluid temperature $T_s(z,t)$ inside the tank with both space z and time t. The first term represents the inertia of the stored fluid, the second term corresponds to the enthalpy fluxes due to charging or discharging with the resulting flow rate $\dot{m}$, the third term is the diffusion inside the storage tank and the last term are the heat losses to the environment. The fluid properties are ρ its density, C_p its specific heat capacity and k its thermal conductivity. A_s is the tank cross-sectional area, which has a perimeter P, and U_s is the overall heat transfer coefficient with the ambient.

In order to solve this PDE, it is first converted into an ODE system, using the method of lines with spatial discretization. The most common discretization scheme used to model the storage tank in 1D from PDE IV.8 is the finite volumes method, also called the multinode model in this case. The tank vertical axis is divided into N layers of the same height Δz. The temperature inside each layer is assumed uniform. This model is easy to implement and requires low computational time for a small number of layers. However, the number of layers chosen has a great impact on the accuracy of the temperature profile in the tank. Indeed, the uniformity of the temperature inside each layer leads to a smoothed temperature profile with a thermocline thicker than it should be. This effect is called numerical diffusion (Powell and Edgar; 2013). It is mitigated when adding more layers but this leads to longer computational time. For the optimization model, which needs very low computational time in order to be used in real-time, the multinode model with 10 layers was chosen. It provides a reasonable estimate of the temperature profile and the energy stored (Scolan et al.; 2020).

For the simulation model, a more accurate representation of the storage tank is required as the model acts as a virtual replacement of the actual plant to test the methodology. The multinode model could be used but a very large number of layers, at least 1000, is needed in order to eliminate the numerical diffusion completely (Untrau et al.; 2023b). Such a methodology would lead to very important computational time, and hence, another spatial discretization scheme was used to convert the PDE into ODE: Orthogonal Collocation on Finite Elements (OCFE). The numerical method is presented in (Untrau et al.; 2023b) in the specific case of a stratified storage tank. OCFE combines the advantages of both orthogonal collocation, where a limited number of discretization points is needed to converge to the actual differential equation solution, and finite elements, where the resolution of the system is fast due to the sparsity of the matrix generated (Carey and Finlayson; 1975). For our model, we chose 15 elements with 25 points each, so 375 discretization points in total.

Natural convection is not represented in Equation IV.8 although it might occur in the storage tank. For example, colder fluid can be charged at the top of warmer fluid when the solar irradiation decreases but is still high enough for heat production. In this situation, the colder fluid will sink inside the storage tank and exchange energy with its surroundings until thermal equilibrium is reached (Pate; 1977). Natural convection can also happen because the top of the tank is more exposed to heat losses and can

therefore cool down faster than the layer of fluid underneath (De Césaro Oliveski et al.; 2003). Natural convection is particularly challenging to be taken into account in 1D models as it involves 3D fluid movements. This phenomenon was neglected in the optimization model to keep it as simple and computationally efficient as possible. Indeed, most approaches to model natural convection in 1D requires conditional structures and are not easily applicable in an optimization framework (Untrau et al.; 2023b). This simplifying assumption leads to temperature inversions inside the storage tank, which would not remain more than a few minutes in the real system. For the simulation model, temperature inversions are corrected regularly by stopping the time integration and computing a new temperature profile which will be used as the initial condition of the next integration period. This new temperature profile is determined by averaging between two temperature profiles, one with reorganized temperatures following the approach from (Franke; 1997) and one with homogenized temperatures following the approach from (Kleinbach et al.; 1993). Indeed, the first approach tends to overestimate the stored energy inside the tank while the second one tends to underestimate it (Pate; 1977). Averaging between both profiles might provide a better estimate of the actual temperature profile in the tank after natural convection took place.

Two 1D models for the storage tank were presented in this subsection. Firstly, a model involving finite volume discretization over 10 computational cells, which neglects natural convection, and which is used for optimization purposes. The second model is based on spatial discretization using OCFE, with 15 elements composed of 25 collocation points, and is used as a representation of the real system in the "simulation model". Temperature inversions are corrected regularly. These differences in modeling are representative of a real application since the optimization model cannot perfectly represent the real system. Thus, it is appropriate to test the DRTO methodology using a simplified model for optimization and a detailed model for simulating the real system behavior. However, these differences in modeling should be kept in mind for the analysis of the case study results.

Pipes

Each pipe of the system represented in Figure IV.1 is modeled in 1D with an energy balance equation. There is no spatial discretization so only the inlet and outlet temperatures, respectively T^{in} and T^{out}, are obtained. Accumulation in the fluid and heat losses are considered, whether the fluid is static or not. The following equation is used:

$$\rho C_p \pi A_{pipe} L \frac{dT^{out}}{dt} = \frac{T_{amb} - T^{out}}{R_{th}} + \dot{m} C_p (T^{in} - T^{out}) \tag{IV.9}$$

Here, A_{pipe} represents the cross-sectional area of the pipe and L its length. The heat transfer between the fluid and the ambient (heat losses), represented by the thermal resistance R_{th}, takes into account the conduction in the insulation layer and the external convection, with a coefficient computed with the Hilpert correlation (Incropera et al.; 2007). However, internal convection and conduction through the wall are supposed to be ideal and are not modeled. Hence, the temperature of the wall is equal to the temperature of the fluid. Mass and energy balances are developed at each mixing valve and flow division, neglecting the accumulation and heat losses.

Pumps

The electricity consumption of the pumps in the solar thermal plant participates to the operating cost of the plant. The pumps are variable speed ones circulating the fluid in the different parts of the plant. Equation IV.10 computes the maximum pumping power when the flow rate is at its maximum allowed value $\dot{m}_{max}$, leading to the largest pressure drop in the circuit ΔP_{max}. The electric power $\dot{P}_{elec}$ is then computed with the actual flow rate $\dot{m}$ and the overall efficiency of the pump η_{pump} in Equation IV.11.

$$\dot{P}_{hydrau} = \frac{\dot{m}_{max}}{\rho} \Delta P_{max}(\dot{m}_{max}) \tag{IV.10}$$

$$\dot{P}_{elec} = \frac{\dot{P}_{hydrau}}{\eta_{pump}} \left(\frac{\dot{m}}{\dot{m}_{max}} \right)^3 \tag{IV.11}$$

The pumps are not described more precisely in the circuit, only their electric consumption is computed. The electric power should be minimized to reduce the operating costs but also the CO_2 emissions associated with heat production.

Representation of the various operating modes

The model for the complete solar thermal plant is obtained by connecting the models for the different elements of the plant: solar field, heat exchangers, storage tank, pumps and pipes. As explained in subsection IV.2.1, the solar thermal plant can be operated with several modes depending on the weather conditions, the storage level and the heat demand. Modeling the different operating modes and the switching from one mode to another is particularly challenging. Indeed, there is a need to describe whether an element is being used or not. An example of such behavior is the temperature in the solar field. The assumption of a linear variation of the temperature inside the solar field only stands when the solar field is in operation and a fluid is flowing through it. Otherwise, another equation should be used. For example, the outlet temperature can be fixed equal to the inlet temperature when the solar field is not in operation. Two conditional equations can be written as follows:

$$\begin{cases} T_{SF}^{out} = T_{SF}^{in} \text{ if } \dot{m}_{SF} = 0 \\ \text{and} \\ T_{SF}^{out} = 2T_{SF}^{mean} - T_{SF}^{in} \text{ if } \dot{m}_{SF} \neq 0 \end{cases}$$

In an optimization framework, Big M formulation can be used to represent such conditional structures. It requires the introduction of a new binary variable y_{SF} representing the existence of a flow rate in the solar field or not, i.e. that is 0 when $\dot{m}_{SF}$ is 0 and 1 otherwise. M is a scalar, much larger than the variable considered. The conditional equations are replaced by inequalities:

$$\begin{cases} -y_{SF}M + T_{SF}^{in} \leq T_{SF}^{out} \leq y_{SF}M + T_{SF}^{in} \\ \text{and} \\ -(1-y_{SF})M + 2T_{SF}^{mean} - T_{SF}^{in} \leq T_{SF}^{out} \leq (1-y_{SF})M + 2T_{SF}^{mean} - T_{SF}^{in} \end{cases}$$

These two inequalities will hold for every $\dot{m}_{SF}$ but the most limiting constraint will impose a value to T_{SF}^{out}. This is a well-known formulation for mixed integer optimization but it can not be used directly in a NonLinear Programming (NLP) problem because it requires a binary variable. Thus, the binary variable was here replaced by a continuous function approximating a binary behavior: a sigmoid function. The expression of a sigmoid function is the following, with β characterizing the steepness of the function and δ the threshold for the variable $\dot{m}_{SF}$:

$$sig(\dot{m}_{SF}) = \frac{1}{1 + exp^{-\beta(\dot{m}_{SF} - \delta)}} \tag{IV.12}$$

If the flow rate in the solar field is below the threshold δ, the sigmoid function is zero and otherwise it is 1. To represent the existence of a flow rate, a small value of δ is chosen. In the real system, a very small flow rate is not implementable by the pumps and valves. Thus, a value of $1kg.s^{-1}$ was chosen to avoid that a very small flow rate impacts the solar thermal plant operation in a non realistic way. The sigmoid is then used in the Big M inequalities in replacement of y_{SF}.

Such a continuous formulation is useful to represent the various operating modes of the solar thermal plant such as the shut down of the solar circuit leading to no exchanged power in heat exchanger 1, or the interruption of supply of solar heat to the consumer through the heat exchanger 2 because there is no solar energy available directly from the solar field or from the storage tank.

IV.3 Input data

The design of the system presented in Section IV.2 is an input of our optimization algorithm along with the heat demand and the weather forecast. The optimization algorithm uses these data to find the optimal operation of the solar thermal plant. The methodology is applied to a detailed simulation model representing the real plant, which undergoes the real weather and heat demand. Our methodology will be tested in a realistic case study and the environmental conditions are real values for the city of Trappes (78), France (coordinates: 48° 46' 39.0000" N, 2° 0' 9.0000" E).

IV.3.1 Weather data

The four parameters used in our model are the following: the Global Horizontal Irradiance (GHI), the Direct Normal Irradiance (DNI), which are both used to compute the solar energy collected in the solar field, the ambient temperature and the wind speed, which are used to calculate the heat losses in the different parts of the solar thermal plant, with the global heat transfer coefficient depending on the wind speed. As explained in Section IV.1, weather forecasts are useful to plan the optimal solar thermal plant operation ahead of time. The actual measurements of the environmental conditions might differ from the forecasted values and that will impact the actual plant operation. Both forecasted and measured values for the four parameters of interest at the chosen location were provided by Météo-France for the whole year of 2021. The weather forecasts are obtained thanks to Météo-France's ARPEGE model with a new

run every 6 hours, providing updated forecasts. The time horizon of the forecasts depends on the run of the day: the runs at 12 am and 12 pm have a time horizon of 103h while it is 73h for the run at 6am and 61h for the run at 6pm. The time step for the values provided is 1 hour. These forecasted values will be used in the optimization algorithm to compute the optimal operation of the solar thermal plant. The same 4 parameters of interest are measured with a meteorological station in Trappes with hourly values. These measurements will be used to represent the actual solar thermal plant operation and will allow the testing of our methodology.

IV.3.2 Heat demand

The heat consumer considered is a DHN. Various industrial, commercial and residential buildings can be part of a DHN (Huang et al.; 2019). Inside the buildings, heat is mostly used for space heating in winter and domestic hot water. Hence, the consumer demand varies seasonally but also daily. Since it is not easy to acquire public data on a DHN heat consumption, the heat demand will be artificially constructed. To simplify this study, an averaged daily heat demand profile was used for every day of the year considered, based on the profile in (Petkov and Gabrielli; 2020) for a residential DHN. In order to build a heat demand profile consistent with the design of the solar thermal plant, the demand from (Petkov and Gabrielli; 2020) was adjusted to ensure the supply of heat during two days relying only on a full storage tank at 80°C. The variable daily profile obtained is plotted in Figure IV.2, with a peak in the demand around 8am and a lower demand around 4pm.

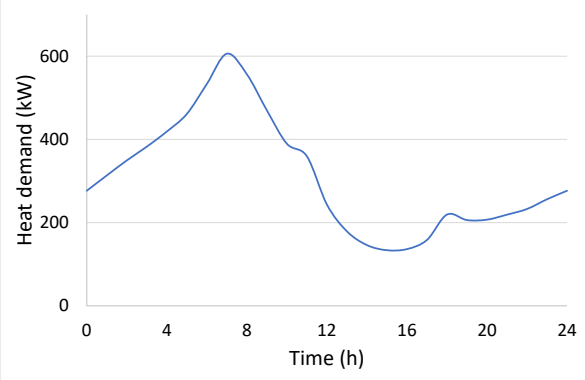

Figure IV.2: Heat demand profile for a day

The return temperature of the DHN is assumed constant and equal to 55°C, so the fluid coming from the consumer side always enters the heat exchanger 2 at , $T^{in}_{consumer} = 55°C$ (see Figure IV.1). The target temperature of the heat demand, T_{demand}, for the consumer flow after collecting the solar energy is fixed, equal to 65°C. This means that the solar heat provided should raise the temperature of the consumer stream as close as possible to 65°C. The gas burner will provide additional heat to reach the target temperature if necessary. However, it is not allowed by the consumer to exceed this temperature. The variable heat demand is represented by a variable flow rate $\dot{m}_{consumer}$ on the consumer side of heat exchanger 2, according to the following equation:

$$\dot{Q}_{demand} = \dot{m}_{consumer} * Cp * (T_{demand} - T^{in}_{consumer}) \tag{IV.13}$$

While $\dot{m}_{consumer}$ and $T^{in}_{consumer}$ are both inputs of our model, the temperature at the outlet of heat exchanger 2 on the consumer side is an output which will be impacted by the operational strategy of the solar thermal plant. This temperature should be as close as possible to the target of 65°C without ever exceeding it. This is a simplified representation of a DHN heat demand, where only the flow rate is variable and the return and target temperatures are fixed. In a real system, both temperatures also vary.

The heat demand is considered variable but perfectly known in advance in this work, which means that it will not be affected by any disturbance during the real-time operation of the solar thermal plant. However, similarly to the uncertain weather forecast presented in subsection IV.3.1, an uncertain heat demand could also be taken into account with our methodology.

IV.4 Optimization methodology

IV.4.1 Two-level algorithm

The objective of our methodology is to determine the optimal flow rate trajectories in the different parts of the plant ensuring the lowest operating costs and satisfying the heat demand. As explained in Section IV.1, storage management in a solar thermal plant might be improved by decomposing the optimization into two hierarchical levels. In our methodology, the first optimization layer, called planning, is in charge of determining the best storage management policy and the second optimization layer, called DRTO, is in charge of the optimal operation of the solar thermal plant. The optimization model presented in Section IV.2 and using finite volume discretization of the storage tank is used for both planning and DRTO. Our real-time methodology is tested on a simulation model, which represents the actual solar thermal plant behavior, assuming perfect tracking of the optimal trajectories. Here the optimization task is separated from the tracking task (which is assumed to be perfect in a first approach), following the method developed by (Kadam et al.; 2002). The two-layer optimization methodology is presented in Figure IV.3. At the initial time, the storage tank is half charged and all other components of the system are at ambient temperature. At first, the planning phase is run, more details on this step are provided in subsection IV.4.2. This step uses weather forecasts to plan the economically optimal operation of the solar thermal plant over several days. Since the available forecasts time horizon is up to 103 hours, this is the time horizon chosen for the planning phase, starting at 12am. This dynamic economic optimization hence benefits from a longer term strategic vision. For the next 6 hours, the simulation model will follow the optimal trajectories for the flow rates determined during the planning phase. After 6 hours, an updated weather forecast is available, allowing the start of the real-time adaptation of the optimal operation. After this time, the planning phase will only be used for storage management, if needed. A new DRTO is run every six hours using a new updated forecast, details on the DRTO step are provided in subsection IV.4.3. The DRTO time horizon chosen is 12 hours, which will be discussed in subsection IV.6.4. The economic objective function of the DRTO can also takes into account an objective on storage management. Several possibilities will be explored in this work. For example, the minimization of

the difference between the planned and actual storage states at the end of the DRTO time horizon will be tested. Between each DRTO run, the behavior of the solar thermal plant will be simulated using the real weather. At the beginning of the DRTO run, the actual state of the system, obtained in the simulation model, will be passed to the optimizer, providing feedback to the DRTO level. The simulation part of the methodology is presented in subsection IV.4.4. In a real implementation, this methodology would be repeated continuously, with a new planning phase computed regularly, in order to optimize the operation of the solar thermal plant throughout the year. In this work, the planning phase is only computed once and the simulation testing the methodology ends after 96 hours because there is no planned storage state available for the next DRTO.

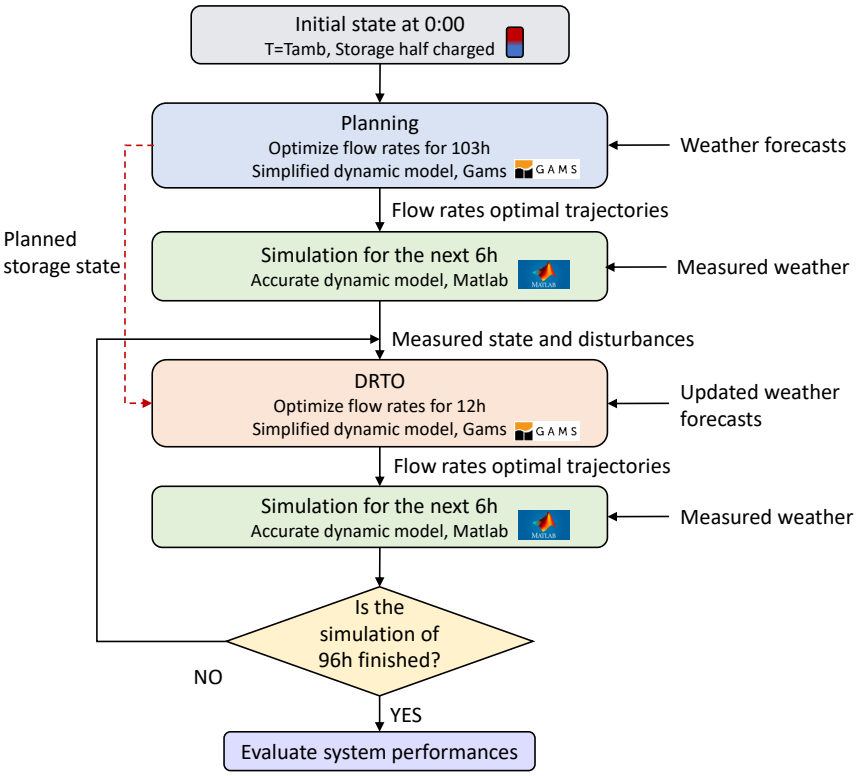

Figure IV.3: Algorithm for the two-level optimization strategy

IV.4.2 Planning

The planning phase is an offline dynamic optimization with an economic objective function. It determines the best operational strategy for the solar thermal plant over 103 hours using weather forecasts. The method for the planning phase was developed in (Scolan et al.; 2020). It benefits from a longer term strategic vision allowing a better use of the storage tank. The degrees of freedom in this optimization are the 6 independent flow rates in the different parts of the solar thermal plant. The dynamic model presented in subsection IV.2.2 is discretized over the whole time horizon, to transform the Differential Algebraic Equations (DAE) into a system of pure algebraic equations that will be solved as a NonLinear Programming (NLP) problem. The time discretization is done with orthogonal collocation on finite elements, following the method in

(Hedengren et al.; 2014), with elements of 1 hour, each containing 9 collocation points. This time discretization was found appropriate in (Scolan et al.; 2020). Using this time discretization, the planning phase takes between 2 and 4 hours to converge to an optimal solution on a laptop with the following characteristics: Intel Core i7-1065G7 1.3GHz. The objective function (OF) to be minimized is the operating costs of the heat production, which entail the electricity consumption of the pumps in the solar thermal plant and the gas consumption of the back up burner. An economic value is given to the stored energy at the end of the time horizon since this energy could be used after the end of the optimization time span, and thus cut down the gas consumption in the future. In order to obtain smooth optimal trajectories for the flow rates, reducing pumping effort and aging of the equipment, an additional term Φ_{var} (explained in (Untrau et al.; 2023a)) is added to the OF with a weight γ_{var}. This weight is adjusted to obtain a good compromise between good economic performances of the plant and smooth trajectories.The formulation of the dynamic optimization problem is presented hereafter:

$$\min_{free\ \dot{m}} OF_{eco} - \gamma_{var}\Phi_{var}, \text{with} \tag{IV.14}$$

$$OF_{eco} = -GasPrice \int_0^{t_f} \dot{Q}_{gas}(t)\mathrm{d}t - ElecPrice \int_0^{t_f} \dot{P}_{elec}(t)\mathrm{d}t + 0.7 HeatPrice\ E_{stored}(t = t_f) \tag{IV.15}$$

The prices used in the cost objective function are the following: $GasPrice$ = 80€/MWh, $ElecPrice$ = 130€/MWh and $HeatPrice$ = 25€/MWh. These prices are specific to a location and time and are here considered constant but could vary throughout the day. Since the stored energy will decrease in quality over time before it is supplied to the consumer, due to heat losses and imperfect heat transfer, a weight of 0.7, which was found to be appropriate by (Scolan et al.; 2020), affects its associated economic benefits.

There are operational constraints in the dynamic optimization problem ensuring a safe operation:

- $T \leq 95°C$ for all temperatures, to avoid overheating and boiling of the fluid, which would damage the equipment
- The pumps have discontinuous operating modes. The flow rate in each pump is defined as follows by the manufacturer guidelines to prevent aging:

$$\begin{cases} \dot{m} = 0 \text{ (corresponding to the pump turned off)} \\ \text{or} \\ 0.3\dot{m}_{max} \leq \dot{m} \leq \dot{m}_{max} \text{ (corresponding to the pump turned on,} \\ \text{with } \dot{m}_{max} \text{ determined by the pump specifications)} \end{cases}$$

- $T^{out}_{consumer} \leq T_{demand}$ forbidding exceeding the target temperature ($T^{out}_{consumer}$ is the temperature of the consumer stream after collecting the solar heat)

The solver CONOPT is used in software GAMS to solve the dynamic optimization problem. The trajectories for the flow rates are initialized with standard operating strategies, ensuring that the local optimum found by CONOPT can be implemented on the actual solar thermal plant. However, the standard operating strategies might not always lead to the respect of all the constraints detailed above. In order to ensure the respect of the constraints and the convergence of the optimization algorithm, the constraints are added progressively. Here are the four steps leading to an optimal solution:

1. Simulate with standard operating strategies, with an upper bound of 120°C for all temperatures and no constraint on the heat demand. Here, there are no degrees of freedom since the flow rates are fixed by the standard operating strategies, and no objective function.

2. Minimize the overheating at the outlet of the solar field, which is the warmest zone of the solar thermal plant at the temperature T_{SF}^{out}. This first optimization is formulated as follows: $T_{SF}^{out} \leq 95 + \lambda_{overheating}$ and the objective function is to minimize the scalar $\lambda_{overheating}$.

3. Minimize the heat demand excess. Here, all temperatures are limited to 95°C and the optimization problem is the following: $T_{consumer}^{out} \leq 65 + \lambda_{demand}$ and the objective function is to minimize the scalar λ_{demand}.

4. Minimize the operating costs of the plant, respecting all the operational constraints.

In the DRTO methodology developed in this work, the planning phase can provide the storage management policy, in terms of stored energy throughout time, to the next optimization level.

IV.4.3 DRTO

The DRTO level corresponds to the real-time adaptation of the optimization methodology. If the weather and load forecasts contain uncertainty, the trajectories derter-mined during the planning phase become sub-optimal. In case of large disturbances, they might even be imposible to track by the controllers. Therefore, it is important to update those trajectories in real-time, relying on updated weather forecasts. Each new DRTO run, performed every 6 hours, retrieves its initial state from the simulation model (as explained in the next subsection). Thus, the new optimal operational strategy is adapted to the current situation. In this work, the triggering of a new DRTO is based on the availability of a new weather forecast. However, conditional triggering could be explored in future work to run a new DRTO every time that it seems necessary. For example, a new DRTO could be run when the trajectories deviate from the reference trajectories (Alonso et al.; 2013). Nevertheless, this approach would require available weather forecasts at any time. The DRTO is an economic dynamic optimization and its formulation is very similar to the planning phase. The dynamic model used is hence the same. There are a few differences between the two optimization layers, which are detailed hereafter. First, the time horizon is shorter than the planning

phase, with the same time discretization. 12 hours are chosen and this choice is further discussed in subsection IV.6.4. The time horizon should be longer than the control horizon to benefit from a better strategic vision. It also has to be short enough to allow real-time implementation and ensure that the forecasts used are accurate ((Wagner et al.; 2018), (Wittmann et al.; 2011)). With 12 hours, the DRTO takes a maximum of 7 minutes to converge (same laptop as the one used for the planning phase), which is appropriate for a real-time implementation. The operational constraints are the same as planning and the degrees of freedom are also the values of the six independent flow rates at each time instant. The convergence of the model is reached by using the same 4 steps as the ones used in the planning phase. The objective function is to minimize the same operating costs, however the term on the storage utilization might be different. In the planning phase, the stored energy at the end of the time horizon is maximized, as it represents useful energy for later use. For the DRTO level, several possibilities are explored and will be discussed in Section IV.6.

- The first possibility is to exclude storage contribution from the DRTO objective function.
- The second possibility is to use the same approach as in the planning phase, namely maximize the stored energy at the end of the DRTO time horizon.
- The third possibility relies on the planning phase. The aim of the DRTO level is to adapt the operational strategy to the current disturbances while trying to follow the plan established previously, based on weather forecasts and a long term strategic vision. To achieve that, the OF incorporates a term minimizing the difference between the planned and the actual stored energies at the end of the DRTO time horizon. An economic value is given to the non-respect of the plan, by multiplying the difference by the price of gas and a weight $\omega = 0.5$ adjusted in (Untrau et al.; 2023a). This represents the fact that the energy that should have been stored but which indeed has not been, will be replaced by gas later. The weight chosen achieves a good compromise between the tracking of the planned storage state and the lowest operating costs. This term is written as follows:

$$\omega.GasPrice.|E_{stored\ planning}(t = t_{f\ DRTO}) - E_{stored\ DRTO}(t = t_{f\ DRTO})| \quad \text{(IV.16)}$$

These three possibilities for the DRTO objective function will be compared in the results in Section IV.6.

IV.4.4 Simulation

Since the methodology developed is a real-time methodology, it has to be tested online on an actual plant. In this work, we use a simulation model solved in MATLAB to represent the actual behavior of the system undergoing the real weather conditions. The dynamic model for simulation takes the optimal trajectories of the flow rates as an input. It forms a DAE system with no degrees of freedom, that is solved with solver ode15s, to compute the temperatures in all parts of the solar thermal plant. As mentioned earlier, perfect control is assumed, so no controllers are taken into account

in the simulation model and the flow rate trajectories are perflectly tracked. The simulation model provides feedback to the DRTO algoritm. Before each new DRTO run, the current system state is retrieved from the simulation and fed to the optimization. No state estimation and data reconciliation steps are included in the methodology. We assume that all states are perfectly measured in first approach. As explained in subsection IV.2.2, the simulation model uses a more precise representation of the storage tank. By starting regularly with the actual system state, the DRTO algorithm reduces model error propagation due to simplifying assumptions in the optimization model, compared to offline dynamic optimization.

The methodology described above has been tested in some case studies, presented hereafter.

IV.5 Case studies

Two distinct time periods will be used in these case studies to show different behaviors of our optimization methodology. In order to choose the time periods, the MAPE (Mean Absolute Percentage Error) between the forecasted and measured GHI are compared for each day of the year 2021 at 12am and for the next 103h, corresponding to the forecast time horizon. Only the GHI values were compared in order to choose the test cases but the DNI values usually follow the same trends. Moreover, the differences between the forecasted and measured values for the ambient temperature and wind speed are smaller and do not impact the solar thermal plant operation as significantly as the solar irradiation. Several optimization strategies using different objective functions will be applied to the test cases chosen.

IV.5.1 July

The first test period starts on July 19^{th} and corresponds to the smallest MAPE of the year (1.2%), meaning that the forecasted GHI is very close to the measured GHI. This is shown in Figure IV.4 where the forecasted and measured GHI for the next 103 hours, starting at 12am (t=0h), are plotted. The general shape of the GHI is well predicted with only small discrepancies. The measured GHI tends to have a slightly lower maximum value than the forecasted GHI. Overall, this forecasted GHI, which will be used in the planning phase, is accurate. The forecasts are updated every 6 hours. In this test case, the updated GHI, which will be used for each new DRTO, are very similar to the one determined at 12am on July 19^{th}. Based on this observation, we expect our optimization methodology to only lead to slight real-time adaptation.

IV.5.2 May

The second test period corresponds to a large MAPE (11.2%) for May 12^{th}. Larger values were observed in the winter but they correspond to very low solar irradiation levels which are less interesting because the solar thermal plant would barely be operated. The forecasted GHI at 12am (t=0h) and the corresponding measured values are

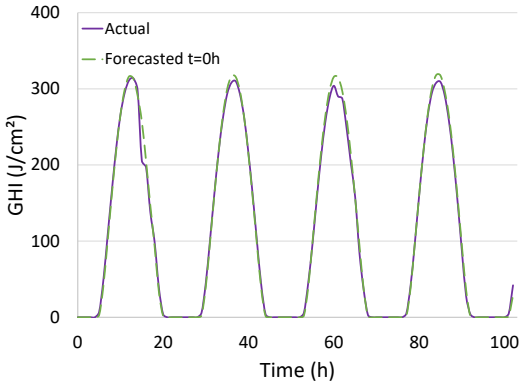

Figure IV.4: Actual and forecasted global horizontal irradiance for the test period in July

plotted in Figure IV.5 in dashed green and solid purple lines respectively. We observe that the solar irradiation on the second day is greatly underestimated by the forecast at 12am, which will be used for the planning phase. This underestimation is corrected in the updated forecasts, provided every 6 hours and used at the DRTO level. For instance, the forecasted GHI on May 13^{th} at 12am (t=24h) is plotted in Figure IV.5 as well, in dashed orange line. This new forecast does not underestimate the actual GHI as much as the one predicted one day earlier. However, discrepancies between the forecasted and measured GHI remain because the solar irradiation is quite variable each day during this time period and those fast variations are not well predicted.

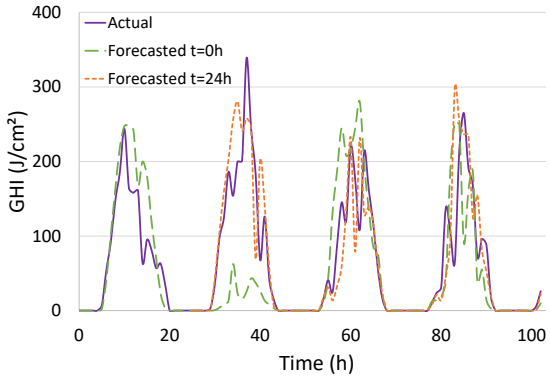

Figure IV.5: Actual and forecasted global horizontal irradiance for the test period in May

IV.5.3 Comparison of several optimization strategies

As explained in subsection IV.4.3, different possibilities to incorporate storage management in the DRTO objective function are explored in this work. The three options are summarized below:

- E (purely Economic): there is no term in the objective function on storage management, the OF is purely economic

- S (maximum Storage): the objective is to maximize the stored energy at the end of the time horizon of each DRTO
- P (following the Planning): the objective on storage is to minimize the difference between the planned stored energy and the actual stored energy at the end of each DRTO

These are only three options but more possibilities could be explored in future work. For example, the objective on storage is here always formulated at the end of the time horizon of the DRTO but an objective formulated as a trajectory over the entire time horizon could be tested. Or the objective could be formulated at a fixed time of the day, the sunset for instance, as used in (Untrau et al.; 2023a) but tested only for one day and a shrinking time horizon.

The three possibilities mentioned above will be tested in simulations in the two case studies (July an May) presented earlier and compared. The comparison will also be made to a simulation following the trajectories determined during planning, which is an offline dynamic optimization. This is summarized in Figure IV.6.

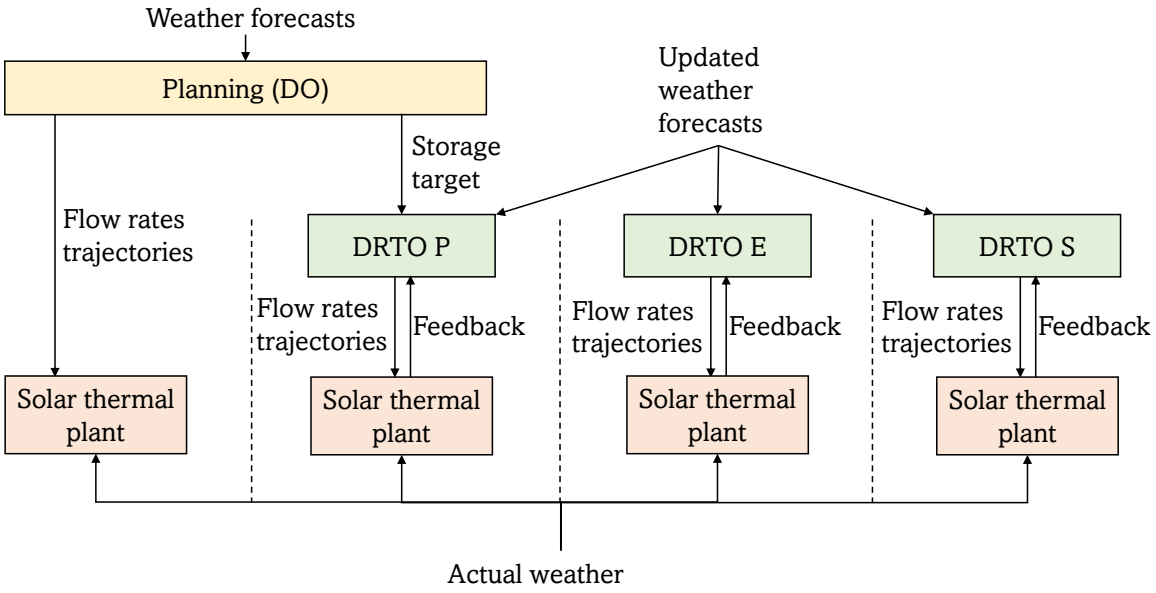

Figure IV.6: Comparison of several optimization strategies

IV.6 Results and discussion

The 4 optimization strategies will be compared using the two different time periods chosen. The results analyzed are simulations results since they represent the real behavior of the system following an optimization strategy. The optimal trajectories (6 transient mass flow rates) obtained with the different strategies will be compared directly as well as the resulting temperatures in the different parts of the plant computed by the "simulation model". Performance criteria will also be computed over the whole simulation horizon. The criteria are the following:

- $E_{supplied}$: quantity of solar heat supplied to the consumer, either directly from the solar field or from the storage tank, at a temperature lower than the target temperature. Any excess heat is not included. $E_{supplied}$ should be as high as possible to reduce gas consumption in the back-up burner in the consumer circuit.
- E_{elec}: electric consumption of the pumps.
- C_{tot}: total operating costs of the plant (electricity and gas consumption)
- $E_{stock\ final}$: quantity of valuable energy (above the consumer return temperature of 55°C) inside the storage tank at the end of the simulation.

The heat demand presented in subsection IV.3.2 corresponds to a total of 29.82MWh for the whole 96 hours.

IV.6.1 Small disturbances: July test period

At first, the test period in July was chosen. Since the weather is correctly predicted for the whole time horizon and there is high solar irradiation available, this represents an ideal case. Indeed, we expect all strategies to satisfy the heat demand. This will allow us to verify that DRTO does not deteriorate the solar thermal plant performances compared to DO due to the frequent updates in the optimal trajectories and the lack of strategic vision.

The performances of the four simulations, following the trajectories determined with the four optimization strategies, are summarized in Table IV.1. Firstly, we observe that the energy supplied is lower than the heat demand of 29.8MWh for all methods. The difference is the largest for DO (about 16%). There are two reasons explaining the differences. First, the solar irradiation is slightly overestimated for most days, as shown in Figure IV.4. The updated forecasts, provided every six hours for each new DRTO, are slightly more accurate but they still tend to overestimate the GHI. Thus, when using the actual weather, the heat production is reduced and the demand is not perfectly satisfied. The second reason are the model and resolution differences between the simplified optimization model and the detailed simulation model representing the real plant. In order to assess the effect of the difference in models only, the 4 optimization strategies were compared in a test with undisturbed weather. This means that the real-time weather does not deviate from the forecasted weather in this test and the same weather inputs were used at each level of the optimization algorithm: planning, all DRTO and simulation of the real plant. Even without any disturbances in the weather, the heat demand is still not perfectly met in the four simulations, and the discrepancy is larger for DO ($E_{supplied}$ is 7.5% lower than the demand for DO and about 5.5% lower for the three DRTO strategies). This stems from the differences in modeling, mostly for the storage tank as detailed in subsection IV.2.2, and in resolution methods, mostly time integration, as explained in Section IV.4. Although the heat demand is met in the optimization model, when the trajectories are used on the detailed simulation model, the performances of the simulated plant are slightly different than expected, they were reduced in this test. Since the DRTO method starts every six hours with the actual state of the system, retrieved from the simulation model, it reduces the model error propagation.

DO is the most expensive strategy since it needs more gas to complete the heat demand. The electricity consumption of the pumps can also be compared in Table IV.1 for the case with the real weather data. We observe a lower electricity consumption for DRTO E. This has to be analyzed along with the stored energy at the end of the simulation. It is the lowest for DRTO E since there is no objective on storage. This strategy collects the minimum solar energy required to satisfy the heat demand, reducing the flow rates in the plant, thus leading to lower electricity consumption. Therefore this strategy is the least expensive in this case. However, the stored energy is lower, which could lead to more gas consumption in the future. DRTO P and DRTO S show very similar performances, with slightly more energy stored at the end of the simulation for DRTO S. In order to better understand the differences in operational strategies between DO, DRTO E, DRTO P and DRTO S, trajectories for various variables are compared.

Table IV.1: Comparison of the performances of the simulated solar thermal plant in July using the different optimization strategies

	Simulation performances			
Performance	DO	DRTO E	DRTO P	DRTO S
$E_{supplied}$ (MWh)	24.86	27.94	27.89	27.82
E_{elec} (MWh)	0.18	0.10	0.18	0.16
C_{tot} (€)	419	162	177	180
$E_{stock\ final}$ (MWh)	15.71	10.44	14.32	14.85

The flow rates in the solar field for the four strategies are compared in Figure IV.7 and the stored energies throughout time are plotted in Figure IV.8. DRTO E uses a lower flow rate in the solar field over the whole simulation horizon, which leads to lower electricity consumption as explained earlier, and to less solar energy collected and stored, even though the final supply to the consumer is the highest. Indeed, in Figure IV.8, the stored energy for DRTO E is lower than for other strategies for the last three days. The differences in stored energy for the other three strategies are small. The flow rate computed with DO increases day after day. We observe that the stored energy for DO is lower than the other strategies on day 1, but increases every day, and it is the largest at the end of the 96h. Because it benefits from a longer-term vision, DO tends to store less at the beginning of the 96h time span. This ensures that the storage is not full for as long as possible, leading to a better solar yield because the temperature of the water entering the solar field is lower (International Energy Agency; 2014). Once the end of the 96h time horizon draws near, the flow rate in the solar field is increased, to maximize solar heat collection and storage. DRTO P tends to follow the same trend while DRTO S uses the same flow rate each day, constantly maximizing solar heat production and storage. Figure IV.9 shows the temperature profile in the storage tank after 12 hours of simulation for DO, DRTO P and DRTO S. We observe that the cold zones for DO and DRTO P are larger than for DRTO S, allowing more storage capacity for the next days. Moreover, the temperature at the top of the storage tank is higher for DRTO P. This is due to the smaller flow rate in the solar field, leading to higher temperatures, and thus higher quality energy stored and leaving more space for future

storage needs .

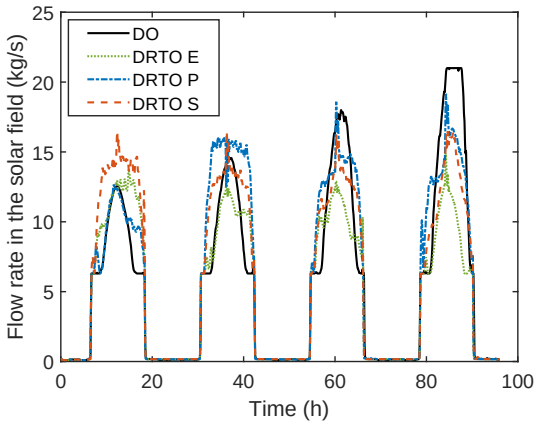

Figure IV.7: Comparison of the flow rates in the solar field in July

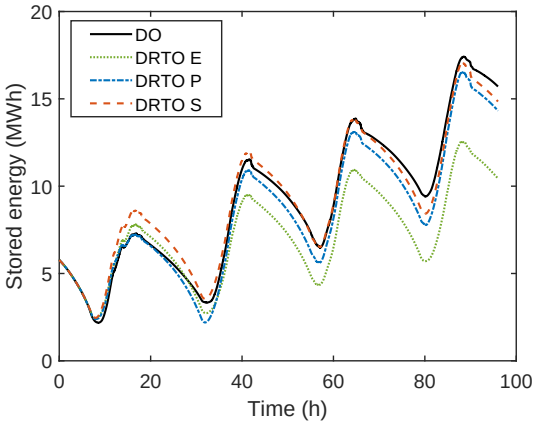

Figure IV.8: Comparison of the simulated stored energies in July

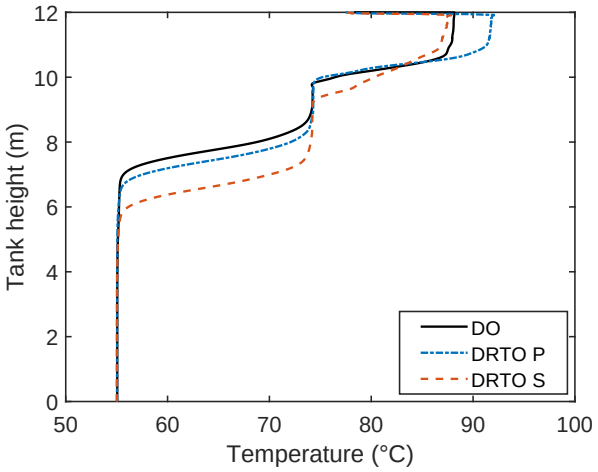

Figure IV.9: Comparison of the simulated temperature profiles in the tank at 12h

This case study shows that DRTO still improves the performances of the solar thermal plant even though the disturbances on the weather are very small. In this case, all DRTO strategies led to lower operating costs. DRTO E stored less solar energy, which might affect future operation, but led, at the same time, to the lowest cost for the 96h time span. However, DRTO P and DRTO S, although using different operational strategies as explained above, led to similar performances for the whole simulation of the solar thermal plant. The next case studies will help to determine which strategy, among DRTO P and DRTO S, should be used in different situations.

IV.6.2 Storage management in mid-season

The second test case is a period in May, typical of mid-season: the solar irradiation is variable, difficult to predict accurately and not high enough throughout the entire day to store sufficient energy to satisfy the heat demand over the entire simulation duration.

The performances achieved with the four optimization strategies are presented in Table IV.2.

Table IV.2: Comparison of the performances of the simulated solar thermal plant in May using the different optimization strategies

	Simulation performances			
Performance	DO	DRTO E	DRTO P	DRTO S
$E_{supplied}$ (MWh)	11.25	15.22	15.91	17.63
E_{elec} (MWh)	0.20	0.05	0.14	0.11
C_{tot} (€)	1512	1174	1131	989
$E_{stock\ final}$ (MWh)	0.76	0.37	0.82	0.87

First, one can notice that DO is the strategy supplying the least energy to the consumer (about 38% of cumulative heat demand), leading to the highest operating cost for heat production (associated to important gas consumption). This can be explained by the error in the solar irradiation forecast used for the planning phase, as shown in Figure IV.5. The initial forecast predicted a very low solar irradiation on the second day whereas the next forecasts and the measures actually show a high GHI. Therefore, the optimal operation on day 2 with DO was to shut down the solar thermal plant. No flow rate is circulating in the solar field, as shown in Figure IV.10 which presents the flow rates in the solar field for the four strategies. Moreover, no heat is supplied to the consumer because the storage tank was emptied the night before, as shown in Figure IV.11 which presents the stored energy throughout time for the four strategies. The stored energy even becomes negative due to heat losses, which means that the average temperature inside the storage tank is lower than the reference temperature corresponding to the return temperature of the consumer stream at 55°C. All three DRTO strategies perform better than DO because they use a better estimate of the solar irradiation. They also all use less electricity for the pumps, with DRTO E leading to the lowest electricity consumption. This is due to lower flow rates, for example a lower flow rate is used in the solar field for all three real-time strategies, as shown in Figure IV.10. DRTO E is the DRTO strategy leading to the lowest amount of energy supplied to the consumer and stored at the end of the simulation. This is because there is no objective on storage and the DRTO algorithm only has a strategic vision of 12 hours. Thus, DRTO E does not store a lot of energy in anticipation of future periods with no or low solar irradiation. This can be seen in Figure IV.11, where the stored energy on day 1 is the lowest for DRTO E, leading to less solar energy available for the next days. Therefore, it is necessary to incorporate a term on storage management in the DRTO objective function. Finally, for this case study, DRTO S allows to supply more solar heat to the consumer than DRTO P, about 6% more heat demand satisfied, reducing the operating cost by 16%. DRTO P includes a term in its objective function to minimize the difference between the planned storage state and the actual stored energy at the end of the time horizon. In this test, the planning was determined using inaccurate weather forecasts, especially on the second day. Thus, the planned storage state is not optimal and tracking it in the real-time phase deteriorates the performances of the solar thermal plant. This can be seen in Figure IV.11, where

the stored energy on the second day for DRTO P is low, even lower than DRTO E.

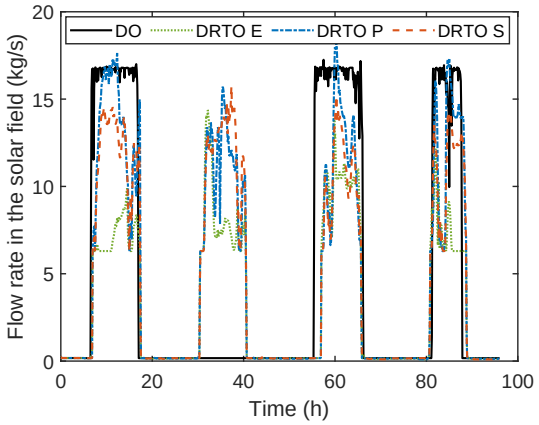

Figure IV.10: Comparison of the flow rates in the solar field in May

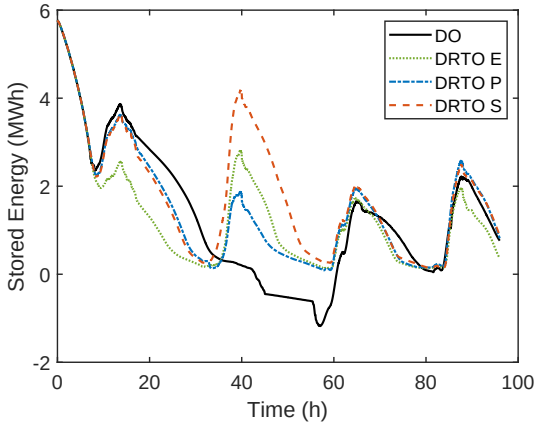

Figure IV.11: Comparison of the simulated stored energies in May

This is confirmed in Figure IV.12, which presents the charge flow rate for DRTO P and DRTO S. We observe that the charge flow rates are similar for both strategies on days 1, 3 and 4. Howerer, on day 2, the charge flow rate for DRTO P is reduced because the algorithm tracks the planned storage state determined with a low solar irradiation on day 2.

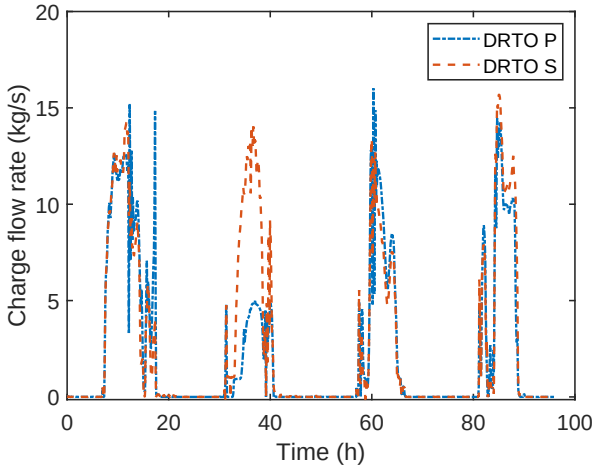

Figure IV.12: Comparison of the charge flow rates for two DRTO strategies

This shows that using the planning phase for storage management can lead to deteriorated performances for the solar thermal plant if the planning is inaccurate. It would be better to re-compute a new planning whenever the weather data differ too much from the forecasted data used for planning. This requires weather data available often and is computationally expensive. Based on the analysis of both case studies in July and May, maximizing the stored energy at the end of the DRTO time horizon leads to the best performances for the heat production: more solar heat delivered to the consumer and stored in the storage tank. So for normal operating conditions, which do not lead to overheating and complete filling of the storage tank, DRTO S seems to be the best strategy, regardless of whether the planning phase is accurate or not. In the

next subsection, an extreme scenario leading to overheating will be studied to assess the best storage management strategy in this situation.

IV.6.3 Storage management in summer: avoiding overheating

A scenario particularly challenging for solar thermal plant operators is when there are several sunny days in a row in summer and the storage tank is full. The solar thermal plant is exposed to overheating, which means that the temperature in the solar field rises too much, leading to thermal expansion and even ebullition (International Energy Agency; 2014). This situation could damage the solar plant equipment and therefore should be avoided. Generally, the solar thermal plant is designed to meet the heat demand during summer, when the solar contribution is the highest (International Energy Agency; 2014). This should prevent overheating, and back-up heaters will be used in other seasons to complete the demand. This is what was observed in the previous case studies: no overheating happened in July and gas was necessary to satisfy the heat demand in May. Nevertheless, extreme scenarios could still happen, and optimization could help to prevent overheating in these scenarios. In the present case study, the test period in July is used. However, we now consider that at the initial time of the 96 hours time span, the storage tank is full, with a uniform temperature of 75°C. This corresponds to a stored energy of 11.61MWh. The maximum theoretical capacity of the storage tank is 23.22MWh when the temperature is uniform equal to 95°C, which is the maximum allowed temperature in the system. In reality, the temperature in the system rarely reaches that level. A full storage is generally defined as the complete filling of the storage tank at a temperature larger than the return temperature of the consumer stream. Additionally, the heat demand has been reduced to a maximum of 334kW. This means that in Figure IV.2, the peak has been reduced to 334kW, which in turns, corresponds to a flow rate of $8kg.s^{-1}$. The total heat demand for the 96 hours of simulation is 25.09MWh in this case. This modified heat demand was artificially built to increase the risk of overheating. The same reduced demand was used at each level of the methodology: planning, DRTO and simulation. The objective of this case study is to find the best storage management strategy to prevent overheating. There are specific strategies that could be employed to prevent overheating, such as night cooling in the solar field (International Energy Agency; 2014) or defocusing of the solar panels (Scolan; 2020). These strategies are not incorporated into our models and optimization methodology. For large solar thermal plants, safety elements are used to handle overheating without damaging the solar field. For example, expansion vessels compensate the increased pressure, safety valves open to release the pressured fluid, or drainback systems completely empty the solar collectors when the temperature reaches a threshold (International Energy Agency; 2015). These elements are not included in our solar thermal plant model. So the only way to prevent overheating, if possible, is to use a smart storage management policy.

The four optimization strategies presented in IV.5.3 have been applied to this extreme scenario. In the case of DRTO S, the DRTO number 9, which starts at 54h did not converge. It corresponds to the middle of day 3, when the solar irradiation is high and after two sunny days during which the storage tank was already filled with hot fluid. When analyzing this convergence fail, we observe that it is due to over-

heating. At some point during the time horizon, the storage tank is completely full, the solar irradiation is high and the heat demand is not very large. The optimization algorithm is not able to respect both constraints: $T \leq 95°C$ (no overheating) and $T^{out}_{consumer} \leq T_{demand}$ (no exceeding of the heat demand). Either more solar heat needs to be evacuated in heat exchanger 2, or the temperature will rise in the solar field above the safety limits. This has been verified by relaxing either constraint, convergence was obtained in both cases. When moving either of the constraint in the objective function, to authorize the violation of the constraint but penalize it, convergence was achieved but the constraint was indeed violated even with a strong penalization. With the two constraints imposed, the optimization is infeasible and the trajectories for the flow rates that would be provided to the simulation model do not verify all physical equations and operational constraints. Thus, the overall numerical integration process was stopped at 54 hours. All three other strategies converged over the whole simulation time span.

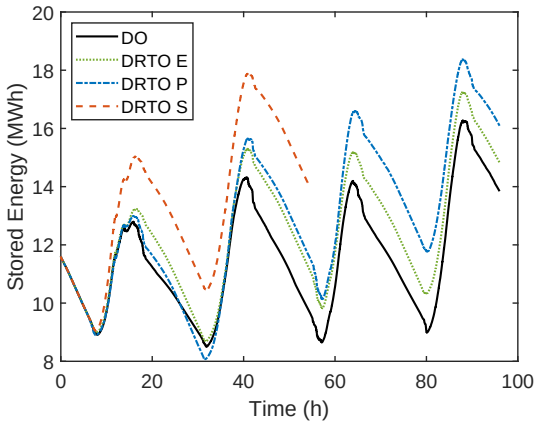

Figure IV.13: Simulated stored energy in July with reduced heat demand

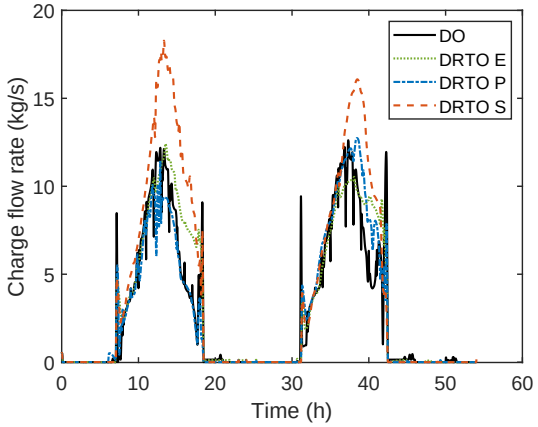

Figure IV.14: Charge flow rate in July with reduced heat demand

Figure IV.13 presents the stored energy throughout time for the four simulations following the four optimization strategies. We observe that the stored energy is much more important for DRTO S, more energy was charged during days 1 and 2. At the hour 54, when DRTO 9 fails for the DRTO S strategy, the initial stored energy is 17% higher than the one obtained with the DRTO P strategy. So during the first two days, the DRTO S strategy stores more energy in the tank, as shown in Figure IV.14. While the three other strategies all use similar charge flow rates, DRTO S uses a higher charge flow rate because its objective is to store as much as possible at the end of each DRTO. In this extreme scenario, this optimization strategy is not suitable because the lack of anticipation leads to an overfull storage tank when the solar irradiation is high, and thus to overheating.

On the first day, all three other strategies lead to the same amount of energy stored, which is the minimal amount. This is because DRTO E does not store additional energy for latter use and DO and DRTO P avoided to store too much to ensure a safe operation for the next days. The simulation with DO presents significantly less solar energy stored than DRTO P (and even DRTO E), although DRTO P follows the storage management policy determined by DO. As explained before, DO stores less energy than expected because it collects less solar energy than expected due to the

errors in the forecasts and the model (see subsection IV.6.1 for the explanations). So the stored energy originally planned in the optimizer, which is the objective used in DRTO P, is larger. This explains why DRTO P stores more energy than DO. This was also observed in (Untrau et al.; 2023a).

Table IV.3 presents the performances of the solar thermal plant for the different optimization strategies. The performances of DRTO S are not computed since the overall process is stopped at 54h after an optimization did not converge. Similarly to the results presented in subsection IV.6.1, DO supplies the least amount of heat to the consumer, 87% of the heat demand, because of the slightly inaccurate weather forecasts and simplifying assumptions in the optimization model.

DRTO E stores less energy at the end of the simulation than DRTO P but the difference is smaller than when the demand was not reduced (only 8% difference compared to the 27% difference in the case study presented in subsection IV.6.1). The difference is small because there is excess energy every day produced in the solar field since the demand is low, so even DRTO E stored this excess heat. Moreover, DRTO P does not store more energy to avoid overheating. DRTO P still leads to more energy stored starting from day 2 because the storage management policy provided by DO allows more storage towards the end of the simulation, once the risk of overheating is handled. The operating costs for DRTO E and DRTO P are similar, slightly larger for DRTO P because it consumes more electricity.

Overall, DRTO P leads to the best performances in the solar thermal plant, with low operating costs and a full storage tank at the end of the simulation, without overheating.

Table IV.3: Comparison of the performances of the simulated solar thermal plant in July when there is a risk of overheating

	Simulation performances		
Performance	DO	DRTO E	DRTO P
$E_{supplied}$ (MWh)	21.76	23.67	23.62
E_{elec} (MWh)	0.15	0.12	0.17
C_{tot} (€)	286	129	140
$E_{stock\ final}$ (MWh)	13.84	14.83	16.09

IV.6.4 Impact of the DRTO time horizon

In this work, a time horizon of 12 hours was chosen for the DRTO. Since the time horizon might affect the operational strategy, a test was conducted to assess its effect. Simulations with DRTO using time horizons of 6 hours and 24 hours were run. First, the computational times of one DRTO algorithm for the three different time horizons were compared in Table IV.4. The computational times are averaged for every test period and DRTO strategy. All time horizons could be chosen for a real-time application, with fast convergence on average. A time horizon of 24 hours might lead to long computational times, with a maximum time of 26 minutes found among all cases,

but it still remains applicable in real-time given that the update frequency is only six hours. Thus, the choice of the suitable time horizon depends on the solar thermal plant performances achieved.

Table IV.4: Comparison of the computational times for one DRTO run for different time horizons

Time horizon (h)	6	12	24
Average time (min)	1	2.5	6
Maximum time (min)	4	7	26

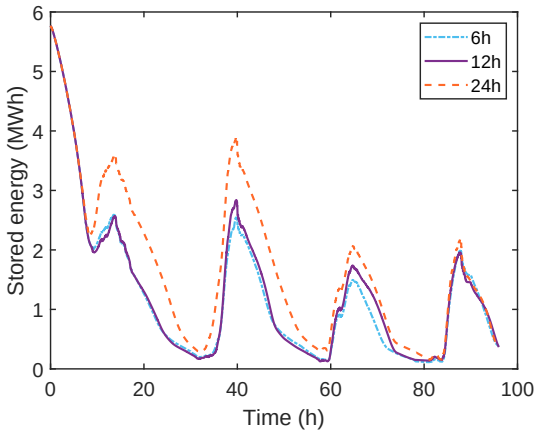

Figure IV.15: Impact of the time horizon for DRTO E in May

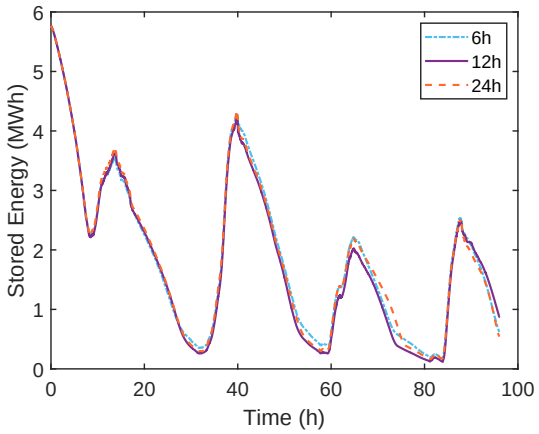

Figure IV.16: Impact of the time horizon for DRTO S in May

Figure IV.15 shows the simulated stored energy throughout time for the test period in May using DRTO E with different time horizons. We observe that the stored energy is higher when using a longer time horizon because the DRTO algorithm can anticipate the need for stored energy. As a result, the supplied energy is larger and the operating costs of heat production lower for the time horizon of 24 hours. On the other hand, Figure IV.16 presents the stored energy for DRTO S. For this strategy, the time horizon does not impact the quantity of energy stored throughout time. The performances of the solar thermal plant are not affected by the time horizon significantly. This is because the storage management is incorporated into the objective function and the DRTO algorithm does not need a long term strategic vision to make the most of the storage tank. A similar analysis can be conducted for DRTO P. Based on this observation, a time horizon of 6 hours, which requires the least computational effort, could be satisfactory.

The simulations were also conducted in July, for both the standard and the extreme scenarios. We noticed more frequent overheating when using a time horizon of 6 hours compared to 12 hours, even for DRTO P. Although storage management is determined by planning in this strategy, having a longer time horizon seems to help avoid overheating in some situations. Therefore, a time horizon of 12 hours is long enough when

using a storage management objective, is computationally acceptable and still provides a few hours of strategic vision to the DRTO algorithm.

IV.7 Conclusion and Perspectives

In this study an economic DRTO methodology for a solar thermal plant was developed and tested online in several case studies. Real data for the weather forecasts and measurements were used. The methodology was tested on a detailed simulation model, representing an industrial plant. Firstly, it has been observed that DRTO improves the solar thermal plant performances compared to DO even when the forecasts used for DO are accurate. This is due to the regular update of the system state with measured values, reducing model error propagation. The main objective of this work was to determine the best storage management policy by comparing several optimization strategies. All optimization strategies aim at minimizing the operating costs from gas and electricity consumption, but they treat the storage management differently. From the different case studies, some guidelines for the optimal operation of a solar thermal plant could be formulated:

- The planning phase should be run to determine if there is a risk of overheating in the following days. A risk of overheating could be defined as a saturation of the storing capacity (complete filling of the tank at high temperature) at one point during the DO.
- If there is no risk of overheating for the following days, the DRTO S strategy should be adopted. This means that the stored energy is maximized at the end of each DRTO time horizon. The maximized stored energy will allow the supply of solar heat later, when no solar irradiation is available, reducing gas consumption for the heat production.
- If there is a risk of overheating, the DRTO P strategy should be adopted. The DRTO P will follow the planned stored energy at the end of each DRTO time horizon. This should avoid overheating by storing energy only if it does not deteriorate the plant operation in the following days.
- A time horizon of 12 hours for the DRTO seems suitable to determine the best operational strategy.
- The planning phase should be updated regularly, especially when the weather forecasts differ a lot from the actual weather conditions.
- Although it did not happen in the case studies presented, the planning phase could fail to converge. Indeed, we showed that the use of planning can help to avoid some overheating situations, but extreme scenarios could lead to overheating predicted even during the planning phase. In this case, the DRTO E strategy should be used because it stores the least energy and collects the minimum amount of solar heat to satisfy the heat demand. Overheating might happen, and safety devices will be activated to protect the solar thermal plant, but DRTO E should reduce the overheating to a minimum. As soon as a new planning phase

converges, which means that the risk of overheating can be handled again, the DRTO S or DRTO P strategy should be adopted again, depending on the guidelines above.

- Overheating can still happen even when following these guidelines, but the occurrences of overheating should be very limited. In case of overheating, safety equipment included in the solar thermal plant must protect the system.

In future work, these guidelines could be tested for more case studies, to formulate more precise criteria for the switching between the different DRTO strategies. Moreover, a criterion on the deviation between the forecasts used for planning and the actual environmental conditions could be formulated to trigger a new planning computation. In this study, the connection between the planning and the DRTO P strategy was to minimize the difference between the planned stored energy and the actual stored energy at the end of the DRTO time horizon. Other possibilities, such as tracking the planned stored energy at a fixed time in the day, sunset for example, could be explored. Finally, future work could focus on improving the models developed, by incorporating the safety equipment used in case of overheating, and add the optimization of these devices in the optimal operation of the plant, and also by modeling non ideal controllers to add them in the detailed representation of the plant.

Acknowledgements

The project leading to this publication has received funding from Excellence Initiative of Université de Pau et des Pays de l'Adour – I-Site E2S UPPA, a French "Investissements d'Avenir" programme.

Bibliography

Alonso, A. A., Arias-Méndez, A., Balsa-Canto, E., García, M. R., Molina, J. I., Vilas, C. and Villafín, M. (2013). Real time optimization for quality control of batch thermal sterilization of prepackaged foods, *Food Control* **32**: 392–403.

Arpornwichanop, A., Kittisupakorn, P. and Mujtaba, I. (2005). On-line dynamic optimization and control strategy for improving the performance of batch reactors, *Chemical Engineering and Processing: Process Intensification* **44**: 101–114.

Brodrick, P. G., Brandt, A. R. and Durlofsky, L. J. (2018). Optimal design and operation of integrated solar combined cycles under emissions intensity constraints, *Applied Energy* **226**: 979–990.

Camacho, E., Rubio, F., Berenguel, M. and Valenzuela, L. (2007a). A survey on control schemes for distributed solar collector fields. Part I: Modeling and basic control approaches, *Solar Energy* **81**(10): 1240–1251.

Camacho, E., Rubio, F., Berenguel, M. and Valenzuela, L. (2007b). A survey on control schemes for distributed solar collector fields. Part II: Advanced control approaches, *Solar Energy* **81**(10): 1252–1272.

Carey, G. and Finlayson, B. A. (1975). Orthogonal collocation on finite elements, *Chemical Engineering Science* **30**(5-6): 587–596.

Caspari, A., Tsay, C., Mhamdi, A., Baldea, M. and Mitsos, A. (2020). The integration of scheduling and control: Top-down vs. bottom-up, *Journal of Process Control* **91**: 50–62.

Clarke, W. C., Manzie, C. and Brear, M. J. (2018). Hierarchical economic MPC for systems with storage states, *Automatica* **94**: 138–150.

Collier, U. (2018). Renewable Heat Policies - Delivering clean heat solutions for the energy transition, *Insights Series 2018 - International Energy Agency* .

Csordas, G., Brunger, A., Hollands, K. and Lightstone, M. (1992). Plume entrainment effects in solar domestic hot water systems employing variable-flow-rate control strategies, *Solar Energy* **49**(6): 497–505.

de Azevedo Delou, P., Curvelo, R., de Souza, M. B. and Secchi, A. R. (2021). Steady-state real-time optimization using transient measurements in the absence of a dynamic mechanistic model: A framework of hrto integrated with adaptive self-optimizing ihmpc, *Journal of Process Control* **106**: 1–19.

De Césaro Oliveski, R., Krenzinger, A. and Vielmo, H. A. (2003). Comparison between models for the simulation of hot water storage tanks, *Solar Energy* **75**(2): 121–134.

De Oliveira, V., Jaschke, J. and Skogestad, S. (2013). Dynamic online optimization of a house heating system in a fluctuating energy price scenario, *IFAC Proceedings Volumes - 10th International Symposium on Dynamics and Control of Process Systems*, Elsevier, Mumbai, India, pp. 463–468.

Delubac, R., Serra, S., Sochard, S. and Reneaume, J.-M. (2021). A Dynamic Optimization Tool to Size and Operate Solar Thermal District Heating Networks Production Plants, *Energies* **14**(23): 8003.

Elixmann, D., Busch, J. and Marquardt, W. (2010). Integration of model-predictive scheduling, dynamic real-time optimization and output tracking for a wastewater treatment process, *IFAC Proceedings Volumes - 11th International Symposium on Computer Applications in Biotechnology*, Vol. 43, Elsevier, Leuven, Belgium, pp. 90–95.

Ellingwood, K., Mohammadi, K. and Powell, K. (2020). Dynamic optimization and economic evaluation of flexible heat integration in a hybrid concentrated solar power plant, *Applied Energy* **276**: 115513.

Engell, S. (2007). Feedback control for optimal process operation, *Journal of Process Control* **17**: 203–219.

Franke, R. (1997). Object-oriented modeling of solar heating systems, *Solar Energy* **60**: 171–180.

Gálvez-Carrillo, M., De Keyser, R. and Ionescu, C. (2009). Nonlinear predictive control with dead-time compensator: Application to a solar power plant, *Solar Energy* **83**: 743–752.

He, Z., Qian, Y., Xu, C., Yang, L. and Du, X. (2019). Static and dynamic thermocline evolution in the water thermocline storage tank, *Energy Procedia* **158**: 4471–4476.

Hedengren, J. D., Shishavan, R. A., Powell, K. M. and Edgar, T. F. (2014). Nonlinear modeling, estimation and predictive control in APMonitor, *Computers & Chemical Engineering* **70**: 133–148.

Hirvonen, J., ur Rehman, H. and Sirén, K. (2018). Techno-economic optimization and analysis of a high latitude solar district heating system with seasonal storage, considering different community sizes, *Solar Energy* **162**: 472–488.

Hosseinnia, S. M., Akbari, H. and Sorin, M. (2021). Numerical analysis of thermocline evolution during charging phase in a stratified thermal energy storage tank, *Journal of Energy Storage* **40**: 102682.

Huang, J., Fan, J. and Furbo, S. (2019). Feasibility study on solar district heating in China, *Renewable and Sustainable Energy Reviews* **108**: 53–64.

Incropera, F., Dewitt, D., Bergman, T. and Lavine, A. (2007). Fundamentals of heat and mass transfer, *John Wiley, 6th edition* .

International Energy Agency (2014). Requirements & guidelines for collector loop installation, *Task 45, Solar Heating & Cooling Program* .

International Energy Agency (2015). Integration guideline, solar process heat for production and advanced applications, *Task 49, Solar Heating & Cooling Program* .

ISO/FDIS 9806 (2017). Énergie solaire - capteurs thermiques solaires - méthodes d'essai, *International Standard* .

Jannesari, H. and Babaei, B. (2018). Optimization of solar assisted heating system for electro-winning process in the copper complex, *Energy* **158**: 957–966.

Kadam, J. V., Schlegel, M., Marquardt, W., Tousain, R. L., Van Hessem, D. H., Van Den Berg, J. and Bosgra, O. H. (2002). A Two-Level Strategy of Integrated Dynamic Optimization and Control of Industrial Processes - a Case Study, *European Symposium on Computer Aided Process Engineering*, Vol. 12, Elsevier, The Hague, The Netherlands, pp. 511–516.

Kalogirou, S. A. (2004). Solar thermal collectors and applications, *Progress in Energy and Combustion Science* **30**(3): 231–295.

Kleinbach, E., Beckman, W. and Klein, S. (1993). Performance study of one-dimensional models for stratified thermal storage tanks, *Solar Energy* **50**(2): 155–166.

Koçak, B., Fernandez, A. I. and Paksoy, H. (2020). Review on sensible thermal energy storage for industrial solar applications and sustainability aspects, *Solar Energy* **209**: 135–169.

Krause, M., Vajen, K., Wiese, F. and Ackermann, H. (2003). Investigations on optimizing large solar thermal systems, *Solar Energy* **73**: 217–225.

Lizarraga-Garcia, E., Ghobeity, A., Totten, M. and Mitsos, A. (2013). Optimal operation of a solar-thermal power plant with energy storage and electricity buy-back from grid, *Energy* **51**: 61–70.

Matias, J. O. and Le Roux, G. A. (2018). Real-time Optimization with persistent parameter adaptation using online parameter estimation, *Journal of Process Control* **68**: 195–204.

Parvareh, F., Milani, D., Sharma, M., Chiesa, M. and Abbas, A. (2015). Solar repowering of PCC-retrofitted power plants; solar thermal plant dynamic modelling and control strategies, *Solar Energy* **119**: 507–530.

Pataro, I. M. L., Roca, L., Sanches, J. L. G. and Berenguel, M. (2020). An economic D-RTO for thermal solar plant: analysis and simulations based on a feedback linearization control case, *XXIII Congresso Brasileiro de Automática*, Virtual event.

Pate, R. A. (1977). *A Thermal Energy Storage Tank Model for Solar Heating*, thesis, Utah State University.

Petkov, I. and Gabrielli, P. (2020). Power-to-hydrogen as seasonal energy storage: an uncertainty analysis for optimal design of low-carbon multi-energy systems, *Applied Energy* **274**: 115197.

Pintaldi, S., Li, J., Sethuvenkatraman, S., White, S. and Rosengarten, G. (2019). Model predictive control of a high efficiency solar thermal cooling system with thermal storage, *Energy and Buildings* **196**: 214–226.

Powell, K. M. and Edgar, T. F. (2013). An adaptive-grid model for dynamic simulation of thermocline thermal energy storage systems, *Energy Conversion and Management* **76**: 865–873.

Powell, K. M., Hedengren, J. D. and Edgar, T. F. (2014). Dynamic optimization of a hybrid solar thermal and fossil fuel system, *Solar Energy* **108**: 210–218.

Rashid, K., Safdarnejad, S. M. and Powell, K. M. (2019). Process intensification of solar thermal power using hybridization, flexible heat integration, and real-time optimization, *Chemical Engineering and Processing - Process Intensification* **139**: 155–171.

Renewable Energy Directive (2018). Directive (EU) 2018/2001 of the European Parliament and of the Council of 11 December 2018 on the promotion of the use of energy from renewable sources, *OJ* **L328/82**.

Saloux, E. and Candanedo, J. A. (2021). Model-based predictive control to minimize primary energy use in a solar district heating system with seasonal thermal energy storage, *Applied Energy* **291**: 116840.

Scolan, S. (2020). *Développement d'un outil de simulation et d'optimisation dynamique d'une centrale solaire thermique.*, thesis, Pau. Publication Title: http://www.theses.fr.

Scolan, S., Serra, S., Sochard, S., Delmas, P. and Reneaume, J.-M. (2020). Dynamic optimization of the operation of a solar thermal plant, *Solar Energy* **198**: 643–657.

Serale, G., Fiorentini, M., Capozzoli, A., Cooper, P. and Perino, M. (2018). Formulation of a model predictive control algorithm to enhance the performance of a latent heat solar thermal system, *Energy Conversion and Management* **173**: 438–449.

Tian, Y. and Zhao, C. (2013). A review of solar collectors and thermal energy storage in solar thermal applications, *Applied Energy* **104**: 538–553.

Tian, Z., Perers, B., Furbo, S. and Fan, J. (2018). Thermo-economic optimization of a hybrid solar district heating plant with flat plate collectors and parabolic trough collectors in series, *Energy Conversion and Management* **165**: 92–101.

United Nations Framework Convention on Climate Change (2015). Adoption of the paris agreement, *21st Conference of the Parties* .

Untrau, A., Sochard, S., Marias, F., Reneaume, J.-M., Le Roux, G. A. C. and Serra, S. (2023a). Dynamic Real-Time Optimization of a solar thermal plant during daytime, *Computers & Chemical Engineering* **172**: 108184.

Untrau, A., Sochard, S., Marias, F., Reneaume, J.-M., Le Roux, G. A. C. and Serra, S. (2023b). A fast and accurate 1-dimensional model for dynamic simulation and optimization of a stratified thermal energy storage, *Applied Energy* **333**: 120614.

Untrau, A., Sochard, S., Marias, F., Reneaume, J.-M., Le Roux, G. A. and Serra, S. (2022). Analysis and future perspectives for the application of Dynamic Real-Time Optimization to solar thermal plants: A review, *Solar Energy* **241**: 275–291.

Wagner, M. J., Hamilton, W. T., Newman, A., Dent, J., Diep, C. and Braun, R. (2018). Optimizing dispatch for a concentrated solar power tower, *Solar Energy* **174**: 1198–1211.

Wang, L., Sundén, B. and Manglik, M. (2007). Plate heat exchangers: Design, applications and performance, *WIT Press* .

Weiss, W. and Spörk-Dür, M. (2021). Global Market Development and Trends in 2020 Detailed Market Data 2019, *Solar Heating and Cooling Programme - International Energy Agency* .

Winterscheid, C., Dalenbäck, J.-O. and Holler, S. (2017). Integration of solar thermal systems in existing district heating systems, *Energy* **137**: 579–585.

Wittmann, M., Eck, M., Pitz-Paal, R. and Müller-Steinhagen, H. (2011). Methodology for optimized operation strategies of solar thermal power plants with integrated heat storage, *Solar Energy* **85**: 653–659.

IV.8 Additional clarifications

- The resulting flow rate $\dot{m}$ from charging and discharging inside the storage tank introduced in Subsection IV.2.2 is equal to $\dot{m}_c - \dot{m}_d$.
- The pipes are modeled in 0D and not in 1D since we do not consider spatial discretization.
- In Chapter III, the IPOPT solver is used because the study is only focused on the storage tank, which lead to a simple model. However, in this chapter, the whole solar thermal plant is modeled, which is more complex. We used CONOPT because we achieved an easier convergence with this solver. If we were able to achieve convergence with IPOPT, this could reduce the computational time.

Conclusion and Perspectives

Greenhouse gases emitted by the combustion of fossil fuels for energy production are directly responsible for climate change. Solar thermal energy represents a good alternative to fossil fuels for heat production, especially at low temperature suitable for some industrial processes and space and water heating. However, the intermittency of the solar irradiation and the uncertainty of its forecast have slowed down its development. Thermal energy storage is required to decouple the heat production and the heat supply. The operation of the solar thermal plant with storage is particularly challenging because of the various operating modes and the need of a good strategic vision to use the storage intelligently. Hence, an efficient methodology ensuring an optimal operation of a solar thermal plant with storage is needed.

In the first chapter of this thesis, the state of the art on the optimization of the operation of solar thermal plants was presented. The design of such systems is often optimized to ensure that the heat demand can be met with minimum investment costs. However, the operation of solar thermal plants is less frequently optimized and usually follows standard operating strategies, based on logic control rules. Although there has been a lot of papers dedicated to advanced controllers, sometimes including an economic objective, dynamic optimization of solar thermal plant is more seldom studied. Furthermore, the work on the operation of solar thermal plants is mostly done for concentrated solar power plants for electricity production. Thus, there is a lack of studies on the optimization of the operation of non-concentrating solar thermal plants with storage for heat production. Such systems have complex characteristics: nonlinear, dynamic, with different time scales and ever-changing environmental conditions. Hence, Dynamic Real-Time Optimization (DRTO) seems particularly well suited to optimize their operation. Indeed, DRTO regularly updates the optimal trajectories using the feedback measurements provided by the real plant, or by a virtual representation of the plant during the testing of the methodology, making sure the trajectories are adapted to the current disturbances. A literature review on DRTO, mostly developed in chemical engineering, shows an improvement in the economic performances of processes operating in variable and uncertain environmental conditions compared to standard operation or offline optimization. A connection between DRTO and a planning phase, which benefits from a longer term strategic vision, is possible. This seems particularly suitable for the storage management in a solar thermal plant. This chapter presented the challenge associated to the operation of solar thermal plants, especially regarding storage management. It highlighted the lack of studies focusing on the DRTO of solar thermal plants, and on the use of a planning phase to improve the use of storage. Therefore, a DRTO methodology using a planning phase was proposed.

The second chapter presented the methodology developed in more details and its testing in a simple case study. Since we did not have access to a real solar thermal plant to test the methodology, a detailed simulation model was used. Perfect control was assumed, so the trajectories determined at the DRTO level were perfectly tracked at the simulation level. The planning phase was performed for 2 days, and then the DRTO was tested online during the first day, with a new DRTO run every hour and a shrinking time horizon ending at the end of the day. The heat demand was considered constant and well known in advance but an artificial disturbance was introduced in the real-time solar irradiation. The DRTO economic objective function included a term for tracking the planned storage state at the end of the day. It was shown that a weight associated with this term has to be adjusted to achieve the best compromise between a

good tracking of the planned stored energy at the end of the day and low operating costs during the day. Then, the performances of the simulated plant following the optimal trajectories for the flow rates obtained with our DRTO methodology were compared to the performances of the plant when the trajectories obtained offline, during the planning phase and without real-time adaptation (Dynamic Optimization, DO), were used. Several case studies were considered, representing three different seasons and with various real-time disturbances. For most case studies, the operating costs were reduced with DRTO thanks to a reduction in electricity consumption from the pumps and an increase in the solar fraction of the heat supply (up to a 35% increase compared to the simulation using DO). The storage state target was reasonably tracked, with a maximum difference of -14% of final stored energy for the simulation using DRTO compared to the one using DO. Therefore, the DRTO methodology developed, using a planning phase, is able to adapt the operating strategy to the current disturbances and updated forecasts, which are more accurate, but also to use a good storage management policy, determined with a planning phase benefiting from a longer term strategic vision.

The third chapter was a focus on the 1D modeling of a stratified storage tank, which is an important part of a solar thermal plant. Because of the large temperature gradient in the thermocline region separating the hot and cold zones, the storage tank is particularly challenging to model. A compromise has to be found between the accuracy of the vertical temperature profile and the stored energy calculated and the computational time, especially for the simulation of complex energy systems and optimization. The traditional spatial discretization scheme, the multinode model, is based on finite volumes and tends to smooth the temperature profile around the thermocline when not enough layers are used. In this chapter, another discretization scheme was presented: Orthogonal Collocation on Finite Elements (OCFE). This scheme offers a good compromise between the fast convergence of orthogonal collocation and the fast resolution of finite volumes. Indeed, orthogonal collocation does not need many discretization points to achieve a good accuracy in the result obtained. Thus, it converges with few discretization points towards the solution of the differential equation. On the other hand, for a given number of discretization points, finite volumes lead to a shorter resolution time. OCFE thus provides a good compromise between the two resolution schemes. Moreover, OCFE has never been applied to the spatial discretization of a storage tank. It was shown that OCFE can achieve a better accuracy for the temperature and energy calculations in a reduced computational time compared to finite volumes. The model was validated against experimental data from a real solar thermal plant. The validation part showed that OCFE can represent the real temperature profile inside the storage tank using four times less discretization points than the multinode model and with a computational time divided by five. Indeed, OCFE with 3 elements and 8 collocation points in each element achieved a slightly better accuracy than the multinode model considering 100 layers in this validation study. Finally, the modeling of natural convection in the 1D storage tank model for optimization studies was discussed, showing the limits of a continuous model suitable for optimization.

Finally, in Chapter IV, the DRTO methodology developed in Chapter II was improved and tested in more realistic case studies. Firstly, the storage tank model in the detailed simulation model representing the real plant was changed for OCFE as introduced in Chapter III. This allowed more accurate and faster simulations. The storage tank model used for optimization was not changed because the computational

time with the multinode model with 10 layers could not be reduced with OCFE. To reduce the computational time with OCFE, less than 10 discretization points would be needed, which would lead to large oscillations in the temperature profile obtained. The planning phase was run once at the beginning and covered the whole simulation period of 96 hours, providing the storage management policy for the whole period, based on weather forecasts. A new DRTO was run every 6 hours, adapting the optimal trajectories for the solar thermal plant flow rates, and a rolling time horizon of 12 hours was used. The economic objective function of the DRTO can include a term for storage management and several possibilities were considered and compared. The case studies used a variable daily heat demand and real weather forecasts and real-time measurements, corresponding to scenarios in summer and mid-season. It was found that maximizing the stored energy at the end of each DRTO run is the best strategy when there is no risk of overheating. Indeed, it provides useful solar heat for latter use, hence reducing the gas consumption of the plant and the operating costs. However, when there is a risk of overheating because the solar irradiation is high compared to the heat demand, it is better to track the planned stored energy at each DRTO, as introduced in Chapter II. Indeed, the planning phase benefited from a longer-term strategic vision, allowing the operating strategy to anticipate the future high solar irradiation and thus reduce the stored energy. When the DRTO tracks this storage management policy, it helps to prevent overheating scenarios.

The work conducted in this thesis shows that DRTO can improve the economic performances of a solar thermal plant compared to offline dynamic optimization. The use of a planning phase avoids a storage management degradation due to a reduced time horizon allowing real-time implementation. A new spatial discretization scheme for the 1D model of a stratified storage tank was proposed, that could improve the accuracy and computational efficiency for simulations and optimizations. It was successfully implemented in the simulation model in this thesis. Finally, guidelines on the storage management at the DRTO level were provided, showing that the planning phase can help to avoid overheating. This work has brought many perspectives, which are detailed below.

The first direction for future work is to improve the storage management in the DRTO methodology. In Chapter IV, it was shown that the optimal storage management strategy at the DRTO level is different whether there is a risk of overheating or not. A precise criteria to switch from one strategy to the other could be determined in future work. This criteria could be a risk of overheating determined during planning or also a real solar irradiation much larger than the forecasted one. The tracking of the planned storage state was here done by minimizing the difference between the planned and the actual stored energy at the end of the DRTO time horizon. Other options could be considered, such as the tracking of the planned storage state at a fixed hour of the day, similarly to the simple test in Chapter II but with a rolling time horizon for the DRTO, or the tracking of the trajectory of the planned stored energy. This could improve the use of storage in the DRTO methodology.

The DRTO methodology could be further improved in several ways. In this thesis, a new DRTO was run at a regular frequency (1 hour in Chapter II and 6 hours in Chapter IV). Conditional triggering could be explored to only re-optimize the operation of the solar thermal plant when it is necessary. For example, a new DRTO could be triggered

by a large disturbance in solar irradiation, but this would require available weather forecasts at any time, or the use of the latest forecasts potentially erroneous. Moreover, the planning phase was used as an offline dynamic optimization performed once, at the beginning of the test, in this work. However, in a real application, the planning phase should be re-optimized regularly, and the criteria triggering a new optimization could be studied.

The resolution of the optimization model could also be improved. A sensitivity analysis could be conducted to determine the best time discretization allowing to capture transient behaviors in the system while still being applicable in real-time. Furthermore, the resolution strategy in this work starts with a dynamic simulation of the system using standard operating strategies and providing an initialization for the variables of the problem. Two constraints are then added and finally the operation of the system is optimized. This strategy was efficient for the case studies but could fail to converge in some other scenarios. Moreover, the resolution of this nonlinear optimization problem leads to obtaining a local minimum. In particular, the optimized trajectories can differ only slightly from the trajectories given as initialization. Other resolution strategies could be explored to ensure the convergence of the algorithm to a global minimum. For example, a stochastic algorithm could be run first to obtain a rough estimate of the global minimum. This estimation would then be refined using a deterministic approach. Or the resolution could be run several times with different initialization trajectories in order to approach the global minimum better and ensure the convergence of the algorithm. However, these modifications to the resolution method should maintain a reasonable computational time. They might be better suited for the planning phase, as the computational time might be prohibitive for a real-time application.

Another direction for future work is to improve the model used for optimization as well as the detailed model representing the real plant to improve the testing of the methodology. The detailed 1D storage tank model has already been modified in the last chapter to increase the accuracy of the results and reduce the computational time, and the new model was validated with real plant measurements. However, natural convection was modeled using a numerical artifice that could not be validated experimentally. On the other hand, the storage tank model used for optimization, although fast, does not provide a good accuracy for the estimation of the temperature profile and the stored energy. Moreover, the modeling of natural convection was not included in this model. Hence, developing fast and accurate models for the storage tank, with an experimental validation, is important. Data-based models, which were not considered in this thesis, could be helpful to build a fast model for optimization. LaTEP is currently working on a data-based model for a District Heating Network (DHN) with a simple production site for optimization studies. As mentioned in the last chapter, the devices or protocols used for cooling down the fluid in the solar field (fans, water cooling) or avoid overheating (defocusing solar collectors, radiative cooling) when necessary should be added to the simplified and detailed models. Additionally, their use could be optimized to minimize their operating cost. Finally, the detailed simulation model could be improved to achieve a more realistic testing of the methodology. In particular, the controllers could be modeled to better reproduce the behavior of the real plant. That way, the optimal trajectories obtained at the DRTO level could be tracked in the presence of disturbances.

Instead of testing the methodology on an improved detailed simulation model, it could also be tested on an experimental apparatus or ideally directly on the real plant. In this case, additional steps of data reconciliation and parameter estimation should be added to exploit the measurements made on the system. These additional steps could be added to the methodology from the test phase on a simulation model in order to reproduce the real behavior of the plant more accurately.

Additionally, the methodology could be tested in more case studies. Firstly, the heat demand considered should be the heat demand of an existing system, industry or DHN, with variations during and between the days. Also, more scenarios should be tested with different weather forecasts and real-time measurements. This extending testing would help to ensure the robustness of the method and might also show behaviors that could not be analyzed in the thesis.

Another direction for future work is the simultaneous optimization of the design of the system and its operation in an offline dynamic optimization.

Finally, this works opens wider perspectives for the optimal operation of multi-energy systems. First of all, the work presented in this thesis could be adapted to other types of solar thermal plants, including solar power plants. But it could also be adapted to optimize other thermal systems operating in uncertain environments. LaTEP is currently working on a DRTO methodology for a solar thermal plant with short-term storage associated to a heat pump and a long-term storage. As intermittent renewable energies are incorporated in larger share in DHN or electric grids, the need for a robust optimal control of the operation of such networks is growing. The methodology developed in this thesis presents interesting characteristics for the future optimal operation of multi-energy networks.

Conclusion et perspectives [français]

Les gaz à effet de serre émis lors de la combustion de combustibles fossiles pour la production d'énergie sont directement responsables du réchauffement climatique. L'énergie solaire thermique représente une bonne alternative aux combustibles fossiles pour la production de chaleur, notamment à basse température pour certains procédés industriels ou le chauffage des locaux et de l'eau. Cependant, l'intermittence du rayonnement solaire et l'incertitude sur sa prévision ont freiné le développement des centrales solaires thermiques. L'utilisation d'un stockage thermique est nécessaire pour découpler la production et la fourniture de chaleur solaire. L'exploitation d'une centrale solaire thermique avec stockage est un défi en raison des multiples modes de fonctionnement et de la nécessité d'une bonne vision stratégique pour utiliser le stockage intelligemment.

Dans le premier chapitre de cette thèse, l'état de l'art sur l'optimisation du fonctionnement des centrales solaires thermiques a été présenté. Le dimensionnement de tels systèmes est souvent optimisé pour assurer la satisfaction de la demande en chaleur tout en minimisant les coûts d'investissement. En revanche, le fonctionnement des centrales solaires thermiques est rarement optimisé et repose généralement sur des stratégies de fonctionnement basées sur des règles de contrôle heuristiques. Bien que le contrôle des centrales solaires soit l'objet de nombreux articles dans la littérature, parfois en y incluant un objectif économique, l'optimisation dynamique des centrales solaires thermiques est plus rarement étudiée. De plus, la majorité des travaux portant sur le fonctionnement des centrales solaires thermiques s'intéressent aux centrales à concentration pour la production d'électricité. Il manque donc d'études portant sur l'optimisation du fonctionnement des centrales solaires thermiques avec stockage, sans concentration et pour la production de chaleur, dans la littérature. De tels systèmes ont des caractéristiques complexes : non linéaires, dynamiques, avec des variations sur différentes échelles de temps et des conditions environnementales toujours changeantes. L'optimisation dynamique en temps-réel (Dynamic Real-Time Optimization, DRTO) semble donc particulièrement bien adaptée pour optimiser leur fonctionnement. En effet, la DRTO met régulièrement à jour les trajectoires optimales en utilisant des mesures de retour fournies par la centrale réelle, ou bien une centrale virtuelle utilisée en phase de développement de la méthode. Cela garantit que les trajectoires optimales calculées sont adaptées aux perturbations réelles. Une revue de la littérature sur la DRTO, qui est principalement développée dans le domaine du génie des procédés, montre qu'elle permet d'améliorer les performances économiques de procédés évoluant dans un environnement variable et incertain comparée à une stratégie de contrôle standard ou une optimisation hors ligne. Il est possible de connecter une phase de planification à la DRTO. La planification bénéficie d'une meilleure vision stratégique à long terme, ce qui semble bien adapté pour la gestion du stockage dans une centrale solaire thermique. Ce chapitre a décrit le défi associé à l'exploitation des centrales solaires thermiques, notamment concernant la gestion du stockage. Le manque d'études portant sur la DRTO appliquée aux centrales solaires thermiques, ainsi que l'utilisation d'une phase de planification pour améliorer la gestion du stockage, a été souligné. Une méthodologie de DRTO utilisant une étape de planification a donc été proposée.

Le second chapitre comporte une présentation plus détaillée de la méthodologie développée, introduite dans le chapitre précédent, ainsi qu'une étude de cas simple

pour la tester. N'ayant pas accès à une centrale solaire thermique réelle et toutes les données associées pour tester la méthodologie, un modèle détaillé pour la simulation du système réel a été créé. Un contrôle parfait a été supposé dans la centrale, les trajectoires optimales déterminées par la DRTO sont donc parfaitement suivies à l'étape de simulation. L'étape de planification a été réalisée sur 2 jours, puis la DRTO a été testée sur la centrale virtuelle pour le premier jour. Une nouvelle DRTO est lancée à chaque heure, avec un horizon de temps jusqu'à la fin de la journée, qui se réduit donc d'une DRTO à l'autre. La demande en chaleur a été choisie constante et connue à l'avance. En revanche, une perturbation artificielle a été introduite sur le rayonnement solaire en temps-réel pour tester la méthodologie. La fonction objectif économique de la DRTO contient un terme pour le suivi de l'énergie stockée planifiée à la fin de la journée. Ce terme est affecté d'un poids, qui a été ajusté pour obtenir le meilleur compromis entre le suivi de l'objectif sur le stockage issu de la planification à la fin de la journée et des coûts d'exploitation journaliers les plus faibles possibles. Ensuite, les performances de la centrale virtuelle qui utilise les trajectoires optimales pour les débits déterminées par la DRTO ont été comparées aux performances obtenues lorsque l'optimisation dynamique hors ligne (Dynamic Optimization, DO) est employée. La DO correspond à l'étape de planification, les trajectoires optimales sont obtenues en avance, en utilisant des prévisions, et sans adaptation en temps-réel. Plusieurs cas d'étude ont été testés, représentant trois saisons différentes et plusieurs scénarios de perturbations en temps-réel. Dans la plupart des cas d'étude, les coûts d'exploitation de la centrale ont été réduits grâce à la DRTO en réduisant la consommation électrique des pompes et en augmentant la fraction solaire de la chaleur fournie (jusqu'à 35% d'augmentation en comparaison à la simulation utilisant la DO). L'objectif sur l'énergie stockée planifiée a été raisonnablement suivi, avec une différence maximale de -14% pour l'énergie finale stockée dans la simulation utilisant la DRTO comparée à celle utilisant la DO. La méthodologie de DRTO développée, s'appuyant sur une phase de planification, est donc capable d'adapter la stratégie de fonctionnement aux perturbations réelles et prévisions mises à jour, donc plus précises, mais aussi d'utiliser le stockage intelligemment grâce à l'usage de la planification qui bénéficie d'une meilleure vision stratégique à long terme.

Le troisième chapitre se concentre sur la modélisation en 1D de la cuve de stockage stratifiée, qui est un composant essentiel de la centrale solaire thermique. En raison du gradient de température très fort dans la région de la thermocline, située entre les zones chaude et froide, la cuve de stockage est particulièrement difficile à modéliser. Un compromis doit être trouvé entre la précision du profil vertical de température et de l'énergie stockée calculés et le temps de calcul, en particulier lorsqu'on s'intéresse à la simulation d'un système énergétique complexe ou à l'optimisation. Le schéma de discrétisation spatial traditionnellement utilisé est le modèle multinode, qui est basé sur les volumes finis en 1D. Ce schéma tend à adoucir le gradient de température au niveau de la thermocline lorsqu'un faible nombre de strates est choisi. Dans ce chapitre, un autre schéma de discrétisation a été proposé : la collocation orthogonale sur éléments finis (Orthogonal Collocation on Finite Elements, OCFE). Ce schéma offre un bon compromis entre la convergence rapide de la collocation orthogonale et la résolution rapide des volumes finis. En effet, la collocation orthogonale ne nécessite pas beaucoup de points de discrétisation pour obtenir des résultats précis et donc converge avec peu de points vers la solution de l'équation différentielle. Par ailleurs, pour un nombre

de points de discrétisation fixé, les volumes finis conduisent au temps de résolution le plus court. L'OCFE présente donc un bon compromis entre ces deux schémas de résolution. De plus, l'OCFE n'a jamais été utilisée pour la discrétisation spatiale d'une cuve de stockage. Dans ce chapitre, il a été montré que l'OCFE conduit à une meilleure estimation des températures et de l'énergie stockée dans la cuve que les volumes finis et cela avec des temps de calcul réduits. Le modèle basé sur l'OCFE a été validé avec des données expérimentales issues d'une centrale solaire thermique réelle. Cette validation a montré que l'OCFE peut représenter le profil réel de température dans la cuve en utilisant quatre fois moins de points de discrétisation que le modèle multinode et avec un temps de calcul divisé par cinq. En effet, l'OCFE avec 3 éléments contenant chacun 8 points de collocation a permis d'obtenir une précision légèrement supérieure aux volumes finis, en considérant 100 strates dans cette étape de validation. Enfin, la modélisation de la convection naturelle dans un modèle de cuve en 1D pour des études d'optimisation a été discutée, montrant les limites d'un modèle continu adapté à l'optimisation.

Enfin, dans le quatrième chapitre, la méthodologie de DRTO développée dans le Chapitre II a été améliorée et testée sur des cas d'étude plus réalistes. Tout d'abord, le modèle de cuve de stockage utilisé pour la centrale virtuelle représentant la centrale réelle a été changé pour l'OCFE introduite dans le Chapitre III. Cela a permis des simulations plus précises et plus rapides. En revanche, le modèle multinode avec 10 strates, utilisé pour l'optimisation, n'a pas été changé car les temps de calcul n'ont pas pu être réduits avec l'OCFE. Afin de réduire encore les temps de calcul avec l'OCFE, il faudrait utiliser moins de 10 points de discrétisation, ce qui conduit à des oscillations importantes dans le profil de température obtenu. La planification est réalisée une seule fois au début puis utilisée pour toute la période de simulation de 96 heures. Elle fournit ainsi la stratégie de gestion du stockage pour toute la période, déterminée grâce à des prévisions météorologiques. Une nouvelle DRTO est lancée toutes les 6 heures afin d'adapter les trajectoires optimales pour les débits dans la centrale aux conditions réelles. Un horizon de temps glissant de 12 heures est choisi. La fonction objectif économique de la DRTO peut inclure un terme concernant la gestion du stockage et plusieurs possibilités ont été explorées et comparées dans ce chapitre. Les cas d'étude utilisent une demande en chaleur variable et des prévisions et mesures météorologiques réelles, correspondant à des scénarios en été et au printemps. Les résultats obtenus montrent qu'il est préférable de maximiser l'énergie stockée à la fin de chaque DRTO, à condition qu'il n'y ait pas de risque de surchauffe dans la centrale. En effet, cette stratégie permet de stocker de l'énergie solaire qui sera utile plus tard, réduisant ainsi la consommation de gaz et donc les coûts d'opération de la centrale. En revanche, lorsqu'il y a un risque de surchauffe parce que le rayonnement solaire est élevé comparé à la demande en chaleur, il est préférable de suivre l'énergie stockée planifiée à chaque DRTO, comme cela a été testé dans le Chapitre II. En effet, la planification bénéficie d'une vision stratégique à plus long terme, ce qui permet d'anticiper les futures périodes de fort rayonnement solaire, et donc de réduire le stockage de l'énergie. Lorsque la DRTO suit cette stratégie de gestion du stockage, cela permet d'éviter des surchauffes.

Les travaux menés dans cette thèse montrent que la DRTO peut améliorer les performances économiques d'une centrale solaire thermique comparée à l'optimisation dynamique hors ligne. L'utilisation d'une étape de planification permet d'éviter une dégradation dans la gestion du stockage due à l'horizon de temps court choisi pour

l'implémentation en temps-réel. Un nouveau schéma de discrétisation spatiale pour le modèle de cuve de stockage en 1D a été proposé, qui pourrait améliorer la précision et réduire les temps de calcul de simulations et d'optimisations. Ce nouveau schéma a été utilisé avec succès dans le modèle de simulation dans cette thèse. Enfin, des lignes directrices concernant la gestion du stockage au niveau de la DRTO ont été formulées, montrant que la planification peut éviter les surchauffes dans la centrale. Ce travail a amené de nombreuses perspectives, qui sont détaillées ci-dessous.

La première direction pour de futurs travaux est d'améliorer la gestion du stockage dans la méthodologie de DRTO. Dans le Chapitre IV, les résultats ont montré que la stratégie optimale pour la gestion du stockage au niveau de la DRTO est différente selon qu'il y a un risque de surchauffe dans la centrale ou non. Un critère précis pour passer d'une stratégie à l'autre pourrait être determiné par la suite. Ce critère pourrait être l'évaluation du risque de surchauffe, déterminé lors de la planification, ou encore un rayonnement solaire réel bien plus important que prévu. Le suivi de l'énergie stockée planifiée a été mis en oeuvre ici en minimisant l'écart entre l'énergie stockée planifiée et réelle à la fin de l'horizon de temps de chaque DRTO. D'autres possibilités pourraient être envisagées telles que le suivi de l'énergie stockée planifiée à une heure fixe de la journée, de manière similaire au Chapitre II mais en utilisant cette fois un horizon de temps glissant, ou bien le suivi de la trajectoire de l'énergie stockée planifiée. Cela pourrait permettre d'améliorer la gestion du stockage dans la méthodologie de DRTO.

La méthodologie de DRTO pourrait également être améliorée de plusieurs façons. Dans cette thèse, une nouvelle DRTO était lancée à intervalles de temps réguliers (1 heure dans le Chapitre II et 6 heures dans le Chapitre IV). Un déclenchement conditionnel pourrait être envisagé pour ne ré-optimiser le fonctionnement de la centrale solaire thermique que lorsque c'est nécessaire. Par exemple, une nouvelle DRTO pourrait être déclenchée par une perturbation importante dans le rayonnement solaire. Cependant, cela nécessite des prévisions météorologiques accessibles à chaque instant, ou l'utilisation des prévisions les plus récentes potentiellement erronées. De plus, la planification a ici été utilisée comme une optimisation dynamique hors ligne réalisée une seule fois, au début de la période de test. Pourtant, dans une application réelle, la planification devrait être ré-optimisée régulièrement, et le critère déclenchant une nouvelle optimisation devrait être étudié.

La méthode de résolution du modèle d'optimisation pourrait également être améliorée. Une étude de sensibilité sur la discrétisation temporelle pourrait être menée pour capturer tous les effets transitoires dans le système tout en étant implémentable en temps-réel. Par ailleurs, la stratégie de résolution du problème d'optimisation utilisée dans cette thèse débute par une simulation dynamique du système utilisant des stratégies de contrôle standard. Cela fournit une initialisation aux variables du problème. Ensuite, deux contraintes sont ajoutées et finalement le fontionnement de la centrale solaire thermique est optimisé. Cette statégie a été efficace pour les cas d'étude testés mais pourrait conduire à un échec de convergence dans d'autres scénarios. De plus, la résolution de ce problème d'optimisation non linéaire conduit à un minimum local. Notamment, les trajectoires optimales obtenues peuvent rester très proches des trajectoires fournies lors de l'initialisation. D'autres stratégies de résolution pourraient être explorées pour faciliter la convergence de l'algorithme vers un minimum global. Par exemple, un algorithme stochastique pourrait être utilisé tout d'abord pour obtenir une estimation

approximative du minimum global. La solution pourrait ensuite être raffinée grâce à un algorithme déterministe. Ou alors, la résolution pourrait être lancée plusieurs fois en utilisant des initialisations différentes pour mieux s'approcher du minimum global et s'assurer de la convergence de l'algorithme. Cependant, ces modifications à la méthode de résolution doivent maintenir un temps de calcul raisonnable. Elles seraient plutôt envisageables pour l'étape de planification, car les temps de calcul risquent de ne pas être adaptés à une application en temps-réel.

Une autre direction pour de futurs travaux est l'amélioration du modèle utilisé pour l'optimisation et du modèle détaillé utilisé pour représenter la centrale réelle pour tester la méthodologie. Le modèle détaillé de la cuve de stockage en 1D a déjà été modifié dans le dernier chapitre pour améliorer la précision des résultats et réduire les temps de calcul. Le nouveau modèle a été validé expérimentalement. Cependant, la convection naturelle est modélisée grâce à un artifice numérique qui n'a pas pu être validé avec les données expérimentales. Par ailleurs, le modèle de cuve de stockage utilisé pour l'optimisation, bien que rapide, ne fournit pas des résultats très précis pour l'estimation du profil vertical de température ou de l'énergie stockée. De plus, la modélisation de la convection naturelle n'est pas incluse dans ce modèle. Il est donc important de développer des modèles précis et rapides pour la cuve de stockage, avec une validation expérimentale. Des modèles basés sur des données, qui n'ont pas été envisagés dans cette thèse, pourraient permettre de créer un modèle rapide pour l'optimisation. Le LaTEP travaille actuellement sur un modèle basé sur des données pour un Réseau de Chaleur Urbain (RCU) avec un site de production simple, pour des études d'optimisation. Par ailleurs, comme mentionné dans le dernier chapitre, les équipements et protocoles utilisés pour refroidir le fluide dans le champ solaire (ventilateurs, refroidissement par eau) ou éviter les surchauffes (défocalisation des capteurs solaires, refroidissement radiatif) quand c'est nécessaire pourraient être ajoutés aux modèles simplifié et détaillé. En outre, l'utilisation de ces équipements pourrait être optimisée pour minimiser leurs coûts d'opération. Enfin, le modèle détaillé représentant la centrale solaire réelle pourrait être amélioré, permettant ainsi des essais plus réalistes de la méthodologie. En particulier, les contrôleurs pourraient être modélisés pour mieux reproduire le comportement de la centrale. De cette façon, les trajectoires optimales obtenues à l'étape de DRTO pourraient être suivies, malgré la présence de perturbations.

Au lieu de tester la méthodologie sur un modèle détaillé de simulation, elle pourrait aussi être testée sur un appareil expérimental ou idéalement sur la centrale réelle directement. Dans ce cas, des étapes supplémentaires de reconciliation de données et d'estimation de paramètres seraient nécessaires pour exploiter les mesures effectuées sur le système. Ces étapes supplémentaires pouraient être ajoutées à la méthodologie dès la phase de test sur un modèle de simulation afin de reproduire plus fidèlement le comportement de la centrale réelle.

Par ailleurs, la méthodologie devrait être testée dans des cas d'étude plus variés. Tout d'abord, la demande en chaleur utilisée devrait être celle d'un vrai système, industrie ou RCU, avec des variations au cours et entre les jours. Plus de scénarios devraient également être testés avec différentes prévisions météorologiques et données en temps-réel. Ce test plus complet de la méthodologie permettrait de s'assurer de sa robustesse et pourrait aussi conduire à des comportements qui n'ont pas pu être

analysés dans cette thèse.

Une autre direction pour de futurs travaux est l'optimisation simultanée du dimensionnement et du fonctionnement de la centrale lors d'une optimisation dynamique hors ligne.

Enfin, ces travaux ouvrent des perspectives plus larges pour le fonctionnement optimal des systèmes multi-énergies. Tout d'abord, le travail présenté dans cette thèse pourrait être adapté à d'autres types de centrales solaires thermiques incluant les centrales à concentration pour la production d'électricité. Mais il pourrait également être adapté à d'autres systèmes thermiques évoluant dans un environnement incertain. Le LaTEP travaille actuellement sur une méthodologie de DRTO pour une centrale solaire thermique avec un stockage à court terme associé à une pompe à chaleur et un stockage intersaisonnier. Alors que les énergies intermittentes sont intégrées en proportions de plus en plus grandes dans les RCU et les réseaux électriques, on a de plus en plus besoin d'un contrôle optimal robuste du fonctionnement de ces réseaux. La méthodologie développée dans cette thèse présente des caractéristiques intéressantes pour le fonctionnement optimal futur des réseaux multi-énergies.

ECOLE DOCTORALE DES SCIENCES EXACTES ET LEURS APPLICATIONS (ED211)

LABORATOIRE DE THERMIQUE ENERGETIQUE ET PROCEDES (LATEP)

Alix Untrau

alix.untrau@univ-pau.fr